Investigation of the Utility of an Electronic Analog Computer in Engineering Problems

by

D. W. Hagelbarger, C. E. Howe, & R. M. Howe

Engineering Research Institute
University of Michigan, Ann Arbor

Project MX-794
(USAF Contract W33-038-ac-14222)
External Memorandum No. 28

Lithoprinted in U.S.A.
EDWARDS BROTHERS, INC.
ANN ARBOR, MICHIGAN
1949

TABLE OF CONTENTS

INTRODUCTION

This report gives the results of a study of an electronic analog computer as a laboratory research tool. The study was undertaken not for a particular problem but rather to investigate the applicability of the computer to applied research. While the treatment is by no means exhaustive, it is hoped that enough data are given on methods of setting up problems and introducing end conditions, accuracy, stability, time required for solutions and other advantages and limitations of this type computer, to enable an experimenter faced with a particular problem to make a critical comparison of this method with others which are available. The approach is that of a text book rather than a hand book and it is believed that the report will not only give an understanding of the principles of an electric analog computer, but also enable an engineer to design and put into operation a computer with the minimum number of pitfalls.

The amplifier, which is the basic element of all the operations, is one described by Ragazzini, Randall and Russell.[1] Some improvements in amplifiers have been made since then such as automatic zero adjust, reduced phase shift at high frequencies, lower grid current in the input stage, etc., however, these are only important when it is desired to push the accuracy to its extreme limit.

We wish to thank Professor Ragazzini for several valuable suggestions received by correspondence.

The report may be divided roughly in to four divisions as follows:

Division I. Introduction and Components of Computer.
Chapters 1 and 2

Division II. Differential Equations with Constant Coefficients.
Chapter 3, 4 and 5

Division III. Differential Equations with Variable Coefficients.
Chapter 6, 7, 8, and 9

Division IV. Study of a Servomechanism.
Chapter 10, 11 and 12

It should be pointed out that a large number of the problems treated here are used as illustrations and ordinarily would not be solved with an analog computer. In some cases, the computer circuit used is not the simplest possible but rather one which shows the general method of proceeding.

No work was done with multiplying circuits (other than functions of time), hence the computer will handle only linear equations. Another useful addition to the computer would be circuits for introduction of backlash, coulomb friction, dead space, and other non linear properties of mechanical systems.

CHAPTER 1

OPERATIONAL AMPLIFIERS AND THEIR USE IN ANALOG COMPUTERS

1.1 DC Feedback Amplifier

In an ordinary vacuum tube amplifier the gain (defined as the ratio of the output voltage to the input voltage) is a function of the circuit elements, including the characteristics of the vacuum tubes. In order to minimize the change in gain of an amplifier caused by changing characteristics of its components, particularly those over which limited control can be exercised, such as the variations in the behavior of vacuum tubes with age and changing voltages, degenerative feedback may be used. For example, in Fig. 1-1 VA is a high gain direct-current amplifier which with a voltage e' applied to its input terminals produces an output voltage of $-e_2$, so that the voltage gain A may be expressed as

$$A = -\frac{e_2}{e'} \tag{1-1}$$

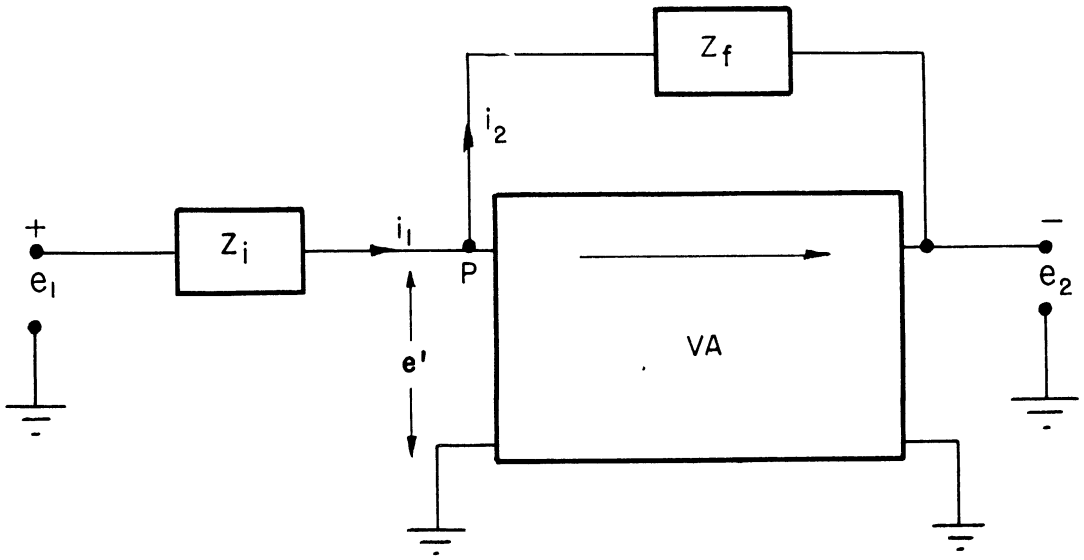

Figure 1-1 Basic dc amplifier with feedback.

Degenerative feedback is obtained by connecting the feedback impedance Z_f from the output of the amplifier VA to the input. The voltage e_1 to be amplified by the system is applied to the input terminals of the amplifier through the series input impedance Z_i.

In order to calculate the net gain of the system cognizance should be made of two facts: first, since the gain of the amplifier VA is very large (greater than 5,000) e' is negligibly small; and second, since the input to VA is connected through a high resistance directly to the grid of the input tube, the current flow from the point P into VA is negligible. Consequently, since the net current flow into the point P must be zero

$$i_1 - i_2 = 0, \tag{1-2}$$

or

$$\frac{e_1 - e'}{Z_i} - \frac{e' - e_2}{Z_f} = 0. \tag{1-3}$$

Since e' is negligible, e' drops out of equation (1-3), which may then be written

$$-e_2 = \frac{Z_f}{Z_i}\, e_1 \tag{1-4}$$

A more exact relation between e_2 and e_1 is

$$-e_2 = \frac{Z_f}{Z_i}\left[\frac{1}{1 + \frac{1}{A}\left(1 + \frac{Z_f}{Z_i}\right)}\right] e_1 , \tag{1-5}$$

as derived by Ragazzini, Randall and Russell.[1] Equation (1-5) reduces to equation (1-4) because, as the amplifier is used,

$$A \gg \left(1 + \frac{Z_f}{Z_i}\right).$$

Equation (1-4) shows that as long as e' is negligibly small, the gain of the system is solely dependent on the ratio of Z_f to Z_i, i.e., it is independent of changing characteristics of the amplifier VA so long as the gain A of the amplifier is large compared with $1 + Z_f/Z_i$.

1.2 Multiplication by a Constant

If the impedances Z_f and Z_i in the operational amplifier of Fig. 1-1 are made equal resistances, for example one megohm each, equation (1-4) shows that the output voltage e_2 will be the negative of the input voltage e_1, i.e., the operational amplifier will perform the simple operation of sign-changing. As a

matter of fact, every operation performed by an operational amplifier will include the operation of sign changing.

If, however, the impedances Z_f and Z_i are unequal resistances, i.e., $Z_f = kZ_i$ (or $Z_i = Z_f/k$) the output voltage e_2 will be k times the input voltage e_1 and of opposite sign. Since k (equal to Z_f/Z_i) may be a positive number either greater or less than unity the magnitude of the input voltage may be multiplied by any desired factor k either greater or less than unity. In practice the multiplication or division by a constant factor greater than 20, except in special cases, is to be avoided.

1.3 Differentiation

If the feedback impedance Z_f is made a pure resistance R_f and the input impedance Z_i a pure capacitance C_i, then the operational amplifier becomes a differentiator, Figure 1-2.

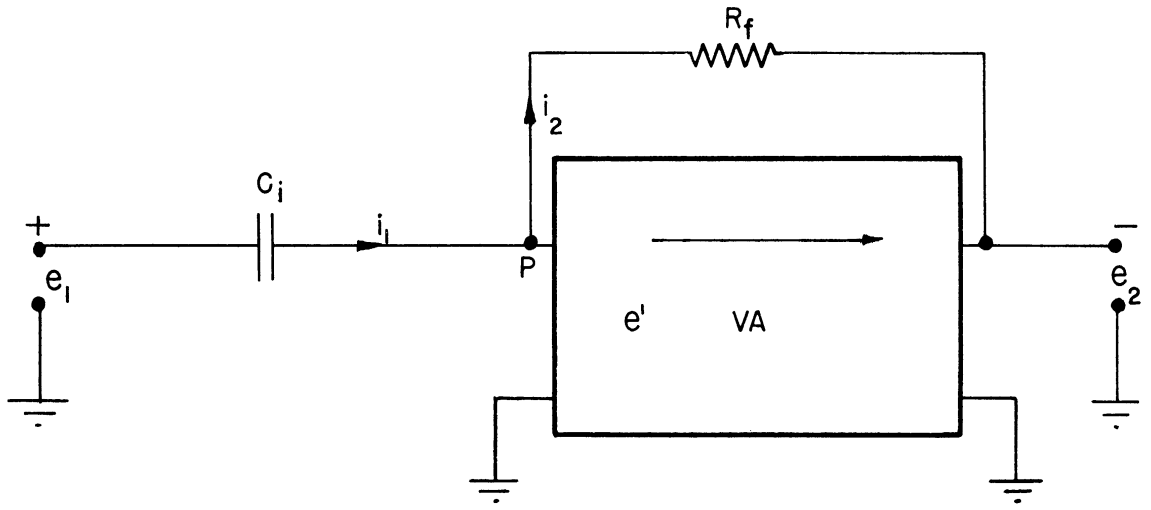

Figure 1-2 A differentiating operational amplifier.

Making the same assumptions as for the derivation of equation (1-4), the summation of the currents at the point P is expressed by equation (1-2), $i_1 - i_2 = 0$. It is readily seen that

$$i_2 = (-e_2 - e')/R_f = -e_2/R_f. \qquad (1\text{-}6)$$

For a capacitor

$$q = Cv, \qquad (1\text{-}7)$$

where q is the charge on the capacitor at any time t, and v is the corresponding voltage across the capacitor. In the case under consideration the voltage across the capacitor C_i is $e_1 - e' = e_1$ (since e' is negligibly small compared with e_1, i.e., the point P is essentially at ground potential). Consequently equation (1-7) may be written

$$q = C_i \ e_1.$$

Differentiating this equation with respect to t gives

$$i_1 = \frac{dq}{dt} = C_i \ \frac{de_1}{dt} \ . \qquad (1\text{-}8)$$

Substituting the values of i_1 and i_2 from equations (1-6) and (1-8) into equation (1-2) and solving for e_2 gives

$$e_2 = - R_f \ C_i \ \frac{de_1}{dt} \ . \qquad (1\text{-}9)$$

Equation (1-9) shows that the output voltage e_2 is the negative of the time derivative of the input voltage e_1 multiplied by the constant R_fC_i. Thus the operational amplifier with the input impedance being that of a capacitor and the feedback impedance a pure resistance may simultaneously perform the operations of differentiation and multiplication by a constant (with sign changing in addition).

If R_fC_i of equation (1-9) is equal to unity (R_f, 1 megohm; C_i, 1 microfarad) differentiation without multiplication by a constant is accomplished. If R_f were 5 megohms and C_1 one microfarad, then the input voltage e_1 would be differentiated and multiplied by the factor -5.

If the input voltage e_1 were sinusoidal ($e_1 = E \sin \omega t$) according to equation (2-9) the output voltage would be

$$e_2 = - R_f \ C_i \ \frac{d}{dt} \ (E \sin \omega t) = - R_f \ C_i \ E \ \omega \cos \omega t. \qquad (1\text{-}10)$$

Equation (1-10) shows that the maximum value of the output voltage e_2 is equal to the constant R_fC_iE multiplied by the angular frequency ω. Thus if R_fC_i were equal to unity and ω equal to 10, the maximum value of the output voltage e_2 would be 10 times E, the maximum value of the input voltage e_1. Should there be some undesired 60 cycles per second voltage (due to pickup, or incomplete filtering in a power supply) applied to the input it would appear in the output as a 60 cycles per second voltage with a magnitude 377 times greater (R_fC_i being equal to unity). Because of this increasing gain with frequency, and various troubles associated with it (e.g., phase shifts for higher frequencies in the dc amplifier), it is advisable to avoid using the operational amplifiers as

differentiators whenever possible.

1.4 The Operator p

In subsequent analysis it will be convenient to use the differential operator p as used in operational calculus. The operator p represents differentiation with respect to time, i.e.,

$$pi = \frac{di}{dt} \quad , \quad \text{or} \quad pe = \frac{de}{dt}$$

Consequently equation (1-9) may be written

$$e_2 = -R_f C_i \; pe_1 \quad . \tag{1-11}$$

Equation (1-11) could have been derived from equation (1-4) in the following manner. Using the differential operator p, equation (1-8) may be written as

$$i_1 = C_i p e_1 \quad , \tag{1-12}$$

where p operates on e_1. However, the properties of the operator p are such that it may be treated as an algebraic quantity. Hence equation (1-12) may be written

$$\frac{e_1}{i_1} = \frac{1}{C_i \, p} \quad . \tag{1-13}$$

Since the impedance of a circuit element is defined as the ratio of the voltage across the element to the current through the element, $1/C_i p$ of equation (1-13) may be considered the operational impedance of the capacitor C_i. Substitution of this impedance, together with the other necessary terms, into equation (1-4) yields equation (1-11).

The operator p designates differentiation with respect to time. The operator 1/p, as may easily be shown, designates integration with respect to time. The advantages of the use of the operators p and 1/p will become evident in later developments.

1.5 Integration

If the impedance Z_i is a pure resistance R_i and the impedance Z_f a pure capacitance C_f then equation (1-4) becomes

$$e_2 = -\frac{Z_f}{Z_i} \; e_1 = -\frac{1/C_f p}{R_i} \; e_1 = -\frac{1}{R_i C_f} \; \frac{1}{p} \; e_1 \quad , \tag{1-14}$$

where 1/p is the integral operator of operational calculus. Thus $\frac{1}{p} e_1$ is the time integral of e_1, and the output voltage e_2 as expressed by equation (1-14) is the negative of the time integral of the input voltage e_1 multiplied by the constant $1/R_i C_f$. Thus the operational amplifier, with the input impedance being a pure resistance and the feedback impedance being that of a capacitor, simultaneously performs the operations of integration and multiplication by a constant. If R_i were 5 megohms and C_f one microfarad then the input voltage would be integrated and multiplied by the factor -1/5.

If the input voltage e_1 were sinusoidal ($e_1 = E \cos \omega t$) according to equation (1-14) the output voltage would be

$$e_2 = - \frac{1}{R_i C_f} \frac{1}{p} (E \cos \omega t) = - \frac{1}{R_i C_f} \frac{E}{\omega} \sin \omega t. \quad (1\text{-}15)$$

This equation shows that the maximum value of the output voltage e_2 is equal to the constant $-E/R_i C_f$ divided by the angular frequency ω. Thus if $1/R_i C_f$ were equal to unity, and ω equal to 10, the maximum value of the output voltage would be 1/10 that of the input voltage. Similarly, for 60 cycles per second e_2 would be 1/377 of e_1. Because of this decrease of magnitude of output voltage with frequency the integrating operational amplifier is not subject to the shortcomings described in connection with the differentiating operational amplifier.

An integrating operational amplifier is shown in Figure 1-3. Since the voltage e' at the input terminals of the amplifier VA is 1/A (less than 1/5,000) of the output voltage e_2, the voltage e' is negligible with respect to e_2 and the point P may be considered at zero potential (relative to ground). Consequently the voltage across the feedback condenser C_f is equal to the output voltage e_2. This fact, as will subsequently be shown, is of importance in setting up the initial conditions of a problem.

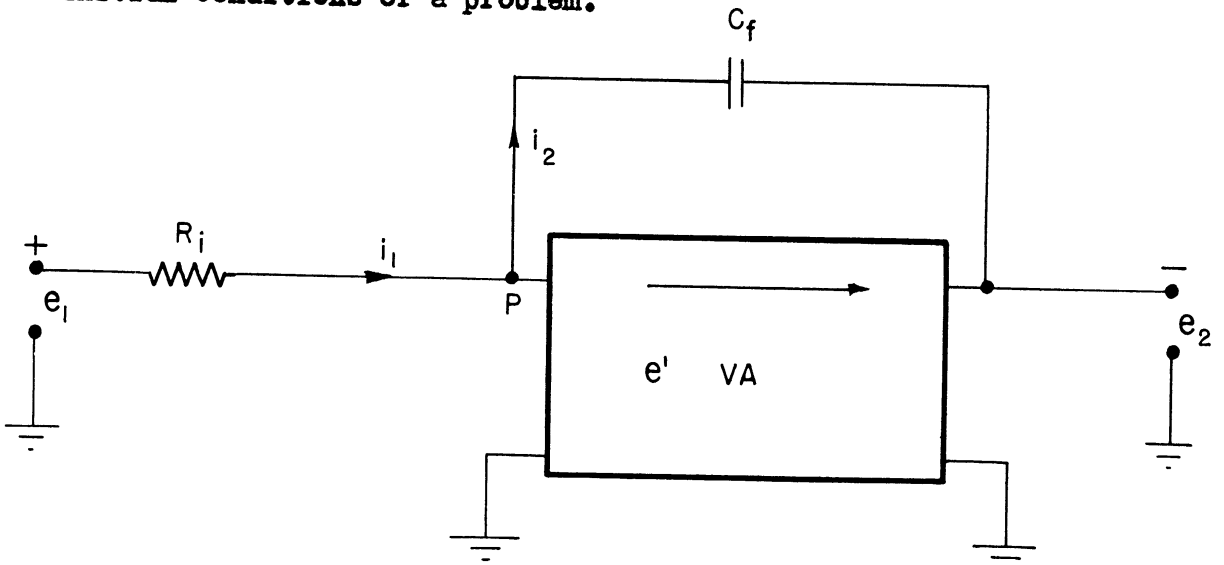

Figure 1-3 An integrating operational amplifier.

1.6 Summation

One of the most important operations performed by the operational amplifier is that of summation, or the adding together of a number of different voltages obtained from different sources. For example, suppose three variable voltages, e_a, e_b and e_c are to be summed. The manner in which this may be done is explained by means of Figure 1-4.

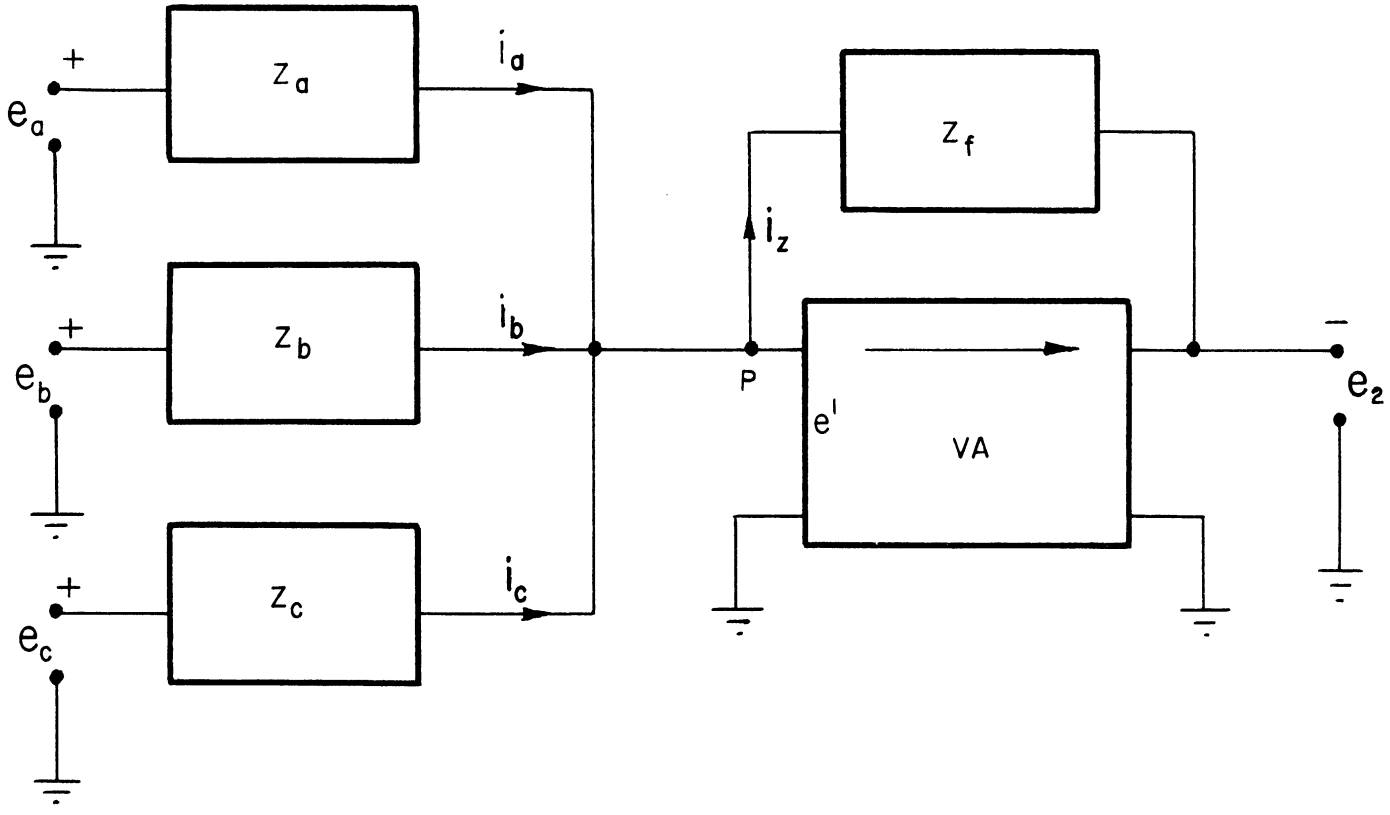

Figure 1-4. Operational amplifier used for summation.

Making the same assumptions as for the derivation of equation (1-4), the sum of the currents at the point P gives

$$i_a + i_b + i_c - i_2 = 0,$$

or

$$\frac{e_a}{Z_a} + \frac{e_b}{Z_b} + \frac{e_c}{Z_c} - \frac{-e_2}{Z_f} = 0.$$

Whence

$$e_2 = -\left(\frac{Z_f}{Z_a}\, e_a + \frac{Z_f}{Z_b}\, e_b + \frac{Z_f}{Z_c}\, e_c\right). \qquad (1\text{-}16)$$

If the feedback impedance Z_f and the input impedance, Z_a, Z_b and Z_c are made equal resistances (say one megohm) the output voltage e_2 is the negative of the sum of the three input voltages, e_a, e_b and e_c. One or more of the input impedances could be given a resistance value different from that of Z_f, thereby multiplying the corresponding input voltage by the value Z_f/Z_i. In case any one of the input voltages is required to have a sign opposite to the others it could be operated on by a sign-changing amplifier before being applied to the corresponding input resistor of the summing amplifier.

1.7 Solving a Simple Differential Equation

There have been described the uses of operational amplifiers for sign-changing, multiplication by a constant factor, differentiation, integration and summation. Some of these operations will now be combined to show how a simple differential equation may be solved.

The differential equation

$$\frac{d^2y}{dt^2} = F(t) \qquad (1\text{-}17)$$

is the equation of motion for a body travelling with an acceleration, F(t), a function of time. F(t) may be zero, in which case the body travels with constant velocity; F(t) may be a constant, in which case the body travels with constant acceleration; or F(t) may be some other function, consistent with the problem being solved.

The analog computer assembly of Fig. 2-5* for solving this equation can be understood more easily if the equation is written in the form

$$\frac{d^2y}{dt^2} - F(t) = 0 \qquad (1\text{-}18)$$

* This is not the simplest computer for this particular equation but it rather serves as a basis from which to develop more complicated computers.

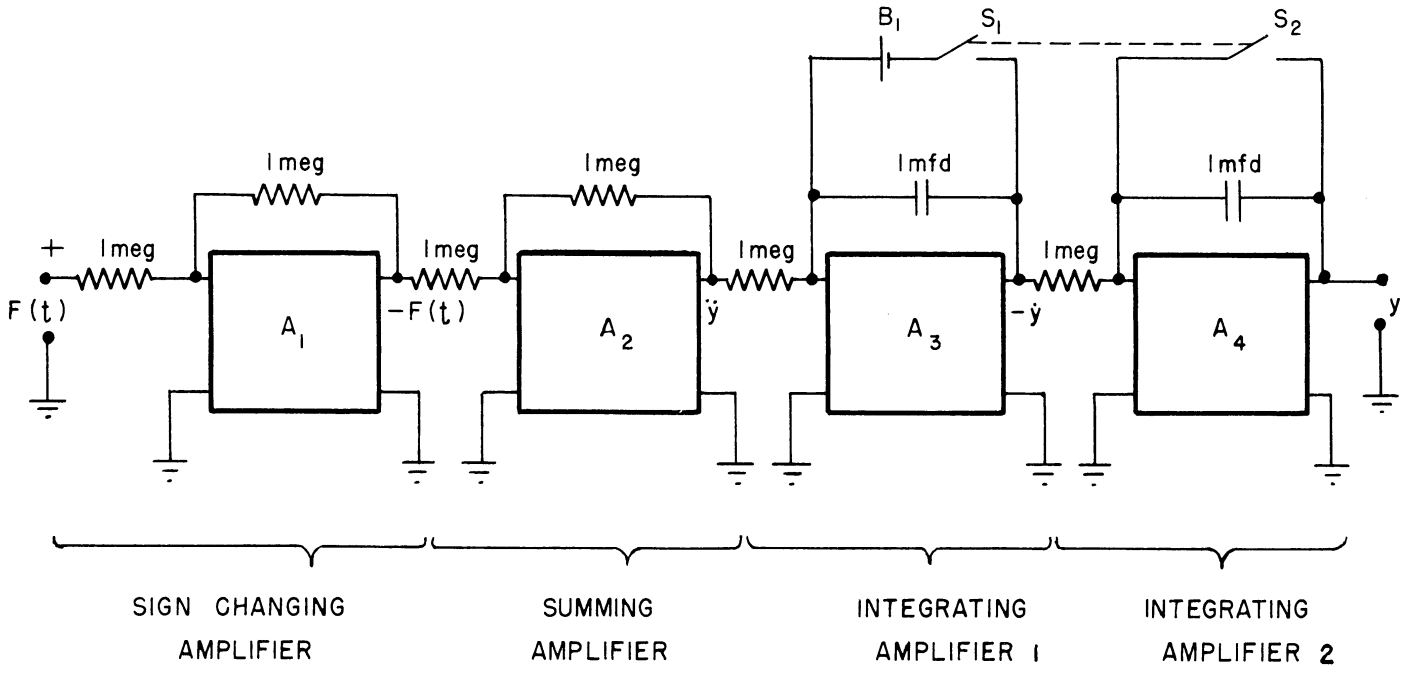

Figure 1-5. Analog computer for equation (1-17).

Four operational amplifiers are used. It is assumed that the output of integrating amplifier 2 will be y. Therefore, since the RC product of the feedback capacitance (1 microfarad) and the input resistance (1 megohm) is unity the input to this integrating amplifier must be $-dy/dt$ or $-\dot{y}$. This follows since the negative of the integrated input is the output. Similarly, the input of integrating amplifier 1 (i.e., the output of the summing amplifier) is $\ddot{y}$.

The function F(t) applied to the input terminals of the sign-changing operational amplifier gives an output voltage which is -F(t) since the gain of this amplifier is -1. The summing amplifier may be looked upon as an operational amplifier adding the two voltages -F(t) and $\ddot{y}$. This can be demonstrated by equating the currents at the point P to zero.

Before equation (1-17) can be solved it is necessary to designate the function F(t) and to state the initial conditions. Suppose we set F(t) equal to a constant (say -1.5 volts, representing an acceleration of -1.5 ft/sec^2) and set the initial conditions, at the time t = 0, at y = 0 and $\dot{y}$ equal to a constant (say 6 volts, representing an initial velocity of 6 ft/sec).

Since the output voltage y of the second integrating amplifier is, for practical purposes, the same as the voltage across the feedback capacitor of the same amplifier, the output voltage y can be made equal to zero by closing the switch S_2, thereby shorting the condenser.

Similarly, the output voltage $-\dot{y}$ of the first integrating amplifier is the same as the voltage across its feedback capacitor and hence the proper initial conditions can be placed on the velocity $\dot{y}$ by making the battery B_1 equal to -6 volts and closing switch S_1.

F(t) can be given its proper value by connecting a 1.5 volt cell across the input terminals of the sign-changing amplifier.

The solution of the problem is obtained by opening switches S_1 and S_2 simultaneously and observing the output voltage y which is, of course, a function of the time t.

If it is desired to observe the velocity $\dot{y}$, the output $-\dot{y}$ of the first integrating amplifier should be connected to the input of another simple sign-changing amplifier and $\dot{y}$ observed at its output terminals.

Figure 1-6 shows the results obtained for the solution of the problem.

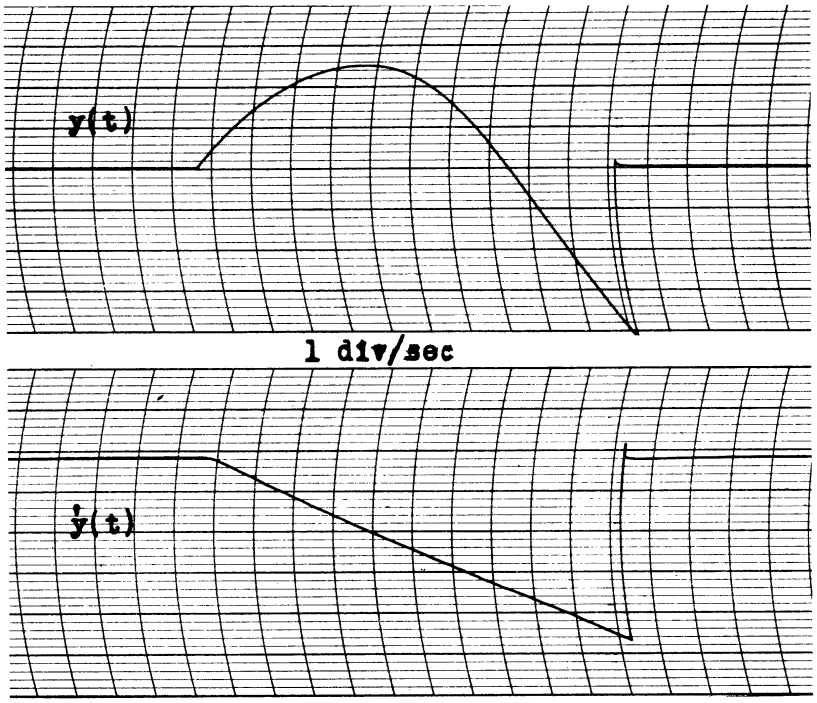

Figure 1-6. The solution of equation (1-17).

1.8 Damped Oscillations

The equation

$$m\ddot{y} + c\dot{y} + ky = 0 \qquad (1\text{-}19)$$

represents the equation of motion of a mass m supported by a spring with elastic constant k, the system being subjected to viscous damping $c\dot{y}$. The analog computer for the solution of this equation is shown in Figure 1-7. Its operation is very similar to that of the computer of Figure 1-5. The computer is set up for the initial conditions, at $t = 0$, of the velocity $\dot{y}$ being zero and of a finite displacement y. The summing amplifier has fed into it voltages proportional to y, $\dot{y}$, and $\ddot{y}$ through input resistors 1/k, 1/c and 1/m respectively to take care of the coefficients of the several terms of the equation. $\dot{y}$ is obtained from $-\dot{y}$ by means of the sign-changing amplifier. Appropriate initial conditions are set up when the switches S_1 and S_2 are closed. The solution of the problem is started by the simultaneous opening of the two switches. As desired the displacement y(t), the velocity $\dot{y}(t)$ or the acceleration $\ddot{y}(t)$ may be observed at the appropriate output terminals.

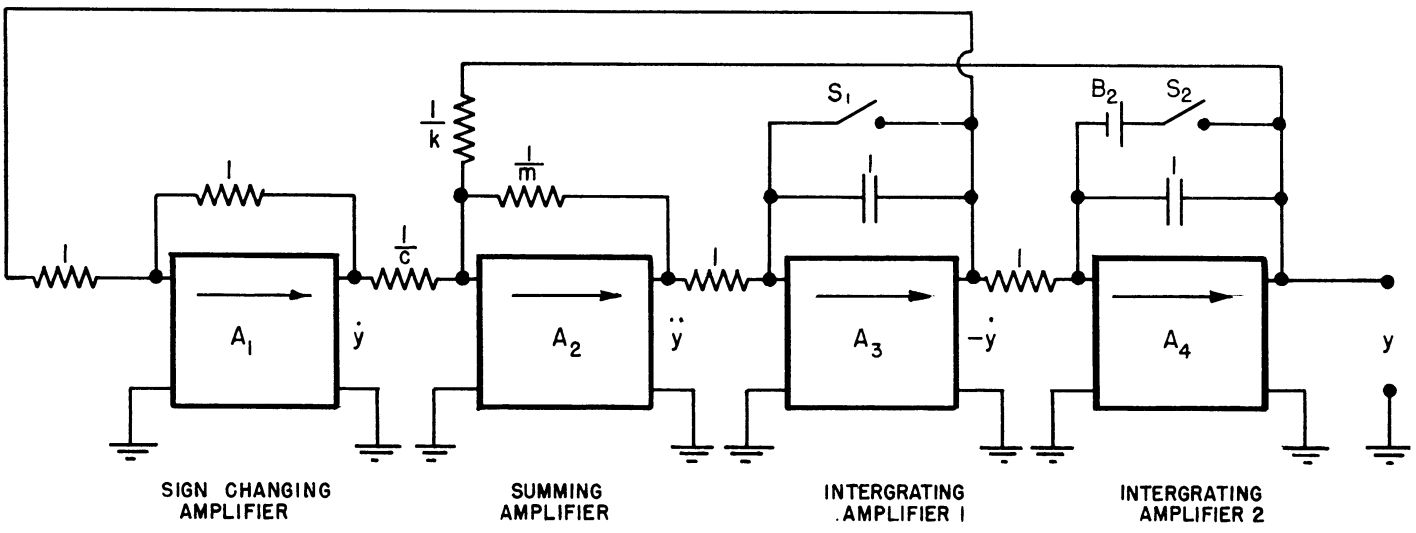

Figure 1-7. Analog computer for solution of equation (1-19) with initial conditions of zero velocity and finite displacement.

It should be noted in Figure 1-7 that the units of the resistances and the capacitances are not indicated. It is very convenient to take the unit of resistance as the megohm and the unit of capacitance the microfarad. The numbers and quantities associated with each of the resistors indicate as many megohms unless otherwise stated. Similarly, the quantities associated with the various capacitances represent that number of microfarads. This practice will be followed uniformly from now on.

The coefficient of $\dot{y}$ is c. It appears in Figure 1-7 as the value 1/c of the input resistor for $\dot{y}$ of the summing amplifier. The same effective result could be obtained by making the input resistance of the sign-changing amplifier 1/c instead of 1, or by making the feedback resistor of the sign-changing amplifier c instead of 1. In either case the output of the sign-changing amplifier would be $c\dot{y}$, and the corresponding input resistor of the summing amplifier would be 1 in place of 1/c. This alternative method is pointed out here because this practice will be followed in many problems.

In Figure 1-8 are shown records of y and $-\dot{y}$ for equation (1-19), for m = 0.25, c = 0.25 and k = 1, with the initial conditions, $y(0) = 6$, $\dot{y}(0) = 0$.

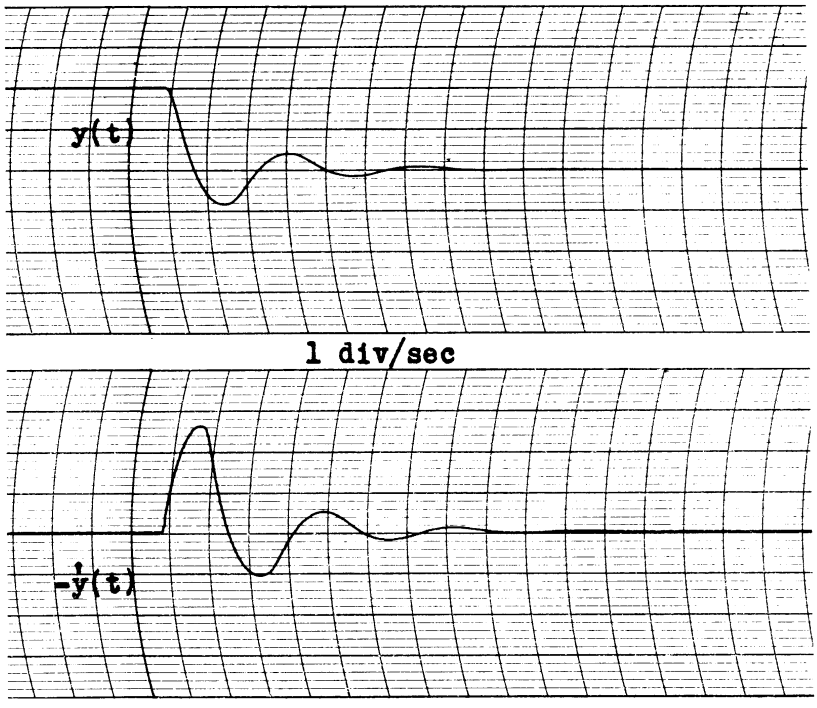

Figure 1-8. Solution of the differential equation of equation (1-19).

1.9 Differential Equations with Variable Coefficients

Differential equations with coefficients which are functions of the independent variable can be solved by electronic analog computers. To this end it is necessary to provide resistance elements which can be made to vary in value in such a way as to obtain the desired variable coefficient values in the computation. For example, if a coefficient were a linear function of the time, t, there could be inserted as a feedback impedance in the appropriate amplifier a linear rheostat the sliding contact of which is made to move linearly with time. Conversely, if a coefficient were inversely proprotional to t a similar device could be inserted as the input impedance of the appropriate amplifier.

The several methods by which these changing resistances can be obtained are discussed more in detail in Chapter 6.

When the coefficients are functions of some of the dependent variables of the equation, or equations, being solved, servomultiplier circuits are used.

The nature of the investigations made by the authors did not make it expedient to undertake any work with servomultipliers. For further information on this phase of the problem reference should be made to other authors.[1,2]

CHAPTER 2

COMPONENTS OF THE SYSTEM

2.1 Direct Current Amplifier

Since the solutions of the differential equations involve steady or slowly changing voltages it is necessary that the basic voltage amplifier of an operational amplifier be a direct durrent amplifier. Figure 2-1 gives the circuit of the direct current amplifier* used in the electronic computing which forms the basis of this report. This circuit is that of a three-stage amplifier of good stability and high gain, having an effective phase shift of 180° (actually 540°). The input and output connections each have one terminal at ground. Any good dc amplifier having similar characteristics could be used. Frost[2] shows a suitable amplifier which has higher gain and more power output than the one shown in Figure 2-1.

The dc amplifier is mounted on a chassis as shown in Figure 2-2. Connections to a power supply distribution box are made by a six-conductor shielded cable, using the six-contact Jones jack shown at the rear of the chassis. Figure 2-3 is a photograph of an amplifier ready for use as an integrator.

The two knobs on the top of the chassis make it possible to change the two variable resistors associated with the input tube. These knobs are to be used for balancing the amplifier for zero dc output. Each amplifier should be carefully balanced before using the computer for the solution of a problem.

To balance a sign-changing or multiplying amplifier the input terminals should be shorted and the resistances adjusted until balance is obtained. For testing the balance a multi-range dc vacuum tube voltmeter of high input resistance is desirable. Rough adjustment can be made using a high scale (say 100 volt scale) and final adjustment by using the lowest scale.

A differentiating amplifier should be balanced in the same manner, mindful of the fact that as the sliding contact of a resistor passes from wire to wire the sudden change of current will be differentiated and give sharp voltage pulses in the output.

An integrating amplifier could be balanced by the same method. In this case balance is obtained when the output remains constant. If an integrating amplifier is unbalanced, a charge will gradually accumulate on the capacitor in the feedback circuit. Before testing for balance this charge should be removed by shorting the capacitor through a low resistance (1,000 ohms). Alternately, balance could be obtained by temporarily shorting the capacitor (as well as the input terminals), and proceeding as in the case of a sign-changing amplifier. In this case, however, the amplifier has zero gain and lacks sensitivity. Experience and the nature of the problem being solved will determine which method should be used in a particular case.

In general it is advisable to disconnect the output of an amplifier while it is being balanced. It is also advisable to test the complete computer or discrete parts of it, for balance, since small unbalances may add up to a large and unacceptable over-all unbalance.

* This circuit is taken from reference 1.

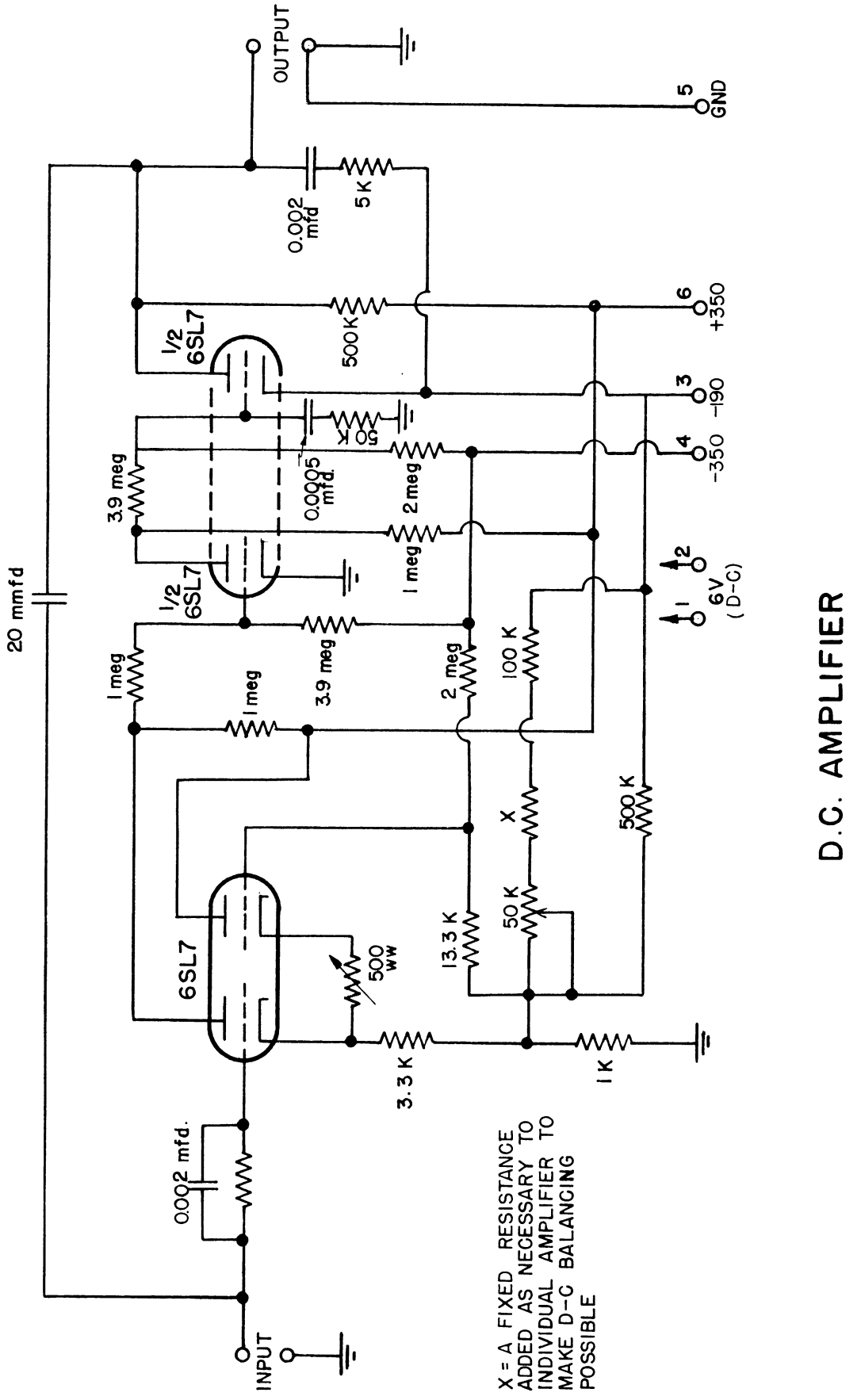

Figure 2-1. Circuit of basic dc voltage amplifier used in an operational computer.

THE POINT A IS CONNECTED TO THE HIGH SIDE OF THE INPUT TERMINALS OF THE AMPLIFIER.

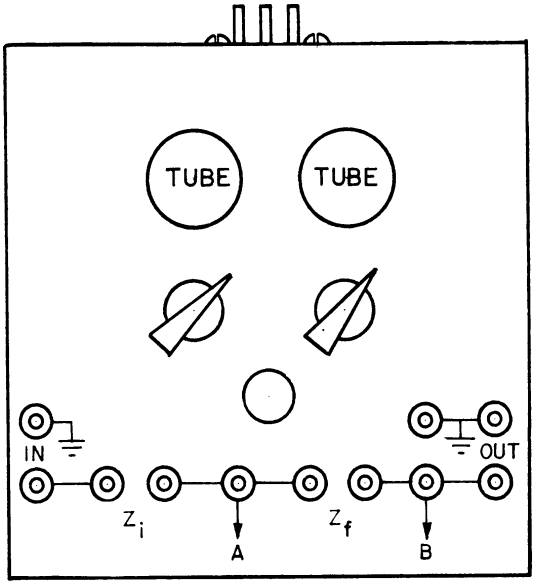

THE POINT B IS CONNECTED TO THE HIGH SIDE OF THE OUTPUT TERMINALS OF THE AMPLIFIER.

AMPLIFIER CHASSIS

Figure 2-2. DC amplifier chassis.

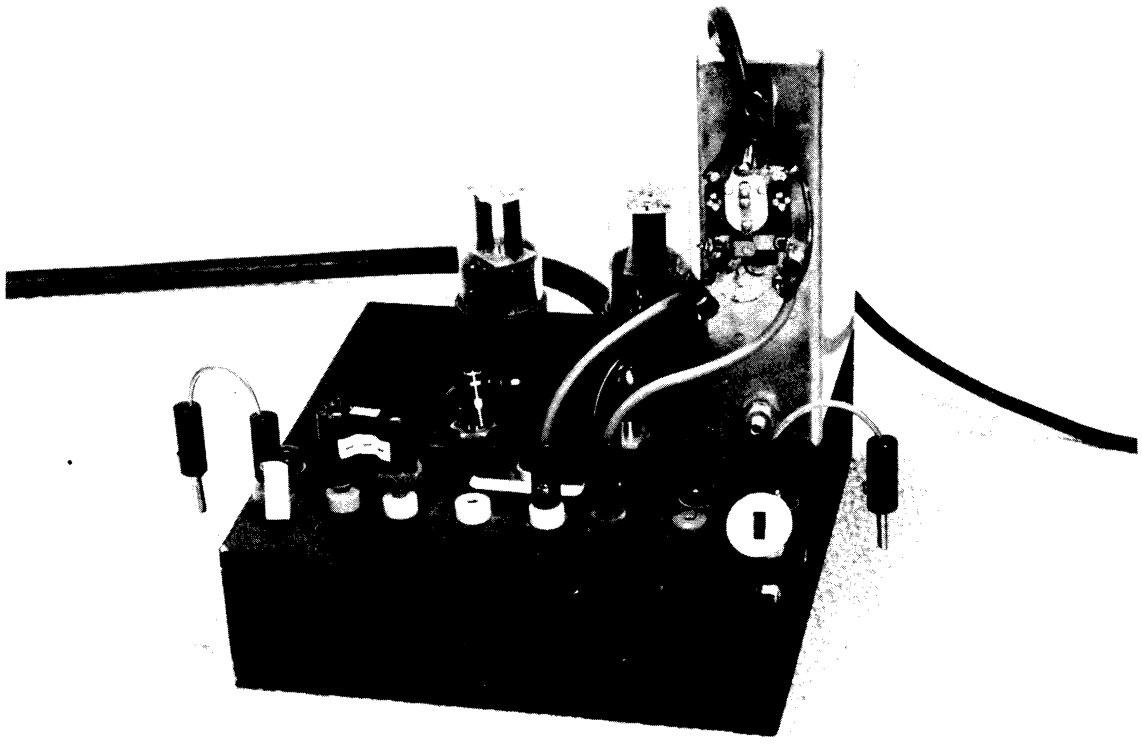

Figure 2-3. Amplifier ready for use as an integrator.

Jacks of the size taking banana plugs are furnished on the amplifier chassis for plugging in feedback and input impedances and the input and output voltages. Where these elements and voltages are plugged in, the spacing of the jacks is 3/4 inch, the correct spacing for General Radio Type 274-M double plugs. In addition, the input and output jacks are placed close enough to the sides of the chassis so that inter-connections of amplifiers can be made with double plugs.

2.2 Resistors, Input and Feedback

The resistors used as input impedance Z_i and feedback impedance Z_f are Continental X-type, ± 1%. Each resistor used as Z_i or Z_f should be measured to within 0.1%. Resistors (and capacitors) used in the feedback and input positions should be matched to each other within 0.1% in order to obtain the proper resistance ratio (or RC product). Carbon resistors should not be used, even if carefully calibrated, because of very poor voltage characteristics. The resistor are mounted on double plugs for convenience in changing circuit constants.

2.3 Capacitors

The impedances used in the feedback circuits of integrators are polystyrene capacitors. These condensers have very high leakage resistance and low dielectric adsorption. The ones used in the computers have one microfarad capacity, are manufactured by Western Electric Company*, and obtained from the Signal Corps. Polystyrene capacitors are commercially available.

The capacitors are arranged for making plug-in connections with double plugs. On top of some of the capacitors is mounted a relay for imposing initial (shorted) conditions. When the initial conditions call for a definite voltage on a capacitor, the relay imposing these conditions is mounted on the battery supplying the voltage. All initial-condition relays are operated simultaneously by a remote "starting" button. Figure 2-3 shows a capacitor with relay mounted on it.

2.4 Power Supplies

Three high voltage power supplies are used, furnishing well-filtered and regulated dc voltages of -190, -350 and +350 volts, respectively, relative to ground. The circuits for the power supplies as constructed for use are shown in Figures 2-4, 2-5, and 2-6.

Each amplifier takes approximately 2.0 ma at +350 volts, 0.5 ma at -350 volts and 2.5 ma at -190 volts. The power supplies should be able to furnish the currents needed for the maximum number of operational amplifiers to be used and to maintain good regulation and low ac ripple. The ac ripple in the power supplies used is of the order of 5-10 mv. (The -190 volt supply is mounted in a small cabinet, the two others together in a large one.)

Suitable power supplies of limited capacity can be obtained with the use of voltage regulator tubes. Such a supply is shown in Figure 2-9.

* Western Electric No. D161270.

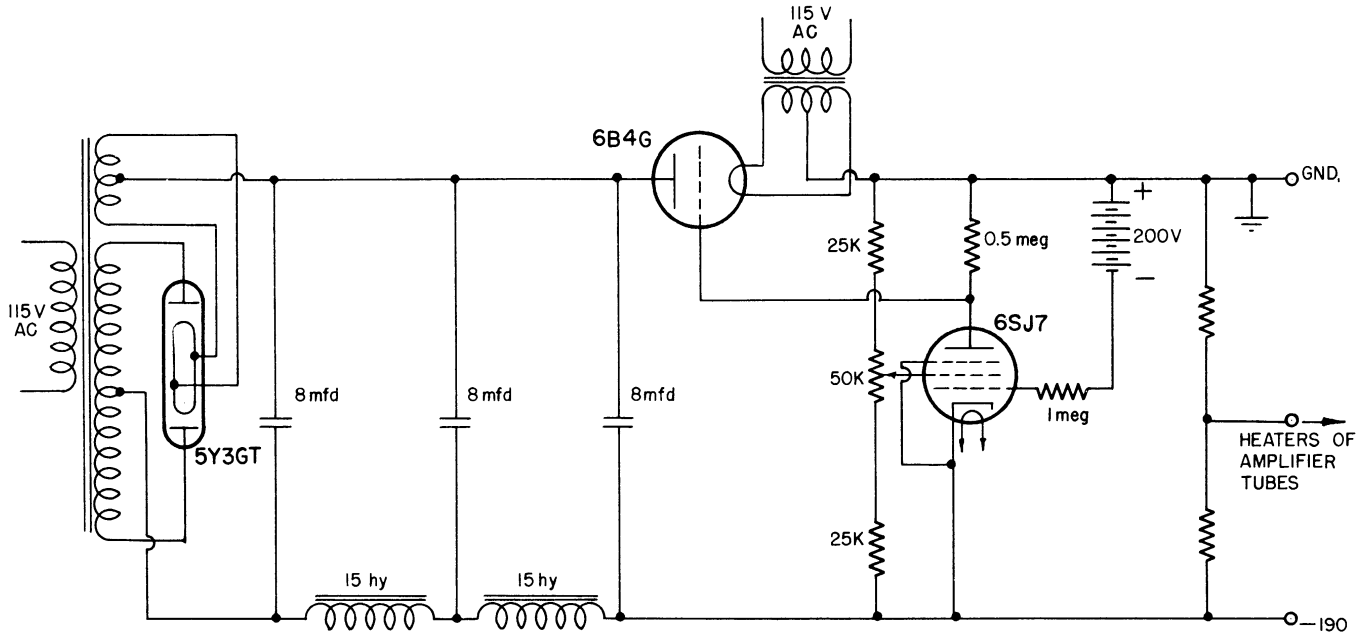

-190 V POWER SUPPLY

Figure 2-4.

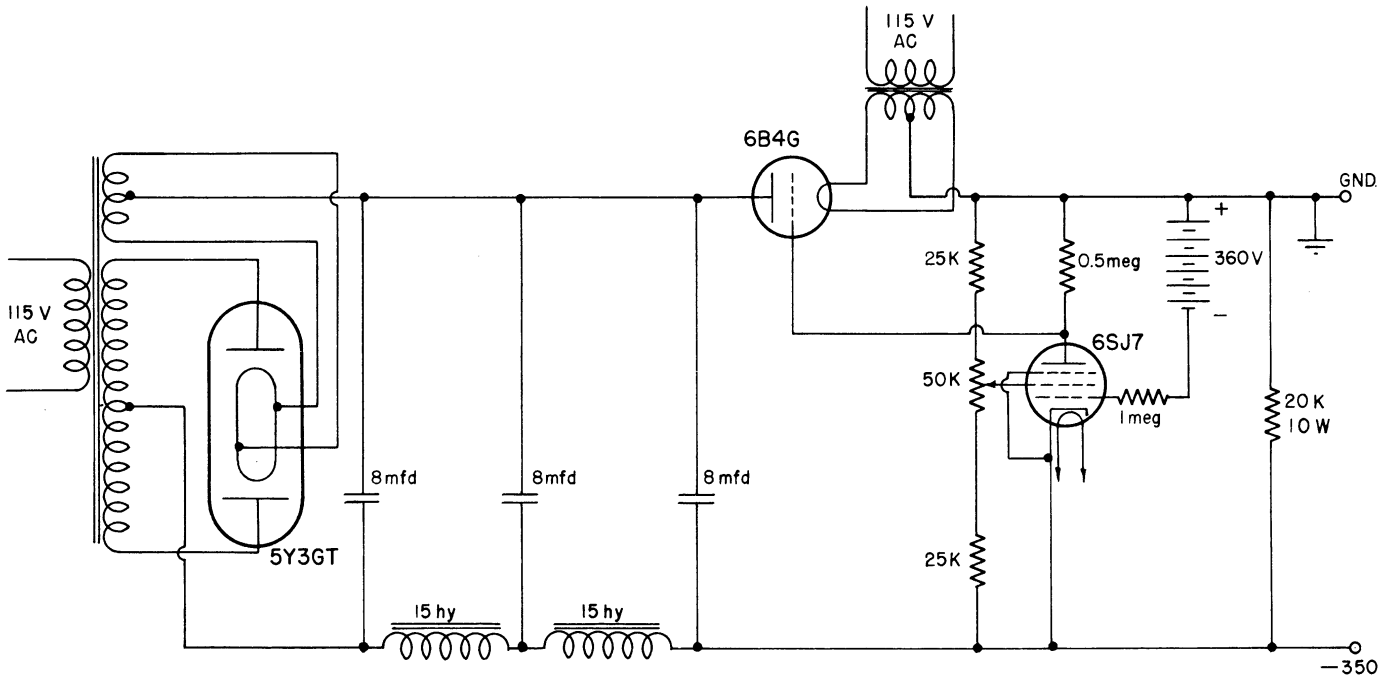

-350 V. POWER SUPPLY

Figure 2-5.

Reference to the dc amplifier circuit (Figure 2-1) shows a voltage difference of 190 volts between the two cathodes of the second 6SL7 tube. In

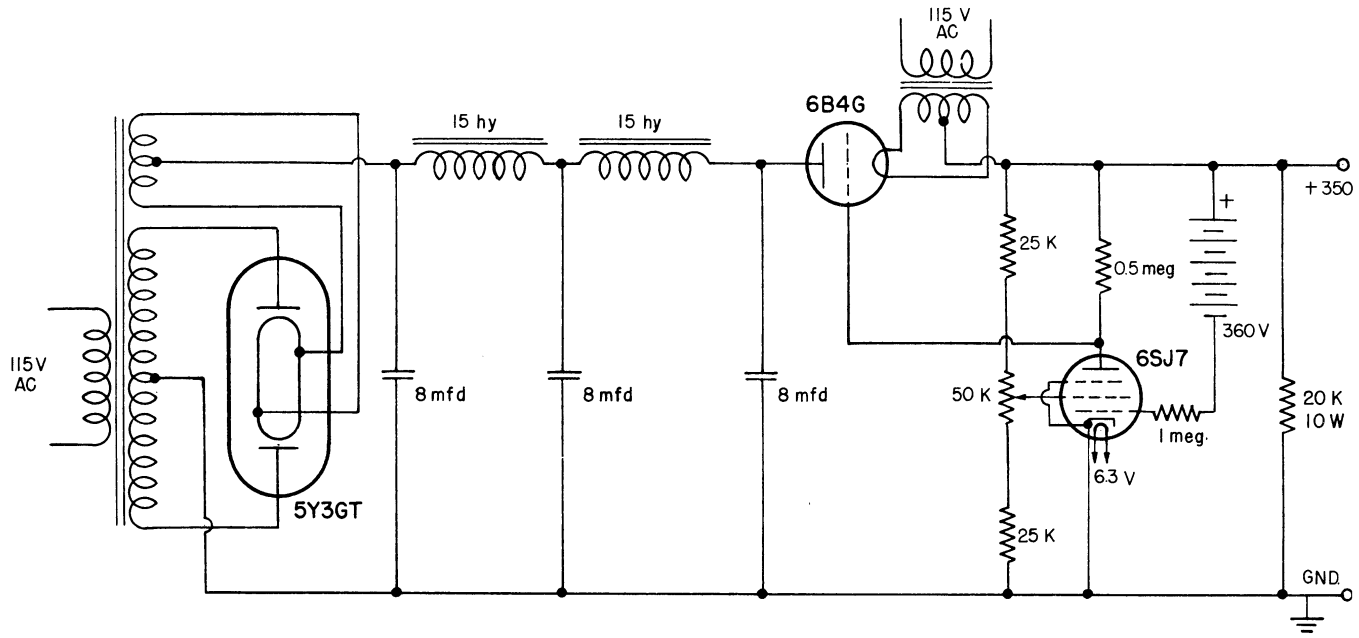

+ 350 V. POWER SUPPLY

Figure 2-6.

order to avoid excessive heater-cathode potential one side of the heater voltage supply was connected to the mid-tap of a resistor across the -190 volt power supply.

2.5 Heater Supply Voltage

In some of the problems solved it was necessary to use one or more differentiating circuits. For this reason the power for the heaters of the amplifier tubes was obtained from a 6 volt storage battery. The use of direct current for the heaters decreased the amount of undesired ac ripple. It is probable that an ac heater supply voltage could be used with computing circuits that do not have differentiating amplifiers.

2.6 Power Supply Distribution Box

The power supply and filament supply voltages are carried to a power supply distribution box by means of shielded cables, plugs and jacks, using a different kind for each source to avoid the possibility of wrong connections. The various voltages are distributed to a number (in our equipment 12) of 6-contact, female Jones plugs for distribution through shielded cables to the respective amplifiers.

2.7 Recording Oscillograph

All solutions were recorded by means of a Brush, Model BL-202, double

channel magnetic oscillograph, which has a frequency range from direct current to 30 cycles per second (up to 100 cycles per second with decreasing amplitude). The sensitivity of the oscillograph is approximately 1.6 mm per milliampere deflection at the pen point. The impedance of the driving coil is 1500 ohms and is critically damped if the impedance of the driving source is 250 ohms. (The manufacturer states that 500 ohms is satisfactory. The performance seems most satisfactory if the driving source impedances is much less than 250 ohms.)

Since full scale deflection of the pen point from median position is 40 millimeters about 25 ma are required to drive the pen with maximum amplitude.

2.8 Impedance Matching DC Power Amplifier

While the operational amplifiers used in the computer have a very low output impedance they can furnish only a small amount of current (approximately 1 ma). Consequently in order to take records of the output voltage of a computer there must be placed between the amplifier and the oscillograph a dc power amplifier with a high input impedance and a low output impedance, capable of furnishing without distortion sufficient current to operate the oscillograph.

Figure 2-7 shows the circuit of a two channel impedance matching dc power amplifier with power supply. Each channel uses two twin 6AS7G triodes connected as cathode followers. Each tube has its elements connected in parallel. In each of the channels one 6AS7G has its grids (connected together) permanently grounded; the other tube has its grids connected to the input voltage terminals in parallel with a one megohm resistor to ground. The output to the oscillograph is taken off of the sliding taps of 100 ohm potentiometers in series with and on the high side of 1000 ohm cathode resistors. Provision is made by means of a switch for connecting the grids of the active tube (of a channel) to ground and simultaneously connecting a 500-0-500 microammeter across the output terminals. By adjusting one of the potentiometers (with a control on the front of the panel) the channel can be balanced for zero output voltage with all grids grounded. Returning the testing switch to the neutral position places that channel of the power amplifier into normal operation. The other channel can be balanced in a similar manner by turning the "testing" switch in the opposite direction.

This dc power amplifier worked very satisfactorily although the combined characteristics of the amplifier and the oscillograph resulted in a slightly non-linear and non-symmetrical response. As a consequance when the ultimum in accuracy of relative deflection is desired it is necessary to replot the oscillograph records using calibration curves. This process is not entirely lost work since the wave forms of the oscillograms are distorted to the eye (particularly wave forms of large amplitude). This is because the recording pen moves in the arc of a circle rather than in a straight line.

The Brush, Model BL-913, dc amplifier is designed to perform the impedance matching operations described above. It has very satisfactory characteristics for use in recording the curves from the computer. It has attenuator steps providing for an input voltage range from 0.001 volt to 300 volts. In addition, its characteristics are such that the combination of the amplifier and recorder gives linear response to 100 cycles per second.

The combination of the two Brush instruments and the selective gain amplifier described in the next section is almost ideal.

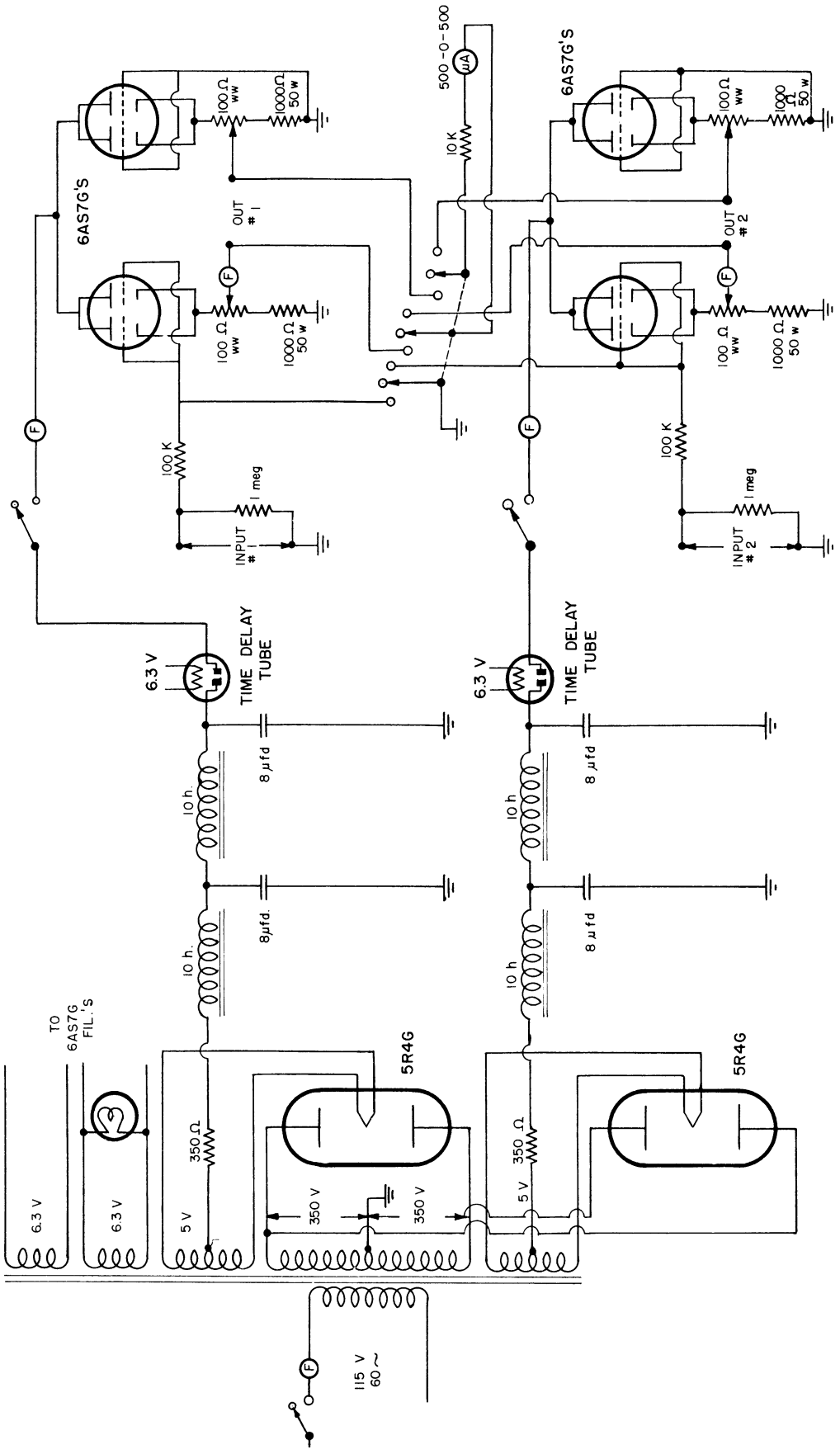

IMPEDANCE MATCHING CATHODE FOLLOWERS FOR BRUSH OSCILLOGRAPH

Figure 2-7.

2.9 Selective Gain Amplifier

Figure 2-8 shows the circuit of a two channel dc amplifier with selective gain. The gain of each channel can be set by a selector switch so that the output voltages is 0.2, 0.5, 1, 2, 3, 5, 7, 10, 20, 40 or 100 times the input voltage. This amplifier is very useful in obtaining suitable amplitudes on the oscillograms, particularly so because the gain factor is definitely known.

Each channel of this amplifier consists of an operational amplifier used as a sign-changing multiplier. The various gains are obtained by introducing with a selector switch suitable input and feedback resistors. These resistors are selected so that their ratios are accurate to within 0.1%. The selective gain amplifiers with power supplies are housed in a single cabinet. Figure 2-9 shows the circuit of the power supply.

2.10 Low Frequency Oscillator

In some instances it is desirable to run frequency response curves of a system to determine the absolute value of the gain and the phase shift. In obtaining information to plot a Nyquist diagram (Chapter 12) for determining the stability of a feedback amplifier this operation is necessary.

For this purpose there was constructed a low frequency oscillator the circuit of which is shown in Figure 2-10. From this oscillator may be obtained frequencies from 0.028 to 5.5 cycles per second in 5 continuously variable steps. The amplitude of oscillation, as well as the wave form of the output voltage, is very dependent upon the amount of feedback. Two feedback controls, for coarse and fine adjustments, respectively, make it possible to obtain the desired amplitude of oscillation. A 500-0-500 microammeter connected in series with a resistance across the output indicates the amplitude of oscillation. Amplitudes of about one-half full scale deflection indicate satisfactory output.

2.11 Frequency Recorder

In the solutions of many problems it is desirable to determine the length of a record (in seconds) as accurately as possible. Since a synchronous motor drives the paper of the oscillograph the speed of the paper depends upon the power frequency. A Leeds & Northrup frequency recorder was used to determine the value of the frequency at the time a record was taken. Since in many cases results involving time measurements could be checked to ± 0.1%, frequency corrections were necessary, the deviations of the local power supply frequency being at times as high as two-thirds of a per cent.

2.12 Equipment for Simulating Variable Coefficients

The equipment for simulating continuous functions by using a resistance that changes in discrete steps consists of the following: (1) a synchronous contactor; (2) units consisting of a stepping relay, a panel for lug-in resistors, and a patch-cord connecting assembly; and (3) a relay control panel.

2.13 Synchronous Contactor

Cam-operated microswitches (Type BS-2RL2), in series with 24 volts dc, give 1, 2, 4 or 8 regularly spaced pulses per second. These cams are about 1 1/8 inches in diameter and have flats machined on the circumference, each flat corresponding to a chord subtending an angle of 45° at the center. Any two of these cams can be mounted on one end of 1/4" shaft driven by a synchronous motor

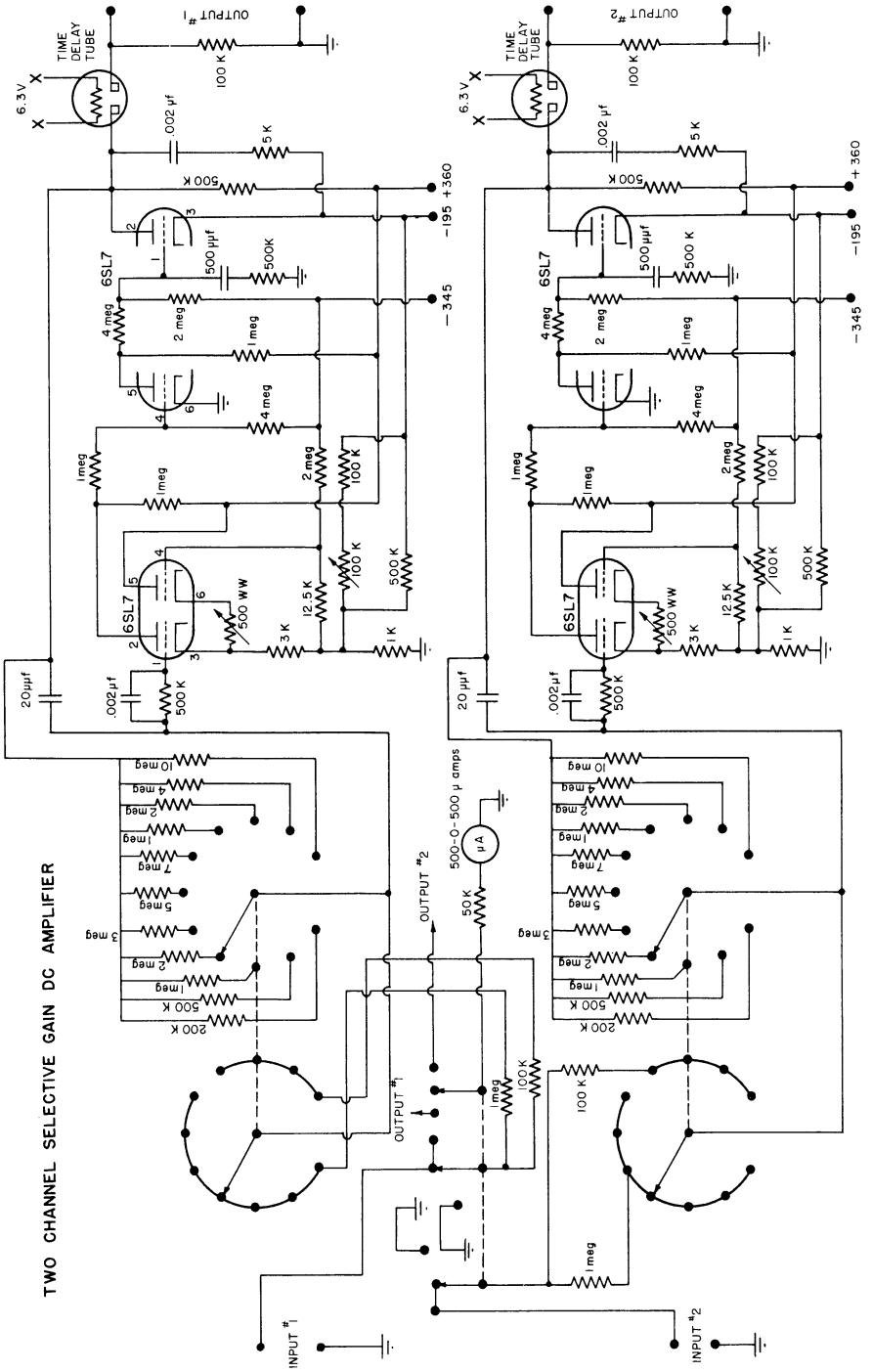

Figure 2-8.

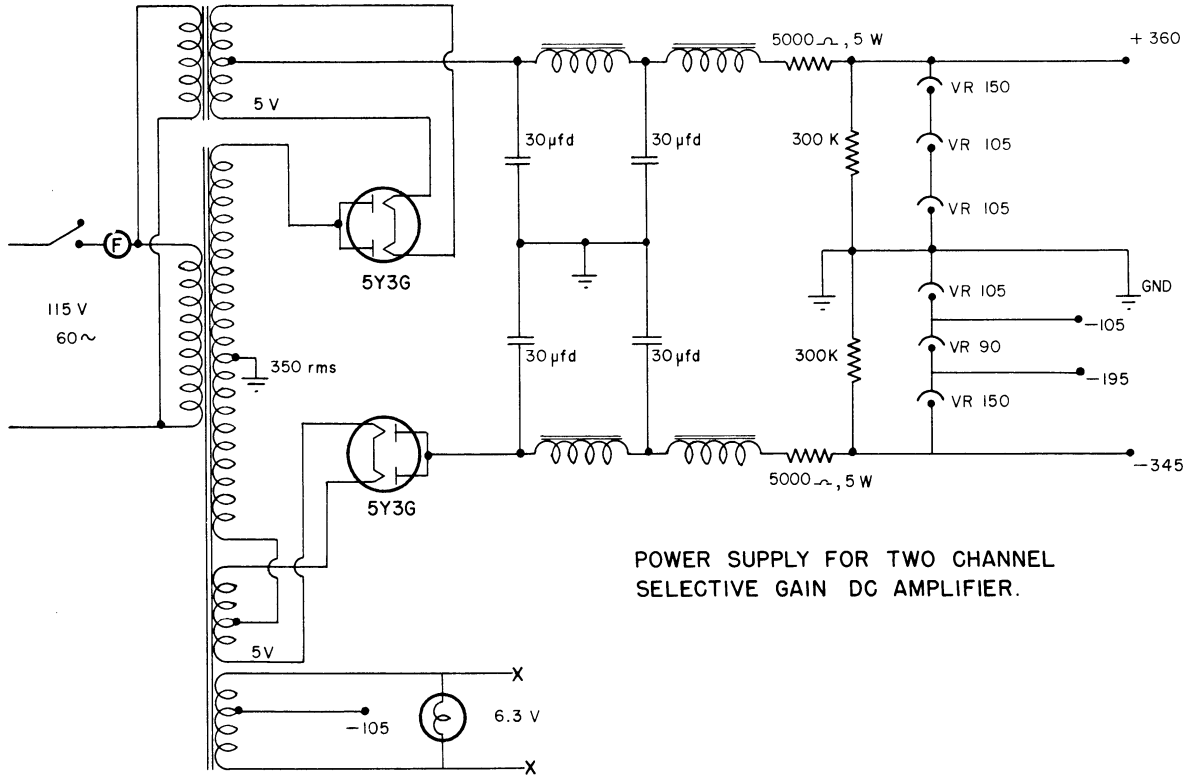

Figure 2-9.

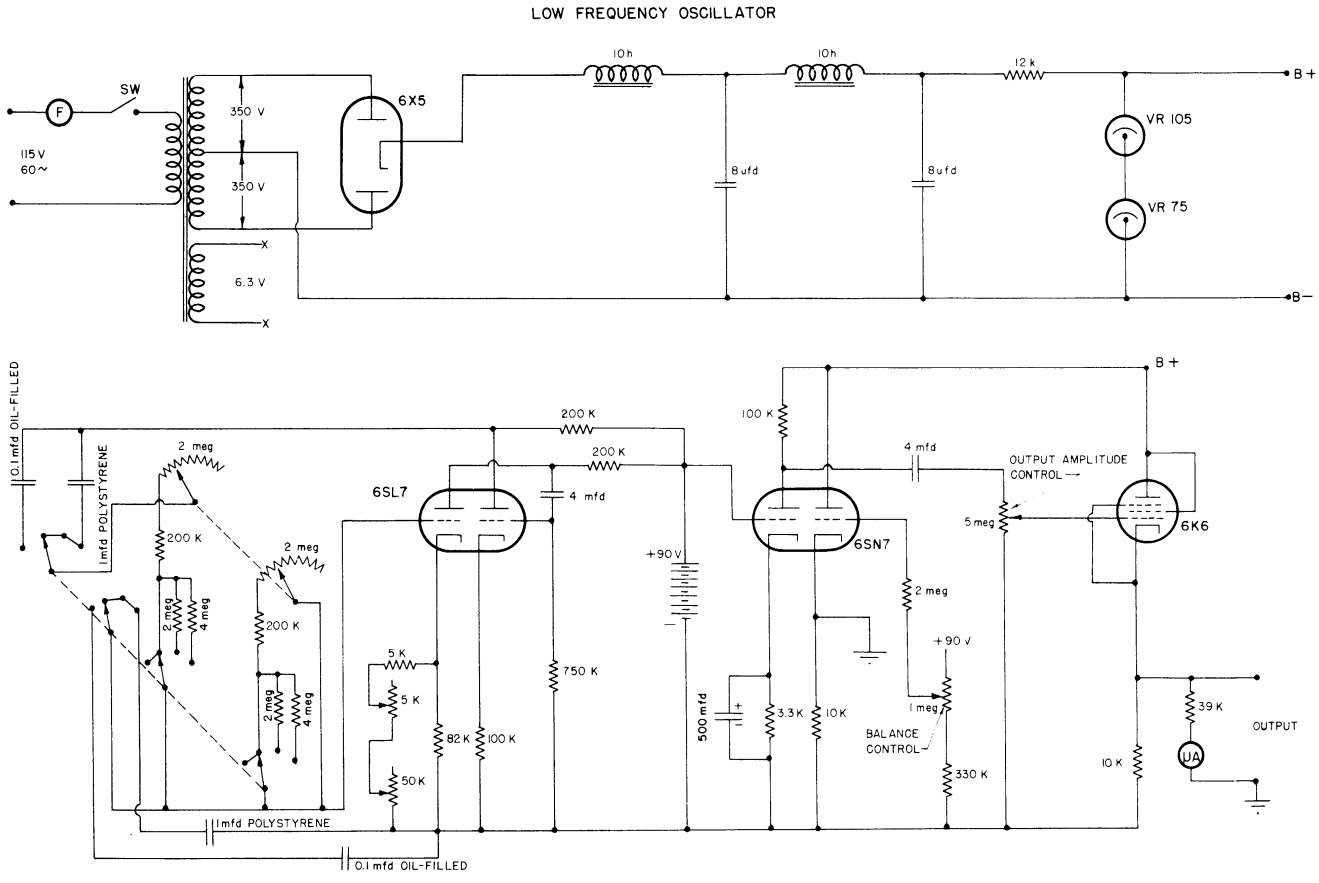

Figure 2-10.

at a speed of one revolution per second. The pulses are used to drive the stepping relays for obtaining resistances which vary in steps. Figure 2-11 shows the basic synchronous contactor assembly. By a remote control switch S_R there can be selected either one of the two pulse rates given by the two cams on the shaft. In practice the one-person cam is always kept in place. A pulse from its microswitch is sent directly to the relay control panel (to be described later) for the purpose of always starting problems on the same "flat" of the other cam used.

2.14 Stepping Relays and Plug-in Resistor Panel

The stepping relays have three levels of 40 contacts.* One level has a non-bridging wiper; the other two levels have bridging wipers. The level of contacts with the non-bridging wiper was used to automatically stop the solution of a problem and to take care of the imposing of and removal of initial conditions. One of the two levels of contacts with bridging wipers was used to connect the wiper to consecutive points on a bank of series connected resistors.

Figure 2-12 is a photograph of a chassis on which are mounted a stepping relay and jacks for making connections to plug-in resistors. Figure 2-13 shows the stepping relay and plug-in resistor circuit.

The forty numbered jacks (Figure 2-13) are permanently connected to corresponding stepping relay contacts. There are also 40 pairs of jacks for receiving General Radio double plugs on which are mounted resistors (Continental X-type). Patch cords with a banana plug on each end are used for connecting the 40 relay contacts to any desired points on the series-connected plug-in resistor assembly.

There are indicated two jacks with leads going to an operational amplifier. If the jack labeled T is connected to one end of the series-connected assembly of resistors, there will appear across these two jacks a resistance which varies in accordance with the position of the stepping relay wiper. For example in Section 6.4 of Chapter 6 there is described in detail the method by means of which a function directly proportional to x^2 can be simulated. In the last column of Figure 6-3 are given suitable values for the plug-in resistors, i.e., the resistance to be added for that step. The first resistor is 5,000 ohms; the second, 30,000 ohms; the third, 60,000 ohms; etc., each resistance being 30,000 ohms more than the preceding one. Contact 1 of the stepping relay should be connected to the point between the 5K and 30K resistors; contact 2, to the point between 30K and 60K; contact 3, to the point between 60K and 90K; etc. As a result there will appear between the two terminals leading to the operational amplifier a resistance of 5K for step 1, 35K for step 2, 95K for step 3, etc.

In this example the total resistance between these two terminals should be 23.4 megohms for step 40. In order to obtain as high a resistance to ground as possible the jacks on the plug-in resistor panel were all mounted on lucite, as may be seen in the photograph of Figure 2-12.

The two stepping relay assemblies used in our experimental work performed satisfactorily except in one respect. They did not at all times fulfill the requirement of having the bridging wipers actually "bridge" in going from one contact to the next. Careful cleaning of contacts seemed to help.

* C. P. Clare Co. Type SD-59 with two bridging wipers and one non-bridging wiper was used.

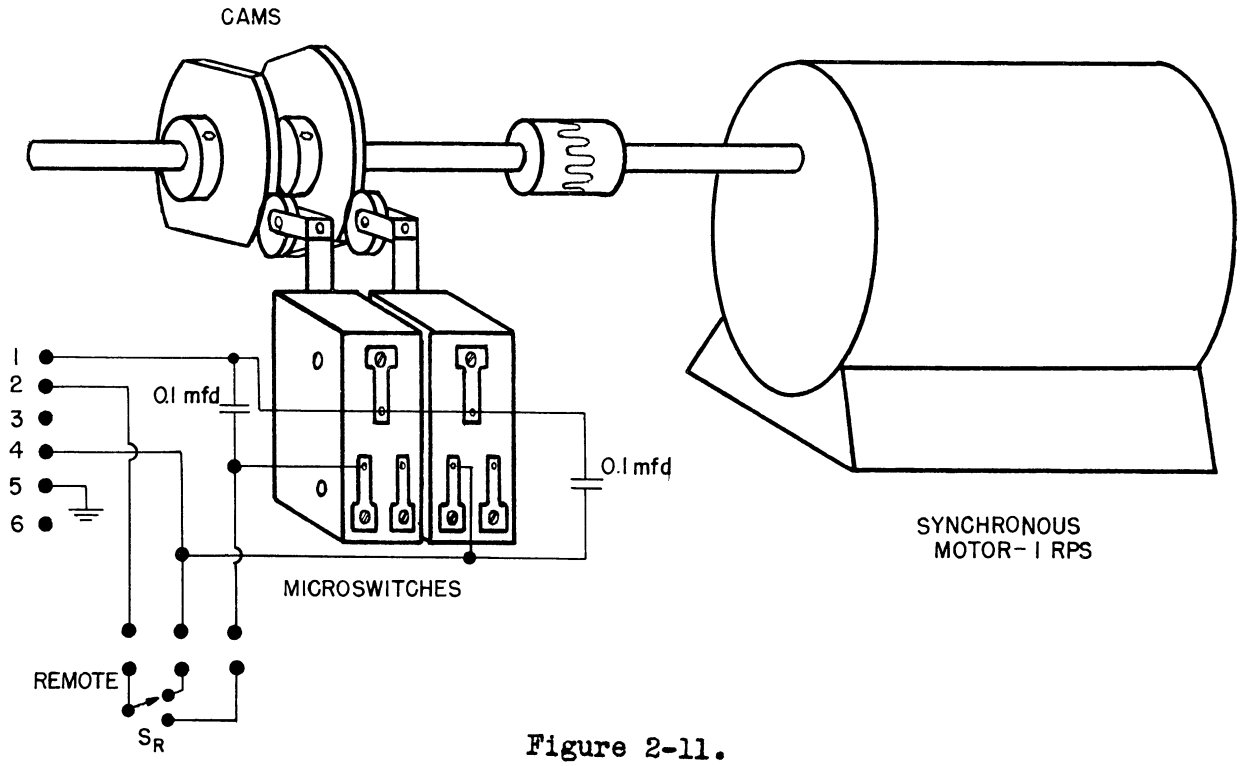

Figure 2-11.

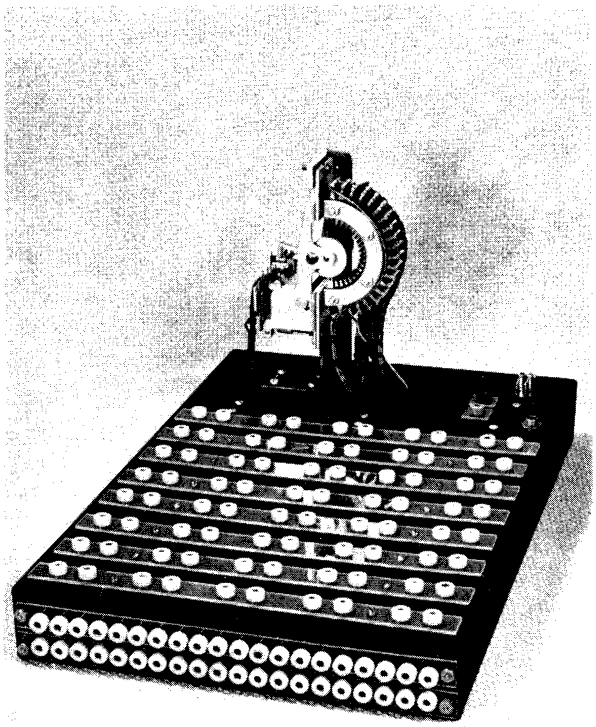

Figure 2-12.

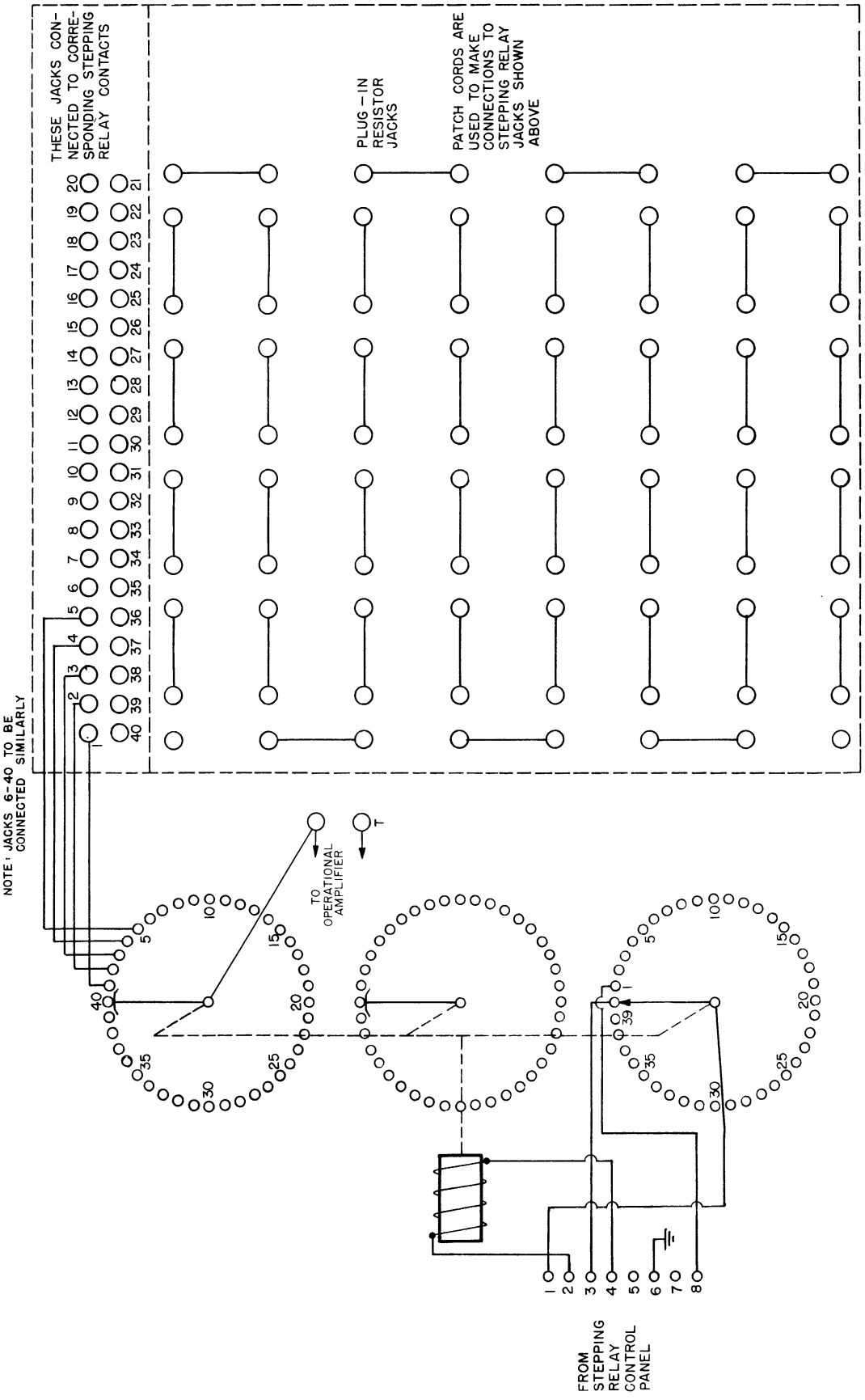
THESE JACKS CONNECTED TO CORRESPONDING STEPPING RELAY CONTACTS
PLUG-IN RESISTOR JACKS
PATCH CORDS ARE USED TO MAKE CONNECTIONS TO STEPPING RELAY JACKS SHOWN ABOVE
NOTE: JACKS 6-40 TO BE CONNECTED SIMILARLY
TO OPERATIONAL AMPLIFIER
FROM STEPPING RELAY CONTROL PANEL
STEPPING RELAY AND PLUG-IN RESISTOR CIRCUIT

Figure 2-13.

2.15 Stepping Relay Control Panel

Figure 2-14 shows the stepping relay control circuit. Provision is made for controlling three stepping relays.

Relay F is the master pulsing relay, its pulsing rate depending upon the two cams on the synchronous contactor and on the position of the remote switch S_R (Figure 2-11).

Relay G, through normally closed contacts, passes pulses from relay F to the coil of stepping relay A. When stepping relay A reaches position 40, relay G is energized and no longer passes pulses. Stepping relay A then stops. Relays H and J performs the same functions for stepping relays B and C.

These three relays G, H and J also play an important part in imposing the initial conditions. When all three of these relays are energized (i.e., when all three stepping relays are on contact 40) power is furnished to the coil of relay L, which is then closed. This removes power from the "locking" contacts on relay M.

Relays L, M, and N perform the functions of automatically imposing and removing the initial conditions. The initial conditions are imposed as soon as all three stepping relays reach contact 40 and are removed as soon as any one of the relays reach point 1.

When relay N is closed, the initial-condition relays are energized, thereby removing the initial conditions. Relay N is controlled by normally open contacts on relay M. If relay M is momentarily energized it remains closed by virtue of its "electrically locking" contacts. These contacts obtain power from normally closed contacts on relay L. (As long as relay M is closed, relay N is closed and all initial conditions are removed.) If relay L is energized (all stepping relays on contact 40) relay M "drops out" and the initial conditions are restored. The initial conditions are not removed until relay M is again energized which is done as soon as any one of the stepping relays reaches contact 1.

The stepping relays always stop on contact 40. When they are in this position relays G, H and J are energized and no longer furnish driving pulses to their respective stepping relays. Relay L is energized, removing power from the "locking" contacts of relay M. Relays M and N are inoperative, no power is furnished to the initial-condition relays and the initial conditions are imposed.

Relay O is the starting relay, controlled by the remote-control momentary-contact starting button S_S. When this switch S_S is closed momentarily, relay O is energized as soon as the next pulse is furnished by the microswitch on the one-per-second cam. Relay O will then remain closed until relay M closes. As soon as relay O closes, connections are made for passing the next pulse from relay F to each of the stepping relays. Actuated by this pulse each stepping relay goes from position 40 to position 1. As soon as contact 40 is left, relays F, G and H open and pulses are continued to be supplied to the stepping relays. Simultaneously relay L drops out, energizing the "locking" contacts of relay M. At the instant any one of the stepping relays reaches contact 1, relay M closes and remains closed. This immediately removes the initial conditions and de-energizes the starting relay O.

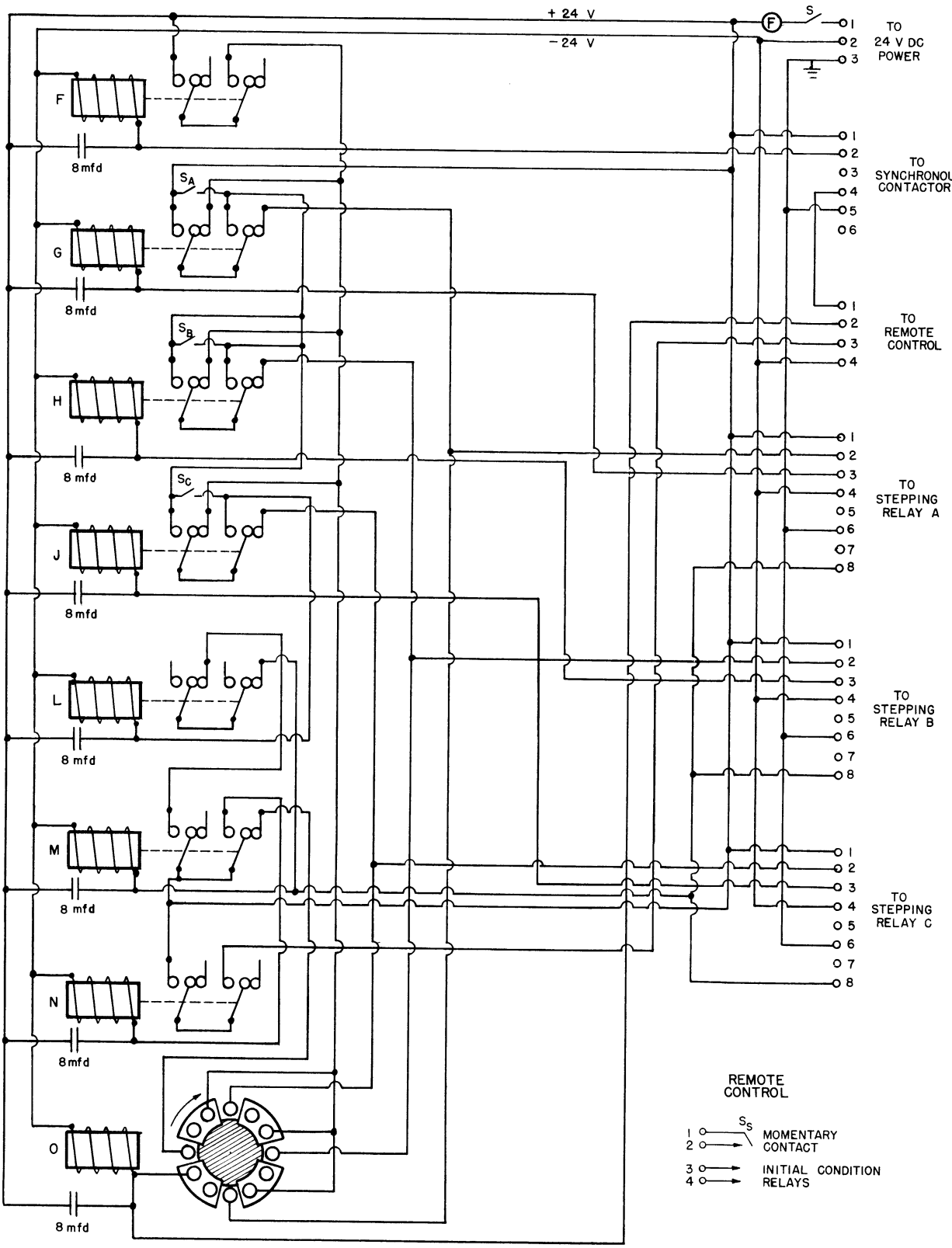

STEPPING RELAY CONTROL CIRCUIT

Figure 2-14.

In case any one or more of the three stepping relays are not used, the corresponding switches S_A, S_B or S_C should be closed. This will then permit normal operation of relay L.

Figure 2-15 shows a complete laboratory set up for solving a fourth order differential equation with variable coefficients. The lettered components can be identified as follows:

A. Low frequency oscillator (not in use).

B. Stepping relay control panel.

C. Synchronous contactor.

D. Stepping relay and plug-in resistor assembly, 1.

E. Stepping relay and plug-in resistor assembly, 2.

F. Power supply, -190 volts.

G. Power supply, -350 volts.

H. Power supply, +350 volts.

I. Power supply distribution box.

J. Two channel selective gain amplifier with power supplies.

K. Impedance matching two-channel dc power amplifier.

L. Two channel oscillograph.

M. Initial condition battery.

N. Potentiometer assembly for fine control of initial condition, (See Figure 5-7).

O. Initial condition battery (used with N).

P. Amplifier in which variable resistance from D is used.

Q. Integrating amplifier.

R. Integrating amplifier.

S. Amplifier in which variable resistance from E is used.

T. Integrating amplifier.

U. Integrating amplifier.

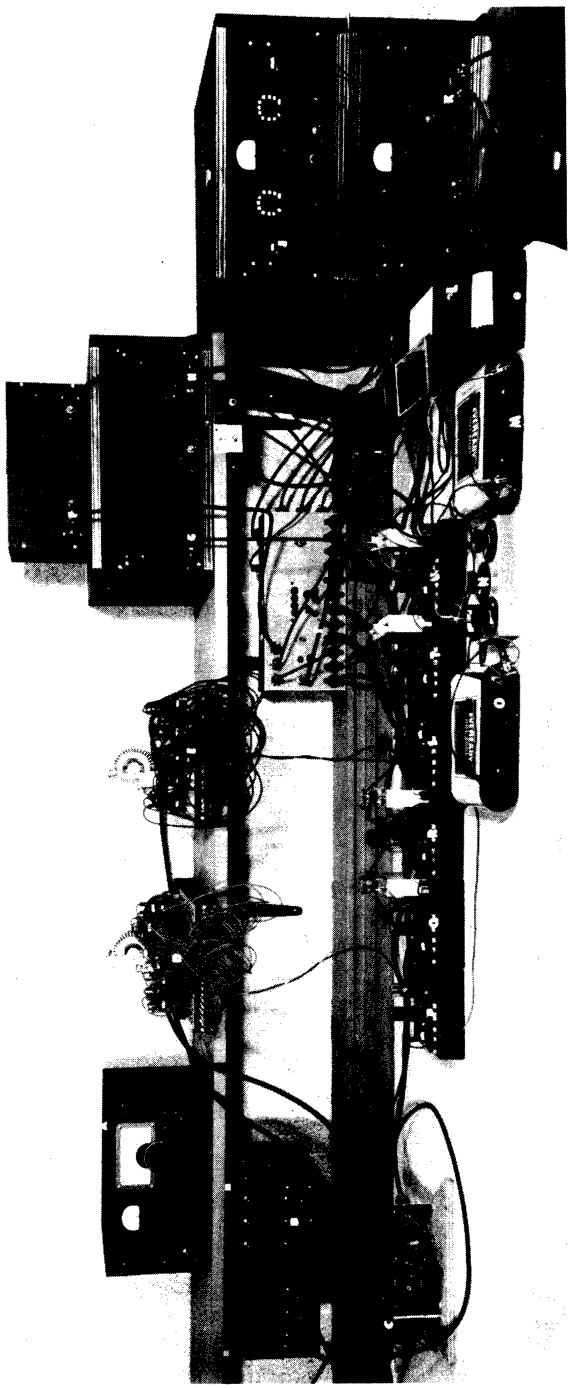

Figure 2-15.

CHAPTER 3

DIFFERENTIAL EQUATIONS WITH ONE INDEPENDENT VARIABLE

In paragraph 1.8 of Chapter 1 is given the solution of equation (1-19) which is a second order differential equation with constant coefficients and one independent variable. The solution obtained for this equation gives the motion of the system uninfluenced by outside "forces" except those of a static nature necessary to set up the initial conditions at the time t = 0. In this chapter there will be shown several examples of the response of a similar system when operated on by outside "forces", or driving functions.

3.1 Response of a System to a Driving Function

In the equation

$$m\ddot{y} + c\dot{y} + ky = F(t), \tag{3-1}$$

F(t) represents the driving function.

Figure 3-1 shows the circuit and a photograph of the computer for determining the response of the system described by the left-hand side of equation (3-1) to an arbitrary driving function F(t). The operation of the computer can be more readily understood if equation (3-1) is rewritten as

$$m\ddot{y} + c\dot{y} + ky - F(t) = 0. \tag{3-2}$$

The outputs of amplifiers A_4, A_3 and A_2 are, respectively, y, $-\dot{y}$, and $\ddot{y}$. Into amplifier A_1 are fed the driving function F(t) through a one megohm resistor and $-\dot{y}$ through a resistor of 1/c megohms. Into amplifier A_2 are fed: (1), the output of amplifier A_1, $c\dot{y} - F(t)$, through a one megohm resistor; (2), y, through a resistance of 1/k megohms; and (3), $\ddot{y}$, through a resistance of 1/m megohms. Amplifier A_2 adds these quantities giving the equivalent of equation (3-2). The response, y, of the system can be observed for any driving function F(t).

3.2 Transient Response to a Step Input Function

A step input function is one which has the value zero for time $t < 0$, and a constant value for time $t > 0$, i.e.,

$$\text{Step function} \rightarrow \begin{cases} F(t) = 0, \text{ for } t < 0, \\ F(t) = A, \text{ for } t > 0, \end{cases} \tag{3-3}$$

where A is a constant.

Figures 3-2, 3-3, and 3-4 give the responses of the system described in the equation

$$0.25\ddot{y} + c\dot{y} + y = F(t), \tag{3-4}$$

where F(t) is the step function described above, A being equal to 1.5(volts), for three different values of c; 0.25, 1.00 and 4.00 respectively. The quantities m and k of equation (3-2) have the values of 0.25 and 1.00, respectively.

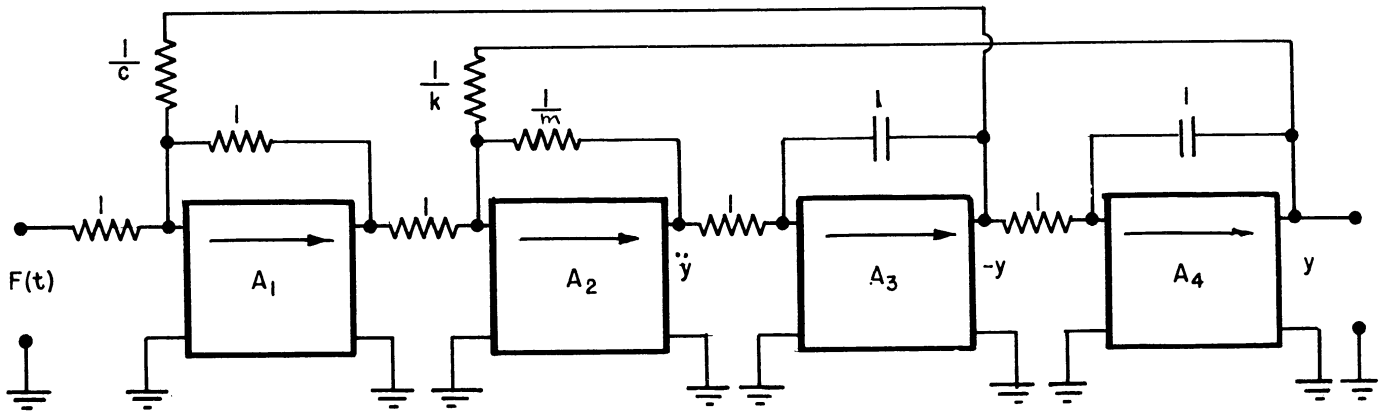

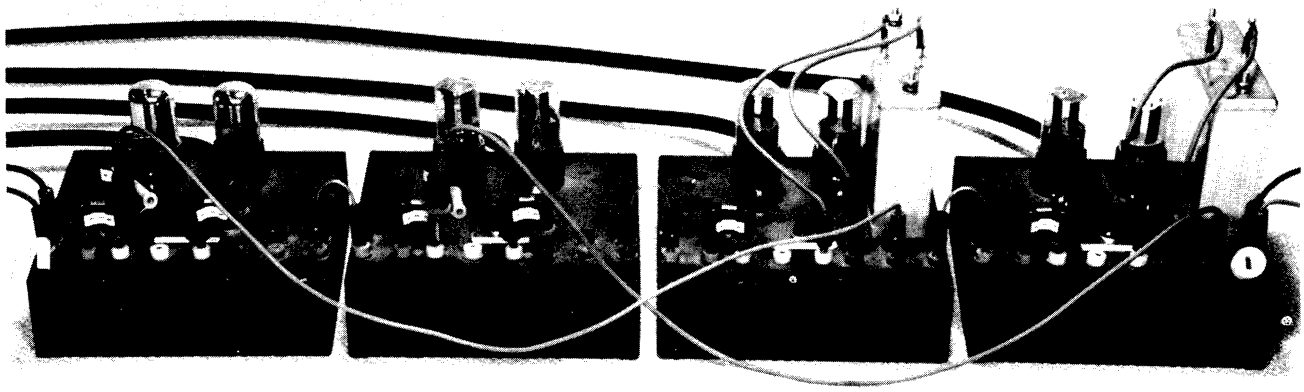

Figure 3-1.

In Figure 3-2 is shown the transient response of the system to a step input, the coefficient c (= 0.25) being such that oscillations take place about a median position corresponding to the steady state position of y. Oscillations will occur whenever c^2 is less than 4km.

The response of Figure 3-3 is obtained when c has the value corresponding to c^2 = 4 km. In this case critical damping occurs, i.e., the steady state position of y is reached in minimum time without oscillations.

Figure 3-4 shows the response when c^2 is greater than 4km. In this case the system is highly overdamped, y reaching its steady state position very slowly.

3.3 Steady State Response to Sinusoidal Input Function

If in Figure 3-1 a sinusoidal voltage, F(t), is applied to the input terminals there will appear at the output terminals a voltage, y, which, after transients have disappeared, will have a sinusoidal wave form of the same frequency as the input. In general the output voltage will differ from the input voltage in both magnitude and phase. Figure 3-5 shows the steady state response to a sinusoidal input function of the system described by equation (3-4) with the constant c equal to 0.25. From records such as these there can be determined by measurements the relative gain (magnitude and phase shift) of the system.

The steady state response of the system to sinusoidal input functions having angular frequencies ranging from 0.67 to 4.15 radians per second was determined experimentally. In Figure 3-6 are shown the absolute values of the ratio of the output to input plotted as a function of the angular frequency. The theoretical values appear as the solid line, the experimental values as the small circles.

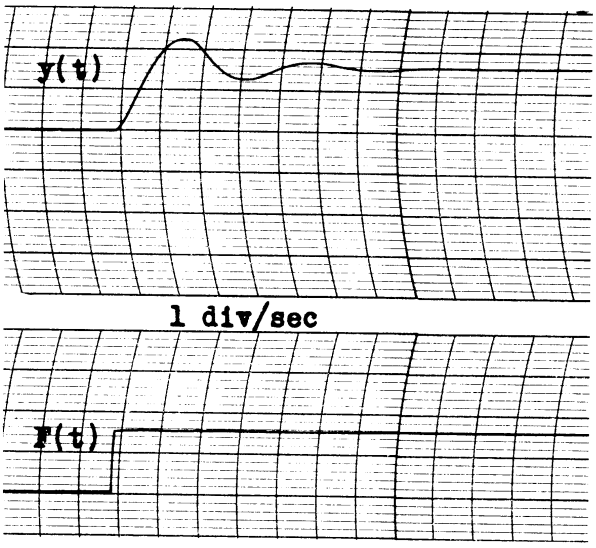

Figure 3-2
Response for less than critical damping.

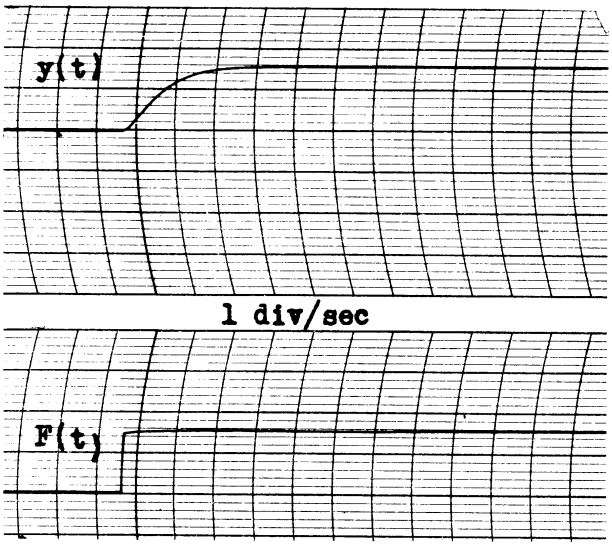

Figure 3-3
Response for critical damping.

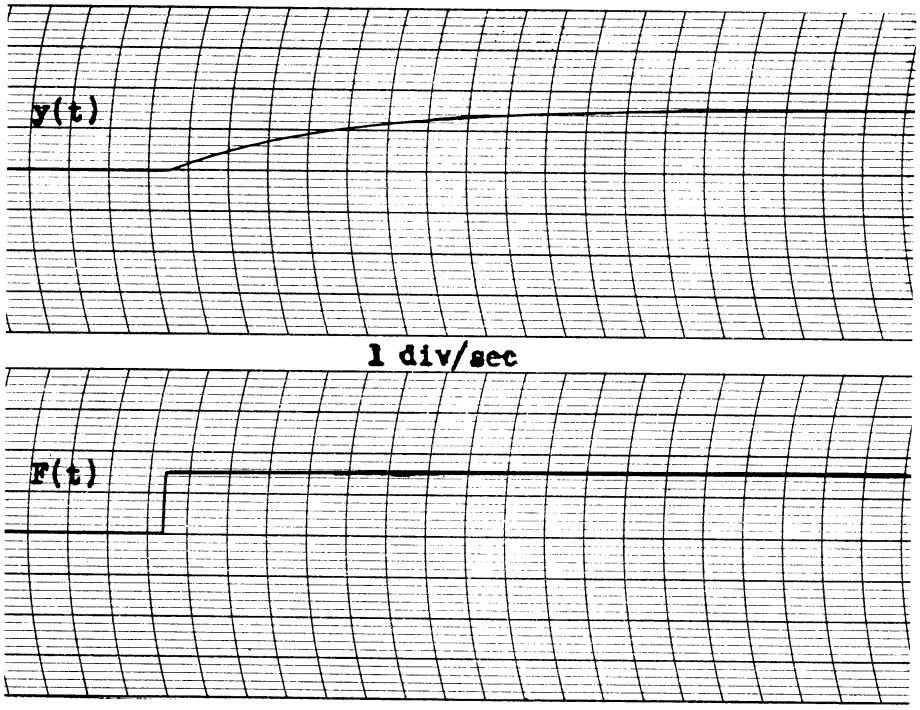

Figure 3-4
Response of an overdamped system.

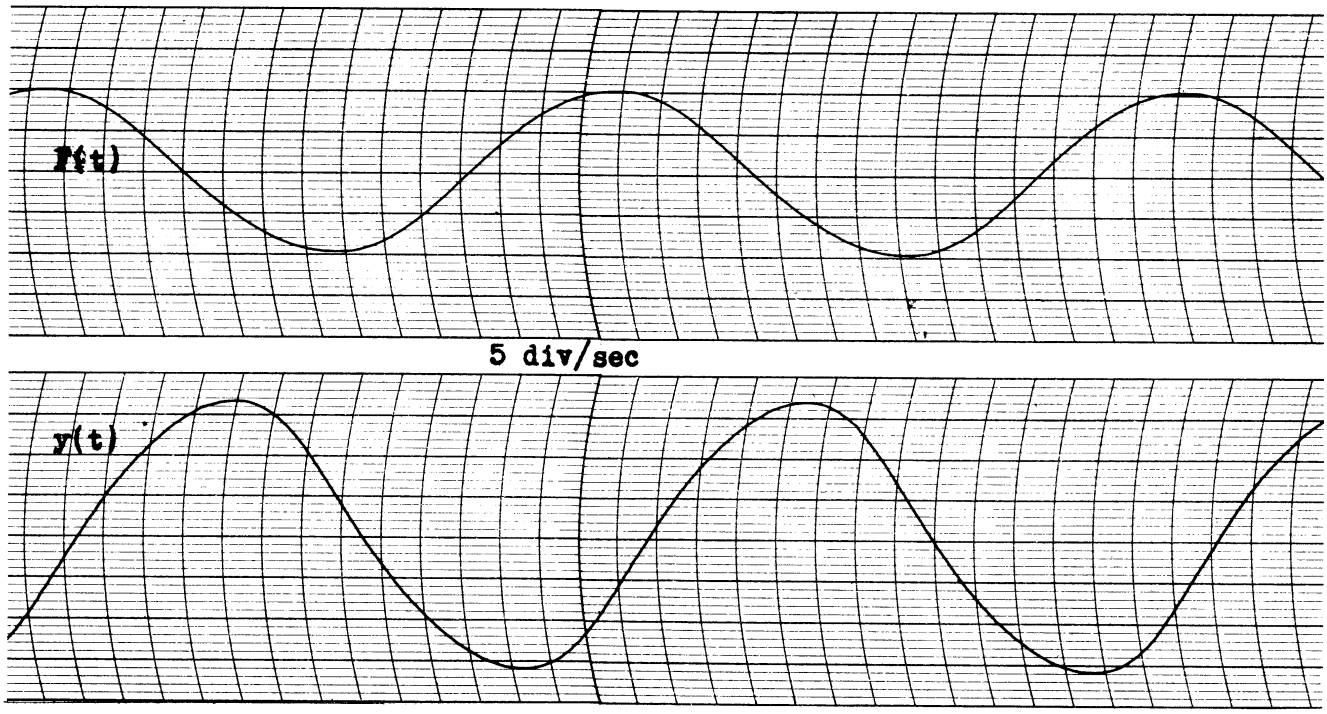

Figure 3-5
Steady state response of system to a sinusoidal driving function of frequency 2.19 radians per second.

Similarly, in Figure 3-7 are shown the theoretical and experimental values of the phase shift.

For a sinusoidal input function, $F(t) = A\,e^{j\omega t}$, equation (3-4), with $c = 0.25$, may be written,

$$0.25\ \ddot{y} + 0.25\ \dot{y} + y = A\,e^{j\omega t}. \qquad (3\text{-}5)$$

For the steady state response the frequency of the output will be the same as that of the input but the amplitude and phase will be different. We may assume then that

$$y = B\,e^{j\omega t}, \qquad (3\text{-}6)$$

where B is a complex number, the magnitude of which is the magnitude of the sinusoidal output and the phase angle of which is the relative phase between output and input.

Differentiating equation (3-6) once to obtain $\dot{y}$ and twice to obtain y, and substituting values of y, $\dot{y}$ and $\ddot{y}$ into equation (3-5) there is obtained after cancelling out $e^{j\omega t}$,

$$(-0.25\,\omega^2 + j0.25\omega + 1)B = A, \qquad (3\text{-}7)$$

or

$$\frac{B}{A} = \frac{1}{1-0.25\,\omega^2 + j\,0.25} = \left|\frac{\text{output}}{\text{input}}\right| \angle\,\text{phase angle} \qquad (3\text{-}8)$$

Values of ω may be substituted into equation (3-8) to obtain theoretical values of the relative magnitude and phase shift of the output. The theoretical values for the plotting of the solid curves of Figures 3-6 and 3-7 were obtained in this way.

3.4 Responses to Other Types of Input Functions

In a manner similar to that described above, responses to a system could be found for other types of input functions. For example, in paragraph 11.2 of Chapter 11 there is described the response of a system to a ramp input function, a ramp function being defined as a function the value of which is zero for $t < 0$ and proportional to the time t for $t > 0$. In paragraph 11.3 of the same chapter there is used as an input function one which, after the time $t = 0$, varies as the square of the time.

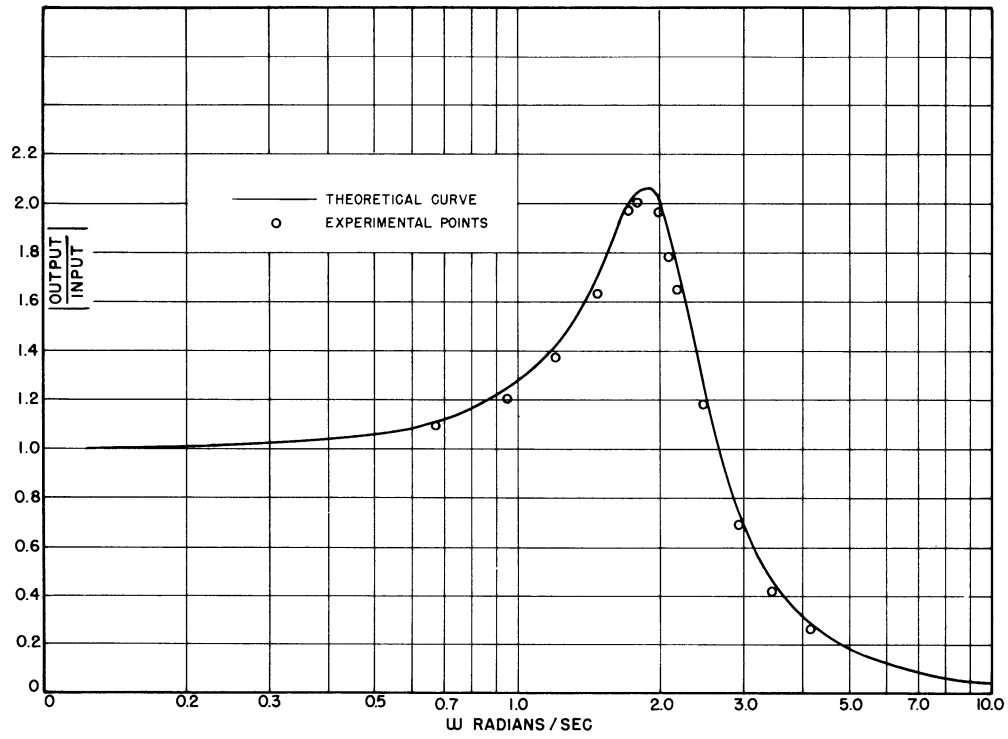

Figure 3-6
Absolute value of gain vs ω .

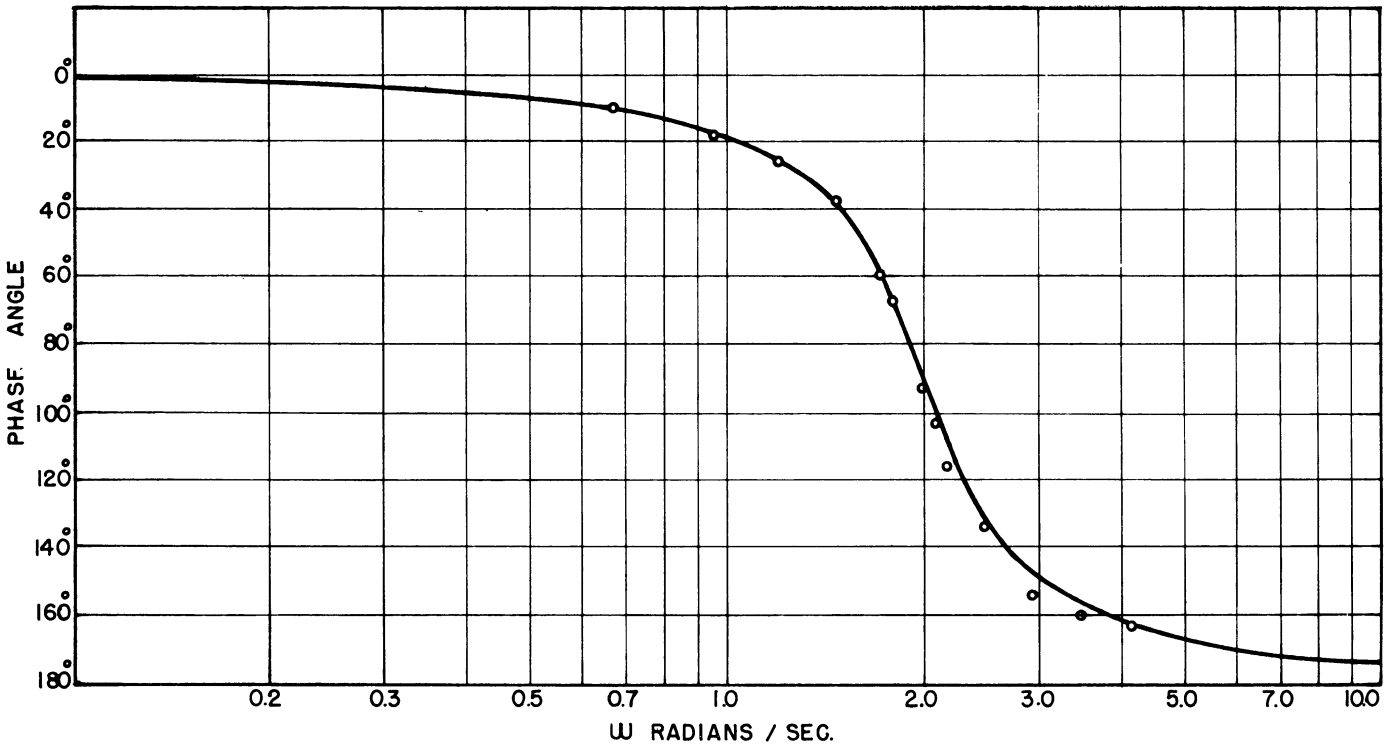

Figure 3-7
Phase angle of gain vs ω .

CHAPTER 4

SIMULTANEOUS DIFFERENTIAL EQUATIONS WITH CONSTANT COEFFICIENTS

To show how simultaneous differential equations with constant coefficients can be solved by the electronic analog computer, there have been chosen two examples: (1), the free vibrations of an undamped two-degree-of-freedom system with spring coupling; and, (2), a dynamic vibration absorber.

4.1 Free Vibrations of an Undamped Two-Degree-of-Freedom System with Spring Coupling [3]

In Figure 4-1 are shown two masses m_1 and m_2 supported by springs with force constants k_1 and k_2 and coupled together by a spring with a force constant k_3. If the masses are confined to vertical motions, the system has two degrees of freedom.

Considering the displacements of m_1 and m_2 to be y_1 and y_2, respectively, with the downward direction as positive, it is easily seen that the two equations of motion are

$$m_1\ddot{y}_1 + (k_1 + k_3)\, y_1 - k_3 y_2 = 0,$$

and

$$m_2\ddot{y}_2 + (k_2 + k_3)\, y_2 - k_3 y_1 = 0. \qquad (4\text{-}1)$$

The computer for the solution of these simultaneous differential equations is shown in Figure 4-2. The upper row of amplifiers in this figure represents the first of the two equations. A_3 and A_4 are integrating amplifiers and A_2 is a summing amplifier. A_1 is a combined multiplying and sign changing amplifier, obtaining its input voltage from the output y_2 of the lower row of amplifiers. A similar explanation could be given for the operation of the lower row of amplifiers representing the other equation. The switches and batteries are used for setting up the initial conditions of the problem.

In the solutions given below the following constants were used for the coefficients of equations (4-1),

$$m_1 = m_2 = 1,$$

$$k_1 = k_2 = 1,$$

Case I $k_3 = 1$

Case II $k_3 = 0.2$.

For all problems solved the initial velocities of both masses were zero, i.e.,

$$\dot{y}_1(0) = \dot{y}_2(0) = 0.$$

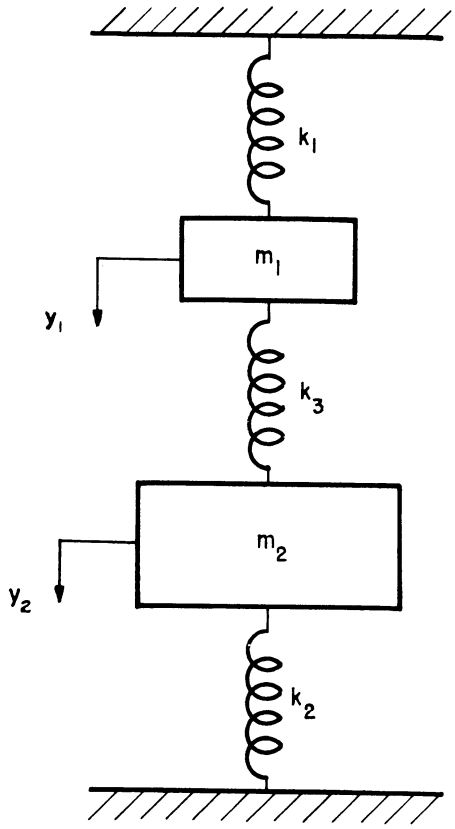

Figure 4-1.
Undamped two-degree-of-freedom system with spring coupling.

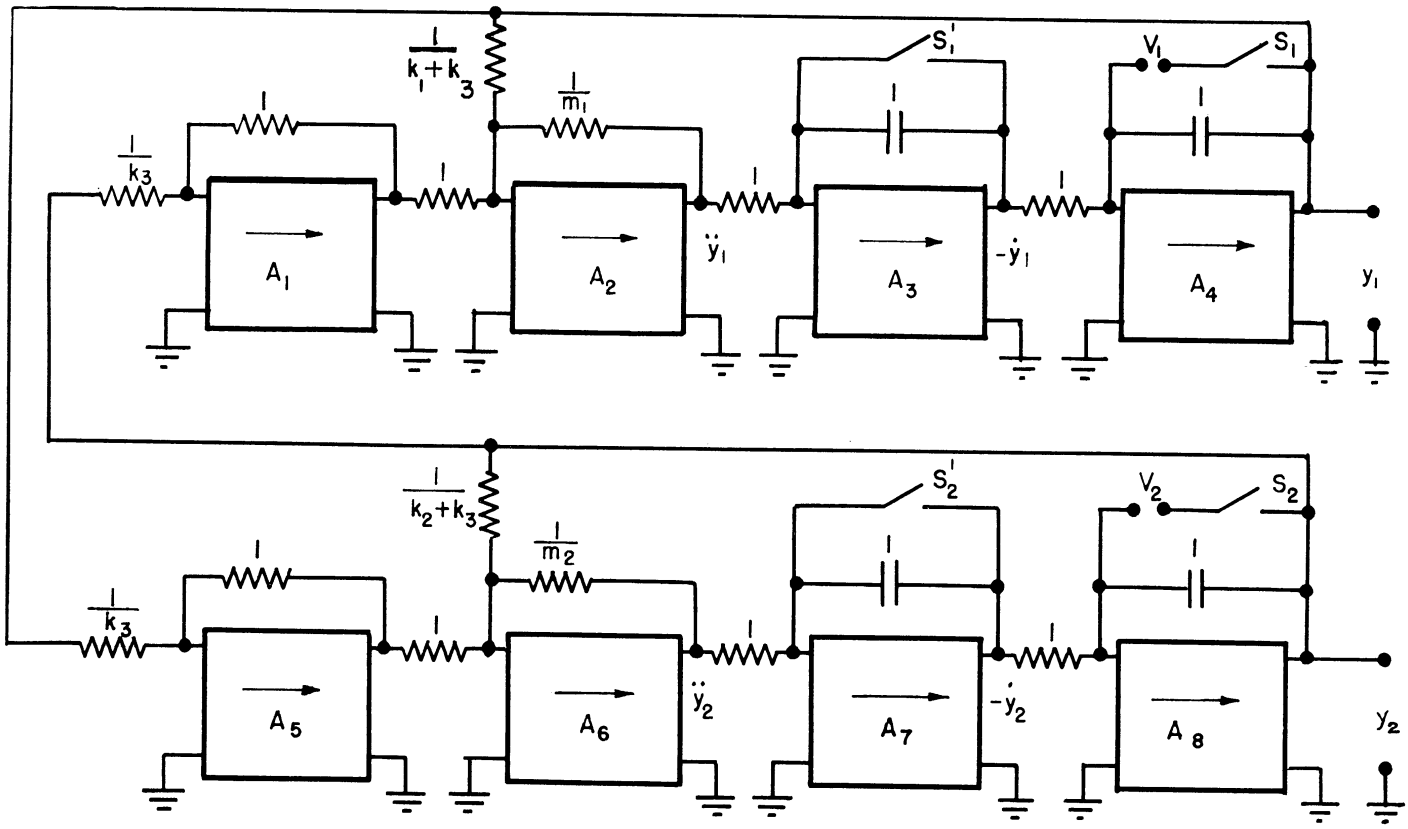

Figure 4-2.
Computer for solving the simultaneous differential equations of equation (4-1).

For both cases I and II three sets of initial displacements were used,

A. $y_1(0) = y_2(0) = V$,

B. $y_1(0) = V$, $y_2(0) = -V$,

C. $y_1(0) + V$, $y_2(0) = 0$, where V = 6 volts.

Case I. $k_3 = 1$

Figures 4-3, 4-4, and 4-5 are records of y_1 and y_2 for the coupling coefficient $k_3 = 1$. For Figure 4-3 the initial conditions were that both masses had zero velocity and equal displacements in the same direction. Both masses oscillate with the same frequency, amplitude and phase. The frequency as measured from the records was 1.001 radians per second, the theoretical frequency being 1.000 radians per second.

The mathematical procedure for computing the theoretical frequency is not given here but may be obtained, with other theoretical considerations, from den Hartog's[3] text.

For Figure 4-4 the masses were initially at rest with equal and opposite displacements. The masses oscillate with the same frequency and amplitude but 180° out of phase with each other. The experimental frequency was found to be 1.733 radians per second, the theoretical value being 1.732.

For Figure 4-5 both masses were initially at rest but m_2 had zero displacement. It is to be noted that energy is transferred back and forth between the two masses. The reality and significance of this fact can be more readily appreciated in the case of a smaller degree of coupling between the two masses, (Figure 4-8).

Case II. $k_3 = 0.2$

Figures 4-6, 4-7 and 4-8 are records of y_1 and y_2 for the coupling coefficient $k_3 = 0.2$, with the same initial conditions, respectively, as for the several examples under Case I. When the two masses were initially at rest with euqal displacements in the same direction (Figure 4-6) the experimental and theoretical frequencies were, respectively, 0.995 and 1.000 radians per second. When the two masses, initially at rest with equal and opposite displacements, oscillated as in Figure 4-7, the experimental and theoretical frequencies were respectively, 1.173 and 1.183 radians per second.

Figure 4-8 clearly shows the transfer of energy back and forth between the two masses. Den Hartog shows that the motion of each mass is the combination of two sinusoidal motions of frequencies corresponding to those of the two "resonance" frequencies (Figures 4-6 and 4-7). If the two "resonance" frequencies are close enough together the phenomenon of beats can be observed. This is clearly seen in Figure 4-8.

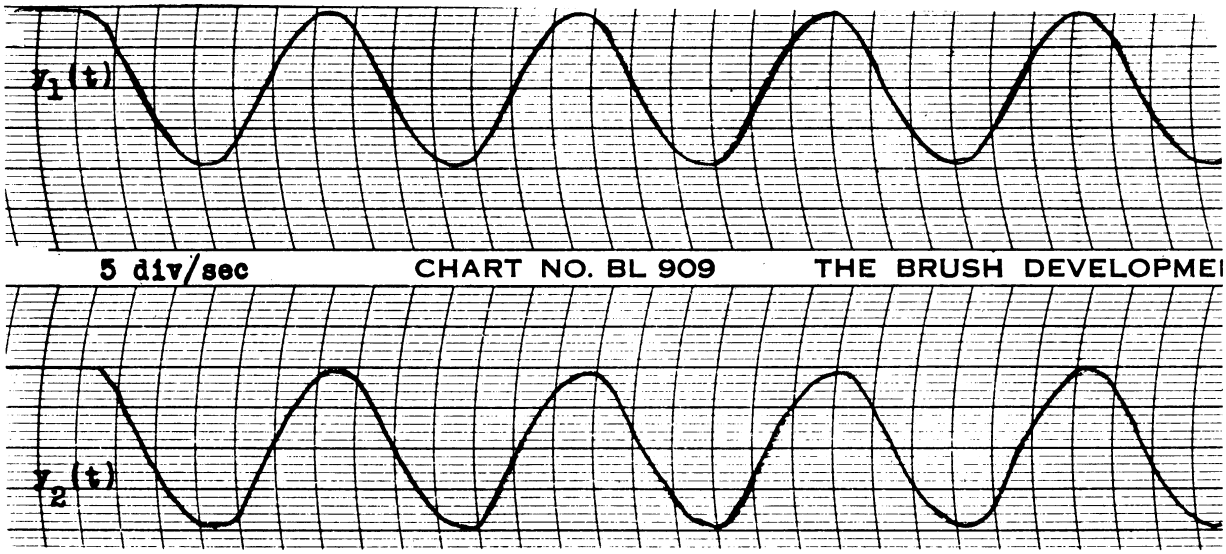

Figure 4-3.

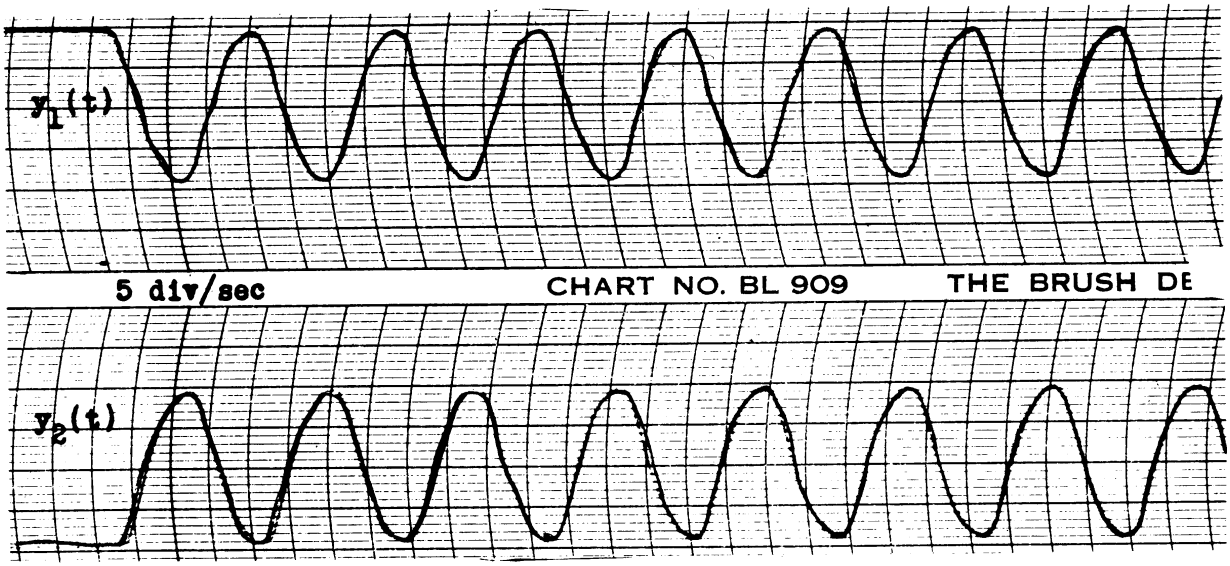

Figure 4-4.

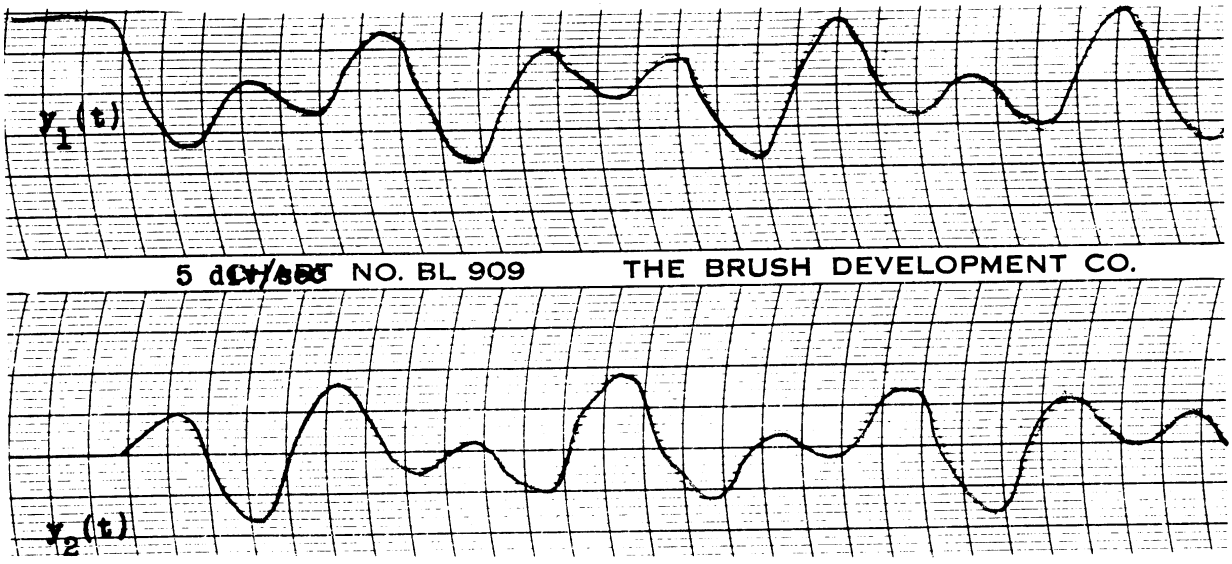

Figure 4-5.

Records of y_1 and y_2 for the coupling coefficient $k_3 = 1$.

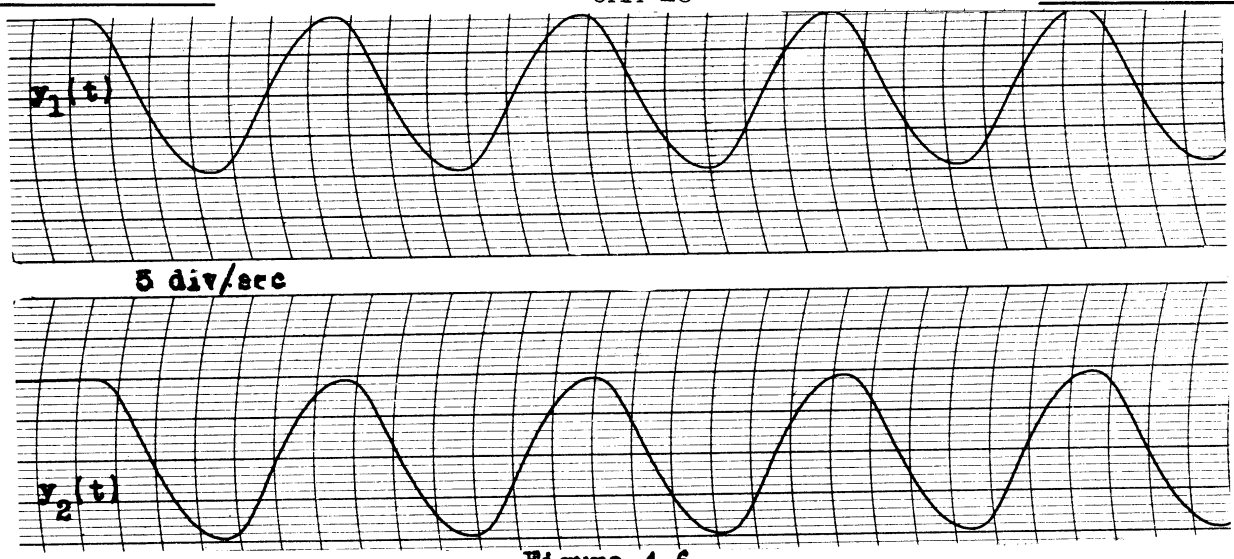

Figure 4-6.

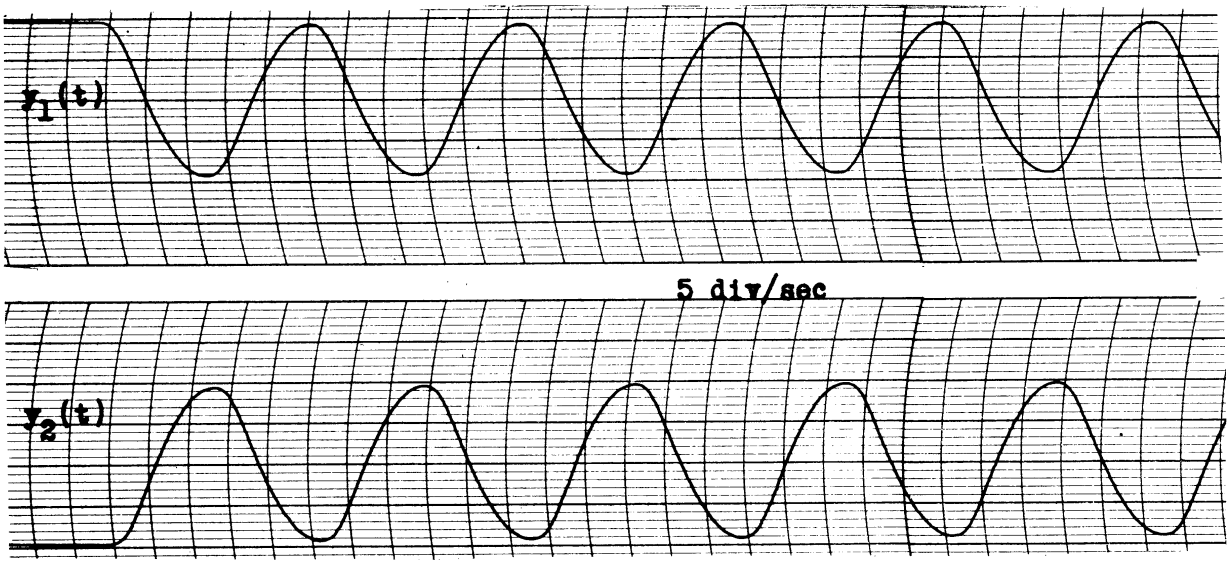

Figure 4-7

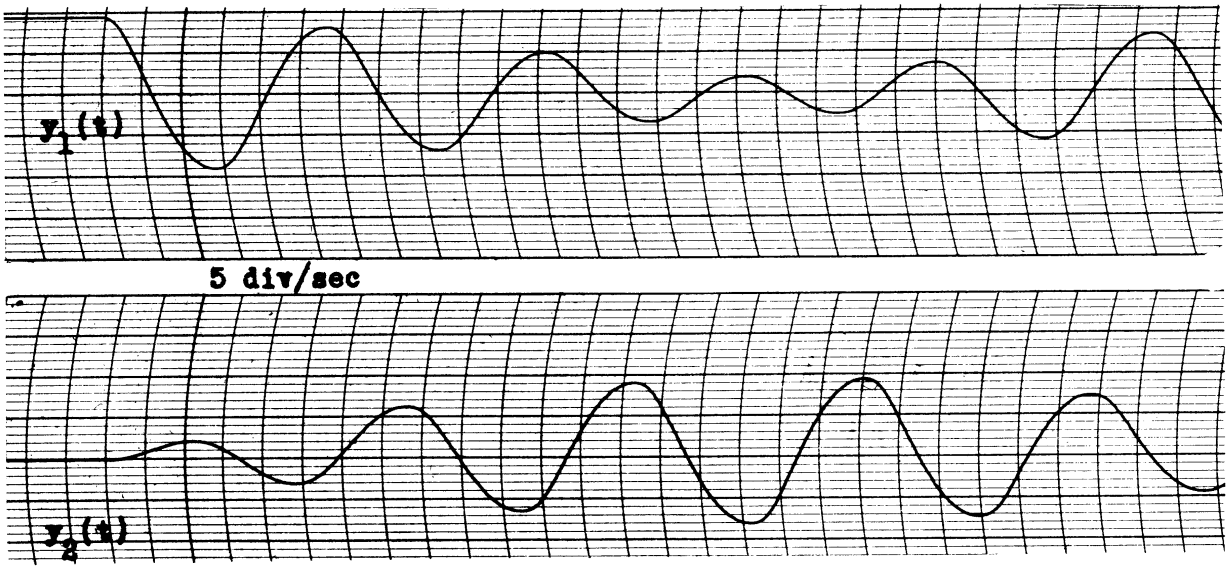

Figure 4-8.

Records of y_1 and y_2 for the coupling coefficient $k_3 = 0.2$.

4.2 Dynamic Vibration Absorber

Equation (3-1) of Chapter 3,

$$m\ddot{y} + c\dot{y} + ky = F(t), \qquad (4\text{-}2)$$

may be considered as representing a mass m attached to a spring with elastic constant k, having a damping force proportional to the velocity of the mass, and acted on by a driving function F(t). In paragraph 3.3 of Chapter 3 it is shown that for a sinusoidal driving function $F(t) = Ae^{j\omega t}$ the motion of the mass, after transients have disappeared, is a sinusoidal motion of constant amplitude and of a frequency equal to that of the driving function.

In Figure 4-9 this system is represented by the mass m_1, spring k_1 and damping device c, the system being subjected to the driving function $F(t) = A\,e^{j\omega t}$.

If there is attached to the mass m_1 a system consisting of another mass m_2 and spring k_2, the values of m_2 and k_2 being so chosen that the resonance $\sqrt{k_2/m_2}$ of this second system is equal to the frequency ω of the driving function, it can be shown[4] that the main mass m_1 does not vibrate at all, and that the auxiliary system (m_2, k_2) vibrates in such a way that the force exerted by it on the mass m_1 is at all times equal and opposite to the driving force $A\,e^{j\omega t}$.

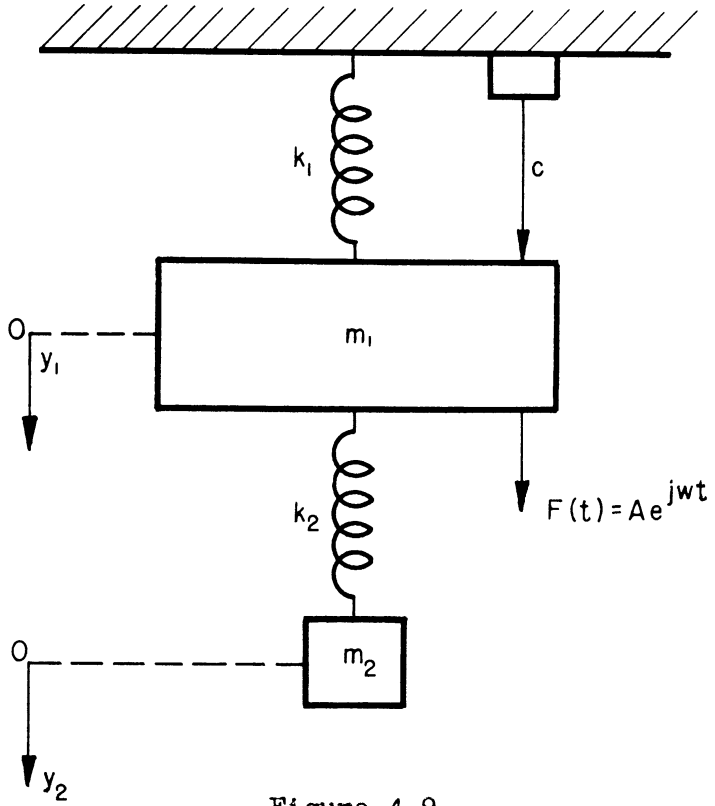

Figure 4-9.
Dynamic vibration absorber.

The differential equations for the complete system shown in Figure 4-9 are

$$m_1\ddot{y}_1 + c\dot{y}_1 + k_1y_1 + k_2(y_1 - y_2) = Ae^{j\omega t},$$

and

$$m_2\ddot{y}_2 + k_2(y_2 - y_1) = 0. \qquad (4\text{-}3)$$

For the purpose of setting up a computing circuit to solve these simultaneous equations they may be written,

$$m_1\ddot{y}_1 + c\dot{y}_1 + (k_1 + k_2)y_1 - k_2y_2 - Ae^{j\omega t} = 0,$$

and

$$m_2\ddot{y}_2 + k_2y_2 - k_2y_1 = 0. \qquad (4\text{-}4)$$

Figure 4-10 shows the arrangement of operational amplifiers for obtaining the solutions of the equations. The operation of the computer can be readily understood from the circuit. The only unusual feature is the assumption of an output $-y_2$ from amplifier A_7. This makes it possible to use one less operational amplifier.

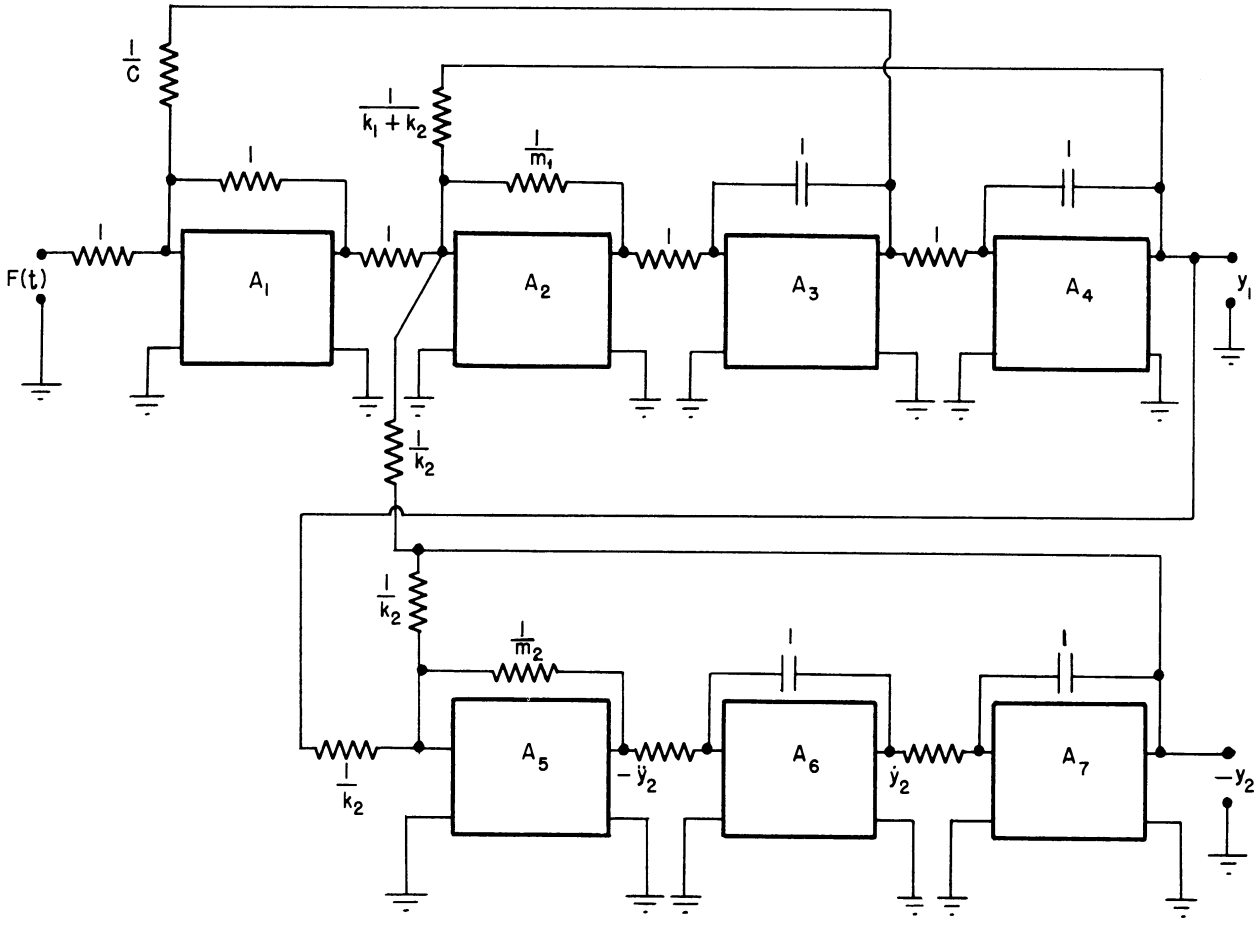

Figure 4-10
Analog computer for dynamic vibration absorber.

The analog computer of Figure 4-10 was set up for $m_1 = 1$, $m_2 = 0.5$ $k_1 = 1$, $k_2 = 2$ and $c = 0.5$. A variable low frequency oscillator was used to furnish the driving voltage $F(t)$ = real part of $Ae^{j\omega t} = A\cos\omega t$. The outputs y_1 and $-y_2$ were observed and the frequency of the input voltage varied until the observed amplitude of motion of m_1 was a minimum (after transients had disappeared).

Having determined the proper driving frequency, the input voltage $F(t)$ was removed and the system permitted to come to "rest", the energy being dissipated by the damping c. Then, with the initial conditions of zero velocity and zero displacement for each mass ($\dot{y}_1 = \dot{y}_2 = y_1 = y_2 = 0$, at time $t = 0$) the sinusoidal driving function was applied and records of y_1 and $F(t)$ taken as shown in Figure 4-11. After initial transients have disappeared, the vibration is negligible. The dashed line shows the steady state amplitude that y_1 would have if m_2 and k_2 were absent. How small this vibration is may be clearly seen in Figure 4-12, where the motion of y_1 is amplified by a factor of 50 as compared with $F(t)$. The reduction of the vibration due to m_2 and k_2 is better than a factor of 60.

In Figure 4-13 there are recorded $-y_2$, the motion of m_2 and the driving voltage $F(t)$. The effect of the driving "force" $F(t)$ on the mass m_1 is seen to be absorbed by the vibrations of m_2 which are seen to be 180° out of phase.

Of some interest is Figure 4-14 which shows the transient and steady state response of the system of Figure 4-9 to a step input function, i.e., a suddenly applied steady force.

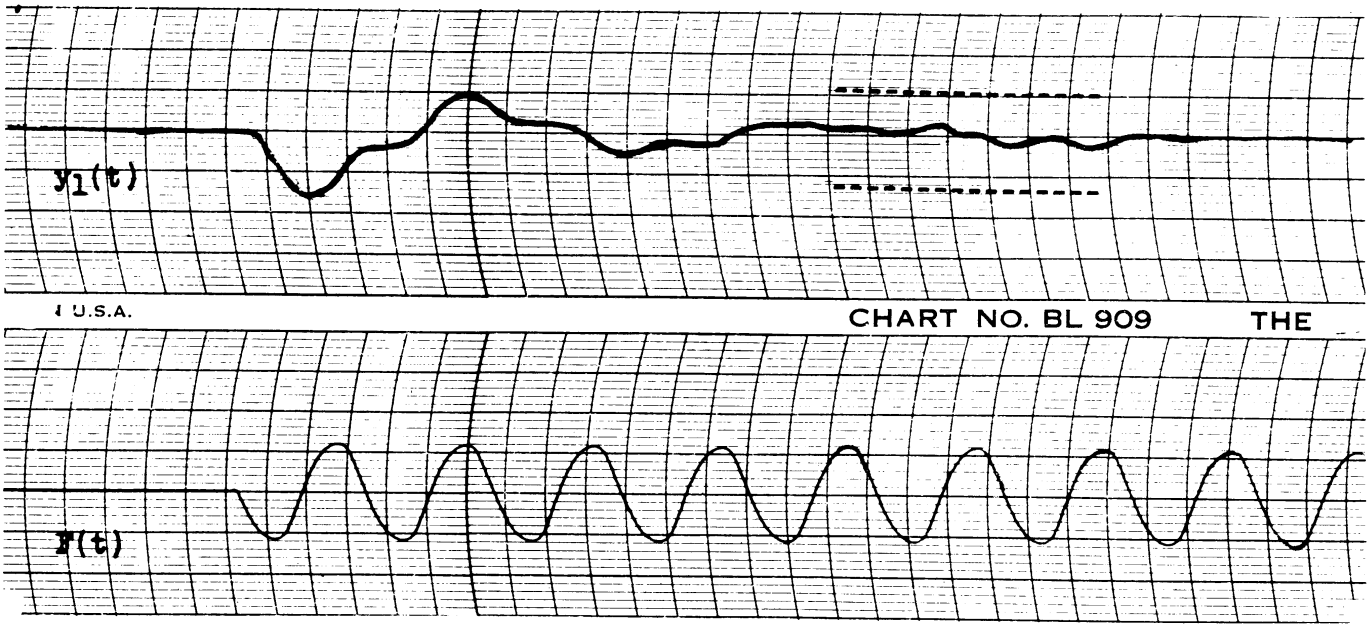

Figure 4-11.
Response y_1 and driving voltage $F(t)$ for a dynamic vibration absorber, y_1 amplified three times more than $F(t)$.

Figure 4-12.
Response y_1 amplified 50 times more than F(t).

Figure 4-13.
Response y_2 and driving voltage F(t) (with equal gains) for a dynamic vibration absorber.

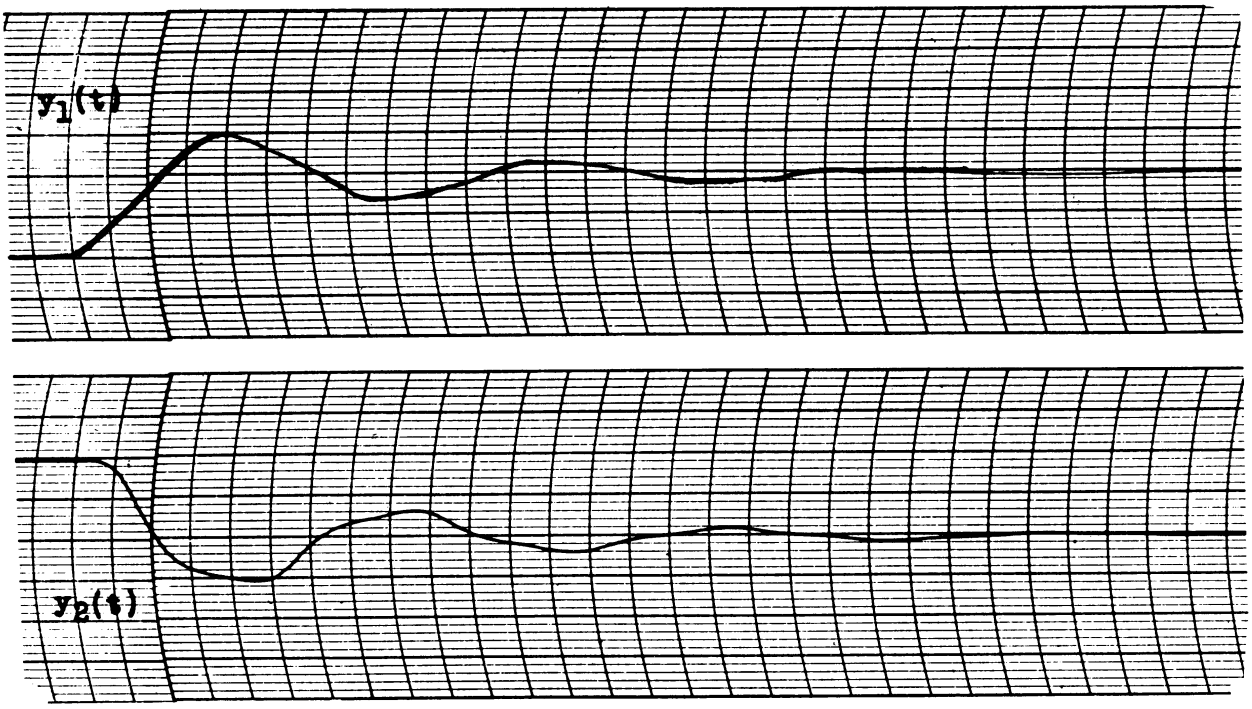

Figure 4-14.
Response of dynamic vibration absorber to a step input function.

CHAPTER 5

BOUNDARY VALUE PROBLEMS

5.1 Static Deflection of Uniform Beams under Uniform Loads

We will now consider the solution of differential equations where not only are there certain given initial conditions but also certain given final or end conditions. As an example of this type of problem we first consider the static deflection of a uniform beam under uniform load.

The differential equation representing the static deflection of a horizontally supported beam of small cross-sectional dimensions in comparison with the length is given by [5]

$$\frac{d^2}{dx^2}\left[EI\ \frac{d^2y(x)}{dx^2}\right] = W(x), \qquad (5\text{-}1)$$

where x is distance along the beam, y is the vertical deflection of the beam, $W(x)$ is the weight per unit length along the beam, I is the area moment of inertia of the cross section of the beam with respect to the central axis, and E is Young's Modulus of Elasticity. For a beam of uniform cross-section both E and I are constant, and we can write Equation (5-1) as

$$EI\ \frac{d^4y(x)}{dx^4} = W(x),$$

or

$$\frac{d^4y(x)}{dx^4} = aW(x), \qquad (5\text{-}2)$$

where $a = 1/EI$ = constant.

It should be noted that the bending moment $M(x)$ at any point along the beam is given by

$$M(x) = EI\ \frac{d^2y(x)}{dx^2} \qquad (5\text{-}3)$$

Since the shear force $Q(x) = \frac{dM(x)}{dx}$, we can write for our uniform beam

$$Q(x) = EI\ \frac{d^3y(x)}{dx^3} \qquad (5\text{-}4)$$

(A) Beam Clamped at Both Ends.

The diagram for a uniform beam clamped at both ends and under a uniform load is shown in Fig. 5-1.

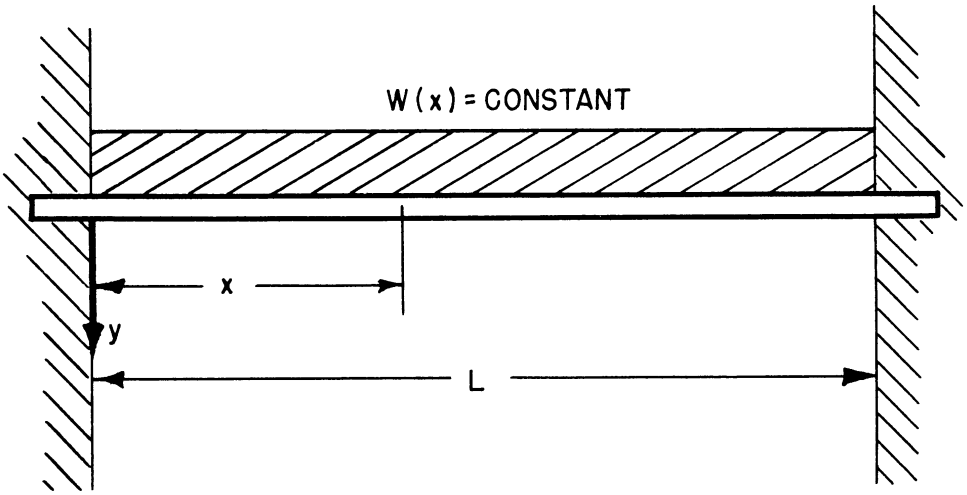

Figure 5-1. Uniform beam clamped at both ends.

If in Equation (5-2) we let aW(x) = V, we obtain for the equation of our beam

$$\frac{d^4y}{dx^4} = V. \qquad (5\text{-}5)$$

Wherever the beam is clamped it has zero deflection and zero slope. Hence we write as our end conditions

$$y(o) = y'(o) = y(L) = y'(L) = 0 \qquad (5\text{-}6)$$

The theoretical solution to Equations (5-5) and (5-6) can be shown to be

$$y(x) = \frac{V}{12}\left(\frac{L^2}{2}x^2 - L\,x^3 + \frac{x^4}{2}\right) \qquad (5\text{-}7)$$

We now proceed to check Equation (5-7) with the analog computer. The circuit for solving equation (5-5) is shown in Fig. 5-2.

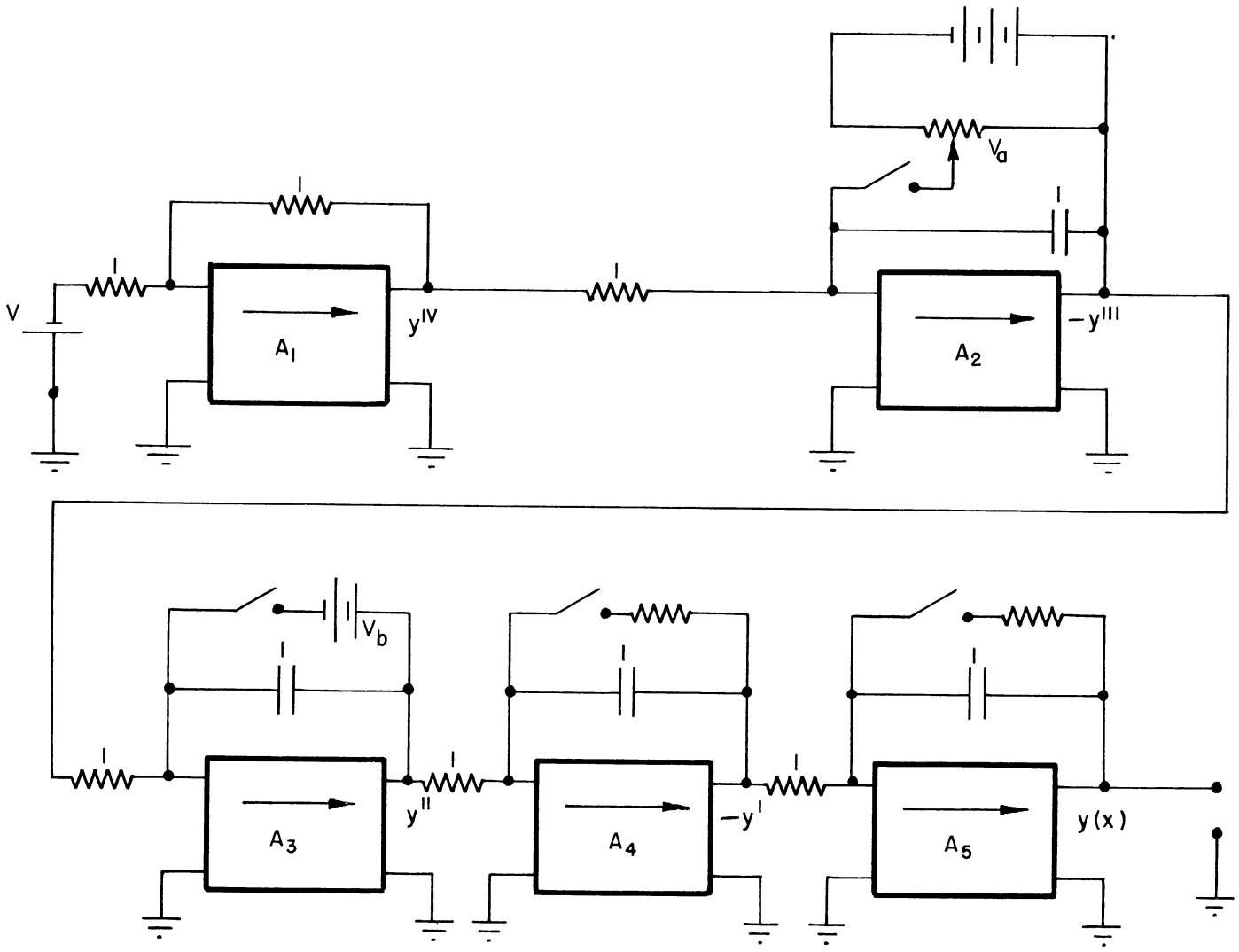

Figure 5-2. Computer circuit for solving uniform beam clamped at both ends and with uniform load.

In solving equation (5-5) with the computer we let the independent variable x (distance along the beam) be time in seconds. Then when we take $\frac{d}{dx}$, we are actually taking the derivative with respect to time.

The conditions $y(0) = y'(0)$ are simulated on the computer by shorting the feedback capacitors of A_4 and A_5 through initial condition relays until the solution of the problem is begun. At $x = 0$ and $x = L$ the bending moment M and the shear force Q have certain definite discrete values, as yet unknown. We denote $\frac{Q(0)}{EI}$ as $-V_a$ and $\frac{M(0)}{EI}$ as V_b. These conditions are simulated by means of battery voltages applied through initial condition relays to the feedback capacitors of A_2 and A_3. The battery voltages are released as soon as the

solution of the problem is begun. The constant V is the input battery voltage to the amplifier A_1 and is measured in terms of recorder deflection units.

The values of initial voltages V_a and V_b are, as stated above, unknown. Note in Fig. 5-2 that we make V_b a fixed battery voltage (of the order of magnitude of 6 volts) and V_a a voltage variable by means of a potentiometer connected across a battery. By changing V_a we can vary the ratio V_a/V_b, and this is sufficient control over the initial voltages V_a and V_b to allow us to obtain a solution to our problem. The technique of finding the solution is as follows:

When the starting button is pressed, all the initial condition relays are energized, the initial conditions $y = 0$; $y' = 0$; $y'' = V_b$, $y''' = -V_a$ are all released, and the solution of the problem begins. Since we have set V_a at an arbitrary value, the ratio V_a/V_b is arbitrary, and the computer solution will probably not be correct, that is, the end conditions $y(L) = y'(L) = 0$ will probably not be met. An example of a first trial solution of this type is shown in Fig. 5-3.

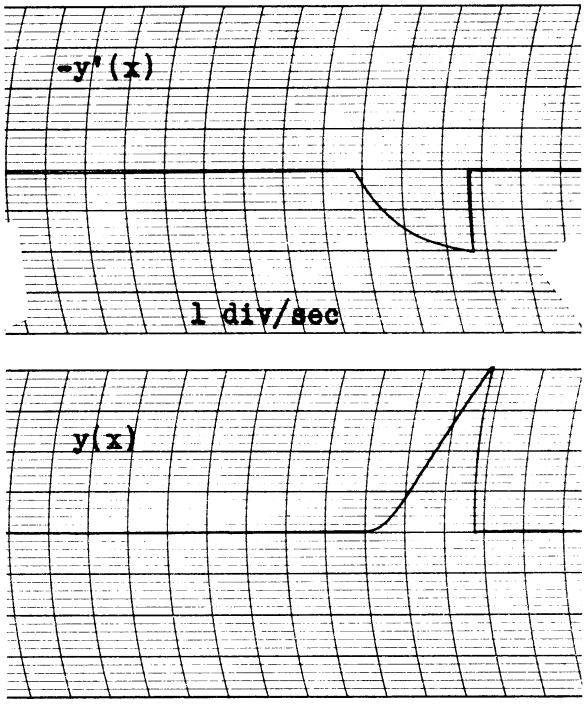

Figure 5-3. First trial solution for uniform beam.

V_a is then changed by means of the pot (thus changing V_a/V_b) and a second trial solution is made. The process is repeated until the exact potentiometer setting is determined for a correct solution, i.e., one for which the y(x) and y'(x) curves pass through zero at the same time. Since y'(x) is merely the slope of y(x), the correct solution is obtained when the minimum of y(x) falls on the zero axis. In Fig. 5-4 are shown several trial solutions where V_a is varied until a nearly correct solution is obtained. In Fig. 5-5 are shown the curves of y, y', y", and y''' for a correct solution.

After a solution which satisfies the required end conditions has been obtained, the length of the beam which that solution represents is carefully measured from the y'(x) curve. The recorder is almost always run on medium speed when obtaining records for these measurements of length, and hence one longitudinal division in Fig. 5-5 represents 0.2 seconds. Using a transparent millimeter rule, it is possible to obtain the length to a hundredth of a second. In this case the L is found to be 3.51 sec.

In our particular problem we have made the length L arbitrary. In the final solution this length L is in fact the length of the solution recorded between end conditions. In a problem where an original length ℓ is specified and a computer solution length L is obtained, we must make a change in variables. This problem is discussed fully in Section 5.2.

We have assumed that $\frac{W(x)}{EI} = V$. By measuring V in terms of recorder deflection, and from the value of L as determined by measuring the length of the computer solution, we can calculate the theoretical deflection curve for our problem from equation (5-7). This curve is shown in Figure 5-6, along with points taken from the computer solution of y(x) shown in Figure 5-5. The small discrepancy of the experimental points is probably because of a slight lag of the recorder pen due to dead space.

Reference to equations (5-3) and (5-4) shows that the bending moment M is proportional to y" and the shear force Q proportional to y''', the constant of proportionality being EI. Therefore the outputs from the computer in which we are more interested in a uniform beam problem will be y, y", and y'''.

It should be pointed out that the ratio V_a, V_b is often very critical in determining the solution with correct end conditions, expecially for the problems in Section 5.2. For this reason the potentiometer which determines V_a is actually made up of three wire-wound potentiometers (see Figure 5-7).

* Notice that the solution continues beyond the point where the end conditions are met. However, we are not interested in the solution beyond this point.

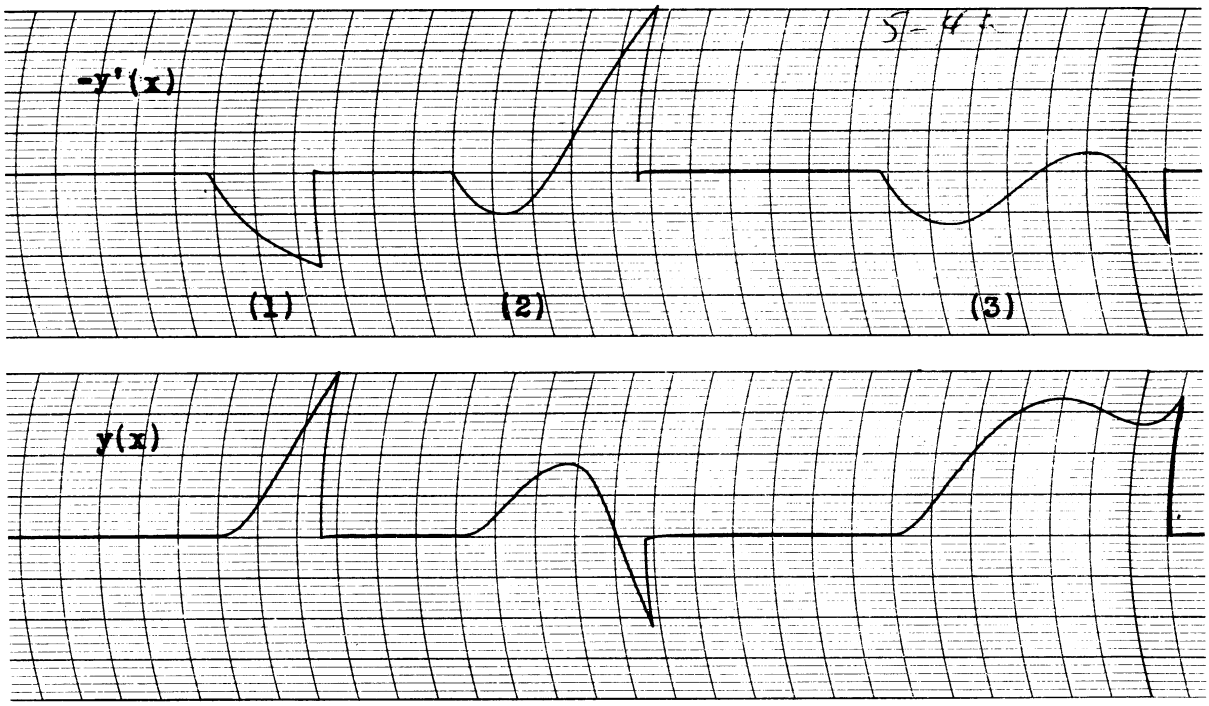

(a)

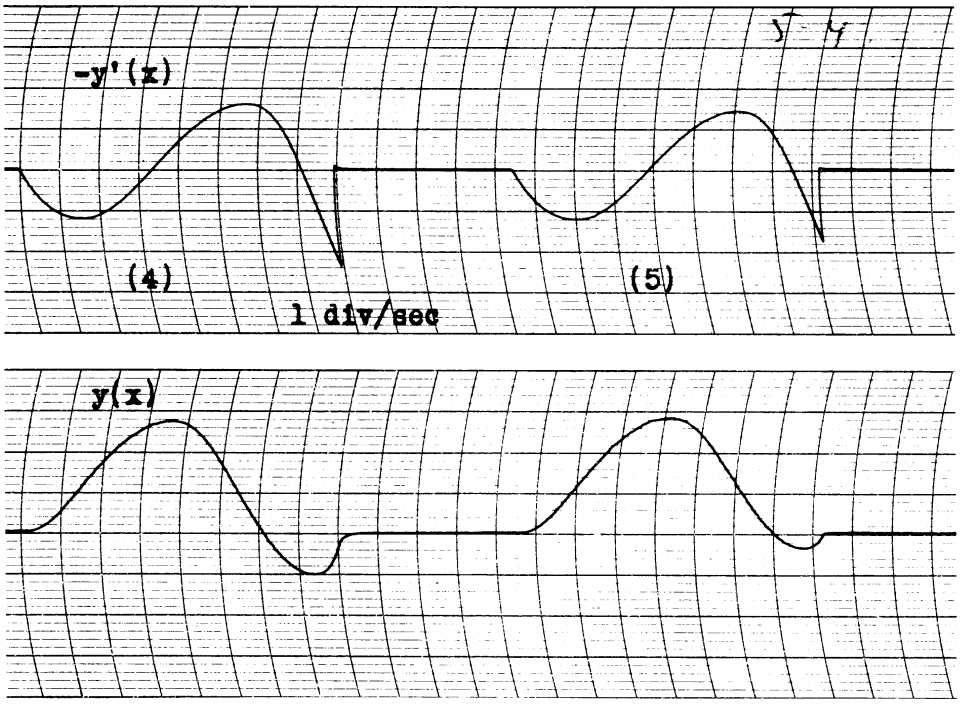

(b)

Figure 5-4. Series of trial solutions in order to obtain a correct solution.

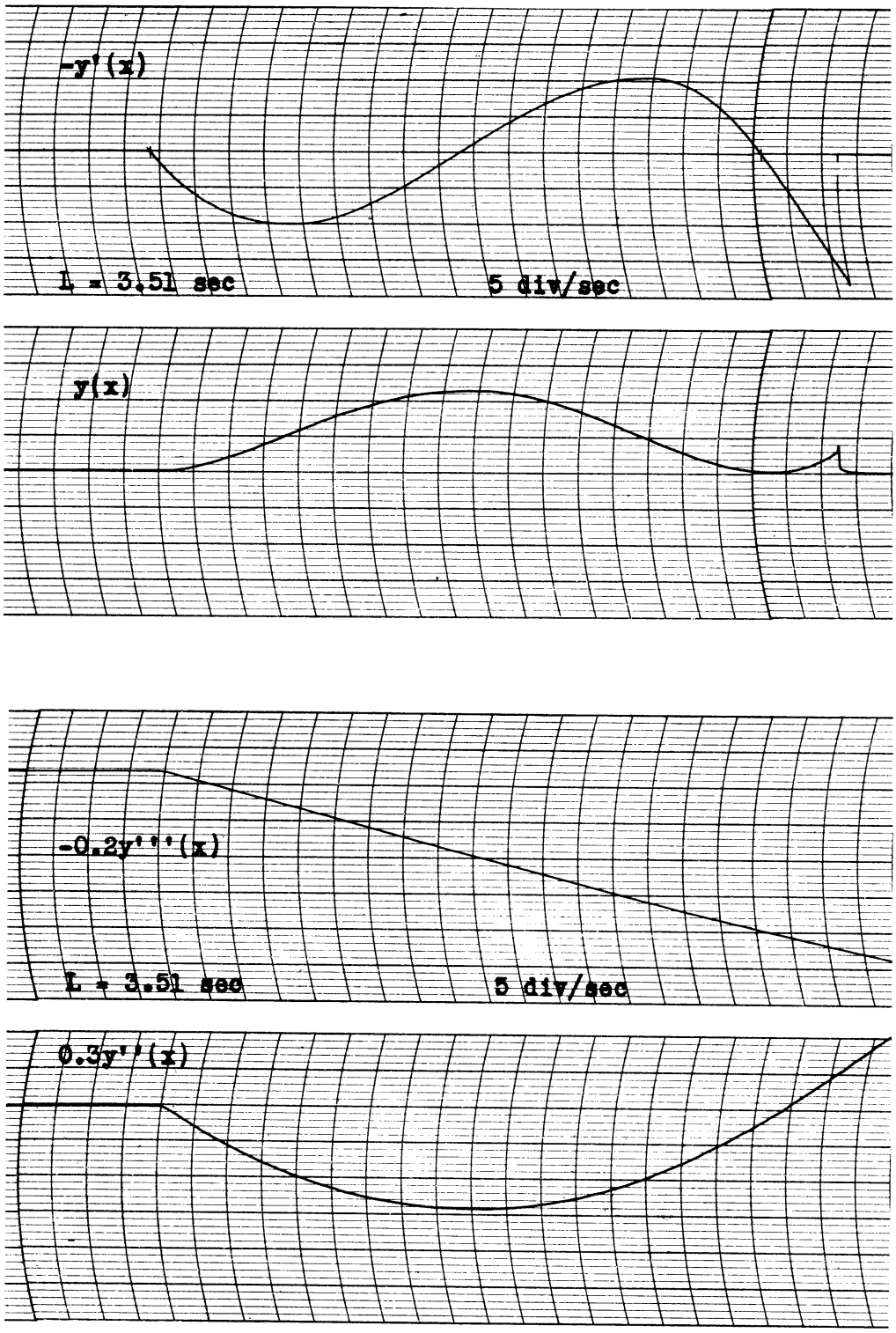

Figure 5-5. Correct solution for uniform beam with clamped ends and under uniform load.

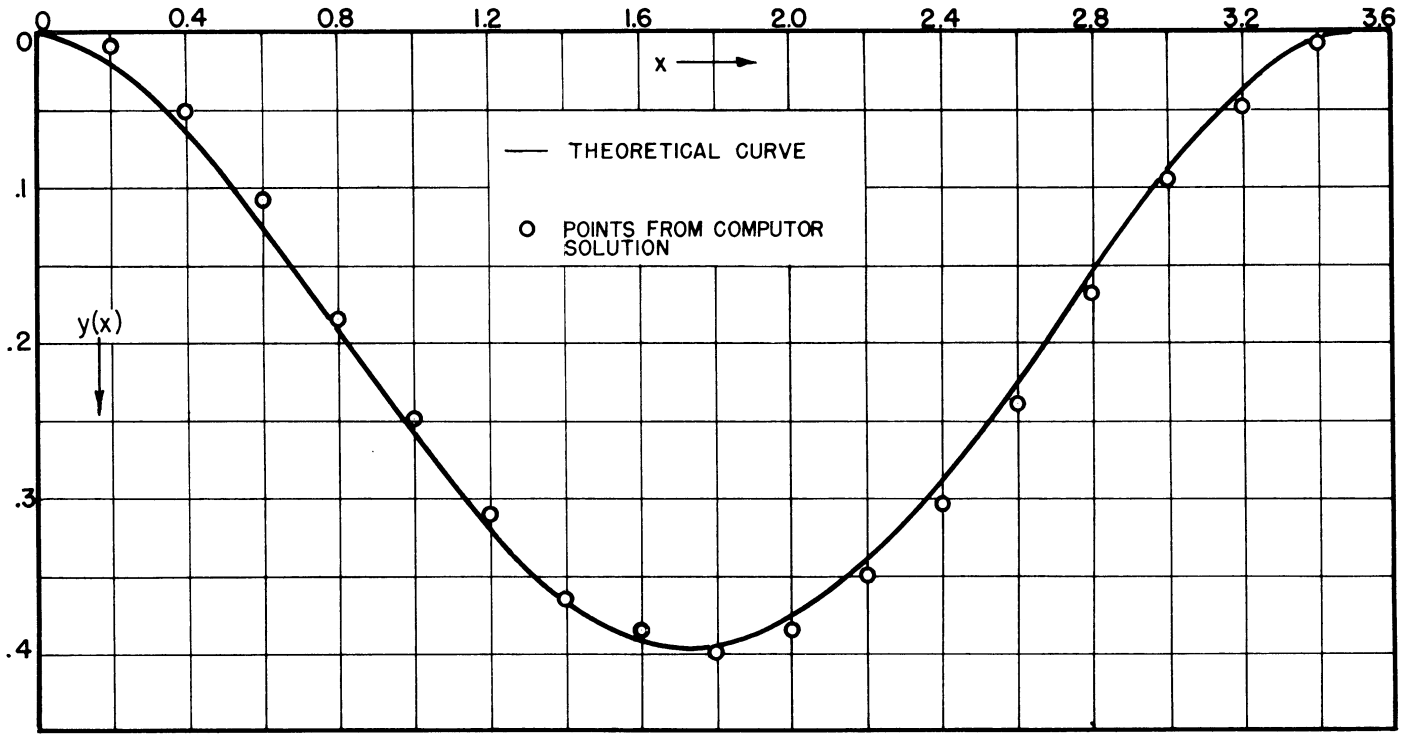

Figure 5-6. Comparison of theoretical and computer deflection curves.

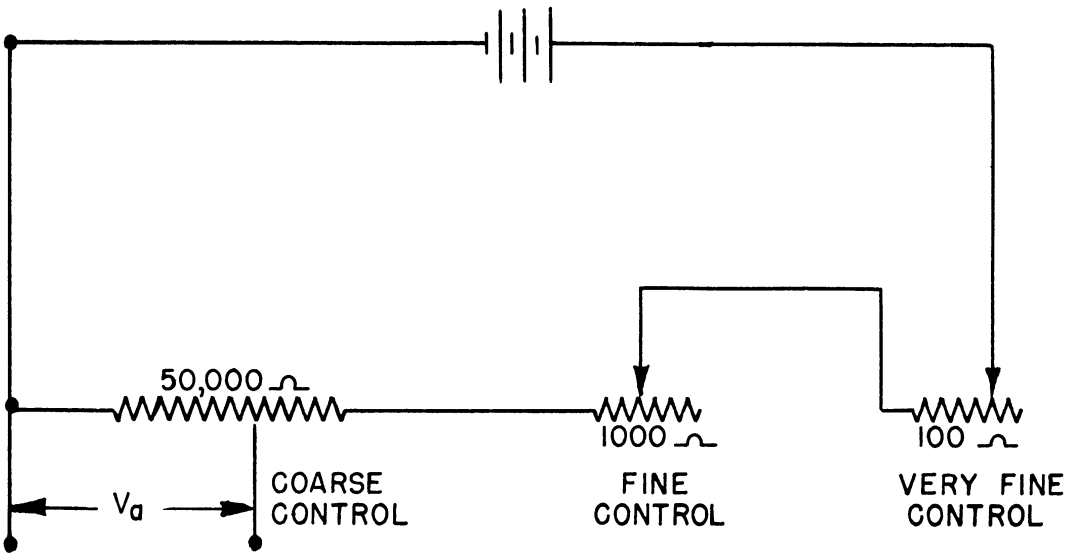

Figure 5-7. Potentiometer for controlling V_a.

(B) Beam Hinged at Both Ends.

The diagram for a uniform beam hinged at both ends and under a uniform load is shown in Figure 5-8.

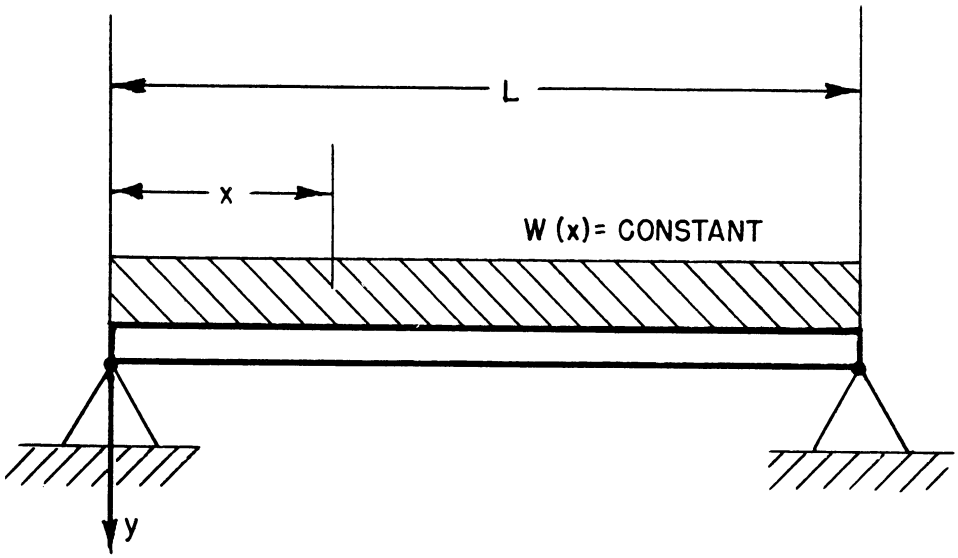

Figure 5-8. Uniform beam hinged at both ends.

When a beam is supported by a hinge, the deflection y(x) and the bending moment EI y"(x) are both zero. Therefore our equation is

$$\frac{d^4y}{dx^4} = \frac{W(x)}{EI} = V \qquad (5\text{-}5)$$

where $y(0) = y''(0) = y(L) = y''(L) = 0$ (5-8)

For this problem and following problems in static deflection of beams we will choose our units of deflection such that V = 1. Thus if V = 7.6 mm on the recorder, 7.6 mm is our unit of deflection.

The computer circuit used to solve equation (5-8) is exactly the same as that shown in Fig. 5-2 with the exception that the feedback capacitors of A_3 and A_5 are initially shorted, and the initial voltages V_a and V_b are applied to the feedback capacitors of A_2 and A_4 respectively, V_a being variable as before. Following the technique described for the clamped beam we vary V_a until we get a solution where y(x) and y"(x) cross the zero axis at the same time, or very nearly the same time. The length L of the solution is determined as the average of the two lengths L_1 and L_2 of y(x) and y"(x) respectively. In general one can get L_1 and L_2 to agree within a few hundredths of a second, The oscillograms of y, y', y" and y"' as recorded from the computer for the hinged beam are shown in Figure 5-9.

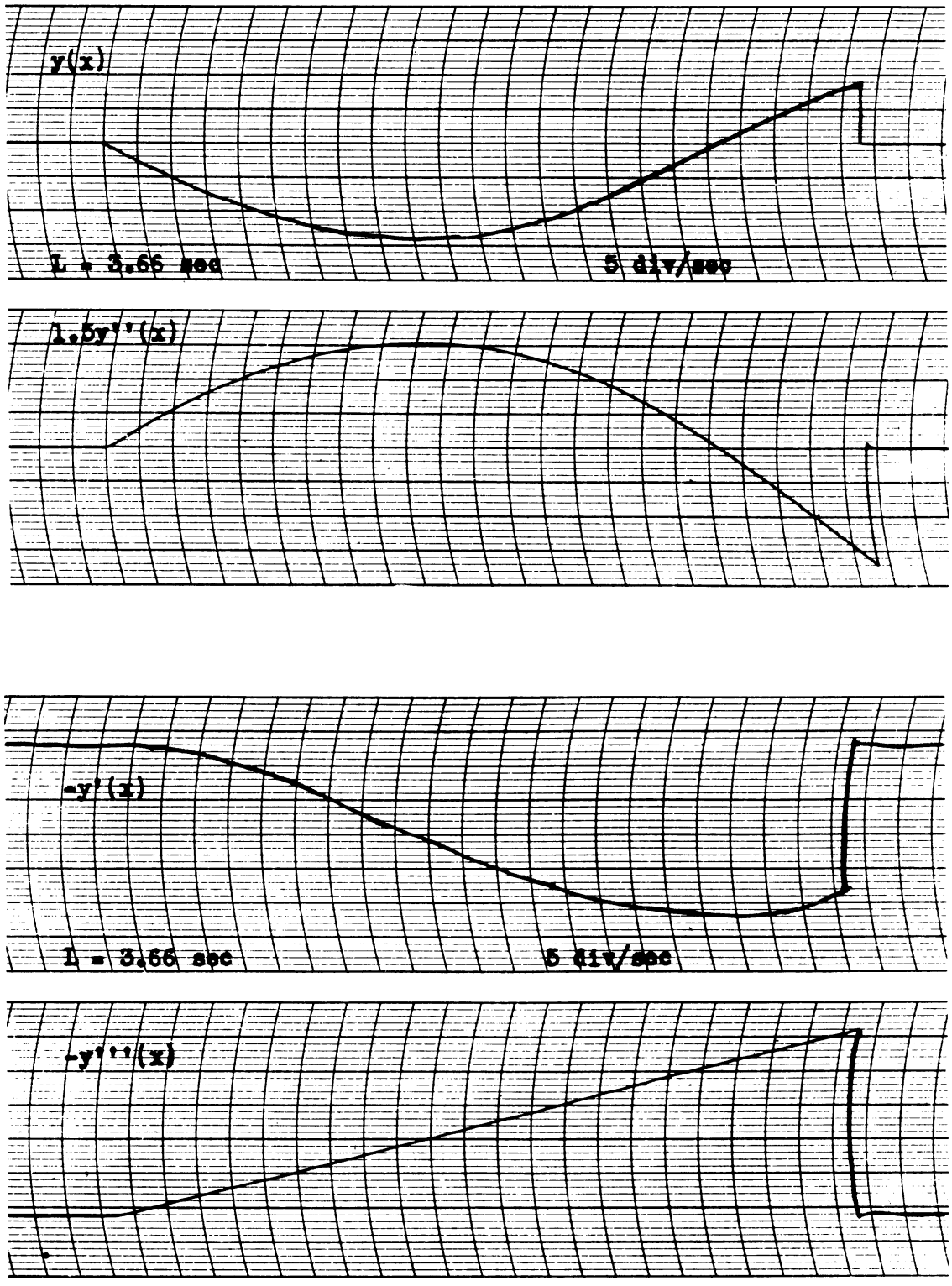

Figure 5-9. Computer solution for uniform beam with hinged ends and under uniform load.

For purposes of simplifying our problem of checking the accuracy of the computer we will assume not only that $V = \frac{W(x)}{EI} = 1$, but that $\frac{1}{EI} = 1$ and hence that $W(x) = 1$. Then we can write

$$M(x) = y''(x) \qquad (5\text{-}9)$$

$$Q(x) = y'''(x) \qquad (5\text{-}10)$$

The following formulas are given for the maximum bending moment and deflection.[6]

$$M_{max} = \frac{wL^2}{8} \qquad (5\text{-}11)$$

$$y_{max} = \frac{5}{384} \frac{wL^4}{EI} \qquad (5\text{-}12)$$

where w = weight/unit length = W(x)

From the computer solution of Fig. 5-9 we find that the length L = 3.664 sec. from (5-11) for w = 1 we have

$$M_{max} = \frac{13.42}{8} = \underline{1.68} .$$

From the computer solution for y'' we obtain

$$M_{max} \text{ (measured)} = \underline{1.70} .$$

The agreement is within the limits of recorder error.

From equation (5-12) for w = 1 and EI = 1 we have

$$y_{max} = \frac{5\ (13.42)^2}{384} = \underline{2.35}$$

From the computer solution for y we find that

$$y_{max} \text{ (measured)} = \underline{2.33}$$

Again the agreement is within our limits of recorder error. It is to be remembered that the M_{max} and y_{max} referred to here are not read directly from the oscillographs of Fig. 5-9 but are subject (1) to a calibration-curve correction (which may change the values by as much as 5%), (2) to a multiplication factor depending on the selected gain of the d.c. amplifier between the computer output and recorder impedance-matcher input, and (3) to a scale factor depending upon

the value of V measured in mm of recorder deflection. For example, in Fig. 5-9 we see that 1.5 y''_{max} is 15.1 mm. From our calibration curves we correct this to 14.4 mm. Now the corrected value of V is found to be 5.64 mm. Hence our final value of M_{max} which is to check with the value from equation (5-10) is

$$M_{max} = \frac{14.4}{1.5 \times 5.64} = 1.70.$$

(C) Cantilever Beam

In the case of the cantilever beam under a uniform load, one end of the beam is clamped and the other end is free. The diagram is shown in Figure 10.

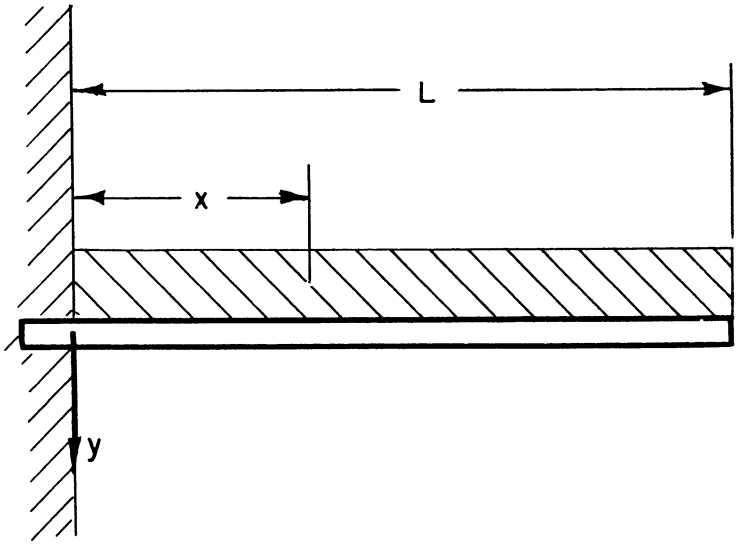

Figure 5-10. Uniform cantilever beam under uniform load.

For the clamped end we have the conditions

$$y(o) = y'(o) = 0 \qquad (5\text{-}13)$$

At the free end the bending moment and shear force are both zero, and our conditions are

$$y''(L) = y'''(L) = 0 \qquad (5\text{-}14)$$

As in the case of the hinged beam we let EI = 1 and w = W(x) = 1 for purposes of simplifying our check of the computer solution. Then our differential equation is

$$\frac{d^4y}{dx^4} = \frac{W(x)}{EI} = 1 \qquad (5\text{-}5)$$

where the end conditions given in equations (5-13) and (5-14). The computer circuit used to solve the cantilever beam problem is exactly the same as that shown in Figure 5-2. The technique for getting the solution is also the same as in the case of the beam clamped at both ends except that V_a is varied until $y''(x)$ and $y'''(x)$ are zero at the same time. Since y''' is the derivative of y'', this will occur when the minimum of y'' lies on the zero axis.

The curves showing y, y', y'', and y''' from the computer are shown in Figure 5-11.

The following formulas give the maximum bending moment and shear for a cantilever beam under uniform load.[6]

$$M_{max} = \frac{w L^2}{2} \qquad (5\text{-}15)$$

$$y_{max} = \frac{w L^4}{8 EI}$$

From the curve showing $y'''(x)$ in Fig. 5-11 the length L is found to be 2.14 sec. For w = 1 and EI = 1 we get from equation (5-15)

$$M_{max} = \frac{(2.14)^2}{2} = 2.29$$

From the computer solution for y'' we obtain

$$M_{max}\ (\text{measured}) = \frac{13.2}{5.92} = 2.23$$

From equation (5-16)

$$y_{max} = \frac{(2.14)^4}{8} = 2.62$$

From the computer solution for y we find that

$$y_{max} = \frac{14.6}{5.92} = 2.47$$

The results for the cantilever beam, while not as accurate as those for the clamped and hinged beams, are still within 7%. Again the inaccuracy in results is probably due more to inaccuracies in recording rather than inaccuracies in the computer, since accuracy in problems where the results depend upon measurements of length rather than deflection (as taken up in the next section of this chapter) are much higher.

In conclusion it should be stated that the presentations made thus far in Chapter 5 showing the solutions of static deflections of uniform beams under uniform loads by means of the analog computer have not been made with the main purpose of acclaiming the computer as an accurate and time-saving means of solving such problems. Problems this simple in nature have already

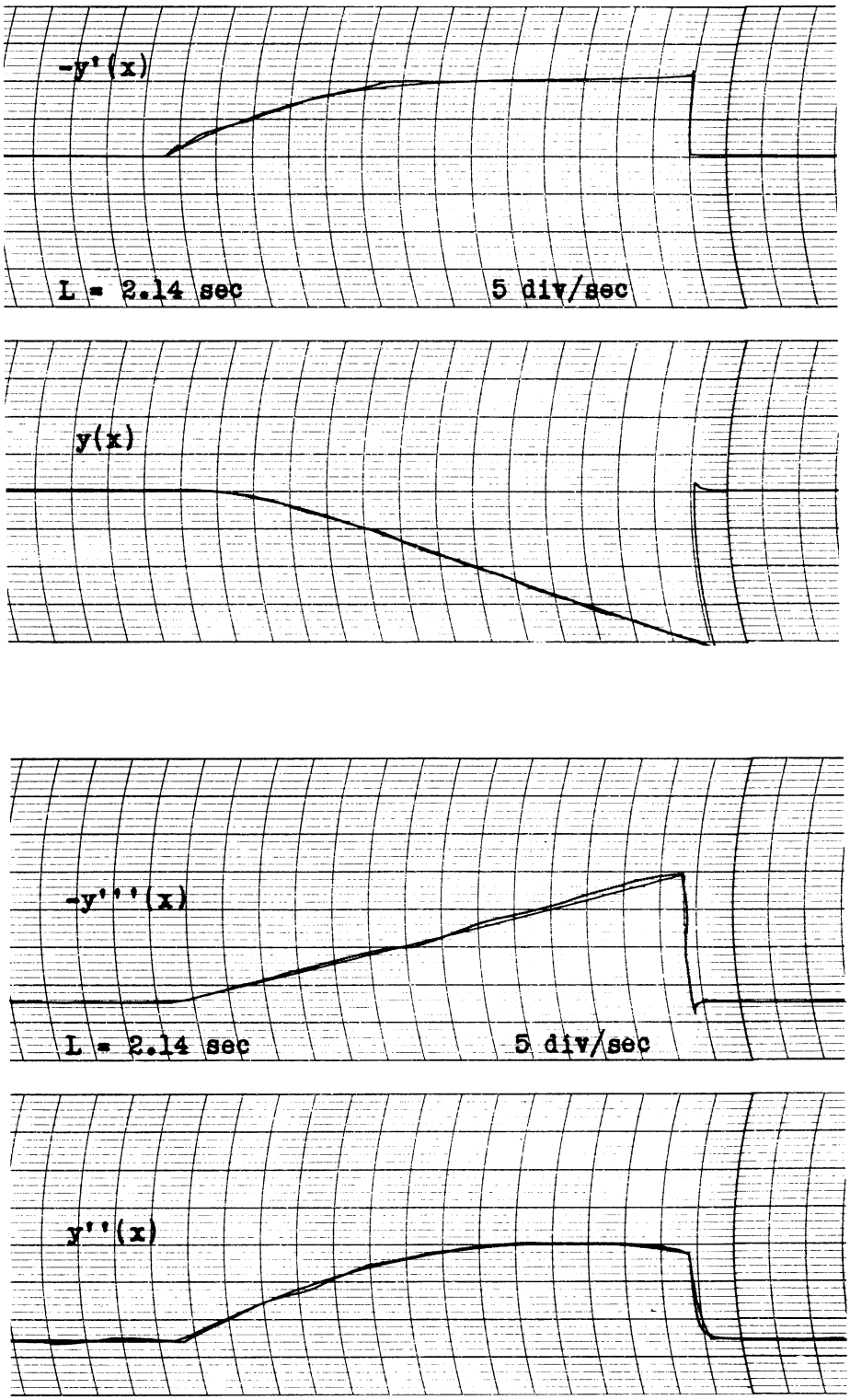

Figure 5-11. Computer solution for uniform cantilever beam under uniform load.

been thoroughly worked out analytically. Rather we have tried to acquaint the reader with the technique of setting up and solving problems with end conditions, an acquaintance which will be very useful in understanding the remainder of Chapter 5 and all of Chapter 9, where the use of the analog computer does show considerable promise as a great time-saving device in more complicated problems.

5.2 Normal Modes of Oscillation of Uniform Beams

In Paragraph 5.1 the equation for the static deflection of a beam with small cross-sectional dimensions in comparison with its length was given as

$$\frac{d^2}{dx^2}\left[EI\,\frac{d^2y(x)}{dx^2}\right] = W(x), \tag{5-17}$$

where x is distance along the beam, y is the vertical deflection of the beam, and W(x) is the load intensity along the beam. To obtain the equation for the lateral vibration of the beam we imagine that the vibrating beam is loaded by inertia forces due to its own mass and acceleration, the inertia force along the beam being given by[7]

$$\text{inertia force} = -\frac{\gamma A}{g}\cdot\frac{\partial^2 y(x,t)}{\partial t^2}, \tag{5-18}$$

where γ is the density of the material of the beam and A is the cross-sectional area. We frequently write

$$\mu = \frac{\gamma A}{g} \tag{5-19}$$

where μ is the mass distribution along the beam. Substituting equation (5-18) for W(x) in equation (5-17) and letting $\mu = \frac{\gamma A}{g}$ we obtain

$$\frac{\partial^2}{\partial x^2}\left[EI\,\frac{\partial^2 y(x,t)}{\partial x^2}\right] = -\mu\frac{\partial^2 y(x,t)}{\partial t^2}, \tag{5-20}$$

which is the general equation for the lateral vibration of the beam.

In studying the normal modes of vibration of the beam we assume that

$$y(x,t) = X(x)e^{j\lambda t}, \tag{5-21}$$

where X(x) is a function only of distance along the beam and is independent of the time t, and where $e^{j\lambda t}$ represents sinusoidal oscillations of frequency λ.

From equation (5-21) it follows that

$$\frac{\partial^2 y}{\partial t^2} = -\lambda^2 e^{j\lambda t} \cdot X(x) \qquad (5\text{-}22)$$

and

$$\frac{\partial^2}{\partial x^2}\left(EI \frac{\partial^2 y}{\partial x^2}\right) = \frac{d^2}{dx^2}\left(EI \frac{d^2X}{dx^2}\right) e^{j\lambda t}, \qquad (5\text{-}23)$$

where E and I are assumed to be functions only of x. Substituting equation (5-22) and (5-23) in equation (5-20) we get

$$\frac{d^2}{dx^2}\left(EI \frac{d^2X}{dx^2}\right) - \mu\lambda^2 X = 0, \qquad (5\text{-}24)$$

which is our fundamental equation for the lateral vibration of a beam. Since equation (5-17) considers only bending forces, the same limitation applies to equation (5-24). Forces due to shear and rotary inertia are neglected. However, these additional forces are taken up in Paragraph 5.3 of this chapter.

In the case of a beam with uniform cross-section where E, I, and μ are constants, we can rewrite equation (5-24) as

$$\frac{EI}{\mu\lambda^2} \frac{d^4X}{dx^4} - X = 0. \qquad (5\text{-}25)$$

It is apparent that equation (5-25) is a linear, 4th order differential equation with constant coefficients, and that therefore it can be set up on the analog computer. However, let us first consider the change of the independent variable.

We denote the length of our uniform beam as ℓ. Then the solution in which we are interested has the range $0 \leq x \leq \ell$ for the independent variable x. From our computer we will obtain a length L for the solution of the problem. Denoting $\bar{x}$ as our new variable, we must have the range $0 \leq \bar{x} \leq L$ for $\bar{x}$. Hence we let

$$\bar{x} = \frac{L}{\ell} x \qquad (5\text{-}26)$$

from which

$$\frac{d}{dx} = \frac{L}{\ell} \frac{d}{d\bar{x}}$$

$$\frac{d^2}{dx^2} = \frac{L^2}{\ell^2} \frac{d^2}{d\bar{x}^2}$$

and in general $\frac{d^n}{dx^n} = \frac{L^n}{\ell^n} \frac{d^n}{d\bar{x}^n}$ (5-27)

Rewriting equation (5-24) in terms of our computer variable $\bar{X}$ we find that

$$\frac{L^4}{\lambda^2 \ell^4} \cdot \frac{d^2}{d\bar{x}^2} \left(EI \frac{d^2 X}{d\bar{x}^2}\right) - \mu X = 0, \qquad (5\text{-}28)$$

and for the beam of uniform cross-section

$$\frac{EIL^4}{\mu \lambda^2 \ell^4} \cdot \frac{d^4 X}{d\bar{x}^4} - X = 0. \qquad (5\text{-}29)$$

For purposes of simplification we let

$$\alpha^2 = \frac{\mu \lambda^2 \ell^4}{EI}, \qquad (5\text{-}30)$$

from which

$$\lambda = \alpha \sqrt{\frac{EI}{\mu \ell^4}}, \qquad (5\text{-}31)$$

and equation (5-29) becomes

$$\frac{L^4}{\alpha^2} \cdot \frac{d^4 X}{d\bar{x}^4} - X = 0. \qquad (5\text{-}32)$$

In equation (5-32), $\frac{L^4}{\alpha^2}$ is a constant which we will denote as C. Then equation (5-32) becomes

$$C \frac{d^4 X}{d\bar{x}^4} - X = 0 \qquad (5\text{-}33)$$

Equation (5-33) is what we set up on the analog computer, where C is a constant which we may choose to give any value. (It is usually given the value unity for a computer solution.) Corresponding to the value of C which we select in setting up the computer, we will find a length L of the computer solution for which the end conditions as determined by the type of beam support being simulated are met. Knowing L and C we can solve for α from the

formula

$$\alpha = \frac{L^2}{\sqrt{C}} \qquad (5\text{-}34)$$

With α determined our problem is solved, for by going to equation (5-31) we can find the frequency of vibration for the type of beam in question by substituting the physical constants E, I, μ and ℓ of the beam.

A. Normal Modes of Oscillation of a Beam with Free Ends.

In the case where both ends of the beam are free (Figure 5-12) the shear and bending moment at each end are zero, and we have as the end conditions of our problem

$$X''(0) = X'''(0) = X''(L) = X'''(L) = 0 \qquad (5\text{-}35)$$

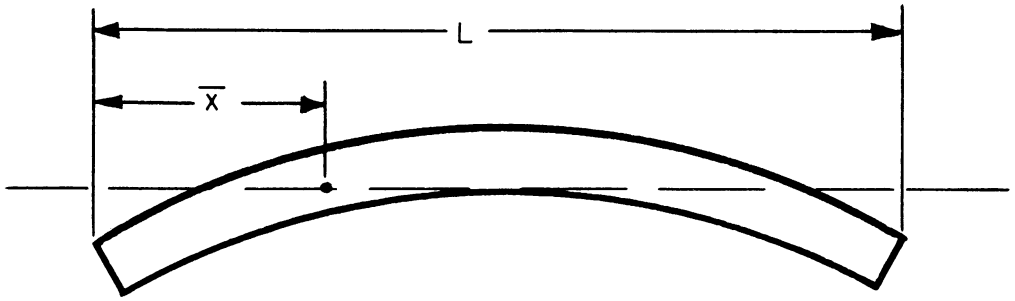

Figure 5-12. "Free-Free" or "Floating" Beam

The equation to be set up on the computer is

$$C\frac{d^4X}{d\bar{x}^4} - X = 0 \qquad (5\text{-}33)$$

where time in seconds on the computer corresponds to the units of $\bar{x}$.

The computer circuit for solving equation (5-33) with the conditions of equation (5-35) is shown in Figure 5-13. Note that the feedback capacitors across A_3 and A_4 are initially short-circuited, and that those across A_5 and A_6 have initial voltages V_a and V_b, V_a being variable by means of the potentiometer shown in Figure 5-7. V_a and V_b are the slope and deflection respectively at each end of our beam necessary to cause it to vibrate in a normal mode of oscillation.

An alternative circuit requiring only four instead of six amplifiers is shown in Figure 5-14. Although the experimental data presented in the rest of this chapter was taken from the computer as set up in Figure 5-13, preliminary tests using the circuit of Figure 5-14 showed improved consistency in consecutive runs, as would be expected with two less amplifiers in the circuit.

The technique of varying V_a until a solution is obtained which satisfies the end conditions of equation (5-35) is described in detail in Section 5.1A, where the static deflection of a beam clamped at both ends is solved on the computer. For the "free-free" beam the proper end conditions are obtained when the minimum (or maximum, depending on the number of the mode) of X" ($\bar{x}$) goes through the zero-axis.

The oscillograms of X, X", and X"' for the solution of the first mode of oscillation are shown in Figure 5-15. In order to make certain that we have a correct solution when we take a record of X($\bar{x}$), a record of X"($\bar{x}$) is taken simultaneously on the second channel. If the minimum of X"($\bar{x}$) falls on the zero axis, we know we have a correct solution for X($\bar{x}$). This procedure becomes more important in obtaining X for higher modes, where the solutions are not likely to repeat.

No difficulty is experienced in obtaining an exact solution for the first mode. The value of V_a is critical enough, however, that the fine control of the potentiometer (Figure 5-7) is necessary in setting V_a.

The length L of the solution is most accurately determined from X"', since here the curve starts out with a finite slope and ends with a finite slope. The technique of measuring L and of applying the proper corrections is discussed in Section 5.4 at the end of this chapter. Since the determination of α depends on L^2 /see equation (5-34)/, the measurement of L is fairly critical.

The following data were obtained from different runs for the length L of the first mode.

4.73 sec
4.72
4.74
4,72
4.71
4.75
4.73
4.74

Av L = 4.730 sec C = 1

From equation (5-34)

$$\alpha = \sqrt{\frac{L^2}{C}} = \frac{(4.73)^2}{1} = 22.39$$

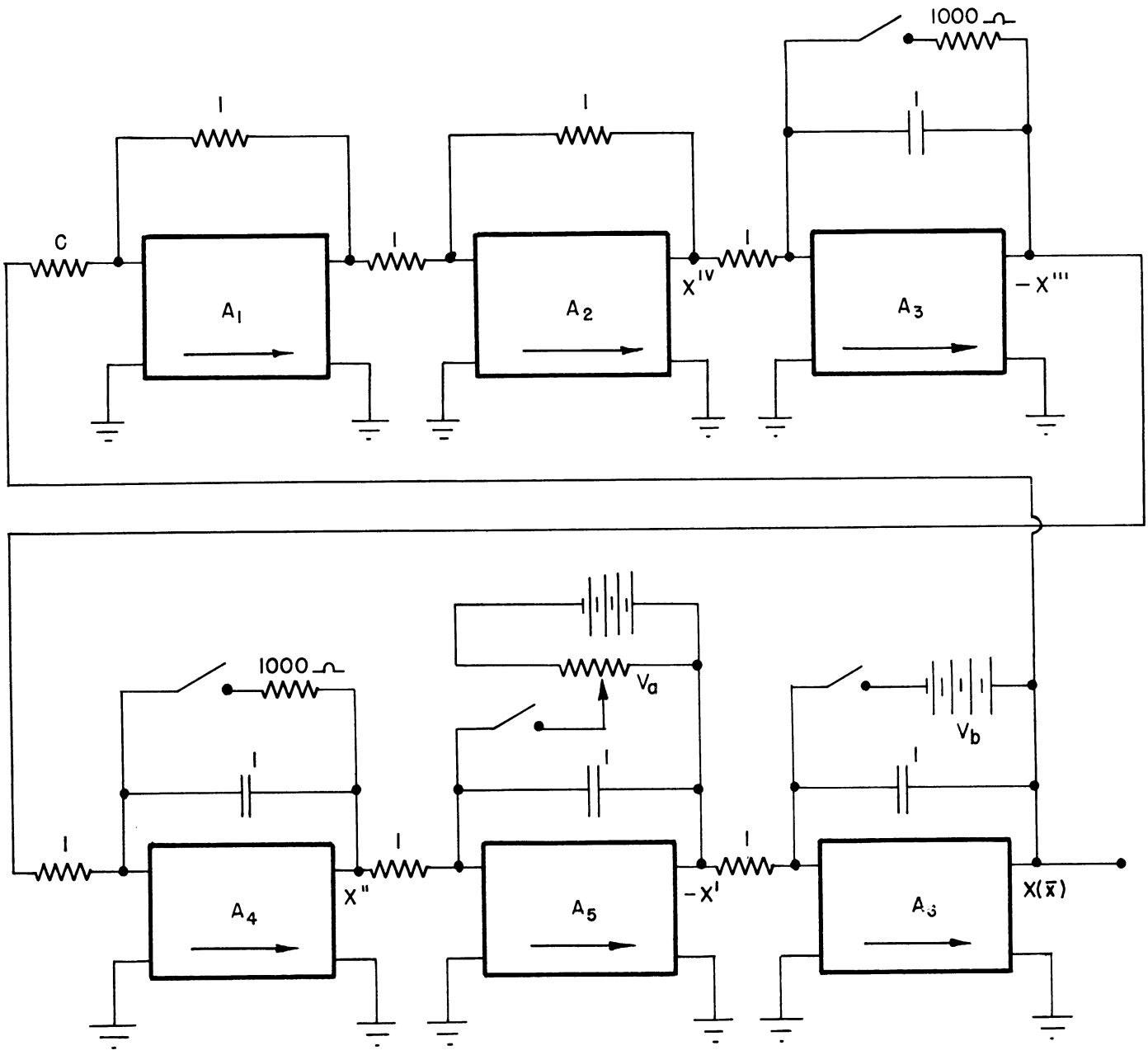

Figure 5-13. Computer circuit for obtaining normal mode solutions of a vibrating uniform beam.

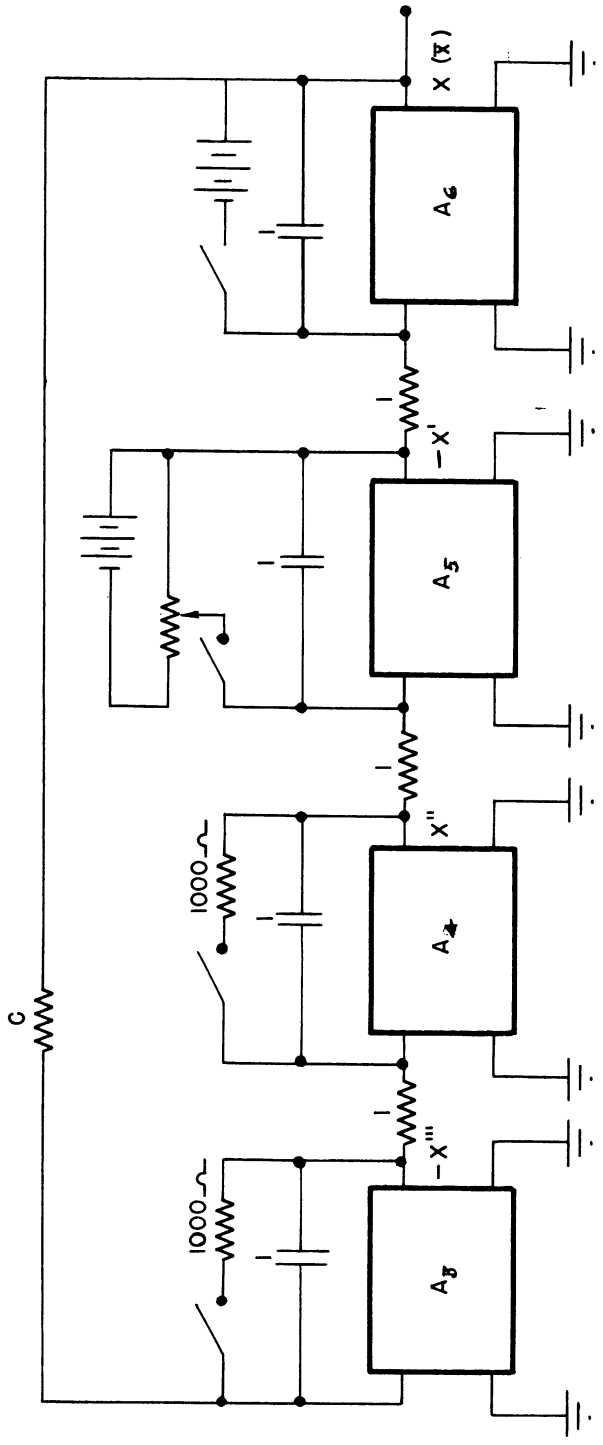

Figure 5-14. Alternative circuit for obtaining normal mode solutions.

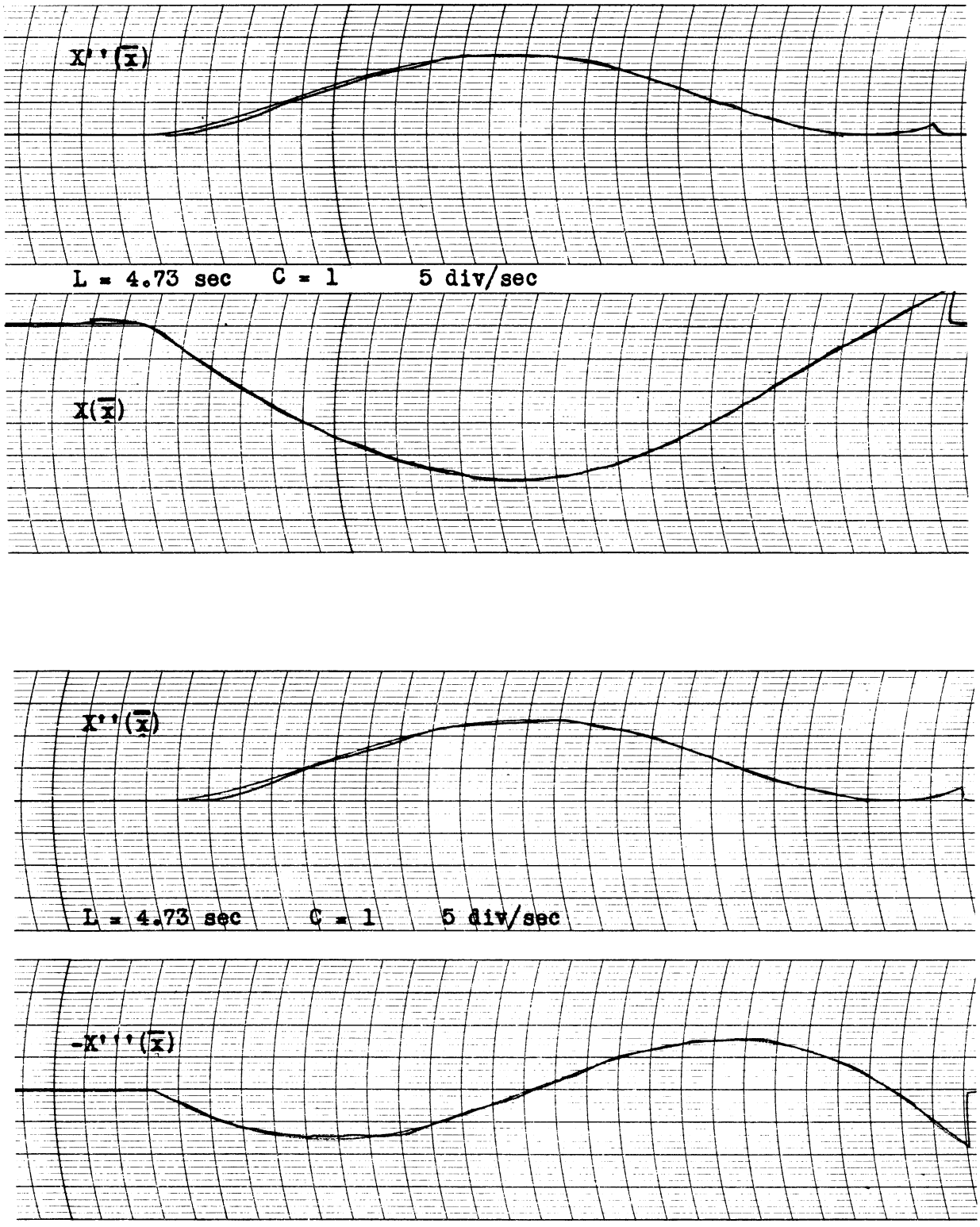

Figure 5-15. First-mode solution for uniform "floating" beam.

Experimental α = 22.39

Theoretical* α = 22.4

The setting of V_a for obtaining the second mode solution is fairly near the setting for the first mode. In the case of the second mode the final setting of V_a is quite critical, and some difficulty may be experienced in obtaining exact repetition of solutions from run to run. In other words while the X" curve maximum may fall 2 mm below the zero axis on a first run, the same X" curve maximum may fall 1 mm above the zero axis on a second run, even though V_a has not changed. However, fifteen or twenty trials are usually enough to obtain several correct solutions for which the proper X" maximum is within 0.1 mm of the zero axis. It is often a question of whether it is quicker to make a large number of runs in order to obtain several exact solutions, or whether it is quicker to take several runs which are almost correct solutions and interpolate the data. The later method is described in detail in the discussion of the third mode.

Oscillograms showing X, X", and X'" for the second mode are seen in Figure 5-16. The following values of the length L were obtained from the X"' curve.

7.84 sec
7.86
7.85
7.85

Avg. L = 7.85 sec C = 1

From equation 5-16

$$\alpha = \frac{L^2}{\sqrt{C}} = \frac{(7.85)^2}{1} = 61.6$$

Experimental α = 61.6

Theoretical* α = 61.7

With the analog computer and associated power supplies which we were using, we found it almost impossible to obtain an exact solution of the third mode, i.e., a solution for which the required minimum or maximum of the X" curve falls exactly on the zero axis. The setting of V_a is very close to the setting for the second mode solution, and for the third mode this setting is so critical that a change in V_a of one part in five-thousand varies the solution considerably. Therefore the very fine control of the potentiometer of Figure 5-7 is used for final adjustments.

The biggest problem, as stated before, is repetition of results due to the extreme critical nature of all initial conditions. The length of time

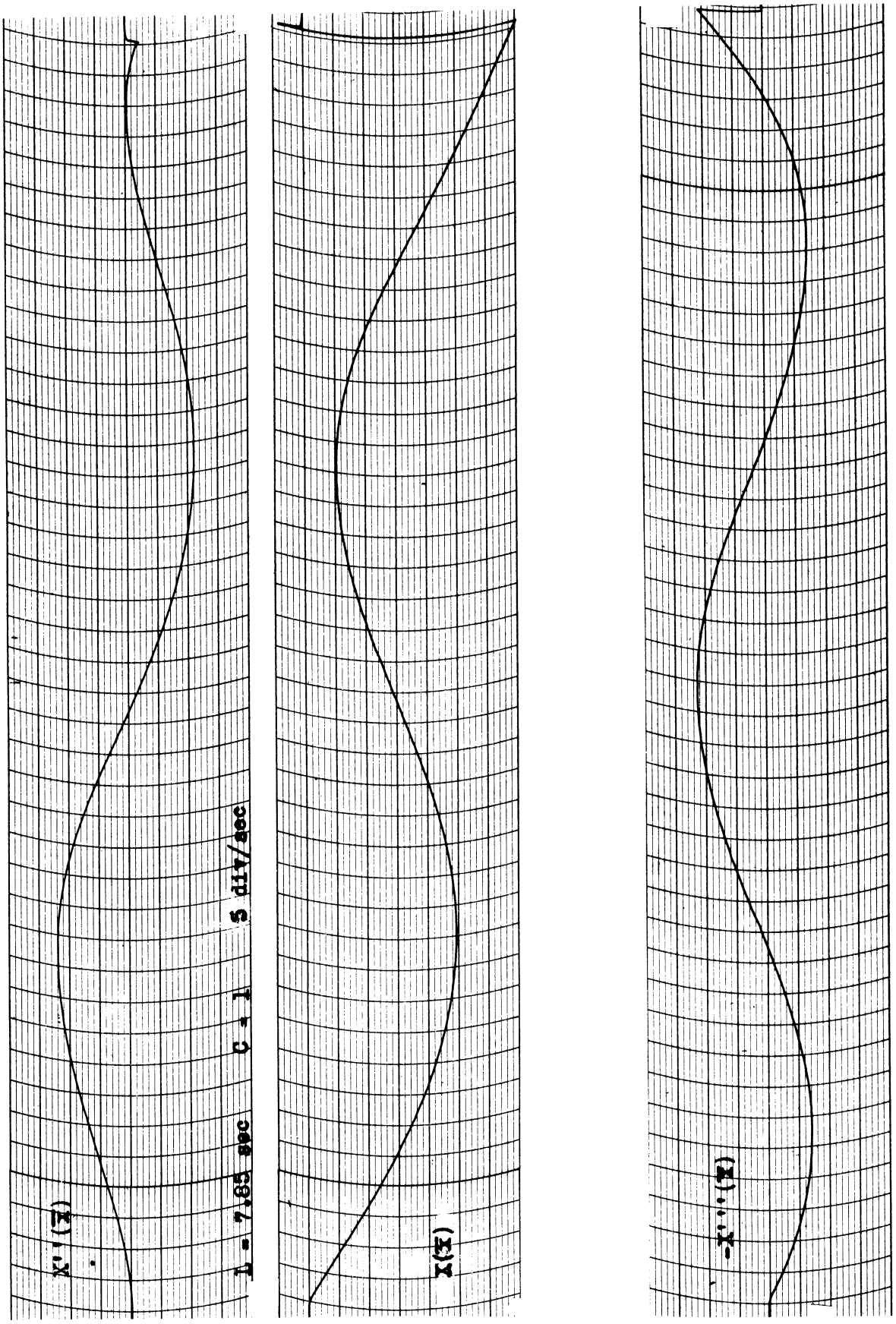

Figure 5-16. Second-mode solution for uniform "floating" beam.

the starting button is left up (i.e., the length of time the capacitors are short-circuited between solution runs) seems to make some difference. Naturally any fluctuations in power supply voltages will change slightly the balance of the amplifiers and cause varying results. Any change in the initial condition battery voltages of more than one part in ten-thousand will cause a noticeable change in the solution form. Contact potentials from the relays may possibly cause trouble. All these effects combine to give inconsistency to the solution forms for the higher modes. One run may give a solution which is close to being correct for the third mode. The next run may go through a fourth mode solution.

A good approximation to the higher mode solutions in the case of a symmetrical beam may be obtained by using only the first half of a near solution since very slight changes in the early part of the solution cause large changes in the latter part. Symmetry will then give the second half of the solution.

Another method of attack for the higher modes is to obtain a number of solutions which are somewhere near the correct solution and interpolate the results to the correct solution. This is in fact the approach we used, and the results seem to be just as accurate as in the cases where an exact solution is obtained. The technique consists of measuring the deflection d in mm of the proper minimum or maximum of the X" curve above or below the zero-axis. Corresponding to that d the length L_d of the nearly correct solution is obtained from where the X'" curve crosses the zero-axis. Values of d above the zero-axis are called positive, below the axis negative. An actual example is shown in Figure 5-17. (Note that in the figure the recorder was run on slow speed; for actual computations the recorder is always run on medium speed.)

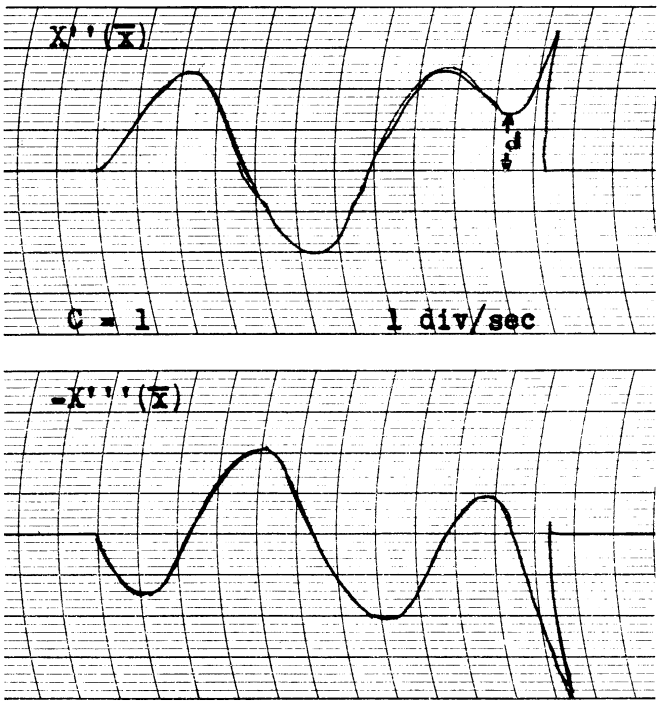

Figure 5-17. Near-correct solution.

* All theoretical values marked with an asterisk come from Den Hartog, "Mechanical Vibrations", Appendix II, V.

The d vs L_d data is then plotted on graph paper and a smooth curve is drawn through the points. Where this curve crosses the axis is taken as the length L of the mode in question.

Data obtained from third mode solutions is shown below.

d	L_d
-7.6 mm	10.54 sec
-6.6	10.605
-5.2	10.71
-2.2	10.88
-0.6	10.97
1.8	11.09
2.8	11.15
4.5	11.235
7.5	11.34

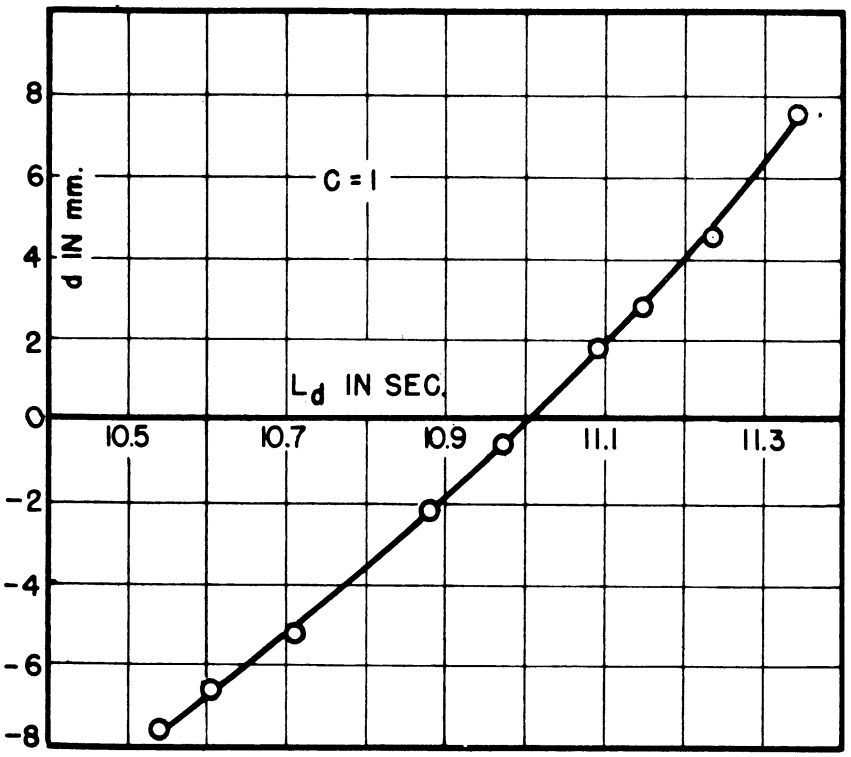

Figure 5-18. Interpolation curve for determining exact solution length L for third mode.

The plot of d vs L_d for the above data is shown in Figure 5-18. Note that a smooth curve can be drawn through the points, and that the length at which the curve crosses the axis d = 0 is determined to within 0.1%.

From Figure 5-18, L = 11.00 C = 1

From equation (5-34)

$$\alpha = \frac{L^2}{\sqrt{C}} = \frac{(11.00)^2}{1} = 121.0$$

Experimental α = 121.0

Theoretical* α = 121.0

The oscillograms of X" and X'" for the third mode are shown in Figure 5-19.

For the fourth mode solution the setting of V_a is of course more critical than for the third mode, so critical, in fact, that to get a solution to even furnish a value of d and L_d for the fourth mode is quite difficult with the equipment in use. From ten to fifty records were generally taken before a suitable solution was obtained, and to get enough points to determine a smooth curve such as shown in Figure 5-18 requires several hours time. However, enough values of d and L_d were obtained as a result of a good deal of perserverance to plot the curve shown in Figure 15-20.

From Figure 15-20

L = 11.89 C = 1/2

From equation (5-34)

$$\alpha = \frac{L^2}{\sqrt{C}} = \frac{(11.89)^2}{\sqrt{2}} = 199.2$$

Experimental α = 199.2

Theoretical* α = 200.0

B. Normal Modes of Oscillation of a Beam with Both Ends Clamped

A beam with both ends clamped is shown in Figure 5-21. As explained in Section 5.1A the end conditions on a beam of this type are

$$X(0) = X'(0) = X(L) = X'(L) = 0 , \qquad (5-36)$$

and from equation (5-33) we have

$$C \frac{d^4X}{d\bar{x}^4} - X = 0. \qquad (5\text{-}33)$$

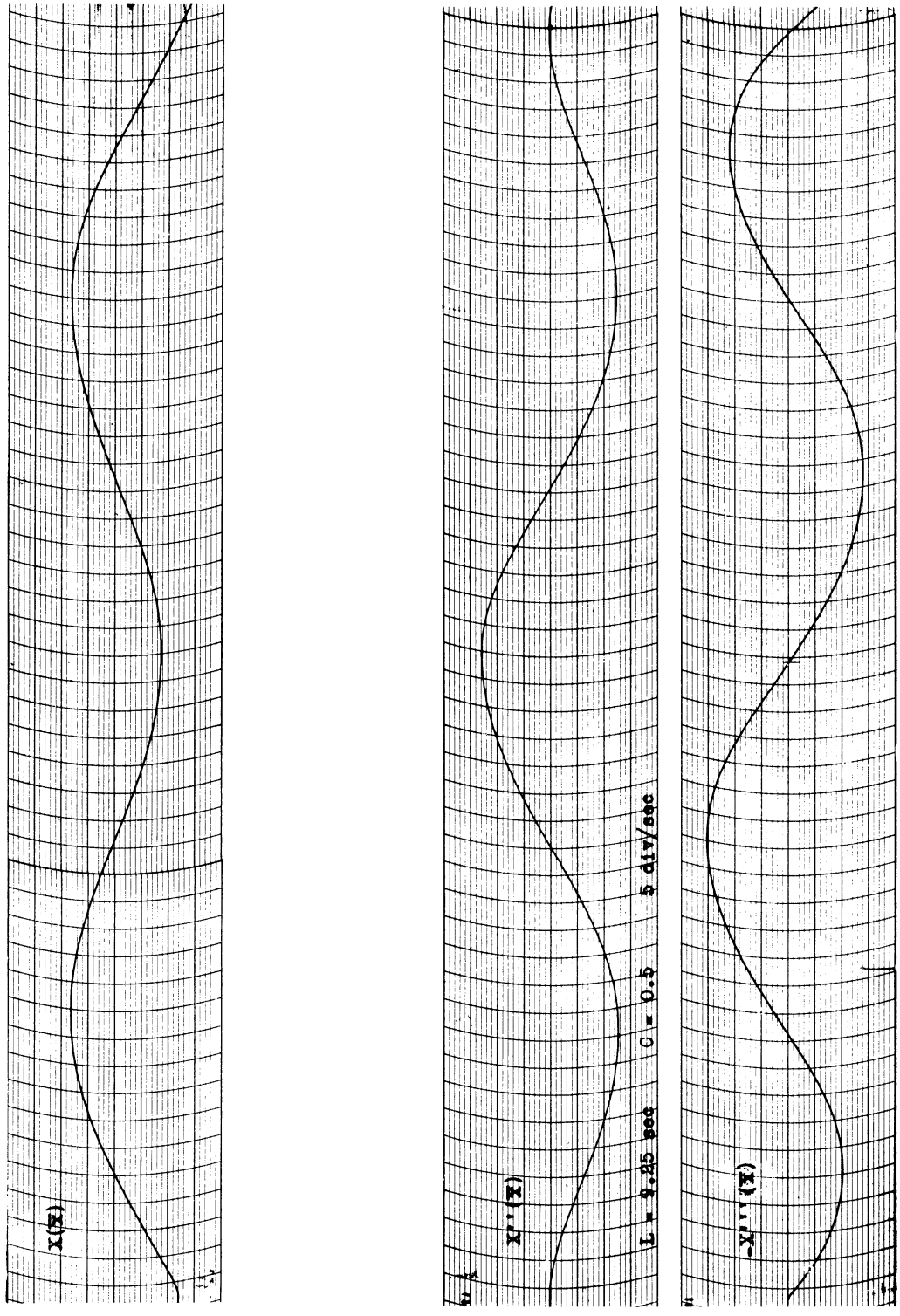

Figure 5-19. Third-mode solution for uniform "floating" beam.

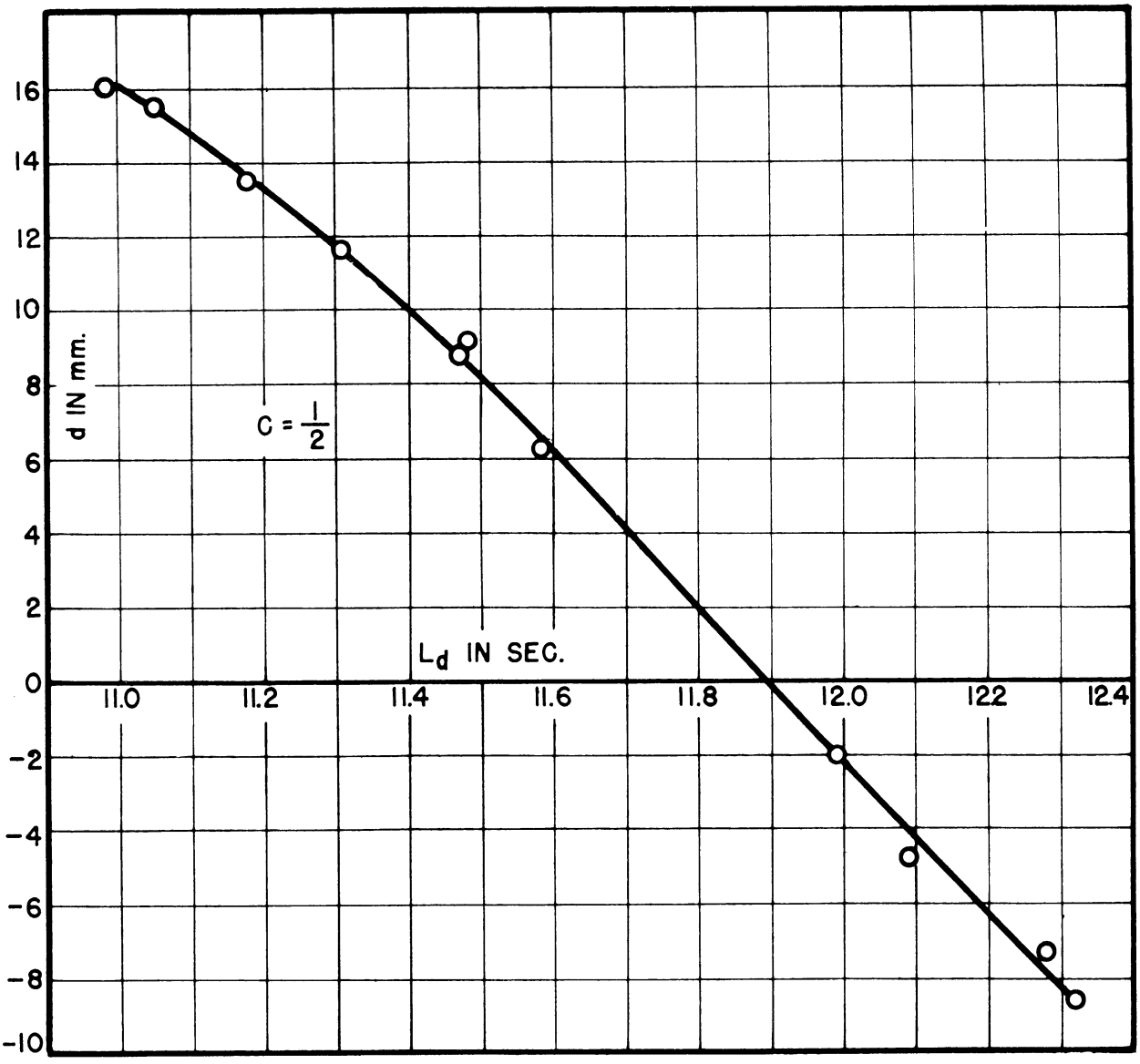

Figure 5-20. Interpolation curve for determining exact solution-length L for fourth mode.

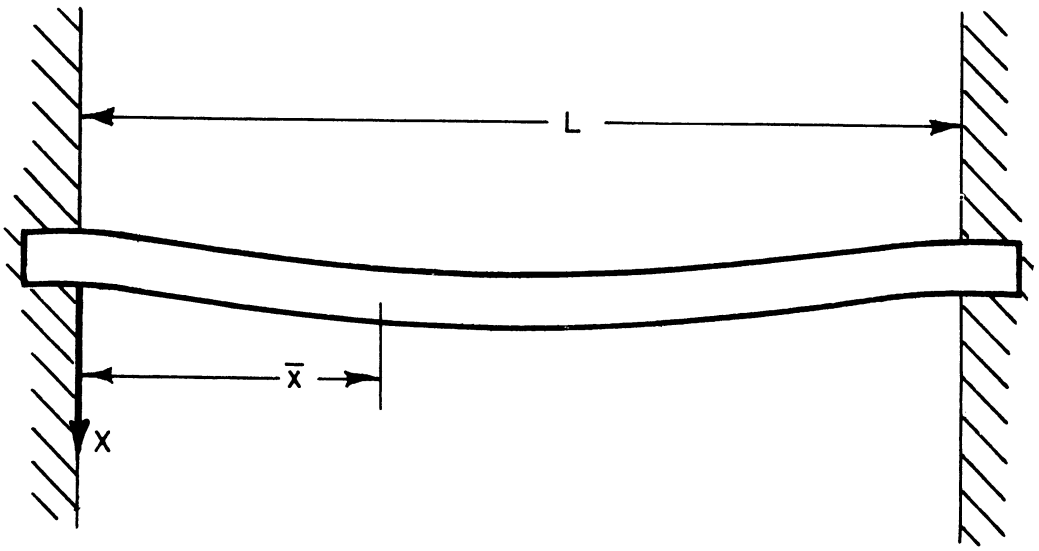

Figure 5-21. "Clamped-clamped" beam.

The computer circuit is exactly the same as the one shown in Figure 5-13 or Figure 5-14 except that the feedback capacitors of A_5 and A_6 are initially shorted, and that the feedback capacitors of A_3 and A_4 have the voltages V_a and V_b applied initially, V_a being variable by means of the potentiometer. As explained in Section 5.1A the initial voltage V_a is varied until a solution satisfying the desired end conditions is obtained. Since X' is the slope of X, both X' and X are zero when the minimum (or maximum, as required) of the X curve falls on the zero axis. The length L of the solution is then determined from the X' curve.

Oscillograms of the X, X" and X"' curves for the first mode are shown in Figure 5-22.

The following values of L were determined for the first mode:

4.740 sec
4.712
4.712

Av L = 4.721 sec C = 1

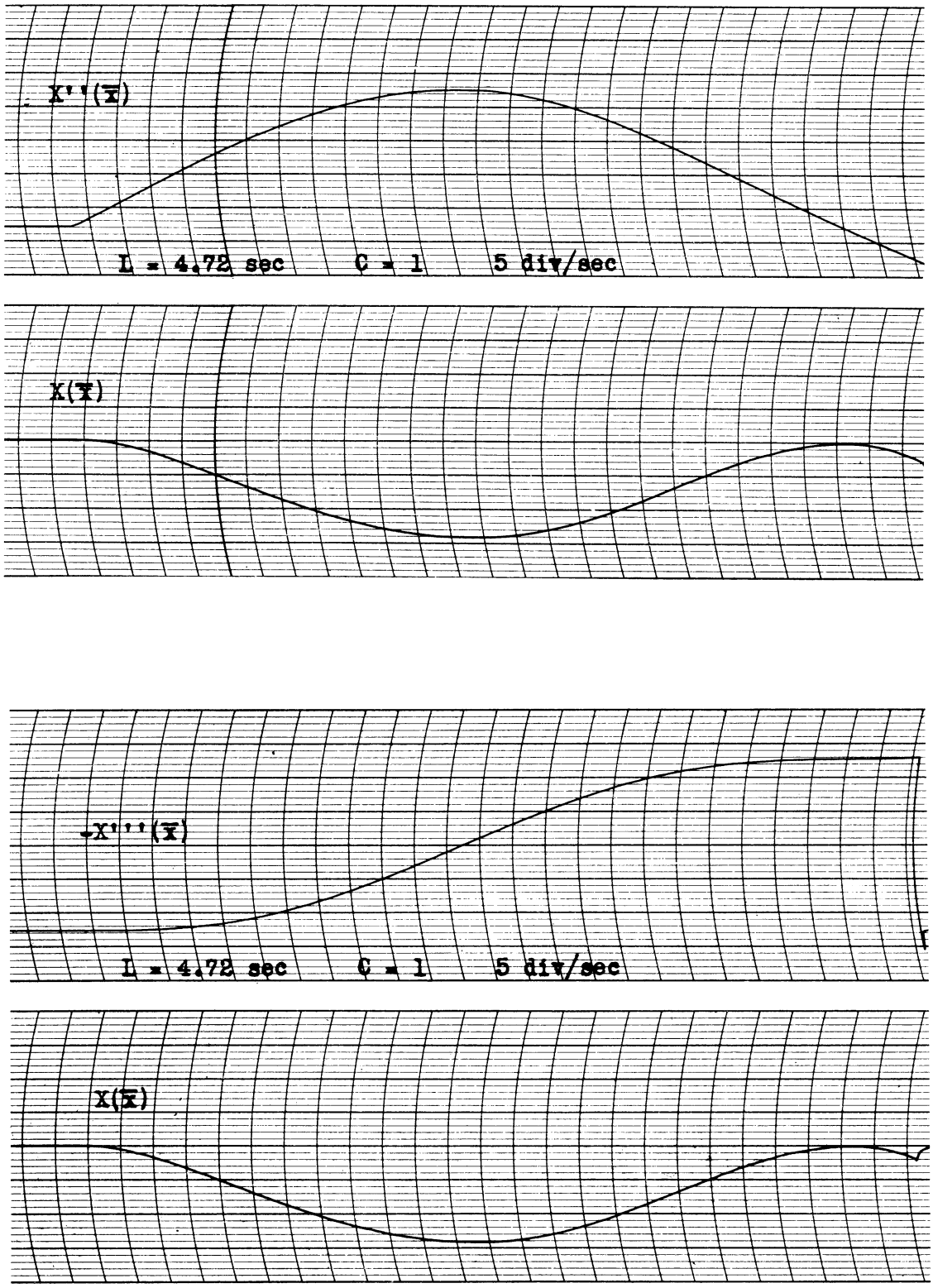

(a)

(b)

Figure 5-22. First-mode solution for uniform "clamped-clamped" beam.

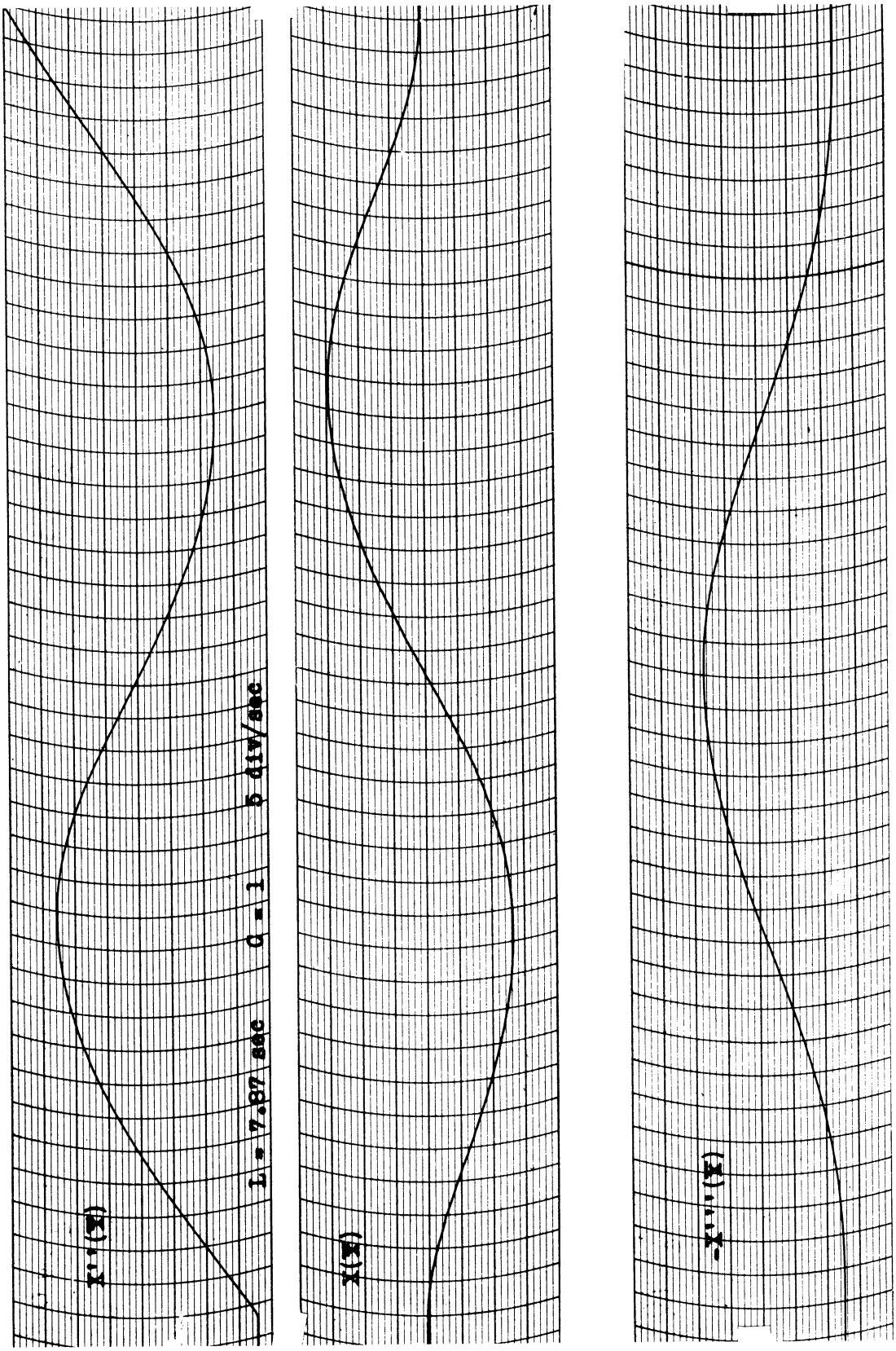

Figure 5-23. Second-mode solution for uniform "clamped-clamped" beam.

From equation (5-34)

$$\alpha = \frac{L^2}{\sqrt{C}} = \frac{(4.721)^2}{1} = 22.3$$

Experimental = 22.7

Theoretical* = 22.4

Oscillograms of the X, X" and X'" curves for the second mode are shown in Figure 5-23.

The length L for the second mode solution was determined from a curve similar to that in Figure 5-18. The calculations are as follows:

$$L = 7.87 \text{ sec} \qquad C = 1$$

From equation (5-34)

$$\alpha = \frac{L^2}{\sqrt{C}} = \frac{(7.87)^2}{1} = 61.9$$

Experimental α = 61.9

Theoretical* α = 61.7

C. Normal Modes of Oscillation of a Beam Hinged at Both Ends.

A beam hinged at both ends is shown in Figure 5-24.

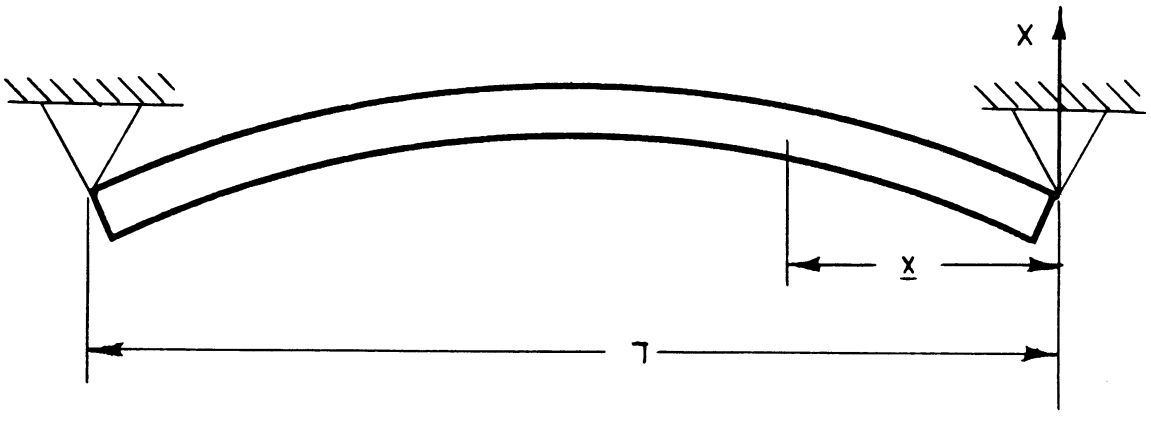

Figure 5-24. "Hinged-hinged" beam.

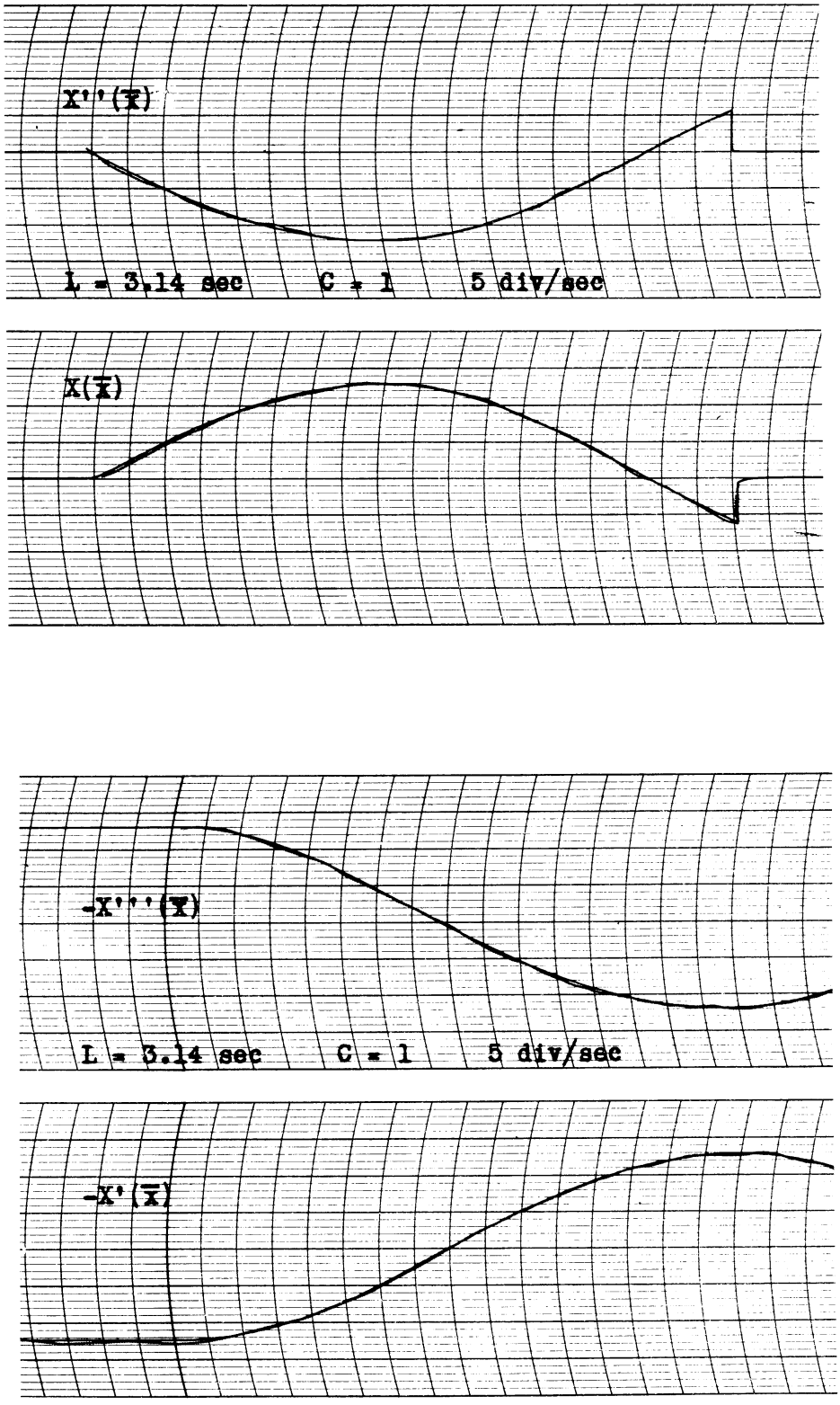

(a)

(b)

Figure 5-25. First mode solution for uniform "hinged-hinged" beam.

As discussed in Section.5.1B, the end conditions in this case are

$$X(0) = X''(0) = X(L) = X''(L) = 0 \qquad (5\text{-}37)$$

The equation to be solved by the computer is

$$C \frac{d^4X}{d\bar{x}^4} - X = 0 \qquad (5\text{-}33)$$

The computer circuit is the same as the one shown in Figure 5-13 or Figure 5-14 except that in this case the feedback capacitors of A_4 and A_6 are initially shorted, and the voltages V_a and V_b are initially applied to the feedback capacitors of A_3 and A_5, V_a being variable by means of the potentiometer

For determining a correct solution the X and X'' curves are recorded. The initial voltage V_a is varied until X and X'' cross the zero axis together. Since the radii of the arcs through which the recording pens swing may be slightly different (for our recorder a difference of about 0.06 mm) the lengths L_0 and L_2 of the solutions are measured on both X and X'' respectively, and then compared to see whether they are equal. If the difference is less than 0.02 sec the average of L_1 and L_2 is taken as the length L of the solution.

Oscillograms showing X, X', X'', and X''' for the first mode are shown in Figure 5-25. The experimental values of L which were determined are shown below

3.142 sec
3.132
3.132

Av L = 3.135 sec C = L

From equation (5-34)

$$\alpha = \frac{L^2}{\sqrt{C}} = \frac{(3.135)^2}{1} = 9.83$$

Experimental α = 9.83

Theoretical* α = 9.87

Oscillograms of X, X', and X'', and X''' for the solution of the second mode are shown in Figure 5-26. The following values of L were obtained:

6.292 sec
6.290

Av L = 6.29 C = L

From equation (5-34)

$$\alpha = \frac{L^2}{\sqrt{C}} = \frac{(6.29)^2}{1} = 39.6$$

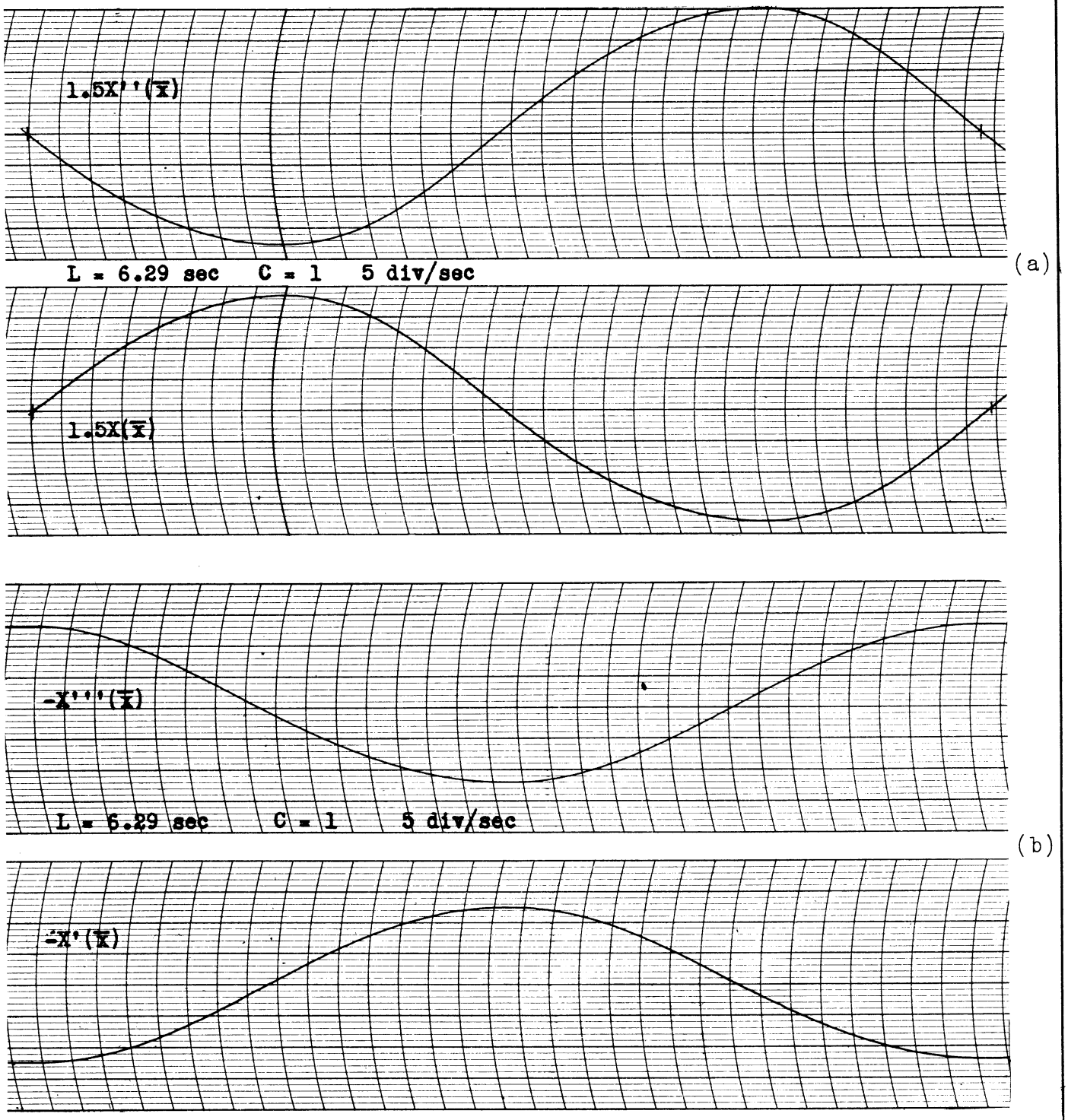

Figure 5-26. Second-mode solution for uniform "hinged-hinged" beam.

Experimental α = 39.6

Theoretical* α = 39.5

The X, X', X" and X"' curves as obtained from the computer for the solution of the third mode are shown in Figure 5-27. In the case of the third mode the setting of V_a has again become very critical, and repetition of solutions again becomes a considerable problem. As a way around this difficulty the same technique of extrapolation is used as was employed for the higher modes of the "free-free" beam.

We let L_o be the length of the X solution and L_2 be the length of the X" solution (see Figure 5-28) and we define $\triangle$ as $L_2 - L_o$. Denoting L_1 as $\frac{L_2 + L_o}{2}$ we can plot $\triangle$ vs. L_1 for different runs. Where the resulting curve crosses the $\triangle$ = 0 axis we have $L_2 = L_o = L$, and our end conditions of equation (5-37) are met. Using this technique we obtained the following value for L:

$$L = 9.44 \text{ sec} \qquad C = 1$$

From equation (5-34)

$$\alpha = \frac{L^2}{\sqrt{C}} = \frac{(9.44)^2}{1} = 89.1$$

Experimental α = 89.1

Theoretical* α = 88.9

In the case of the fourth mode the same procedure of interpolation to determine L is used as for the third mode. The experimental value of L was obtained:

$$L = 12.61.$$

From equation (5-34)

$$\alpha = \frac{L^2}{\sqrt{C}} = \frac{(12.61)^2}{1} = 159.0$$

Experimental α = 159.0.

Theoretical* α = 157.9

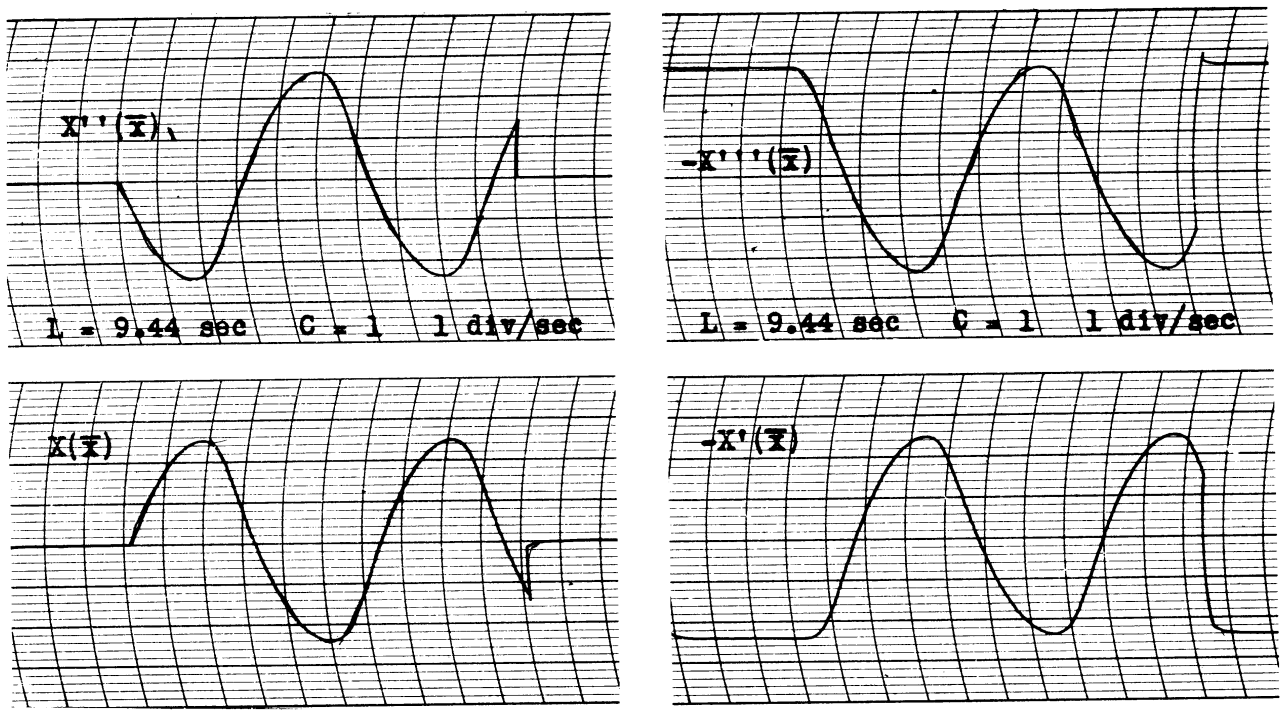

Figure 5-27. Third-mode solution for uniform "hinged-hinged" beam.

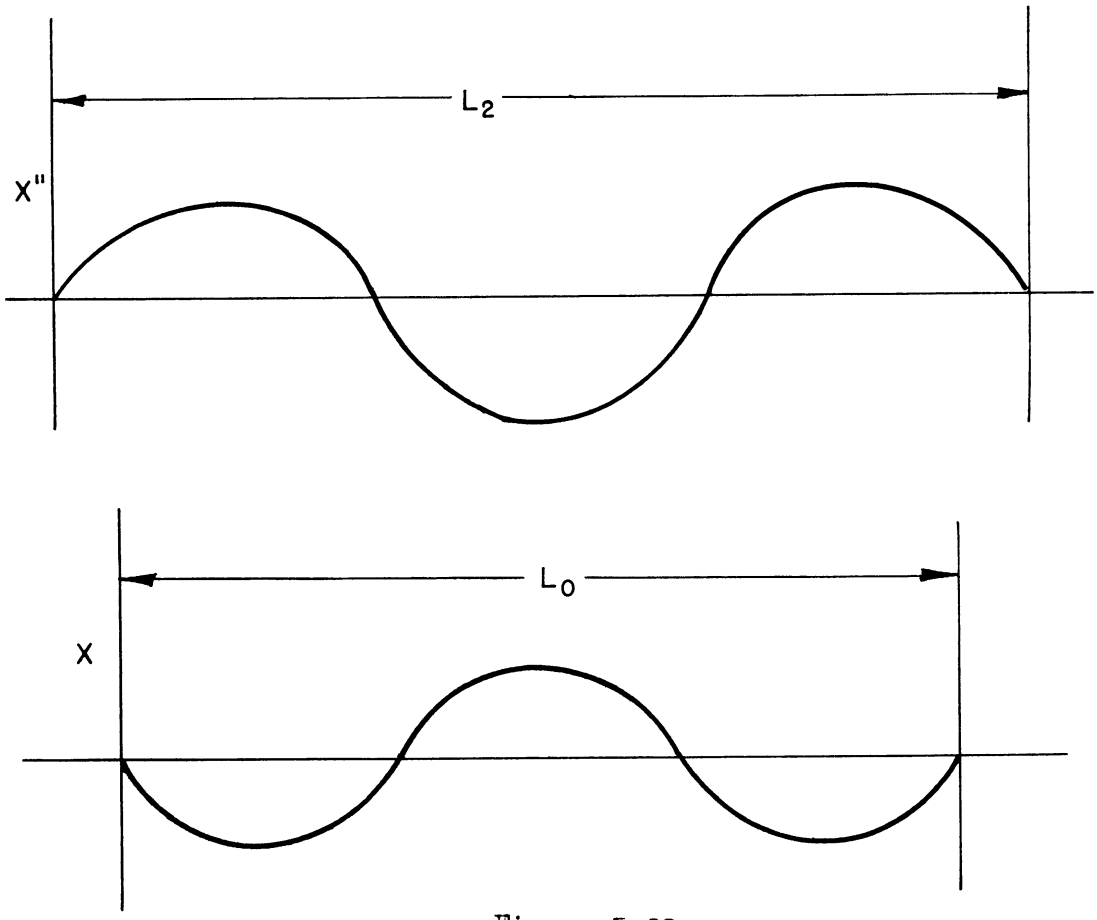

Figure 5-28.

D. Normal Modes of Oscillation of a Cantilever Beam

The cantilever beam is shown in Figure 5-29.

The end conditions (see Paragraph 5.1C) are as follows:

$$X(0) = X'(0) = X''(L) = X'''(L) = 0 \qquad (5\text{-}38)$$

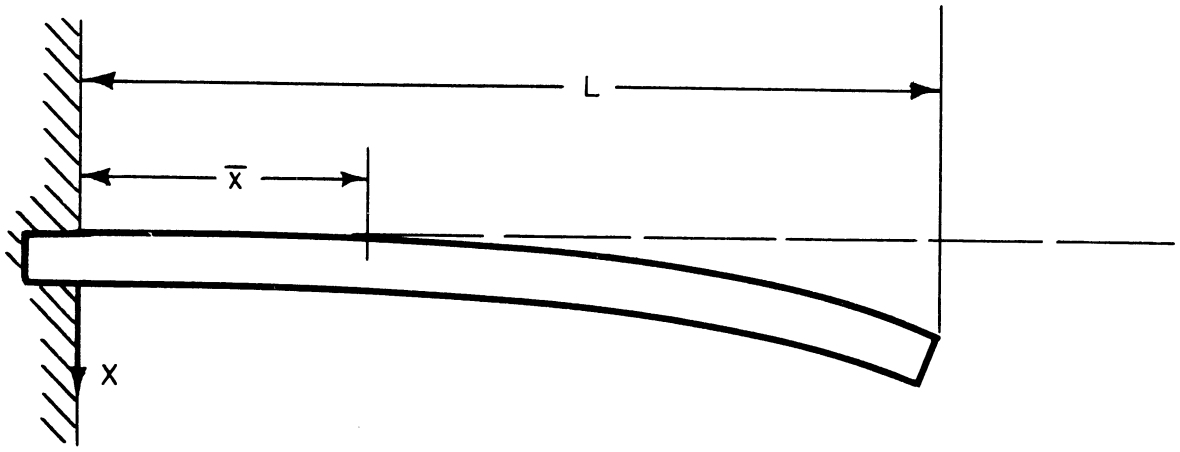

Figure 5-29. Cantilever beam.

The differential equation to be solved is

$$C \frac{d^4X}{d\bar{X}^4} - X = 0 \qquad (5\text{-}33)$$

The computer circuit for solving equation (5-33) with end conditions of equation (5-38) is exactly the same as the circuit of Figures 5-13 or 5-14 with the exception that the capacitors of A_5 and A_6 are initially shorted and that the voltages V_a and V_b are initially applied to the capacitors of A_3 and A_4. V_a is varied until the curves X'' and X''' are both zero at the same time, i.e., when the minimum or maximum of X'' lies on the zero axis. The length L of the solution is then measured, the beginning of L being taken from the X'' curve and the end from the X''' curve. Any pen-arc difference between the two pens must be considered.

The oscillograms of X, X', X'' and X''' are shown in Figure 5-30. The values of L as determined for the first mode were

1.89 sec
1.88
1.88

Av L = 1.88 sec C = 1

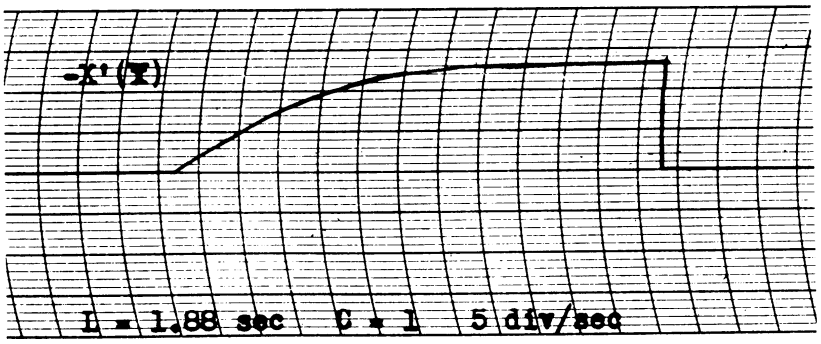

(a)

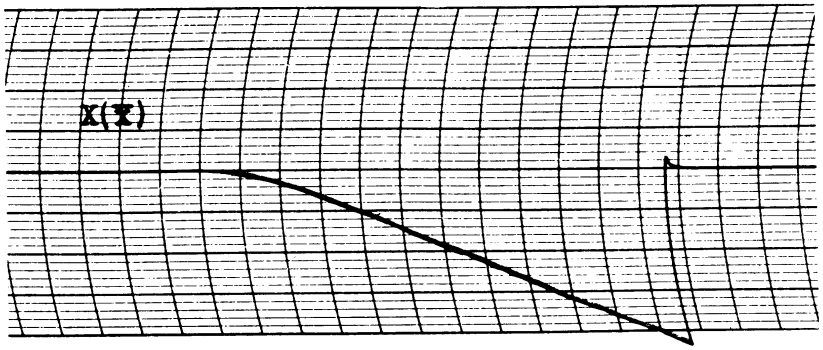

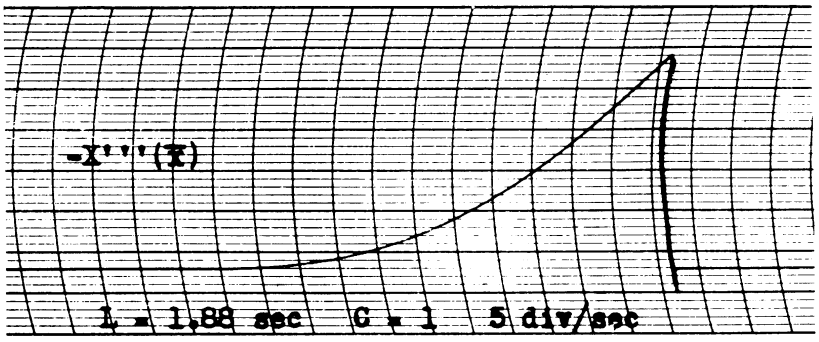

(b)

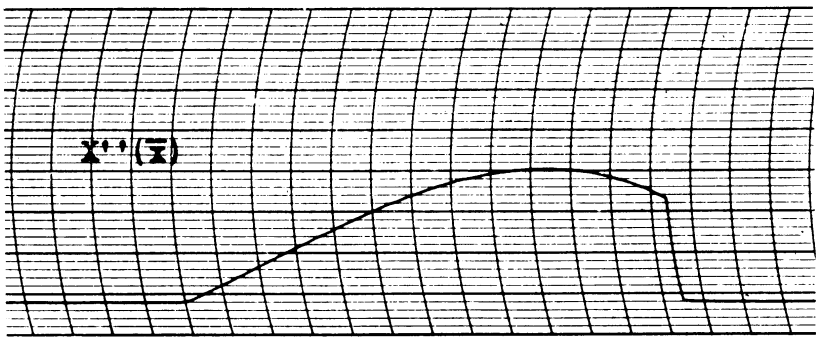

Figure 5-30. First-mode solution for uniform cantilever beam.

From equation (5-34)

$$\alpha^2 = \frac{L^2}{\sqrt{C}} = \frac{(1.88)^2}{1} = 3.53$$

Experimental α = 3.53

Theoretical* α = 3.52

The computer curves for X, X', X" and X'" for the second mode are shown in Figure 5-31. The experimental values of L were

4.728 sec
4.724

Av L = 4.73 C = 1

From equation (5-34)

$$\alpha^2 = \frac{L^2}{\sqrt{C}} = \frac{(4.73)^2}{1} = 22.4$$

Experimental = 22.4

Theoretical* = 22.4

The third mode curves for X, X" and X'" are given in Figure 5-32. The value of L was determined as

$L = 7.86_4$ sec C = 1

From equation (5-34)

$$\alpha = \frac{L^2}{\sqrt{C}} = \frac{(7.864)^2}{1} = 61.8$$

Experimental α = 61.8

Theoretical* α = 61.7

Summary of Results - Determination of Normal Modes of Oscillation of Uniform Beams.

Values of α

A. "Free-Free" Beam

	Experimentsl	Theoretical*
1st Mode	22.4	22.4
2nd Mode	61.6	61.7
3rd Mode	121.0	121.0
4th Mode	192.2	200.0

* Den Hartog, "Mechanical Vibrations", Appendix II, V.

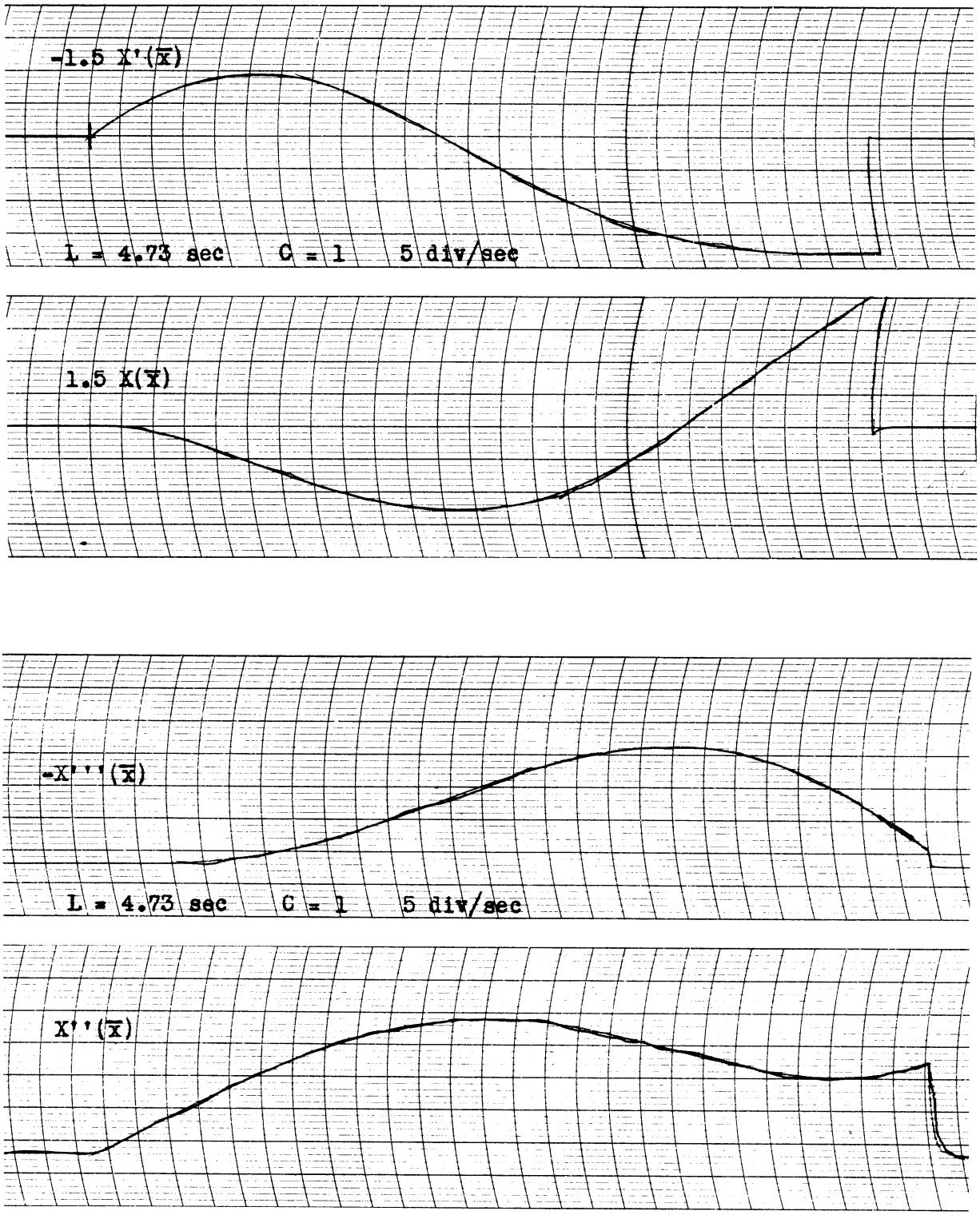

Figure 5-31. Second-mode solution for uniform cantilever beam.

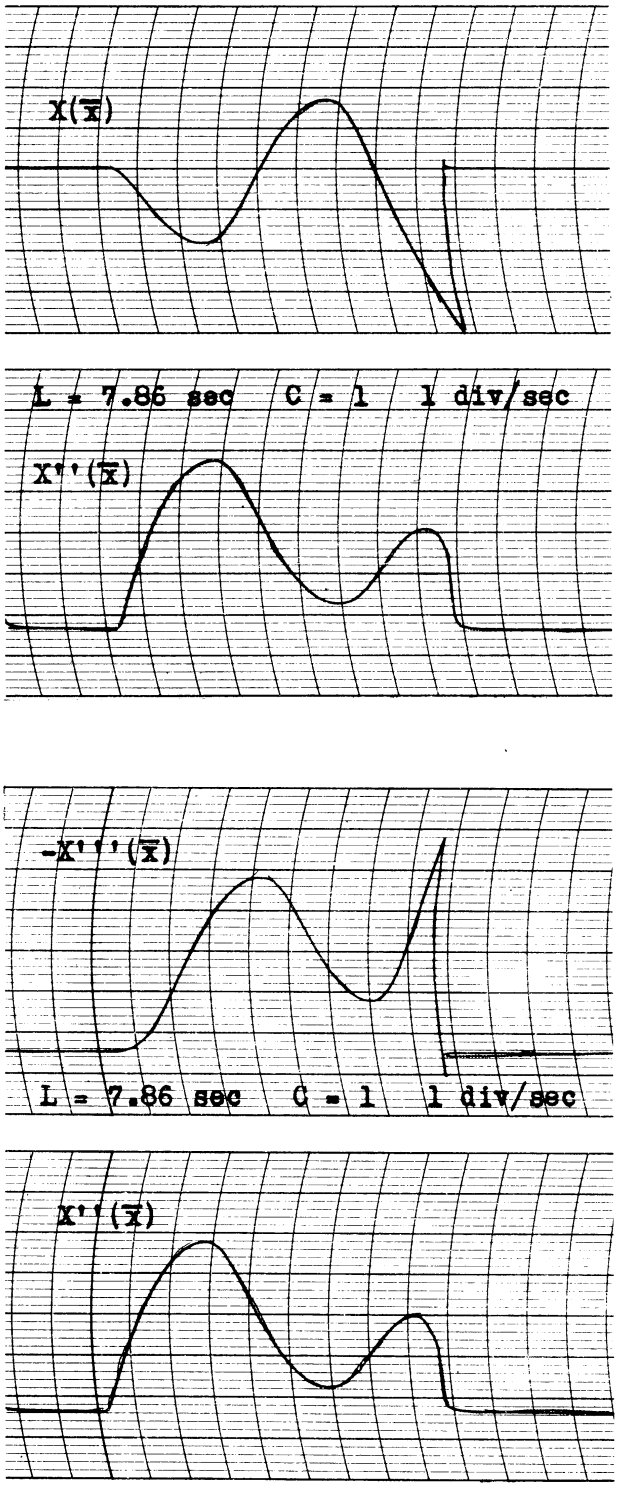

(a)

(b)

Figure 5-32. Third-mode solution for uniform cantilever beam.

B. Beam Clamped on Both Ends

	Experimental	Theoretical*
1st Mode	22.3	22.4
2nd Mode	61.9	61.7

C. Beam Hinged on Both Ends

	Experimental	Theoretical*
1st Mode	9.83	9.87
2nd Mode	39.6	39.5
3rd Mode	89.1	88.9
4th Mode	159.0	157.9

D. Cantilever Beam

	Experimental	Theoretical*
1st Mode	3.53	3.52
2nd Mode	22.4	22.4
3rd Mode	61.8	61.7

Note: frequency = $f = \frac{\alpha}{2\pi}\frac{EI}{\mu l^4}$

5.3 The Effect of Shearing Force and Rotary Inertia on the Normal Modes of Oscillation of Uniform Beams.

In Paragraph 5.2 we considered the cross-sectional dimensions of the uniform beam as small compared with the length, and we obtained equation (5-20) as the fundamental equation.

$$\frac{\partial^2}{\partial x^2}\left[EI\,\frac{\partial^2 y(x,t)}{\partial x^2}\right] = -\mu\,\frac{\partial^2 y(x,t)}{\partial t^2} \qquad (5\text{-}20)$$

However, for beams where the cross-sectional dimensions are not small in comparison with the length, or for modes of vibration of higher frequencies, it is of considerable importance to consider the effect of shear forces and rotary inertia. Considering these forces the differential equations for lateral vibration of a uniform beam becomes [8]

$$EI\frac{\partial^4 y}{\partial x^4} + \mu\frac{\partial^2 y}{\partial t^2} - \frac{\mu}{A}\left(I + \frac{EI}{k'G}\right)\frac{\partial^4 y}{\partial x^2\,\partial t^2} + \frac{\mu^2 I}{A^2 k'G}\frac{\partial^4 y}{\partial t^4} = 0 \qquad (5\text{-}39)$$

where k' is a numerical factor depending on the shape of the cross section and G is the modulus of elasticity in shear.

For studying the normal modes of oscillation we assume that

$$y(x,t) = X(x)e^{j\lambda t} \quad . \tag{5-21}$$

Substituting y(x,t) as given by equation (5-21) in equation (5-39) we obtain

$$EI\frac{d^4X}{dx^4} + \lambda^2\frac{\mu}{A}\left(I + \frac{EI}{k'G}\right)\frac{d^2X}{dx^2} - \lambda^2\mu\left(1 - \frac{\lambda^2\mu I}{A^2k'G}\right)X = 0, \tag{5-40}$$

where $0 < x < \ell$, ℓ being the length of the beam. We wish to change the independent variable so that $0 < \bar{x} < L$ and hence we write that

$$x = \frac{\ell}{L}\bar{x} \quad , \tag{5-41}$$

from which

$$\frac{d^n}{dx^n} = \frac{L^n}{\ell^n}\frac{d^n}{d\bar{x}^n} \tag{5-42}$$

Then equation (5-40) becomes

$$\frac{EIL^4}{\ell^4}\frac{d^4X}{d\bar{x}^4} + \frac{\lambda^2\mu L^2}{A\ell^2}\left(I + \frac{EI}{k'G}\right)\frac{d^2X}{d\bar{x}^2} - \lambda^2\mu\left(1 - \frac{\lambda^2\mu I}{A^2k'G}\right)X = 0 \tag{5-43}$$

Dividing equation (5-43) by $\lambda^2\mu$ we obtain

$$\frac{EIL^4}{\lambda^2\mu\ell^4}\frac{d^4X}{d\bar{x}^4} + \frac{IL^2}{A\ell^2}\left(1 + \frac{E}{k'G}\right)\frac{d^2X}{d\bar{x}^2} - \left(1 - \frac{\lambda^2\mu I}{A^2k'G}\right)X = 0. \tag{5-44}$$

We introduce the following dimensionless parameters:

$$m = \frac{E}{k'G} \quad , \tag{5-45}$$

$$R = \frac{\text{radius of gyration}}{\text{length of beam}} = \frac{1}{\ell}\sqrt{\frac{I}{A}} \quad , \tag{5-46}$$

and

$$\alpha = \lambda \sqrt{\frac{\mu \ell^4}{EI}} \qquad (5\text{-}47)$$

Rewriting equation (5-44) in terms of these parameters we get

$$\frac{L^4}{\alpha^2} \frac{d^4X}{d\bar{x}^4} + R^2L^2 (1 + m) \frac{d^2X}{d\bar{x}^2} - (1 - \alpha^2 m R^4) X = 0$$

Dividing through by $1 - \alpha^2 mR^4$ it follows that

$$\frac{L^4}{\alpha^2(1 - \alpha^2 mR^4)} \frac{d^4X}{d\bar{x}^4} + \frac{R^2L^2(1 + m)}{1 - \alpha^2 mR^4} \frac{d^2X}{d\bar{x}^2} - X = 0, \qquad (5\text{-}48)$$

where $0 \leq \bar{x} \leq L$

For purposes of analysis by means of the computer we rewrite equation (5-48) as

$$\frac{L^4}{\bar{\alpha}^2} \frac{d^4X}{d\bar{x}^4} + \frac{L^2}{N} \frac{d^2X}{d\bar{x}^2} - X = 0, \qquad (5\text{-}49)$$

where

$$\bar{\alpha}^2 = \alpha^2 (1 - \alpha^2 m R^4) \qquad (5\text{-}50)$$

and

$$\frac{1}{N} = \frac{R^2 (1 + m)}{1 - \alpha^2 m R^4} \qquad (5\text{-}51)$$

If as in equation (5-32) we let

$$C = \frac{L^4}{\bar{\alpha}^2} \qquad (5\text{-}52)$$

and

$$D = \frac{L^2}{N} , \qquad (5\text{-}53)$$

Equation (5-49) becomes

$$C \frac{d^4X}{d\bar{x}^4} + D \frac{d^2X}{d\bar{x}^2} - X = 0. \qquad (5\text{-}54)$$

Equation (5-54) is what we set up on the computer. For a "free-free" beam the end conditions are[9]

$$X''(0) = X'''(0) = X''(L) = X'''(L) = 0. \tag{5-35}$$

The computer circuit for solving equation (5-54) with the end conditions of equation (5-35) is shown in Figure 5-33. The initial voltage V_a is varied until the end condition $X''(L) = X'''(L)$ is satisfied. The length L is then measured from the X''' curve, and $\bar{\sigma}$ and N are calculated from the following formulas derived from equations (5-52) and (5-53):

$$\bar{\sigma} = \frac{L^2}{\sqrt{C}} \tag{5-55}$$

$$N = \frac{L^2}{D} \tag{5-56}$$

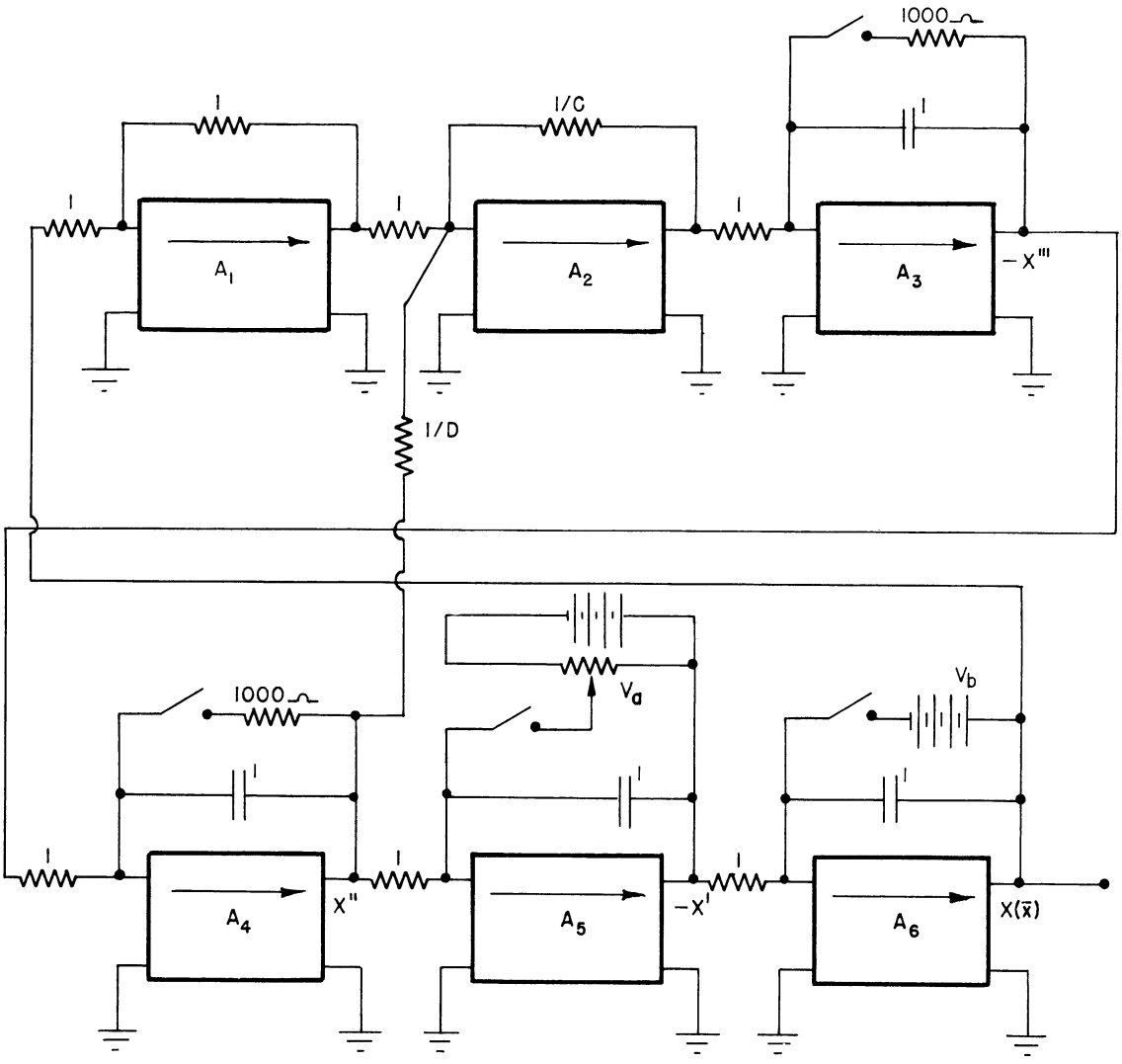

Figure 5-33. Computer circuit for obtaining normal mode solutions where shear and rotary forces are considered.

The constant D is varied on the computer in order to calculate the values of $\bar{\alpha}$ for a wide range of N. In each case the length L of the solution is measured and N and $\bar{\alpha}$ are calculated. The effect of the constant D is to make L shorter, i.e., to lower $\bar{\alpha}$. Enough solutions of $\bar{\alpha}$ and N were obtained for various values of D to enable a continuous curve to be drawn representing $\bar{\alpha}$ vs N for a wide range of N. Curves of this type as obtained from computer data are shown in Figure 5-34 for the first four modes.

It should be remarked here that the effect of the additional feedback loop $D\frac{d^2X}{d\bar{x}^2}$ in the computer is to make the value of V_a much less critical. Naturally, the larger the value of D, the less critical V_a will be. For $D > 0.5$ it is fairly easy to get exact solutions of the third mode and for $D > 2$, exact solutions of the fourth mode are possible. For small values of D the method of interpolation described in Section 5.2A was used in obtaining the length L for higher modes.

In Figure 5-35 the percentage change in $\bar{\alpha}$ due to the ratio N is plotted for the first four modes. In this case

$$\% \text{ change} = \frac{\bar{\alpha}_0 - \bar{\alpha}}{\bar{\alpha}} 100 \text{ where } \bar{\alpha}_0 \text{ is the frequency constant } \alpha \text{ for } D = 0 \text{ (i.e., } R = 0) \text{ as obtained in Section 5.2A.}$$

We will now derive R in terms of N and $\bar{\alpha}$. Multiplying equation (5-50) by equation (5-51) we find that

$$\frac{\bar{\alpha}^2}{N} = R^2 \alpha^2 (1 + m), \tag{5-57}$$

From equation (5-51)

$$\alpha^2 = \frac{1}{mR^4} \left[1 - NR^2 (1 + m)\right] . \tag{5-58}$$

Substituting the expression for α^2 given in equation (5-58) into equation (5-57) we obtain

$$\frac{\bar{\alpha}^2}{N} = \frac{(1 + m)}{mR^2} - \frac{N(1 + m)^2}{m} ,$$

from which

$$R^2 = \frac{1}{\frac{m\bar{\alpha}^2}{N(1 + m)} + N(1 + m)} \tag{5-59}$$

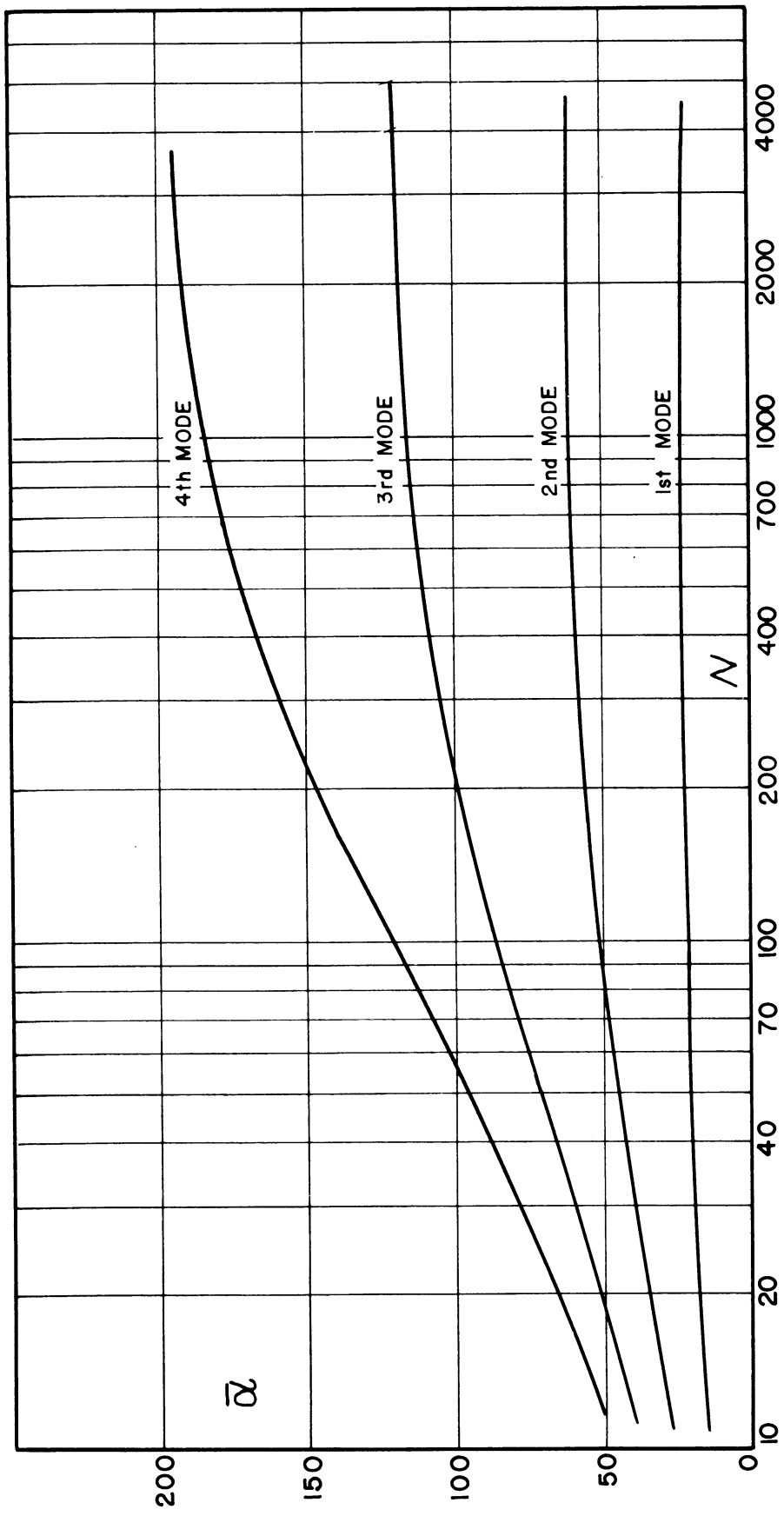

Figure 5-34. $\bar{\alpha}$ vs N for the first four modes.

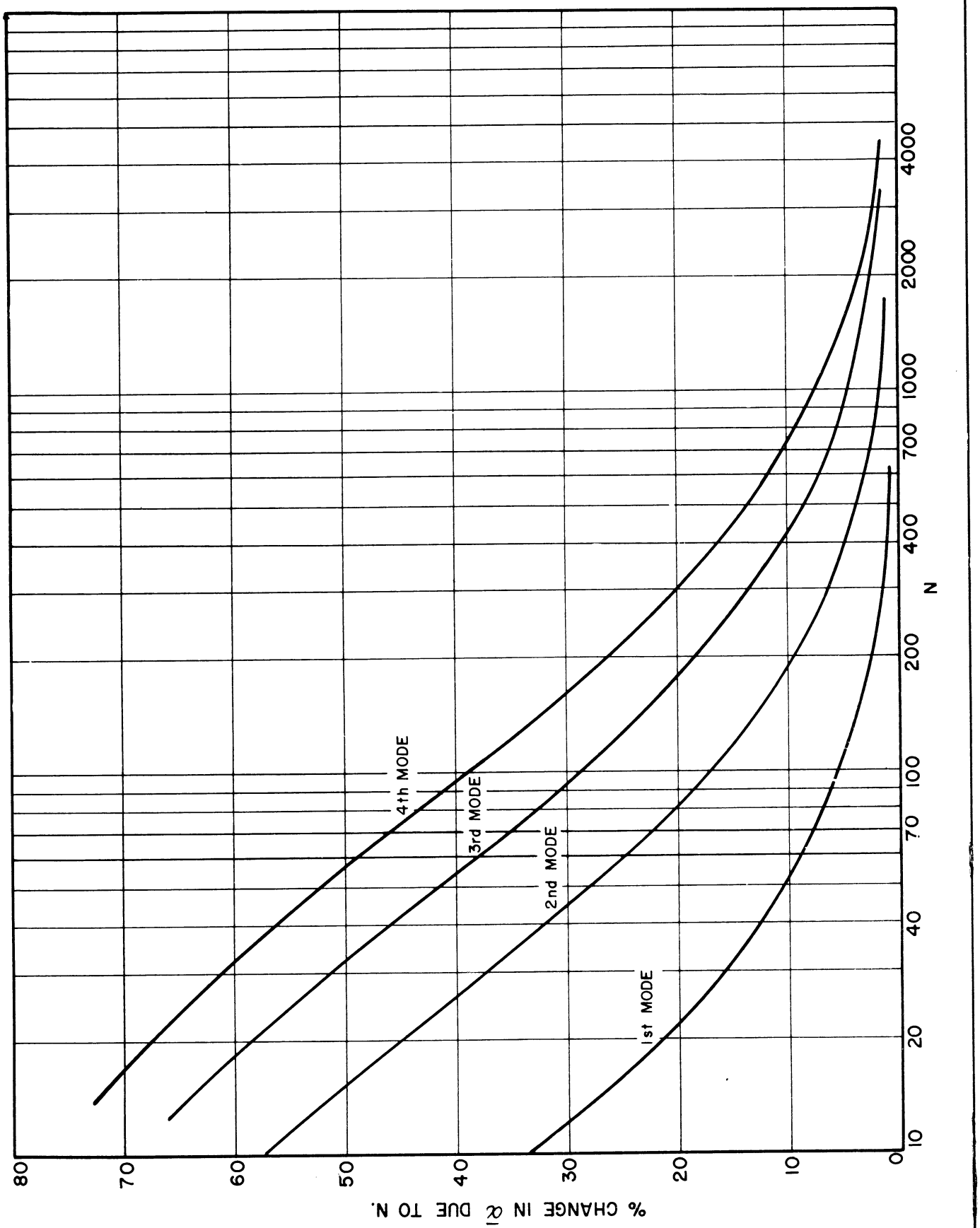

Figure 5-35. Percentage change in $\bar{\alpha}$ due to N, plotted against N for the first four modes.

From equation (5-57) we have

$$\alpha = \frac{\bar{\alpha}}{R\sqrt{N(1+m)}}, \qquad (5\text{-}60)$$

and from equations (5-59) and (5-60)

$$\alpha = \bar{\alpha}\sqrt{\frac{m\bar{\alpha}^2}{[N(m+1)]^2} + 1}. \qquad (5\text{-}61)$$

Knowing the relationship between $\bar{\alpha}$ and N from the curves in Figure 5-34 or Figure 5-35, we can calculate the curves for α vs R from equations (5-59) and (5-60) for any particular type of beam. As an example, we calculated the α vs R curves for a steel beam of rectangular cross-section. The following values of the constants were used to calculate m:

$$E = 30 \times 10^6 \text{ lbs/in}^2$$

$$G = 12 \times 10^6 \text{ lbs/in}^2$$

$$k' = 2/3$$

Then from equation (5-45)

$$m = \frac{E}{k'G} = \frac{30}{2/3 \times 12} = \frac{30}{8} = 3.75$$

For m = 3.75 equations (5-59) and (5-60) become

$$R^2 = \frac{1}{0.79\,\frac{\bar{\alpha}^2}{N} + 4.75N}$$

and

$$\alpha = \frac{0.459\,\bar{\alpha}}{R\sqrt{N}}$$

The curves of α vs R for a rectangular steel beam are shown in Figure 5-36. Oscillograms of $X(\bar{x})$ and $X''(\bar{x})$ for various values of R are shown in Figures 5-37, 5-38, 5-39 and 5-40 for the first, second, third, and fourth modes respectively. Note how the $X(\bar{x})$ curve flattens out as the beam gets stubbier (i.e., as R gets larger). In fact for the first and third modes the $X(\bar{x})$ curve actually stays entirely on one side of the axis for larger values of R. This of course cannot be the actual physical case since it would mean that the center of gravity of the beam would no longer be fixed. The reason for this discrepancy is that the end conditions, equation (5-35) given by Timoshenko are incorrect. The correct end conditions for a free-free beam are that the bending moment M and shearing force V are zero at both ends. When shear and rotary inertia are considered, these are no longer proportional to the second and third derivatives respectively but are given by:[10]

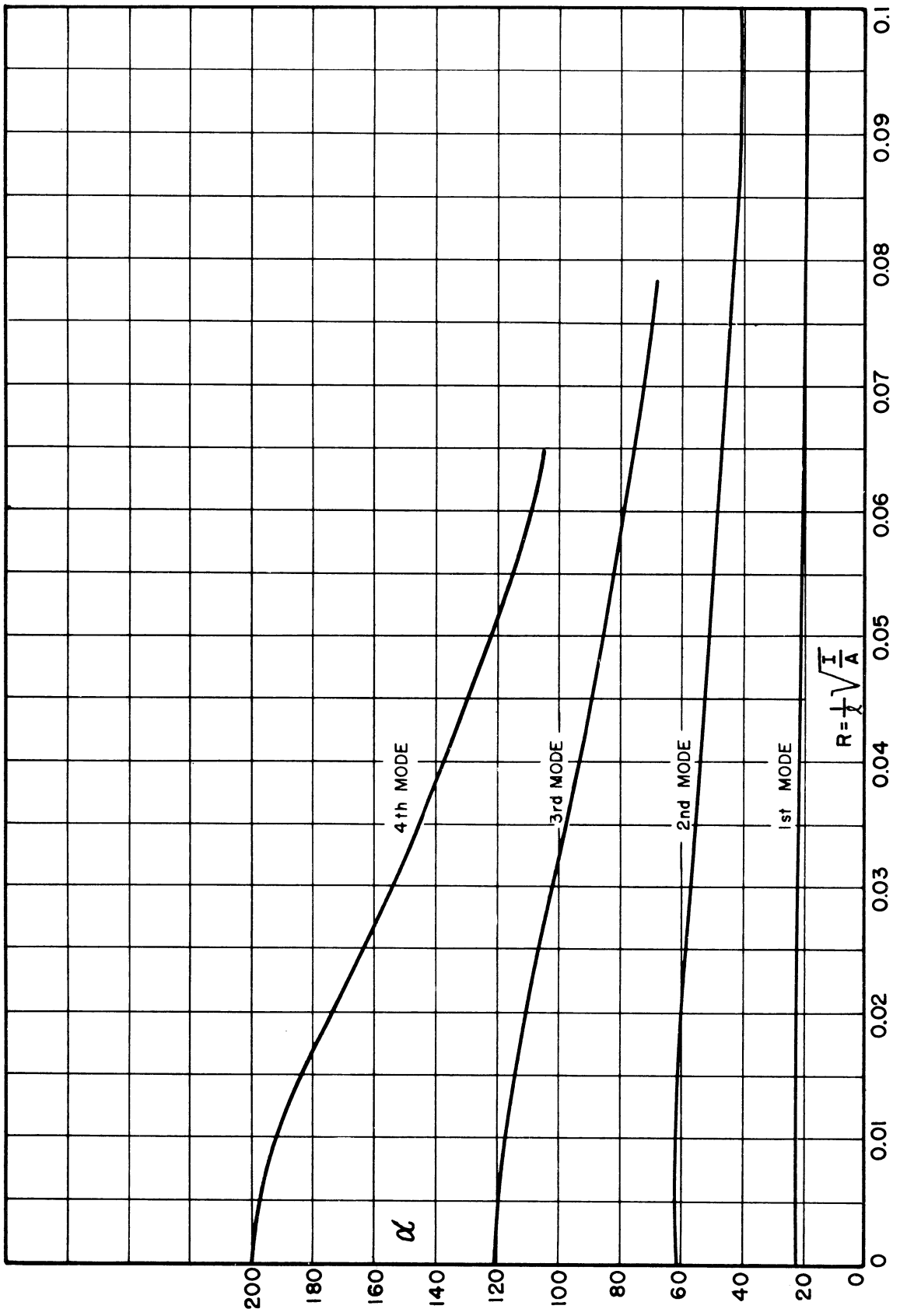

Figure 5-36. α vs R for a uniform rectangular steel beam.

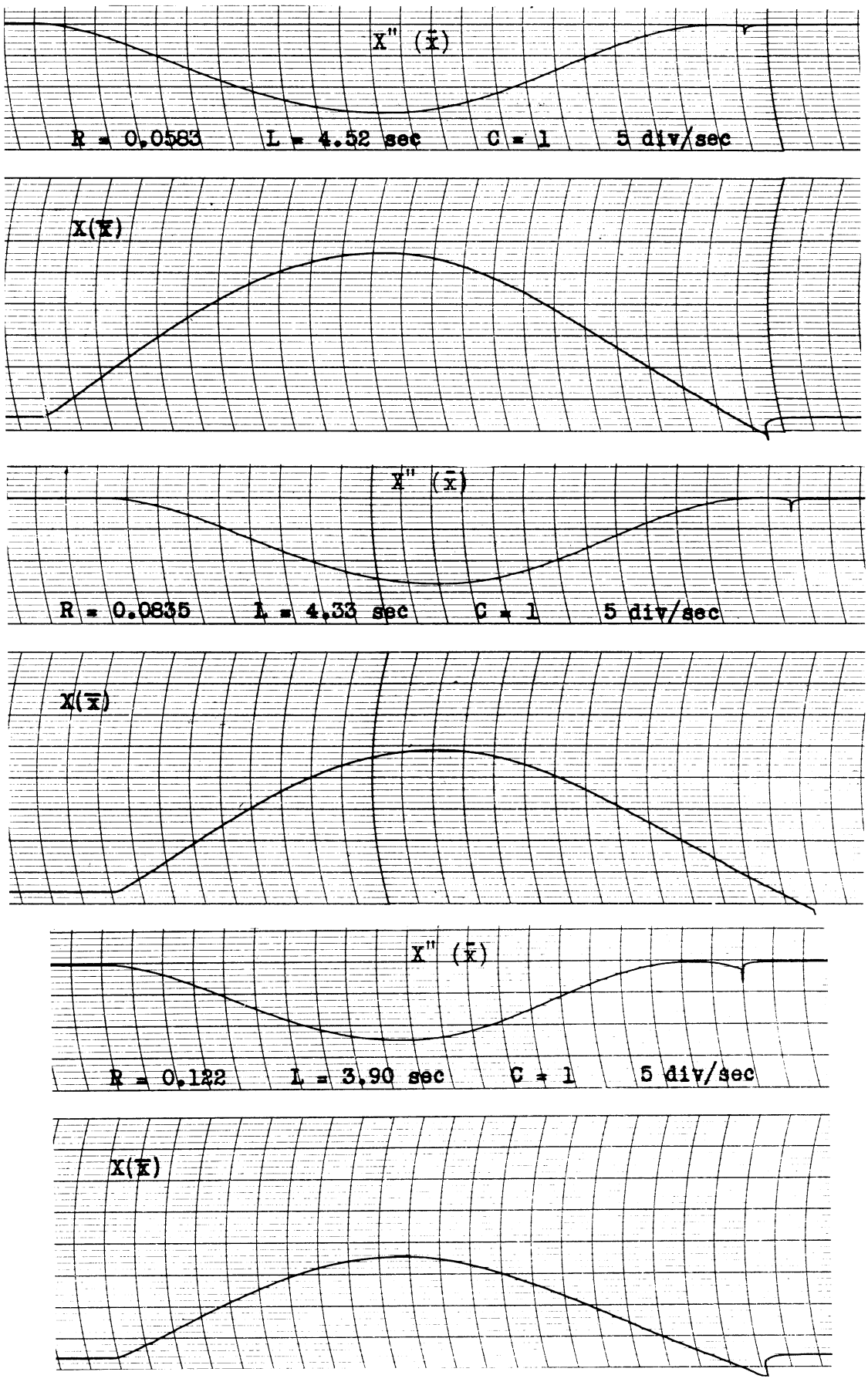

Figure 5-37. First-mode solutions considering shear and rotary inertia forces.

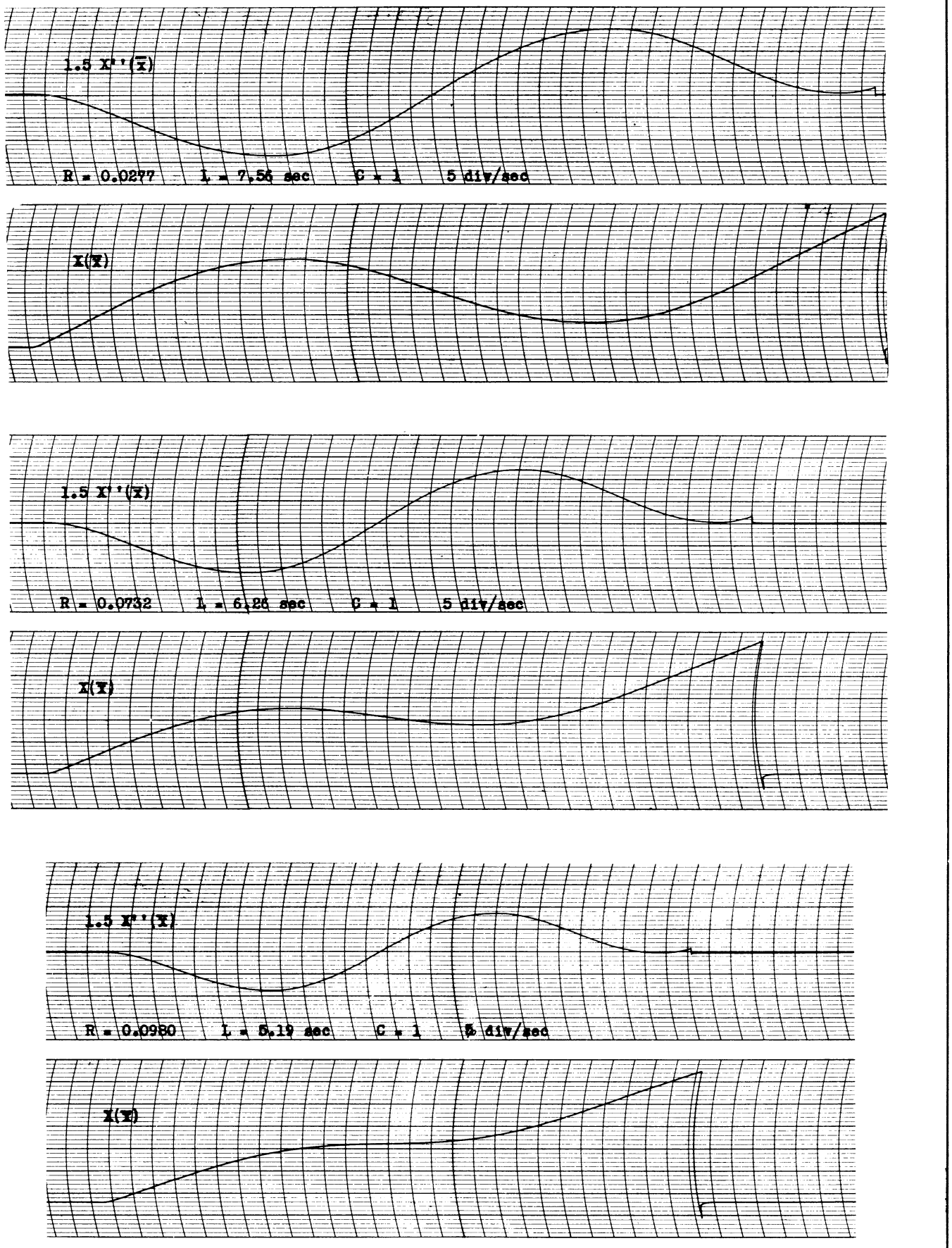

Figure 5-38. Second-mode solutions considering shear and rotary inertia forces.

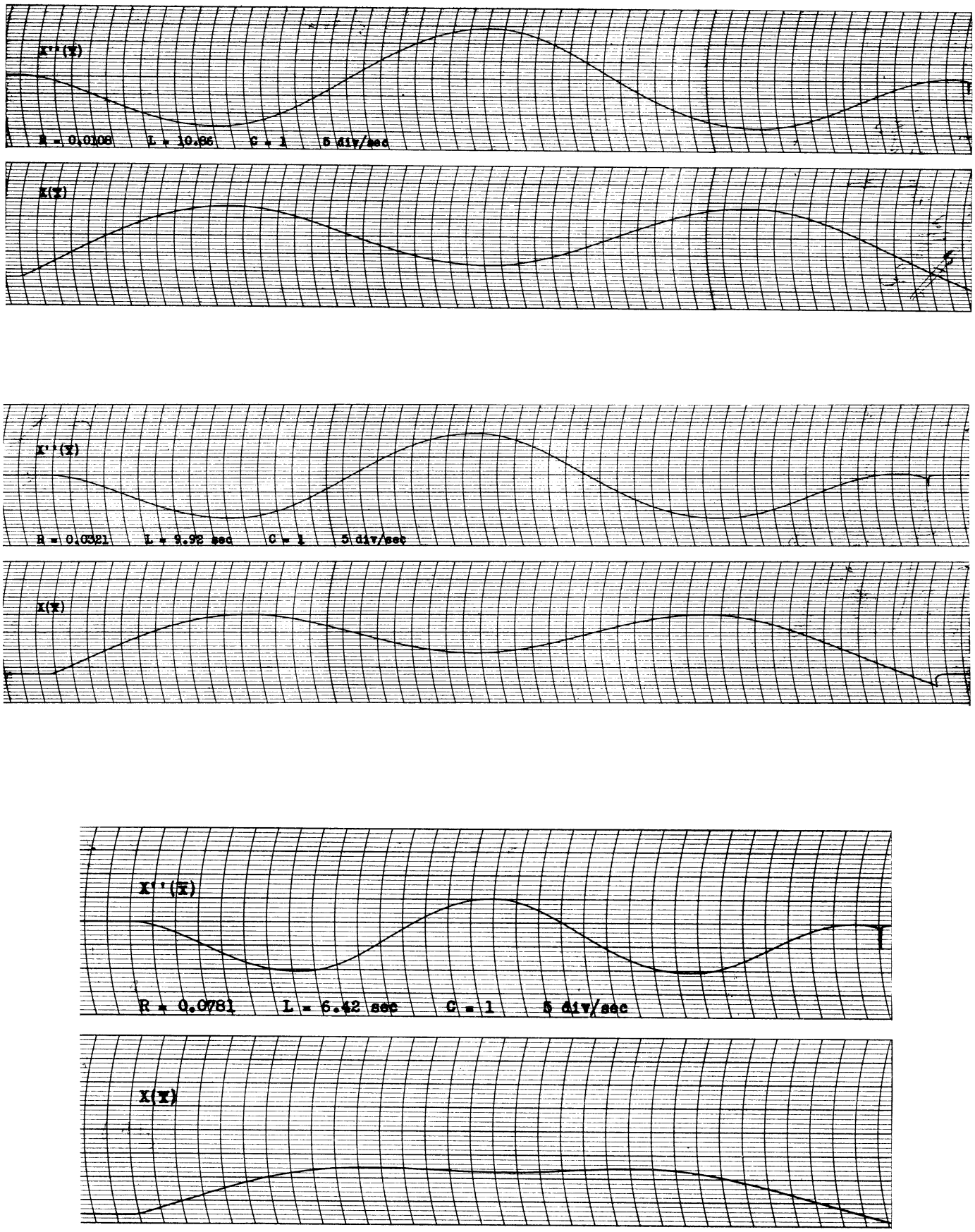

Figure 5-39. Third-mode solutions considering shear and rotary inertia forces.

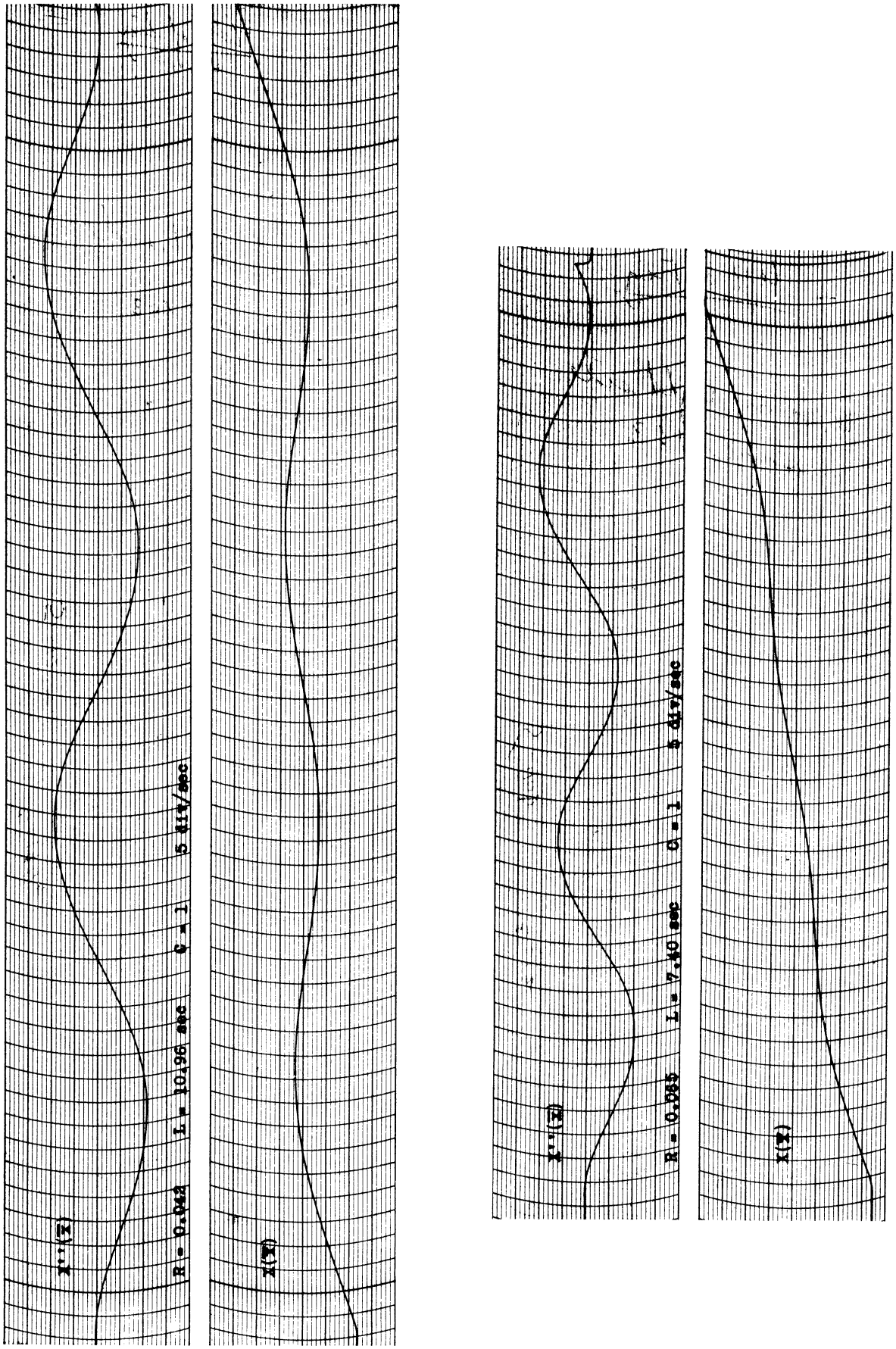

Figure 5-40. Fourth-mode solutions considering shear and rotary inertia forces.

$$M = EI \left(\frac{\partial^2 y}{\partial x^2} + \frac{\rho \lambda^2}{k'AG} y \right) \qquad (5\text{-}62)$$

$$V = \left(\frac{EI}{1 - \frac{\rho I \lambda^2}{k'AG}} \right) \left(\frac{\partial^3 y}{\partial x^2} + \left(\frac{\rho \lambda^2}{k' AG} + \frac{\rho \lambda^2}{E} \right) \frac{\partial y}{\partial x} \right) \qquad (5\text{-}63)$$

How much these inaccuracies effect the frequencies of oscillation is a question which must be investigated further.

5.4 Measurement Techniques in the Solution of Vibrating-Beam Problems.

In paragraphs 5.2 and 5.3 the frequencies of normal modes of vibration of uniform beams were determined using the analog computer. The solution of the problem involved finding the length L between satisfied end conditions. The frequency constant δ then varied as L^2 (see equation 5-34). Hence the accuracy of the measurement of L is of great importance in determining the accuracy of δ In order to measure L on the recorder chart-paper an output is selected which has a finite slope at the ends of the beam, such as the X"' curve in the case of the "free-free" beam.

This makes it possible to determine accurately where the curve crosses the zero axis. Due apparently to a small pen-lag, the X"' curve for a "free-free" beam is slightly rounded at the beginning instead of appearing as a sharp, clean angle when it changes from zero slope to a finite slope. In order to get accurate starting point, we extend the first part of the curve back to the origin along a straight line and take this crossover point as our starting point. Reference to Figure 5-41 will clarify this.

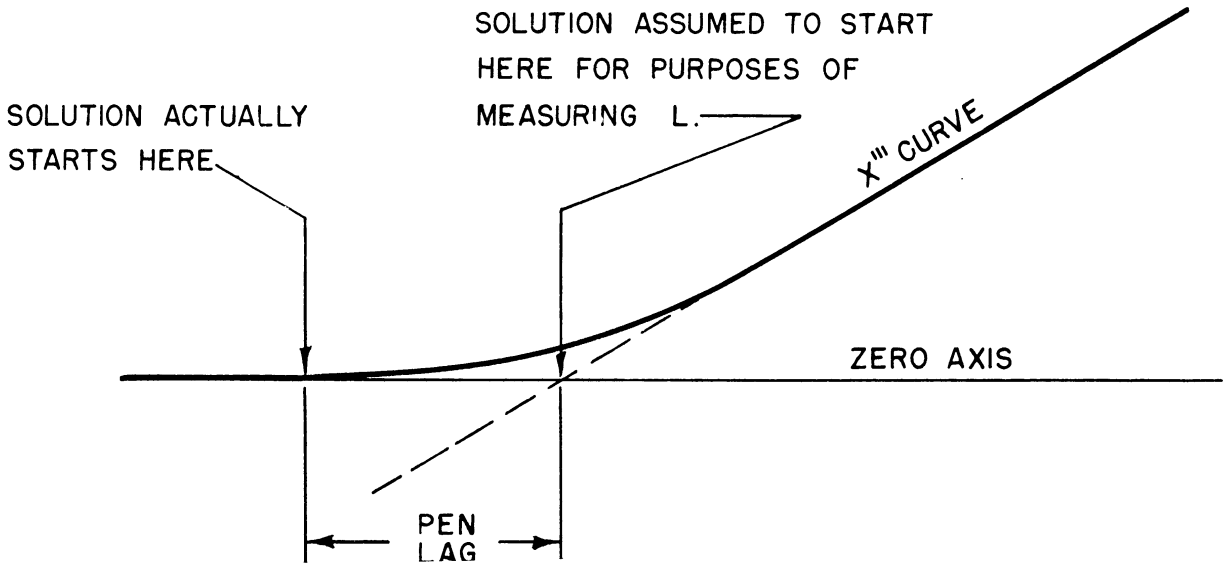

Figure 5-41. Pen-lag effect, greatly exaggerated.

Since the X'" curve crosses the zero axis at the end of the solution with the same slope it had at the beginning, the pen lag should be the same and the error will cancel out. Actually, this pen lag only amounts to between 0.02 and 0.04 second when the recorder is run on medium speed (5 divisions per second). But since our results indicate that we are measuring the length L correctly to within 0.02 second, the pen lag is a measurable effect.

One possible alternative method of overcoming the pen-lag effect is to increase the gain of the X"' input to the recorder by a large factor, while at the same time clipping off the amplitudes which would force the pen off scale. In Figure 5-42 is shown an oscillogram using this technique. The clipping was achieved by loading the output of the intermediate selective-gain amplifier with 25,000 ohms. Note that the X"' curve crosses the axis almost at right angles, since the gain factor is 20.

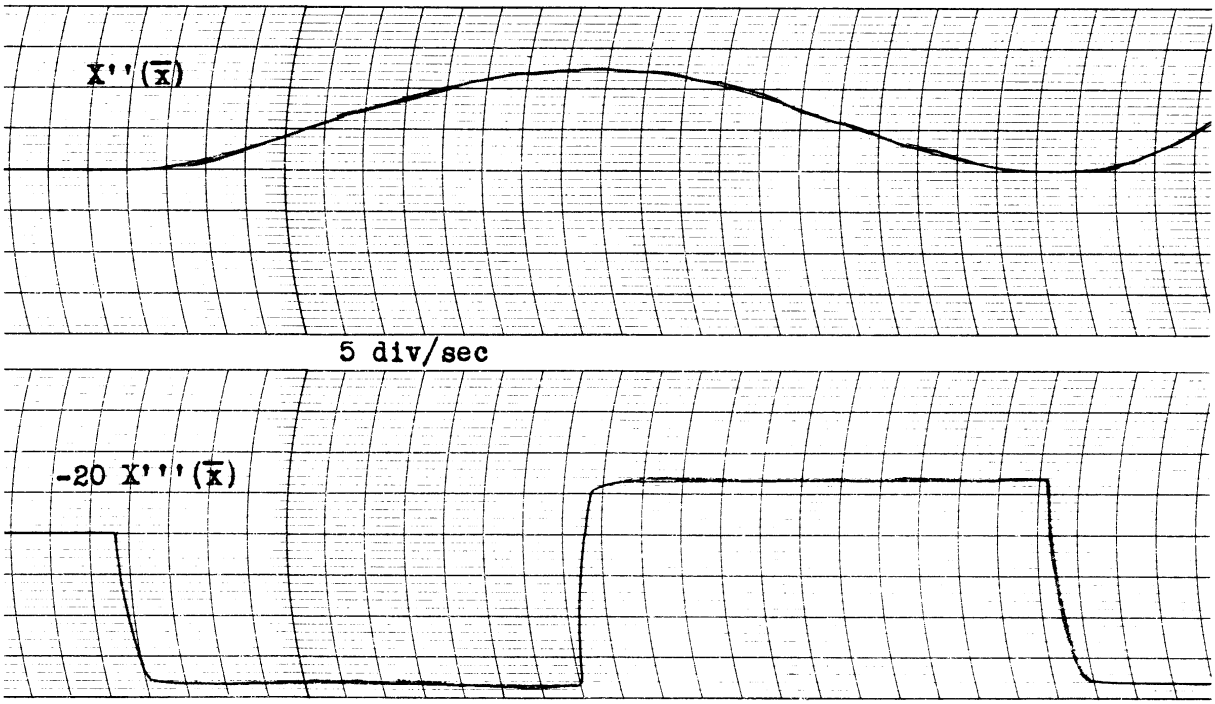

Figure 5-42. X"'($\bar{x}$) amplified to reduce pen-lag effect.

After the length L is measured from the X"' record, several corrections must be considered if maximum accuracy is to be obtained. The first of these corrections involves calibration of the recorder chart paper against a synchronous clock run from the same 60 cycle system as the recorder input. The error in the printed lines marking off seconds (slow speed) or fifths of seconds (medium speed) is determined. For our recorder this error was found to be about 0.2%.

A second correction arises from the fact that the rollers which pull the chart-paper through the recorder are driven by a synchronous motor, the speed of which will of course very directly with the 60 cycle line frequency. We found the variation in the 60 cycles in our case to be ± 0.4 cps. A frequency-recorder was run continuously while normal mode

solutions were being taken on the Brush Oscillograph, and the line frequency was noted at the time of each solution. The necessary linear correction was applied to L if the frequency at the time of the record was different from 60 cps.

Another important consideration is the accuracy of components in the computer. All components were measured to 0.1%. However, an additional method of insuring that a high degree of accuracy exists in the computer for the vibrating beam problem is to calibrate each pair of integrators as part of a second order differential equation analog with zero damping. All components in the circuit are made equal to unity. Hence when the system is given a pulse, it should go into oscillations of period 2π. The components in the integrators are adjusted slightly until the period of oscillation is exactly 6.283 seconds as read in chart divisions on the recorder paper. (The period must of course be corrected for the line-frequency error in each case.) If the integrators of the circuit are calibrated in this manner, the correction due to discrepancy between second-markings on the chart and a synchronous clock is eliminated. This means that the chart-division is then our unit of time rather than the second, the difference in the two units being equal to the discrepancy mentioned above. This procedure of calibration was followed for all solutions in this chapter.

CHAPTER 6

METHODS OF OBTAINING VARIABLE COEFFICIENTS

6.1 Introduction

In Chapter 5 there were solved a number of problems involving the static deflections and normal modes of oscillation of uniform beams. In many cases, however, the beam may not be uniform and may have non-uniform loading. In these cases some of the coefficients will not be constant.

Bessel's Equation and Legendre's Equation are common examples of differential equations with variable coefficients. The equation of motion of a rocket involves variable coefficients because of, among other things, the decrease of mass with the consumption of fuel.

In solving differential equations with constant coefficients the values of the coefficients determine the relative (fixed) gains of the operational amplifiers. In order to take care of variable coefficients, it is necessary to actually, or effectively, cause the gains of the proper operational amplifiers to change appropriately. A fairly obvious method is to vary the values of feedback resistors or input resistors. Another method is shown in Figure 6-1.

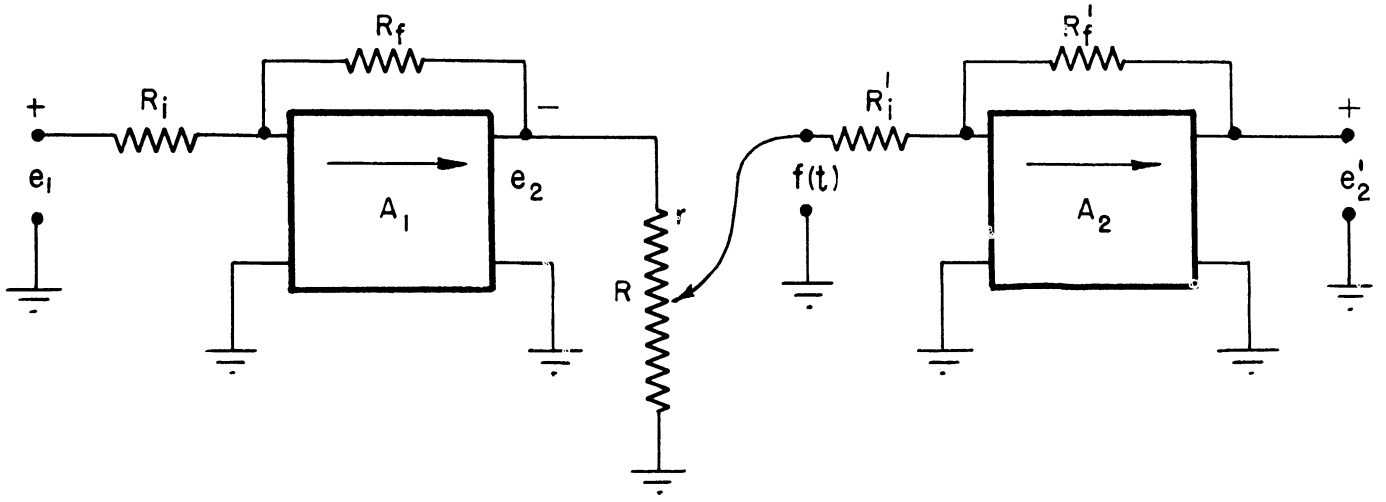

Figure 6-1. A method for obtaining variable gain.

If it is required to have $f(t)$ as a variable coefficient of e_2, the output voltage of amplifier A_1, it would seem possible to place across the output e_2 a potentiometer R and cause the sliding contact on R to move in such a way as to obtain from it the desired voltage $f(t)\, e_2$.

However, a dilemma is encountered. If the value of R is made too small, the amplifier A_1 will be unable to furnish sufficient current to maintain a linear output for all voltages. If the value of R is made too large, the additional current which flows to the next amplifier through r, that portion of R between the sliding contact and the high side of the potentiometer, will cause f(t) to differ from the expected value. For example, if the sliding contact is placed at the electrical center of a 50,000 ohm potentiometer and the input resistor, R_L, to the next amplifier is made 1/2 megohm, the effective voltage input will be approximately 2.5 per cent less than $e_2/2$ as would have been expected. Because of these difficulties it nas seemed advisable not to use this method for obtaining variable coefficients.

6.2 Cam Operated Variable Resistances

A standard practice for obtaining a variable resistance is to cut a cam of such a shape that when the cam is rotated it moves the sliding contact of a linear rheostat so as to vary its resistance in such a way as to obtain the desired function. While this method has, in many instances, produced satisfactory results there are definite limitations. The accuracy can be no better than the linearity of the rheostat or the precision of the cam and connecting link. Furthermore, there is a definite limit to the ratio between maximum resistance and minimum resistance that can be maintained with accuracy. In the solutions of some problems described later, resistance ratios (maximum to minimum) as high as 4800 are used. It would be difficult, indeed, to have a cam operated linear rheostat produce this range of resistance values and at the same time maintain accuracy.

6.3 Non-Linear Potentiometers

In some instances cam operated linear rheostats (or potentiometers) are replaced by non-linear potentiometers driven at constant speed. These non-linear potentiometers are obtainable* with almost any desired curve of resistance versus rotation - sine, consine, tangent, square root, logarithmic, special empirical relationships, etc. The accuracy is of the order of magnitude of one per cent.

6.4 Simulation of Continuously Variable Functions by Resistance Changes in Discrete Steps.

To simulate continuously variable functions there can be used feedback and input resistors that vary in discrete steps, and automatic stepping relays can be used to connect in the desired resistance. The manner in which this is done is described in Section 2.14.

Reference to the computer circuits already presented shows that in virtually every case there are two integrating circuits immediately preceding the output voltage representing the solution of the problem. It is proposed to simulate continuously variable functions by making the resistance steps such that at the end of each step $\leq R \Delta t$ would be exactly proportional to the integral of the continuously variable function.

* For example, from Fairchild Camera and Instrument Corporation, Jamaica, N.Y.

For example, suppose it is desired to simulate a function which is directly proportional to x^2, taking s steps for each unit value of x, i.e., if x were expressed in centimeters, there would be s steps per centimeter. In Figure 6-2, x^2 is plotted against x in units of 1/s. This means that the

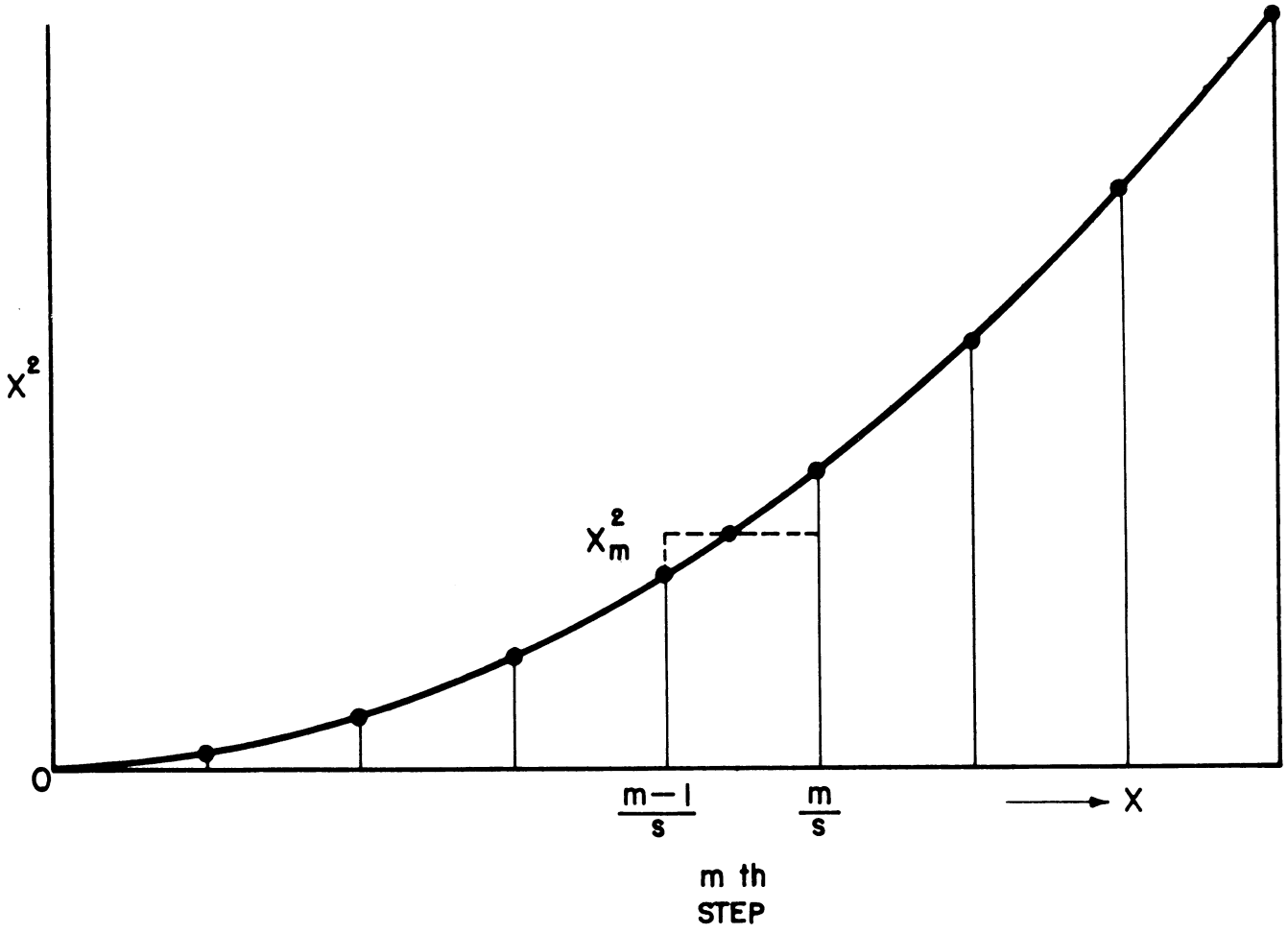

Figure 6-2.

successive points plotted are 1/s, 2/s, 3/s, ... m-1/s, m/s, ... n/s, for a total of n points or steps. For the mth step there is chosen an ordinate x_m^2 such that the area of the rectangle is equal to the area under the curve. x_m^2 is determined by the relation

$$x_m^2 \cdot 1/s = \int_{(m-1)/s}^{m/s} x^2\,dx = 1/3s^3 \left[m^3 - (m-1)^3 \right] \qquad (6\text{-}1)$$

or

$$x_m^2 = 1/3s^2 \left[m^3 - (m-1)^3 \right] \qquad (6\text{-}2)$$

This value of x_m^2 is proportional to the resistance required during the mth step to simulate the function x^2 for that step. Consequently we may write as the resistance R_m required for the mth step

$$R_m = Mx_m^2 = M/3s^2 \left[m^3 - (m-1)^3 \right] \qquad (6\text{-}3)$$

where M is an arbitrary constant multiplying factor necessary to give the resistances the proper magnitudes to be used in the operational amplifiers. The coefficient $M/3s^2$ may be replaced by K so that

$$R_m = K \left[m^3 - (m-1)^3 \right] \qquad (6\text{-}4)$$

In Figure 6-3 is shown a partial tabulation of the computation of suitable resistors for a total of 40 steps. The K of equation (6-4) equals 5000 ohms here. The fourth column gives the value of resistance in the circuit (input or feedback impedance) for each step. The last column gives the resistance to be added for each step to the resistance already in the circuit to give the proper resistance for that step.

m = xs	m^3	$m^3-(m-1)^3$	R_m (ohms)	$R_m - R_{(m-1)}$ (ohms)
1	1	1	5K	5K
2	8	7	35K	30K
3	27	19	95K	60K
4	64	37	185K	90K
5	125	61	305K	120K
35	42875	3571	17.855 meg	1.02 meg
36	46656	3781	18.905	1.05 meg
37	50653	3997	19.985	1.08 meg
38	54872	4219	21.095	1.11 meg
39	59319	4447	22.235	1.14 meg
40	64000	4681	23.405	1.17 meg

Figure 6-3. Partial tabulation of the computation of resistances suitable for simulating a function proportional to x^2 in 40 steps.

If the "stepping" resistance is used as the feedback impedance of an operational amplifier it is necessary to determine the value of the input resistance R_i to give the amplifier a gain of unity when $x^2 = 1$. Since $R_m = Mx_m^2$, for the general case $R = Mx^2$ and for the particular case of $x^2 = 1$, $R_i = M$.

Since $M = 3s^2K$,

$$R_i = 3s^2K \qquad (6\text{-}5)$$

In the example given above K = 5000. For 4 steps per unit length, R_i = 240,000; for 2 steps per unit length, R_i = 60,000.

In order to simulate an arbitrary function f(x) by taking s steps for each unit value of x it can be shown that

$$R_m = M\left[s \int_{m-1/s}^{m/s} f(x)\, dx\right] \qquad (6\text{-}6)$$

where

f(x) = the function to be simulated
s = the number of steps per unit value of x
m = the number of the step for which the calculation is being made
R_m = the resistance in the circuit for the mth step
M = an arbitrary constant to give proper magnitudes of resistances.

The series resistance to be added algebraically for the mth step is

$$R_m - R_{m-1} ,$$

where R_{m-1} = the resistance in the circuit for the (m-1)th step.

A number of differential equations with variable coefficients will be solved in the following chapters.

CHAPTER 7

SOLUTION OF BESSEL'S EQUATION BY MEANS OF THE ANALOG COMPUTER

7.1 Introduction

It was felt that a classic linear differential equation with variable coefficients such as Bessel's equation would serve as an excellent example of the accuracy attainable with the analog computer when the coefficients are varied in steps instead of continuously. Bessel's equation is

$$\frac{d^2y}{dx^2} + \frac{1}{x}\frac{dy}{dx} + \left(1 - \frac{n^2}{x^2}\right) y = 0. \qquad (7\text{-}1)$$

The computer circuit for solving equation (7-1) is shown in Figure 7-1. The x^2 input resistor to A_1 is simulated by means of 40 steps. The values of the

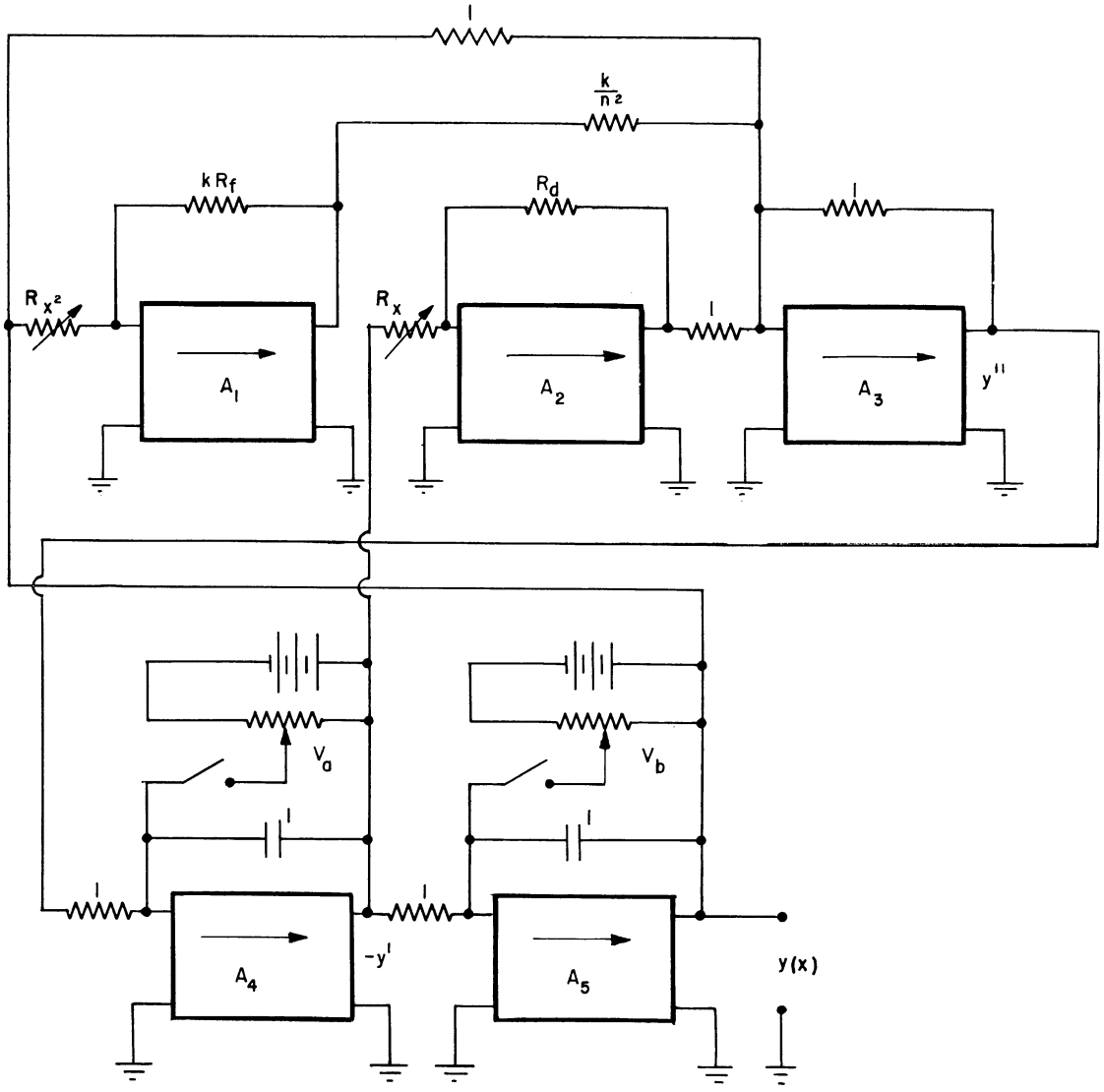

Figure 7-1. Computer circuit for solving Bessel's equation.

resistors selected are exactly those given in the example in Chapter 6, Section 6.4. The x input resistor to A_2 is also simulated in 40 steps, the first step being 100 K, the second 300 K, the third 500 K, etc., up to 7.9 meg.* The independent variable x is, of course, time in seconds for the computer. We will use three different stepping speeds for the relays -- 1, 2, and 4 steps per second. If s is the number of steps/sec., the value of R_f in thousands of ohms required to give A_1 a gain of unity for x = 1 is given by the following equation (see Section 6.4):

$$R_f = 15s^2 \quad . \tag{7-2}$$

Similarly

$$R_d = 200\ s \quad . \tag{7-3}$$

The factor k in Figure 7-1 is merely a constant factor inserted to keep the gain of A_1 not greater than the order of magnitude of unity for any step.

We will consider only those solutions of equation (7-1) termed "Bessel's functions of the first kind" and denoted by $J_n(x)$.

7.2 Bessel's Function of Order Zero

The initial conditions for Bessel's function of order zero are:

$$J_o(o) = 1 \qquad J_o'(o) = 0 \quad . \tag{7-4}$$

The initial voltage V_a in Figure 7-1 is made zero by replacing the potentiometer with a 1000 ohm resistor in series with the shorting-relay. V_b is made finite. When the starting button is pressed, the stepping relays start, causing the initial conditions to be simultaneously released, and the solution of the problem begins. The voltage V_b is varied until the $J_o(0)$ curve on the recorder reads 10 divisions for these runs.

Oscillograms of the J_o and J_o' curves are shown for 1, 2, and 4 steps/sec. in Figures 7-2, 7-4, and 7-6 respectively. In Figures 7-3, 7-5, and 7-7, the experimental points are plotted against the theoretical J_o curves as obtained from values in Jahnke and Emde, "Tables of Functions." Note how the accuracy of the computer increases when a higher number of steps per second are used.

7.3 Bessel's Functions of Orders Between Zero and One

The initial conditions for Bessel's functions of orders between 0 and 1 are

$$J_n(o) = o, \quad J_n'(o) = \quad , o\ n\ 1 \quad . \tag{7-5}$$

In this case the capacitor across A_5 is initially shorted and the voltage V_a is made finite. (Since the functions $1/x$ and $1/x^2$ in the computer circuit are very large but certainly not infinite at x = 0, it makes

* It would be more correct to use a step approximation for $1/x^2$ rather than the reciprocal of the step approximation for x^2. The same follows for $1/x$.

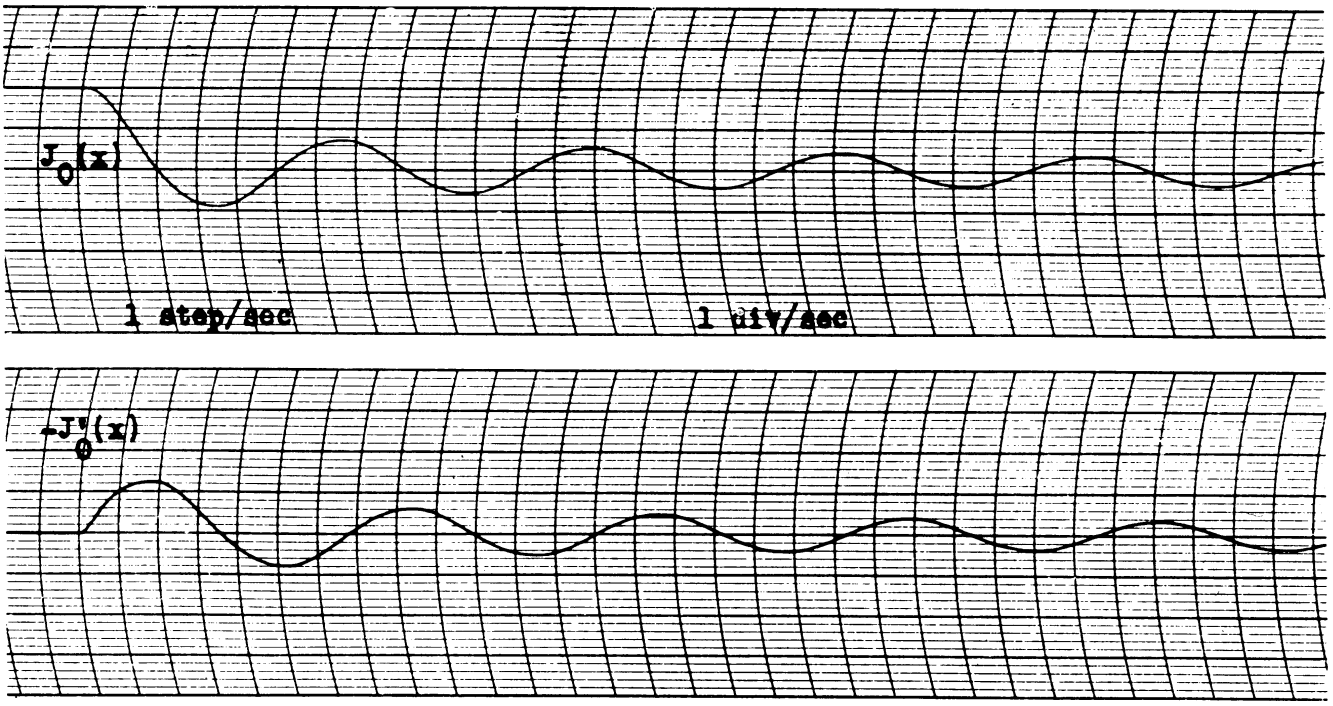

Figure 7-2. Computer solution for $J_0(x)$; one step per second.

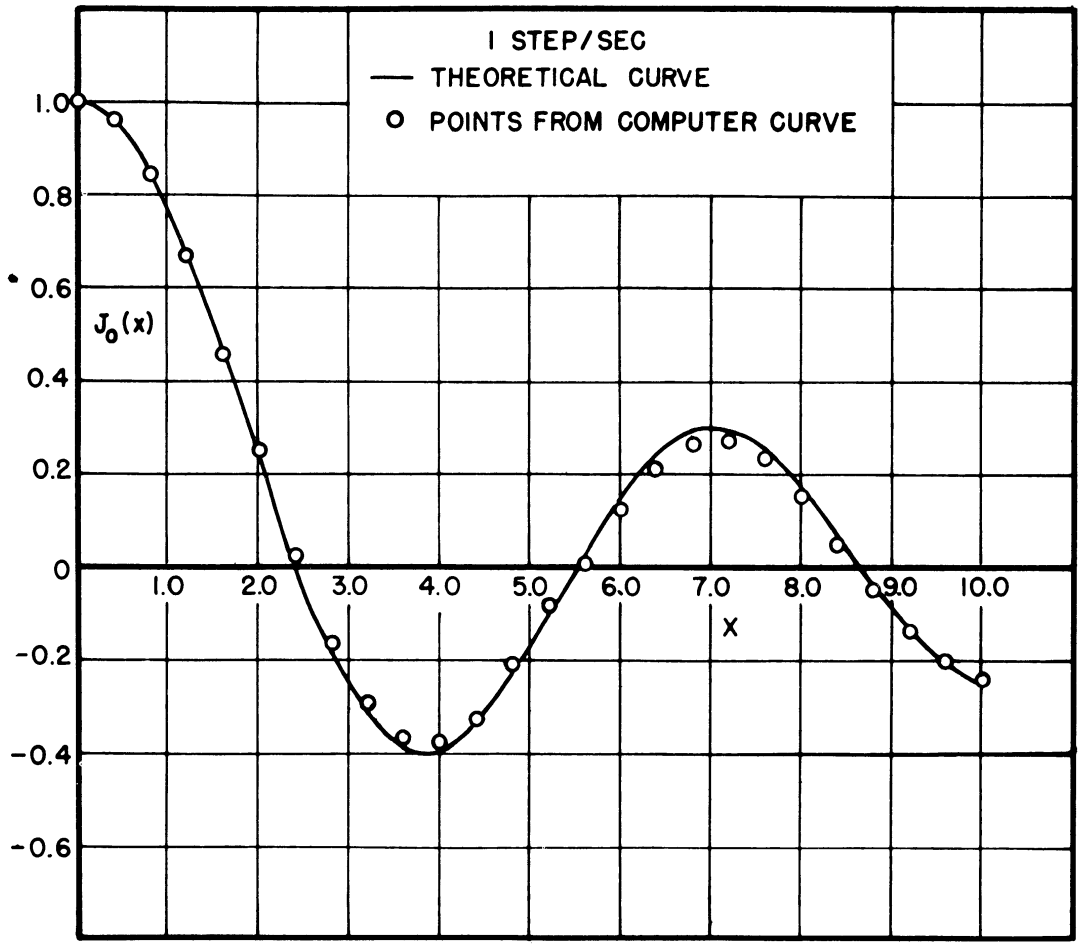

Figure 7-3. Theoretical J_0 curve with computer solution; one step per second.

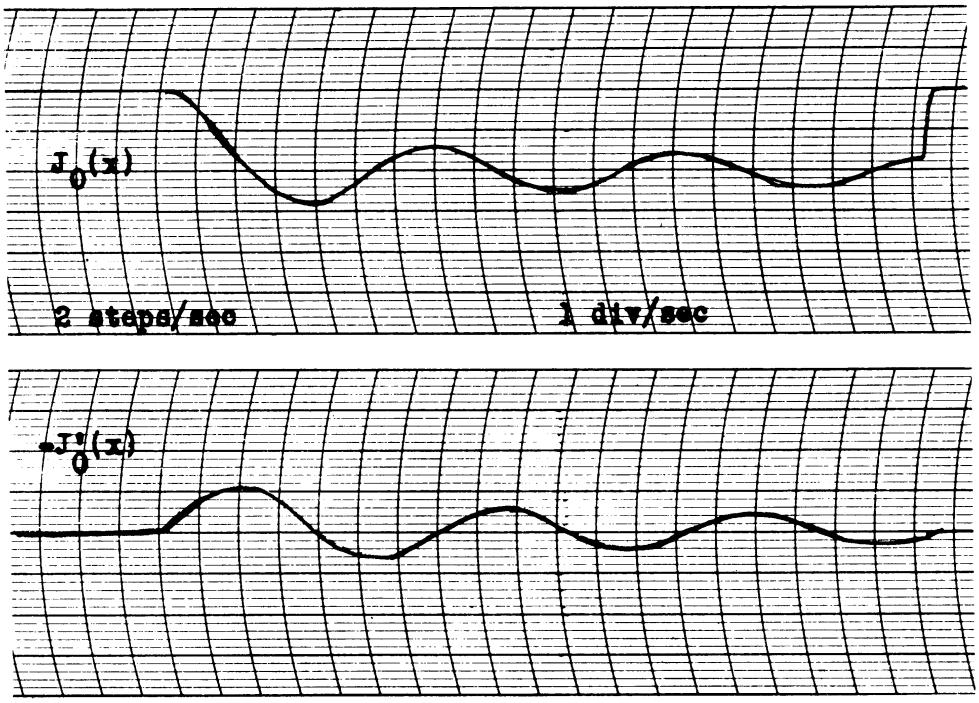

Figure 7-4. Computer solution for $J_0(x)$; two steps per second.

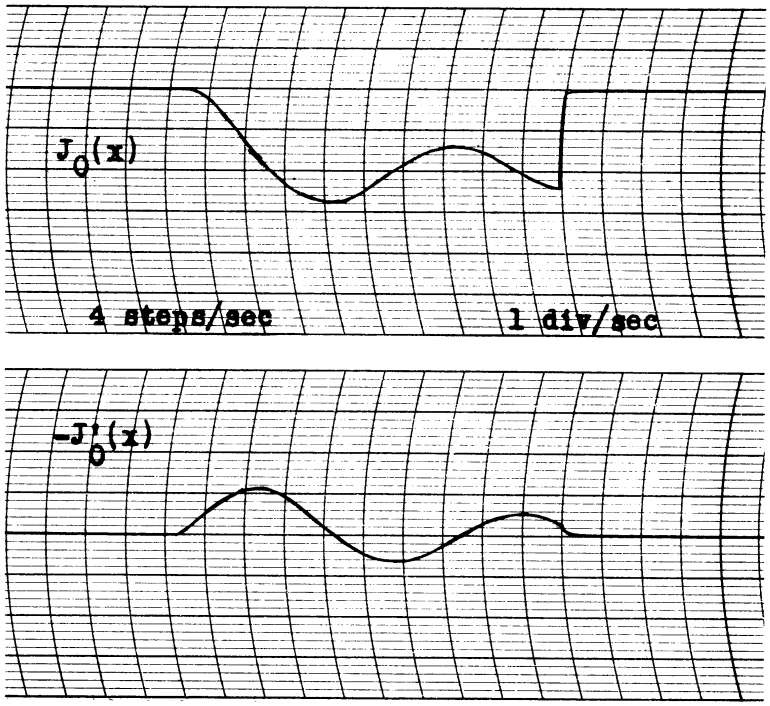

Figure 7-5. Theoretical J_0 curve with computer solution; two steps per second.

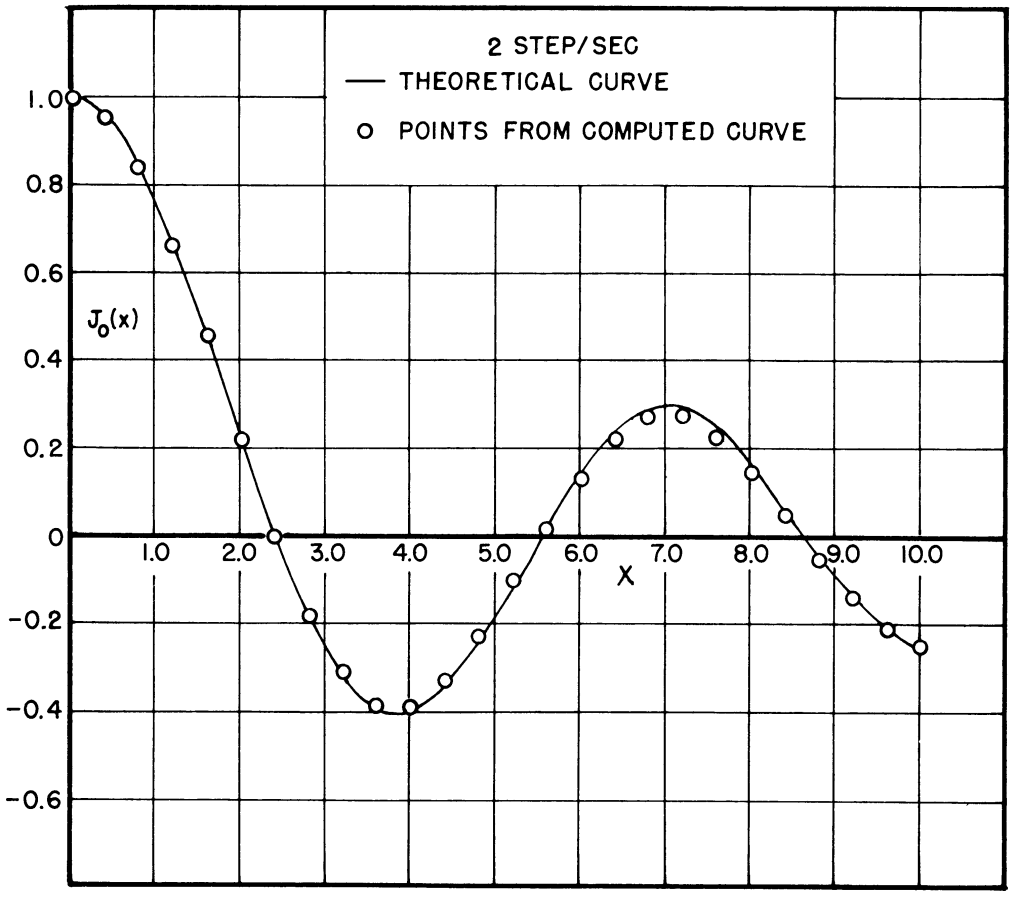

Figure 7-6. Computer solution for $J_0(x)$; four steps per second.

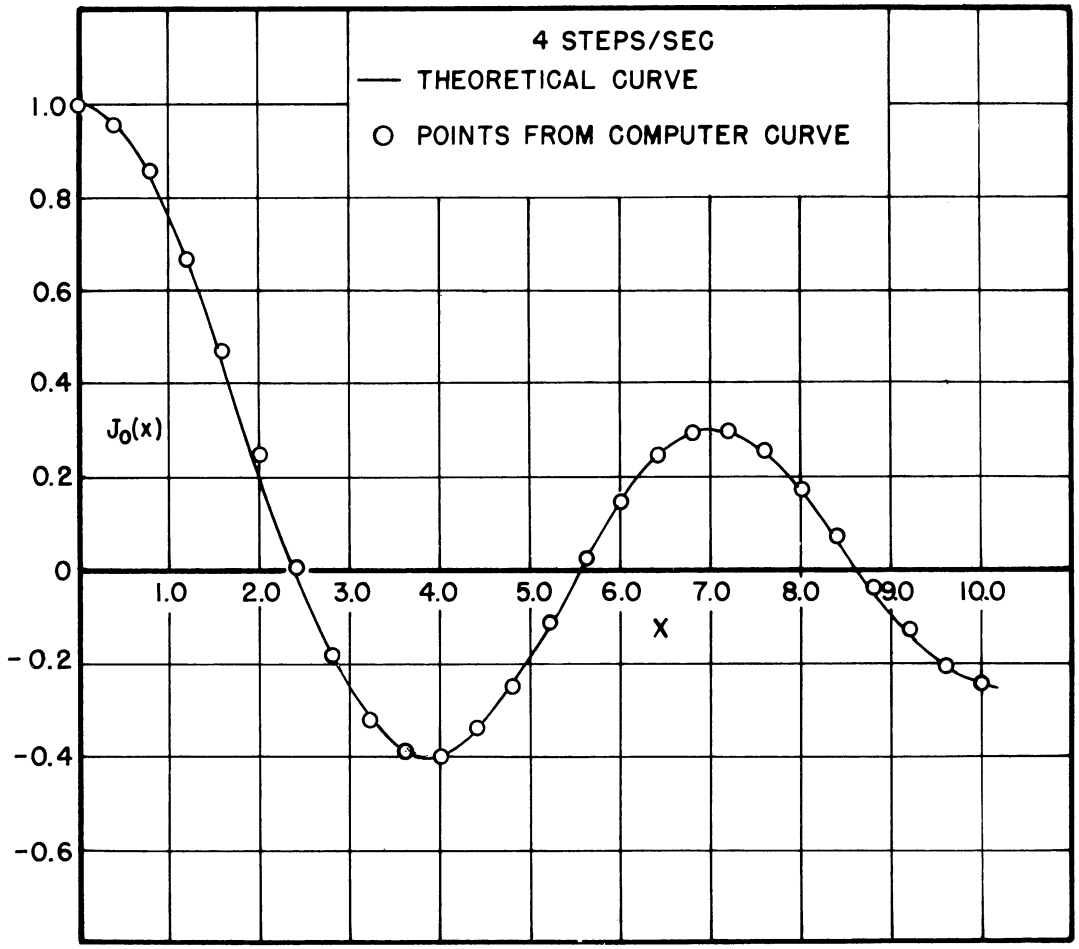

Figure 7-7. Theoretical J_o curve with computer solution; four steps per second.

no sense to attempt to make V_a infinitely large.) Care must be taken not to make V_a so large that any of the amplifiers are driven to cut off in the first step. For example, note that when n = 1/4, we make k = 1/16 so that A_1 has a gain of $\frac{(240)}{5 \times 16} = 3$ for the first step. A good range for V_a is around 6 volts. The value of V_a is varied slightly until the J_n curve has its first maximum at the desired deflection on the recording paper.

Oscillograms of $J_n(x)$ and J_n' for n = 1/4, 1/3, 1/2, and 3/4, along with plots of the computer curves against the theoretical curves from Jahnke-Emde, are shown in Figures 7-8 to 7-15.*

* A Brush BL-913 dc amplifier was used for checking the computer curves against the theoretical curves for all solutions J_n other than J_o. This eliminated the necessity of calibration corrections, since the Brush Amplifier is quite linear. However, the computer curves shown in the figures were taken using the dc impedance matcher of our own design, since two channels were available. We had only one Brush Amplifier on hand.

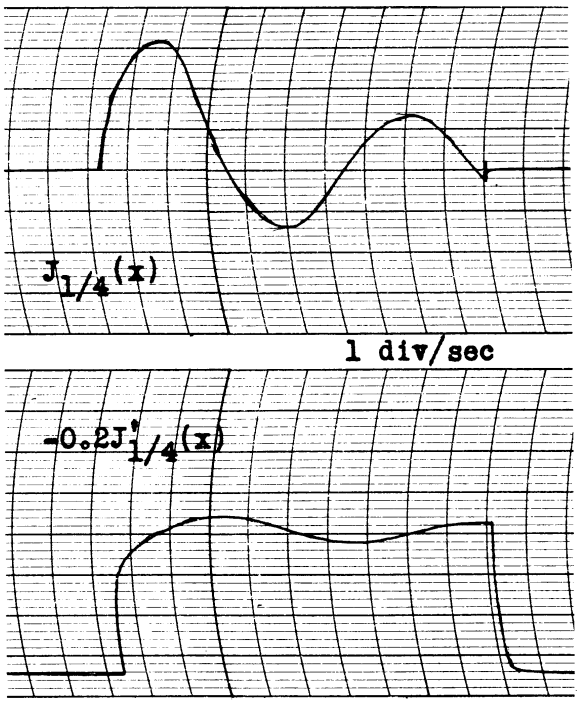

Figure 7-8. Computer solution for $J_{1/4}(x)$.

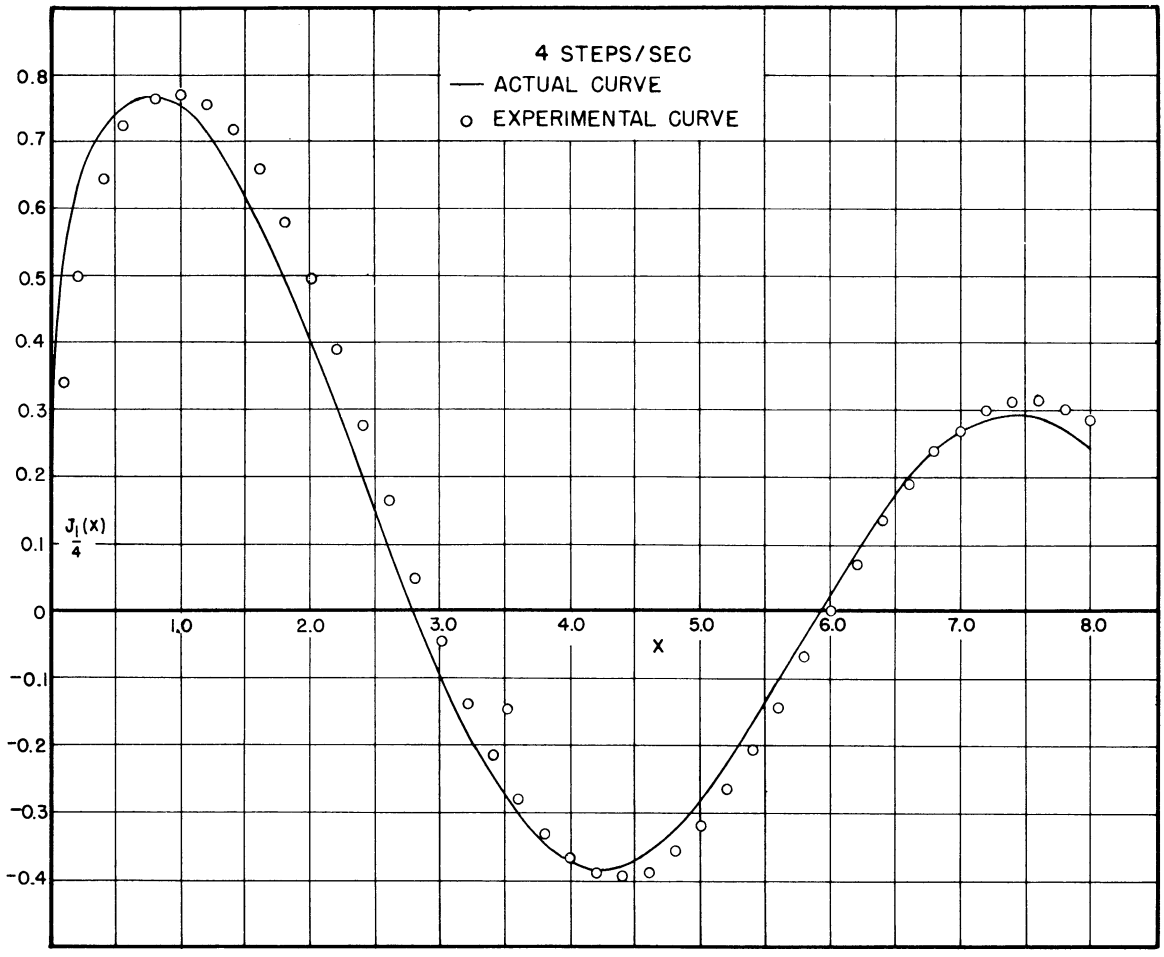

Figure 7-9. Theoretical $J_{1/4}$ curve with computer solution.

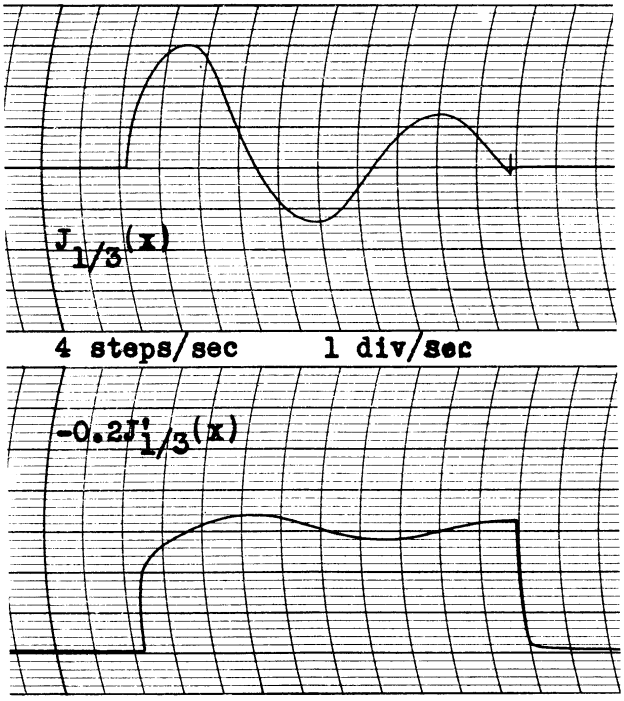

Figure 7-10. Computer solution for $J_{1/3}(x)$.

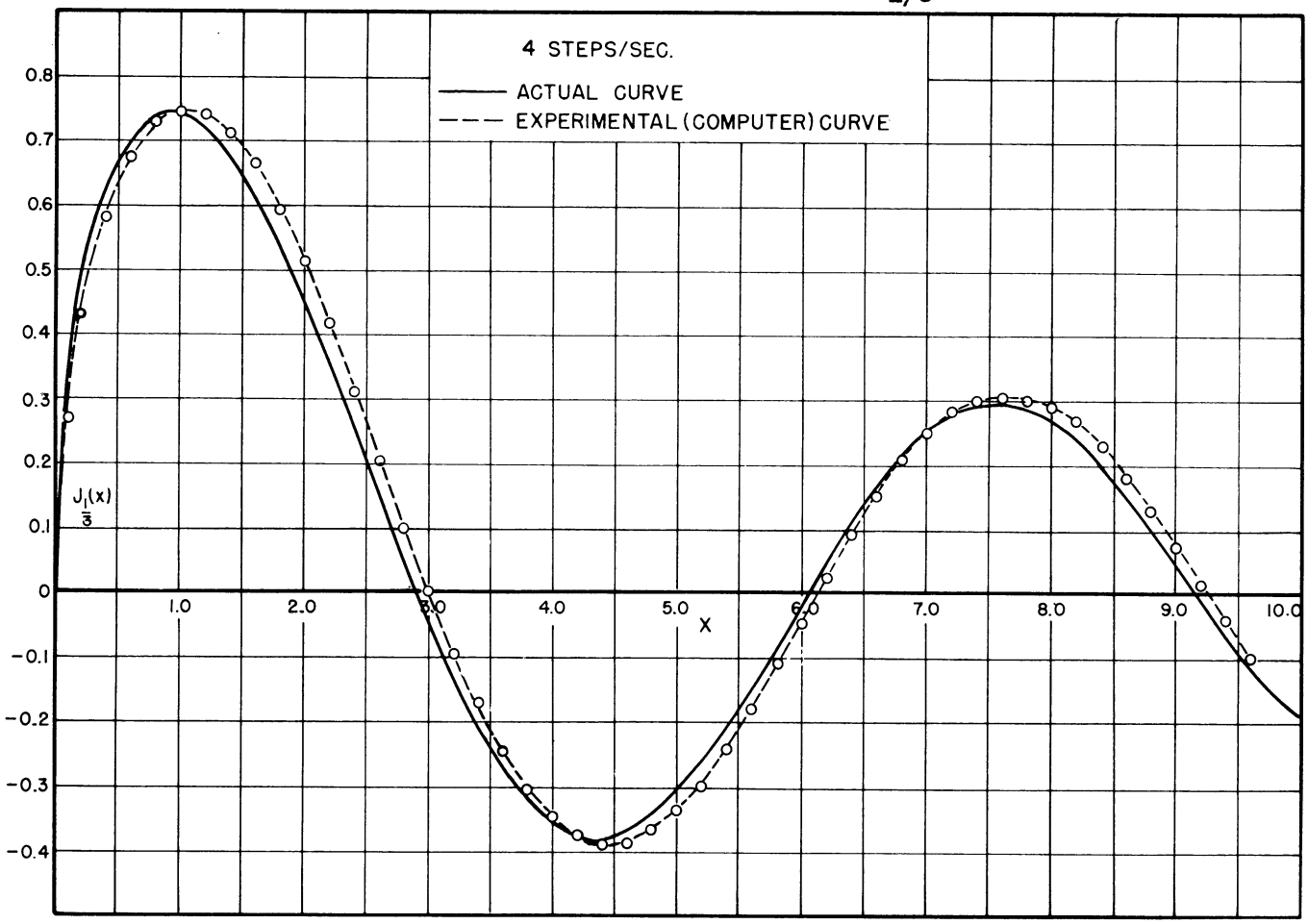

Figure 7-11. Theoretical $J_{1/3}$ curve with computer solution.

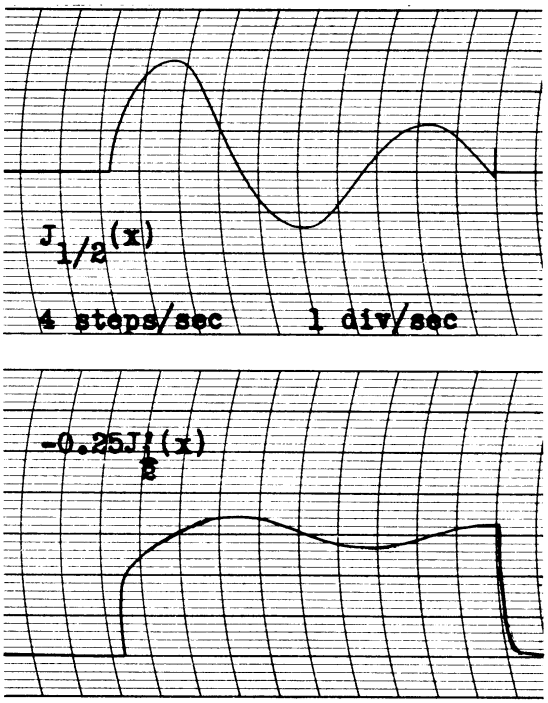

Figure 7-12. Computer solution for $J_{1/2}(x)$.

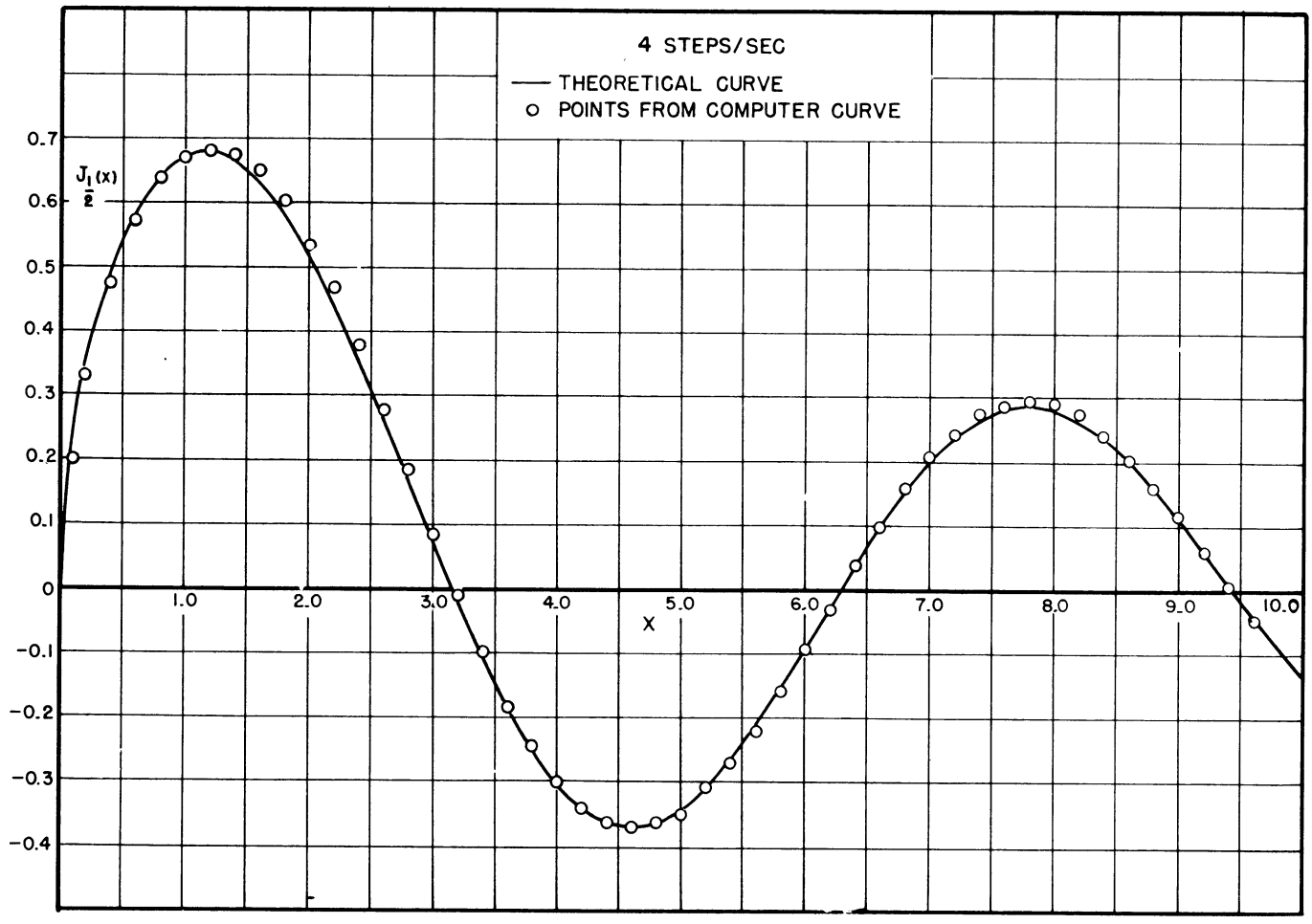

Figure 7-13. Theoretical $J_{1/2}$ curve with computer solution.

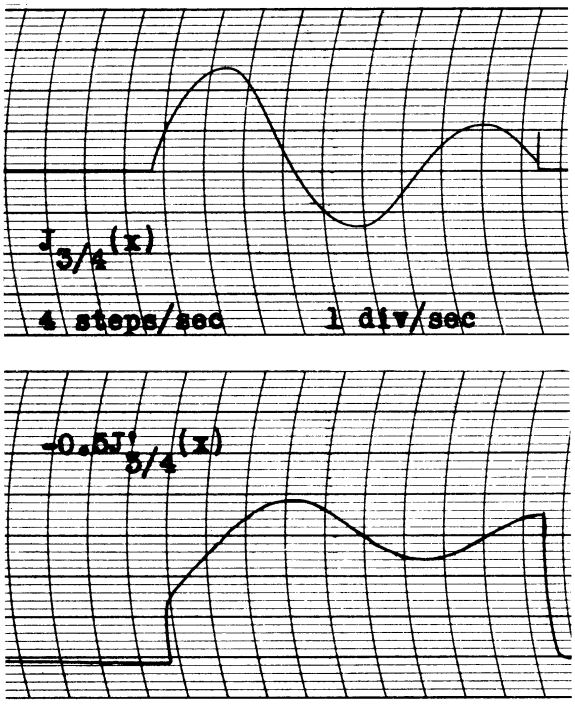

Figure 7-14. Computer solution for $J_{3/4}(x)$.

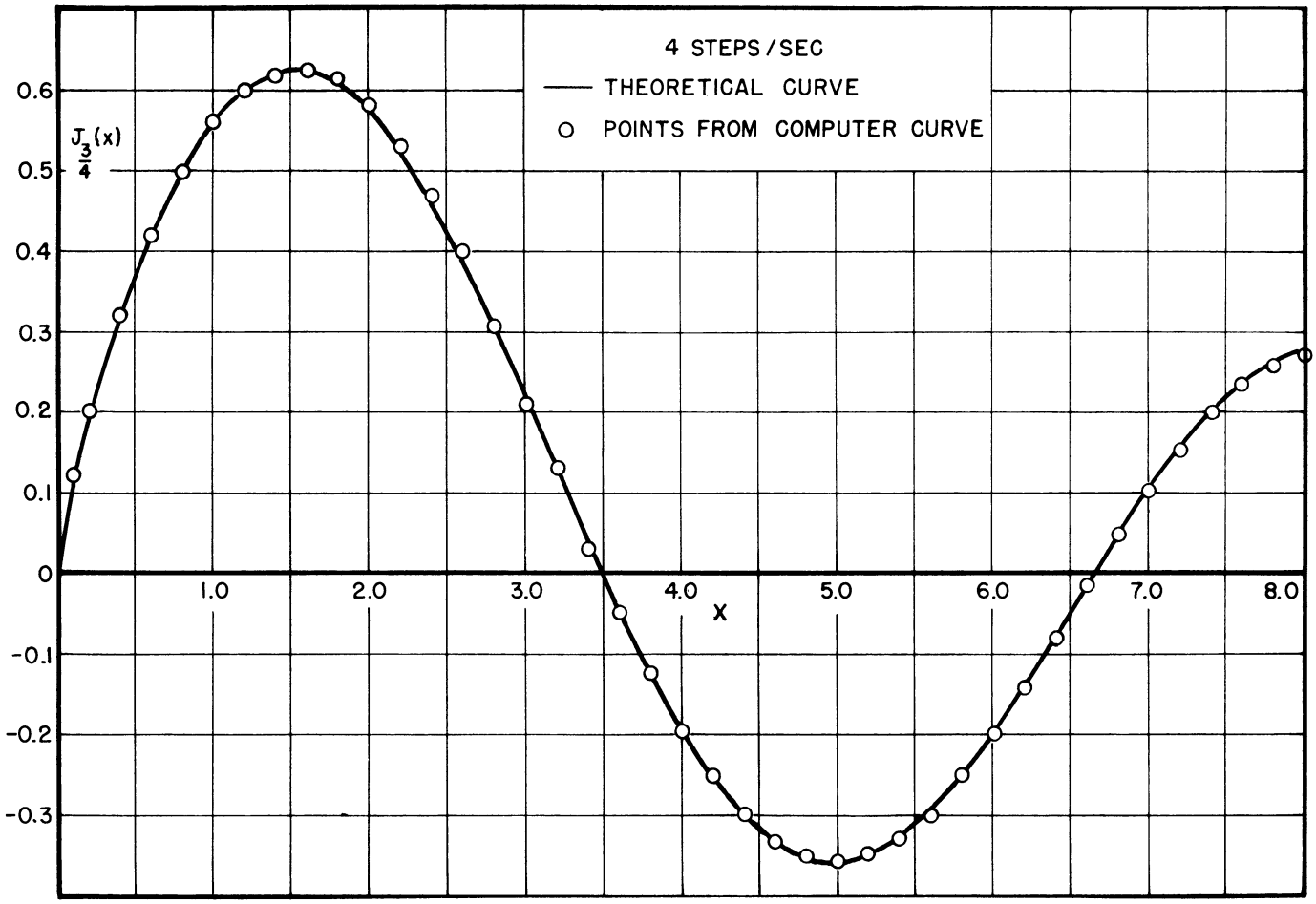

Figure 7-15. Theoretical $J_{3/4}$ curve with computer solution.

Four steps per second were used for all solutions in this section.

7.4 Bessel's Function of Order One.

The initial conditions for Bessel's function of order one are

$$J_1(0) = 0, \quad J_1'(0) = \text{constant} \tag{7-6}$$

The initial slope V_a is varied until the first maximum of the J_1 curve is the desired deflection on the record. Four steps per second were used.

In Figures 7-16 and 7-17 is shown the oscillogram of $J_1(x)$ and $J_1'(x)$ from the computer, along with the check of the computer solution against the theoretical $J_1(x)$ curve from Jahnke-Emde.

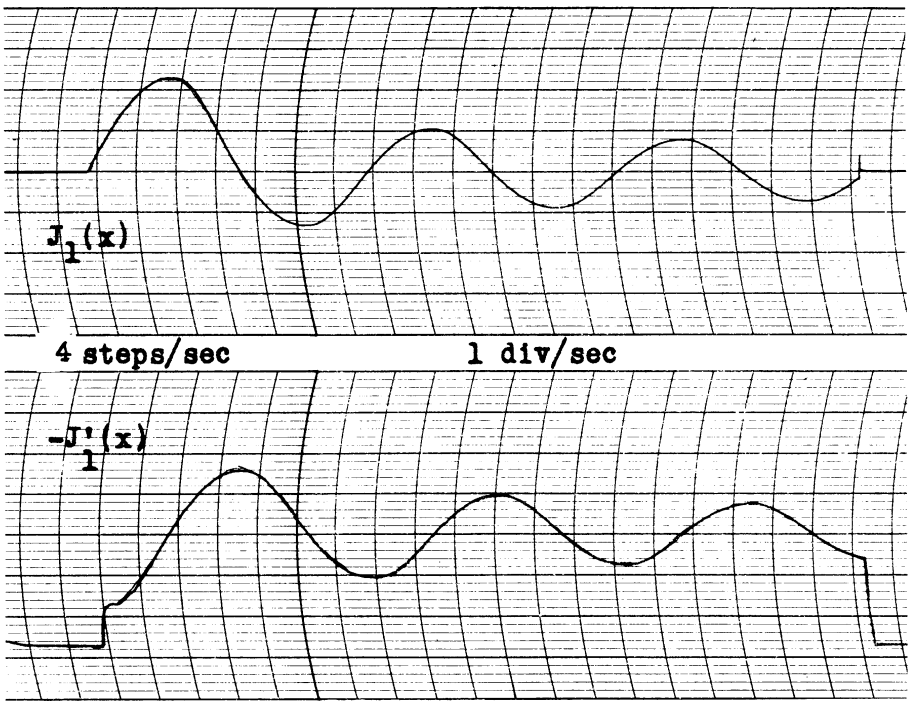

Figure 7-16. Computer solution for $J_1(x)$.

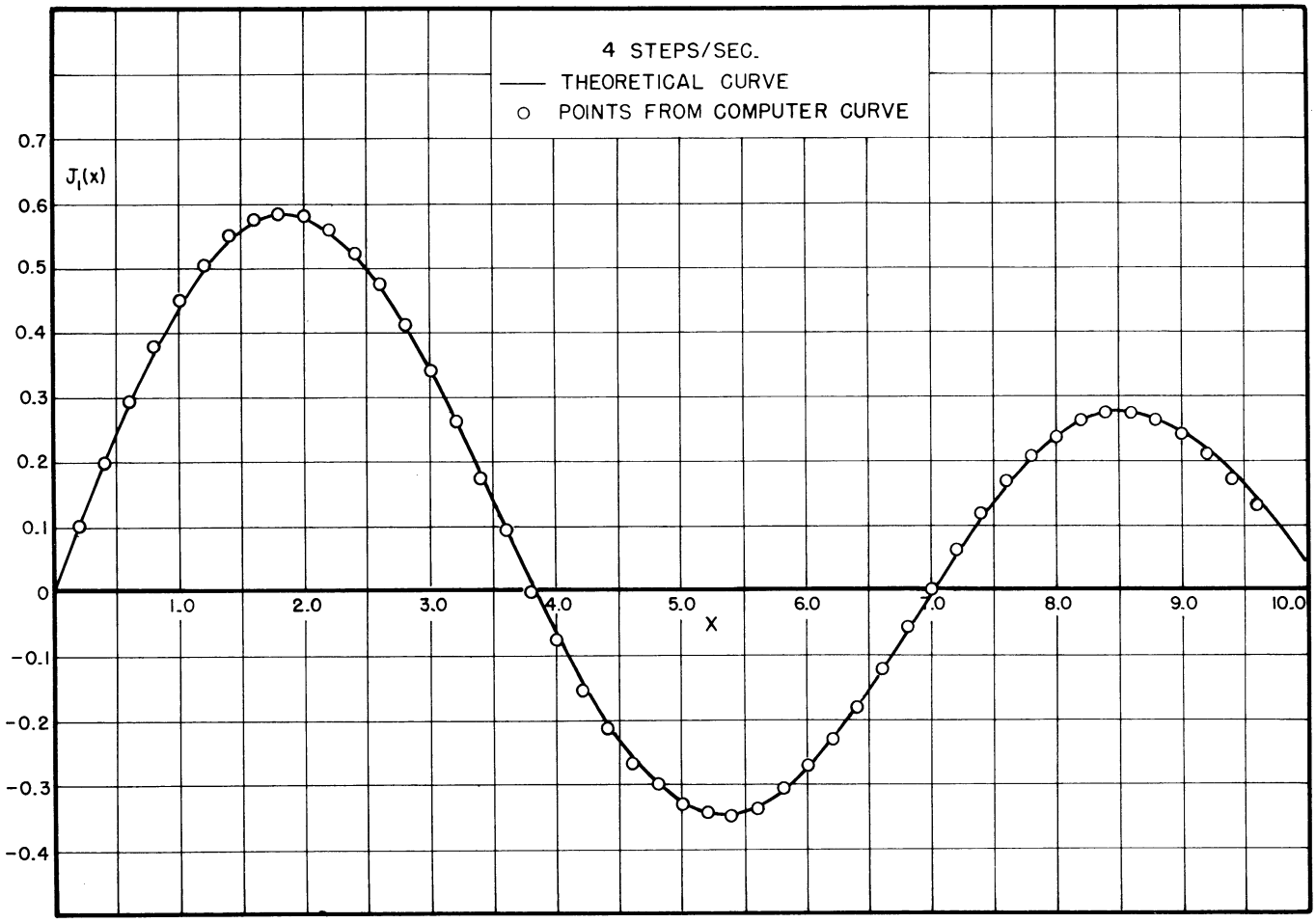

Figure 7-17. Theoretical J_1 curve with computer solution.

7.5 Bessel's Functions of Order Greater than One.

The initial conditions of $J_n(x)$ for $n > 1$ are

$$J_n(0) = 0, \quad J_n'(0) = 0, \; n > 1 \quad . \tag{7-7}$$

Both feedback capacitors across A_1 and A_2 are initially short-circuited. The generation of the solution despite zero input is caused by the initial instability of the system. For higher values of n this initial instability [due to the negative sign of the y term in equation (7-1)] lasts longer and is much more pronounced. In order to prevent the computer from going to cut-off on one or more amplifiers before the J_n curve reverses slope, it is necessary to balance all amplifiers very carefully before attempting any solutions.

Oscillograms of $J_n(x)$ and $J_n'(x)$ are shown in Figures 7-18 to 7-23 for n = 2, 3, and 4. The plots of the shapes of the computer curves against curves from Jahnke-Emde are also shown.

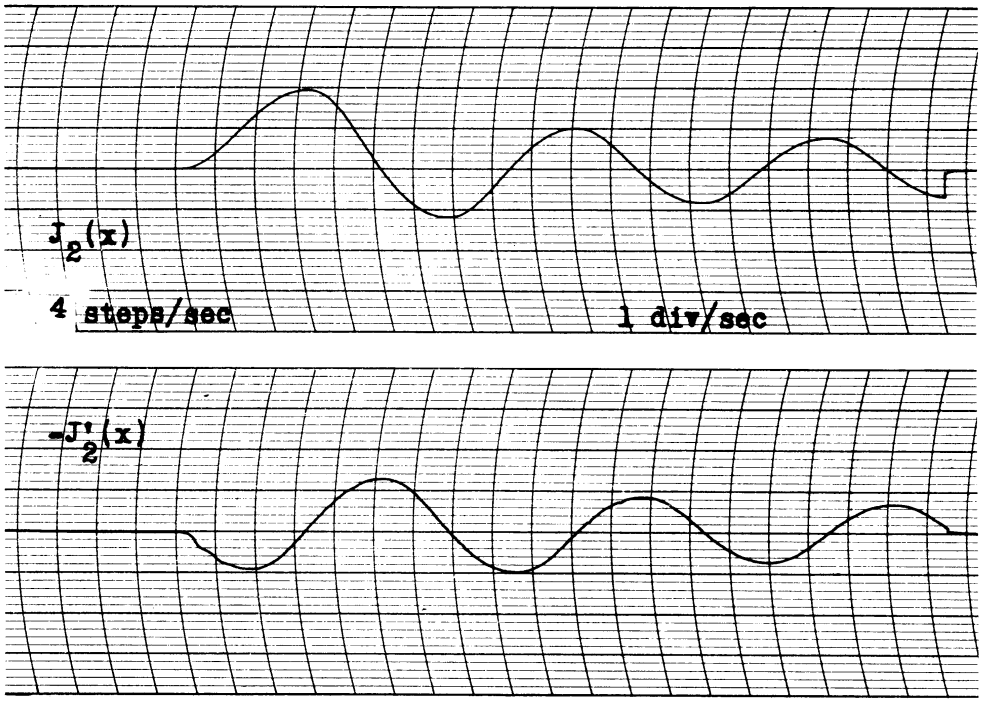

Figure 7-18. Computer solution for $J_2(x)$.

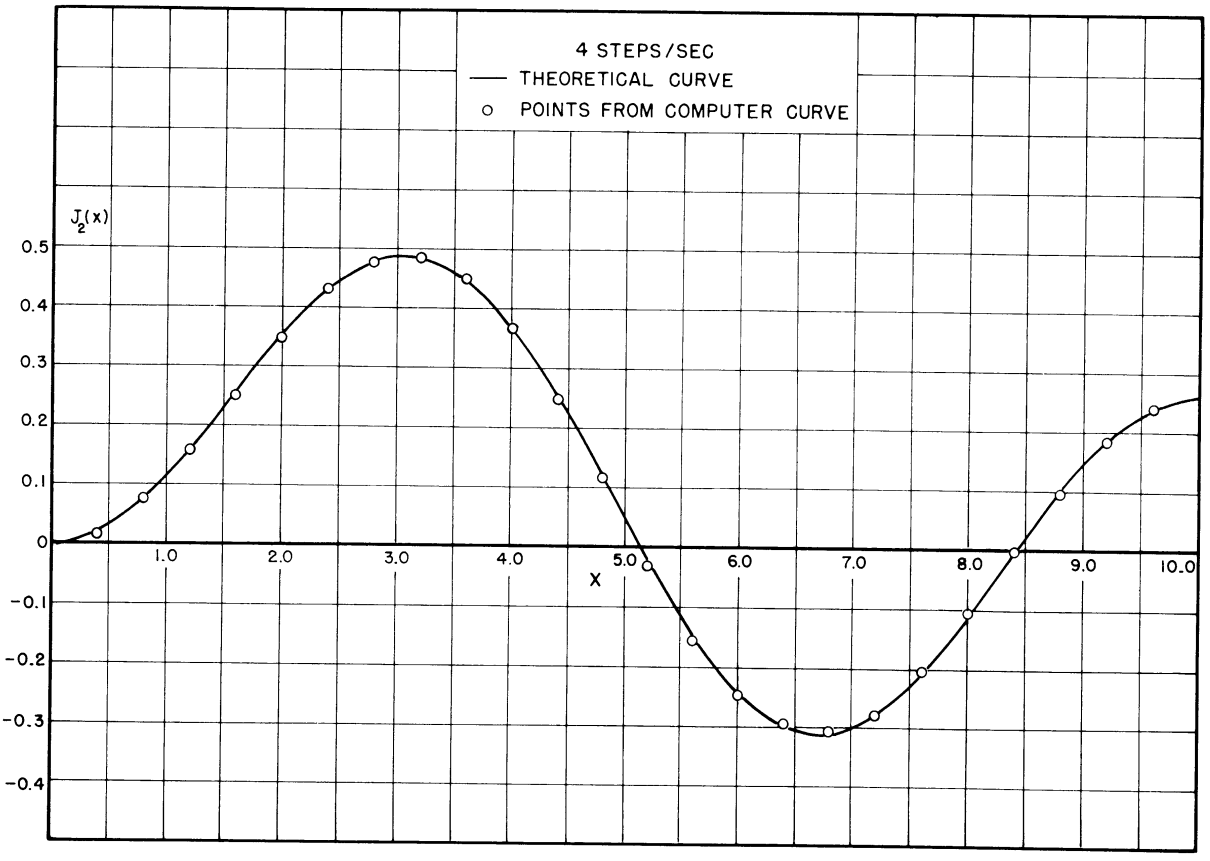

Figure 7-19. Theoretical J_2 curve with computer solution.

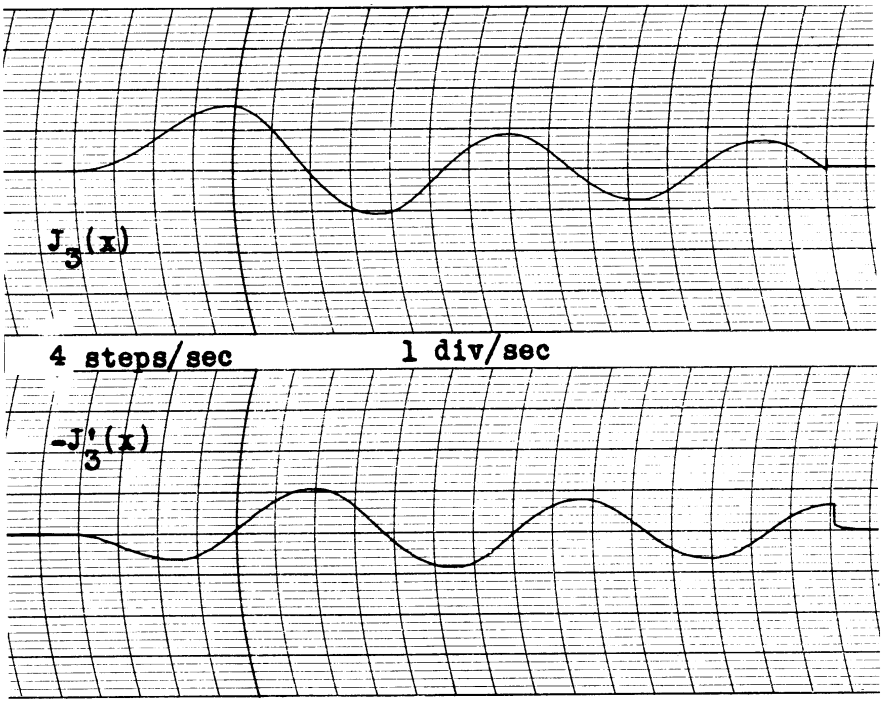

Figure 7-20. Computer solution for $J_3(x)$.

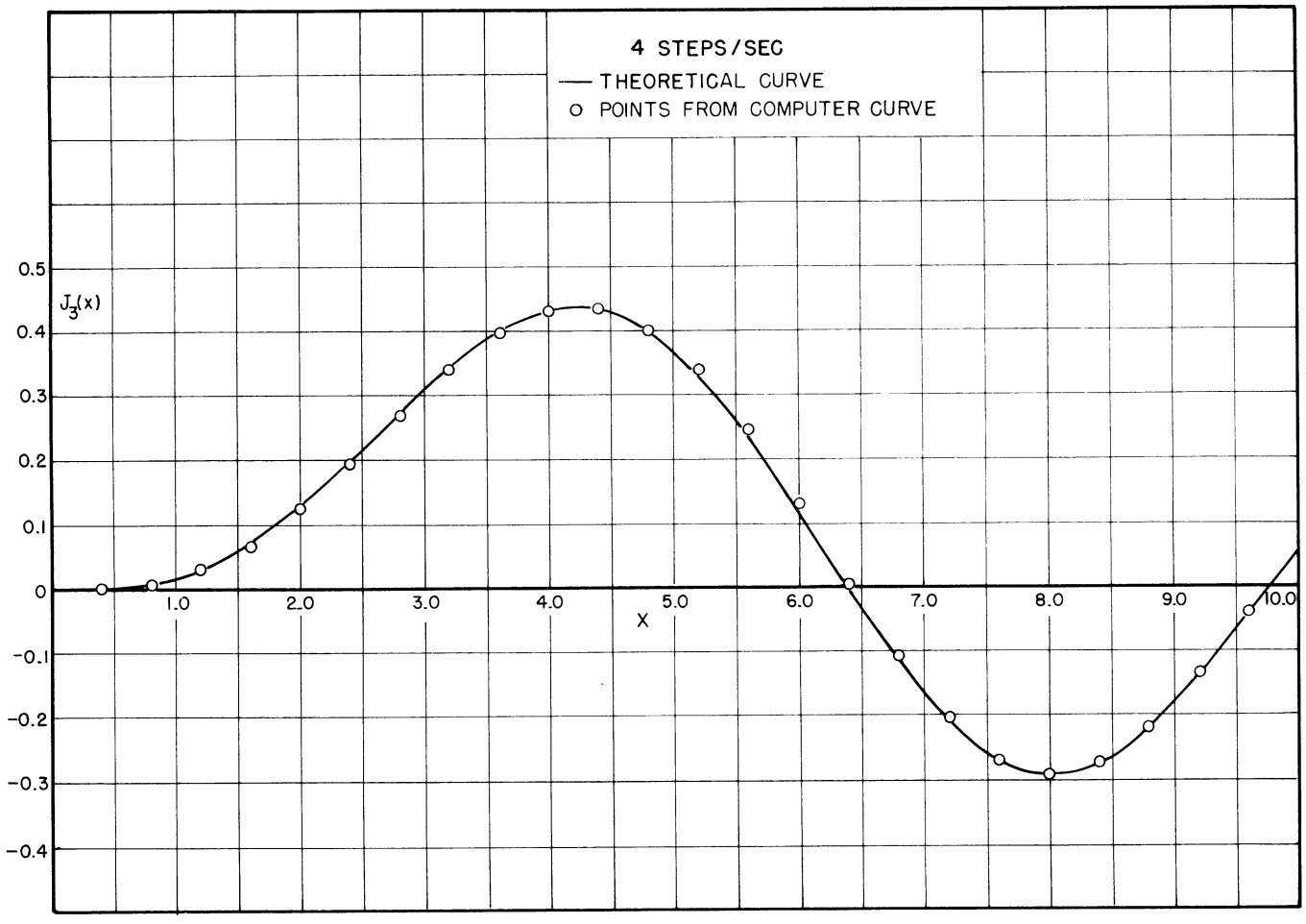

Figure 7-21. Theoretical J_3 curve with computer solution.

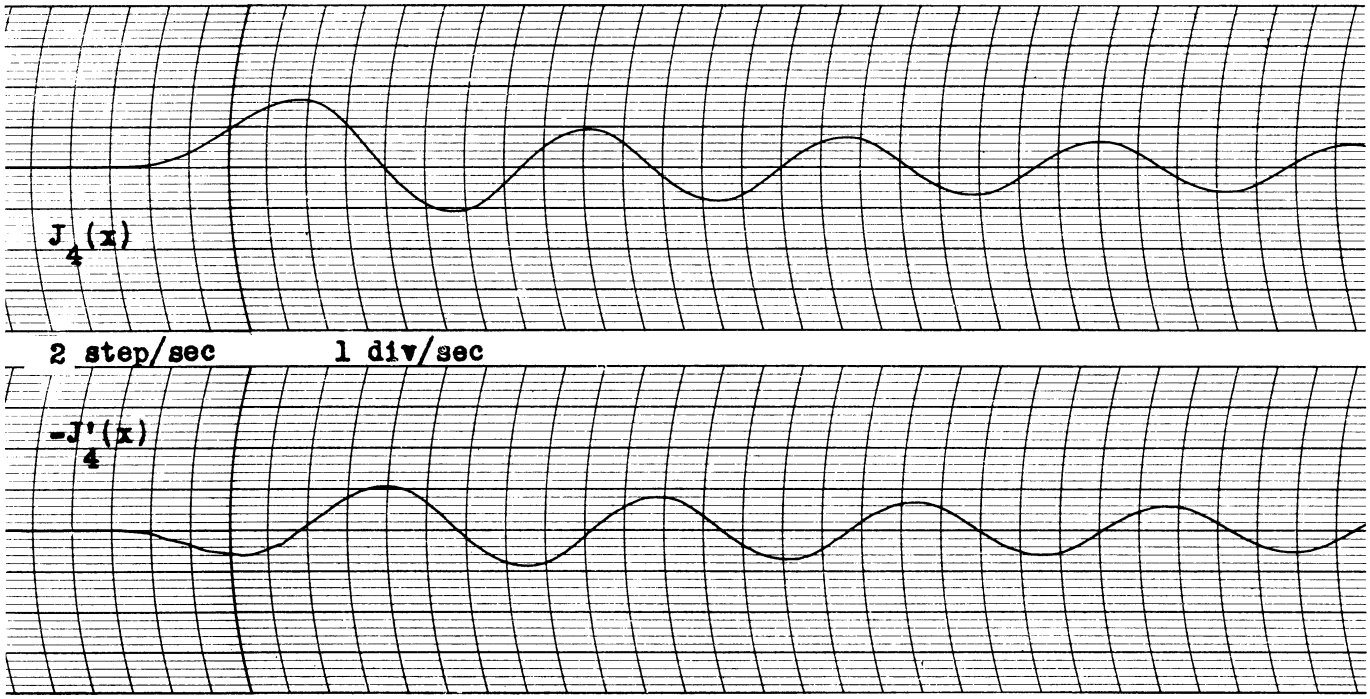

Figure 7-22. Computer solution for $J_4(x)$.

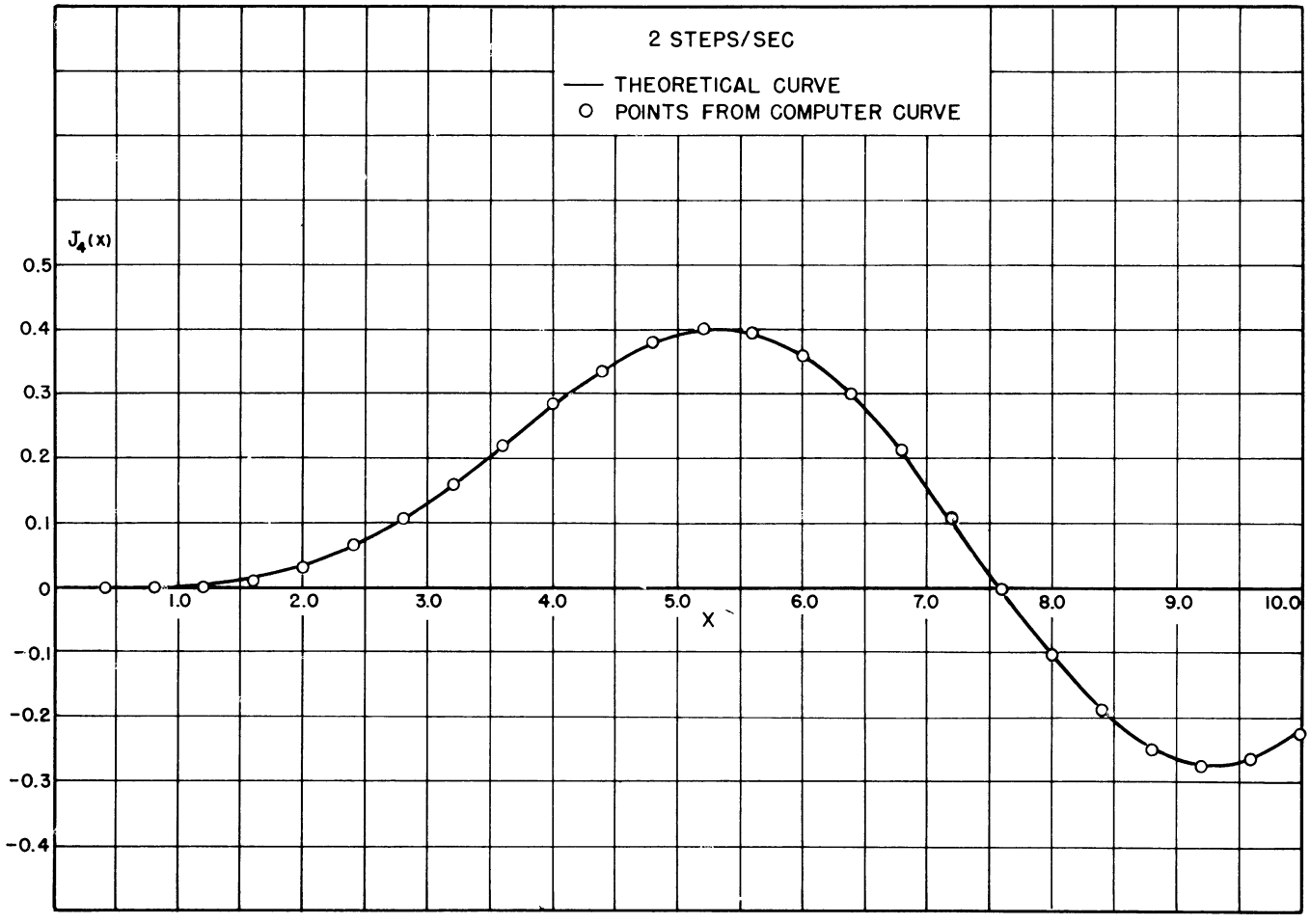

Figure 7-23. Theoretical J_4 curve with computer solution.

In the following table the first nine roots of $J_5(x)$ as obtained from a computer solution (recorded on medium speed) are compared with the values given in Jahnke-Emde. The oscillogram of $J_5(x)$ is shown in Figure 7-24.

Root Number	Experimental Root	Theoretical Root
1	8.78	8.78
2	12.34	12.34
3	15.68	15.68
4	18.96	18.96
5	22.18	22.22
6	25.40	25.43
7	28.61	28.63
8	31.78	31.81
9	34.93	34.98

A correction for variation in 60-cycle line frequency was included in the above experimental values.

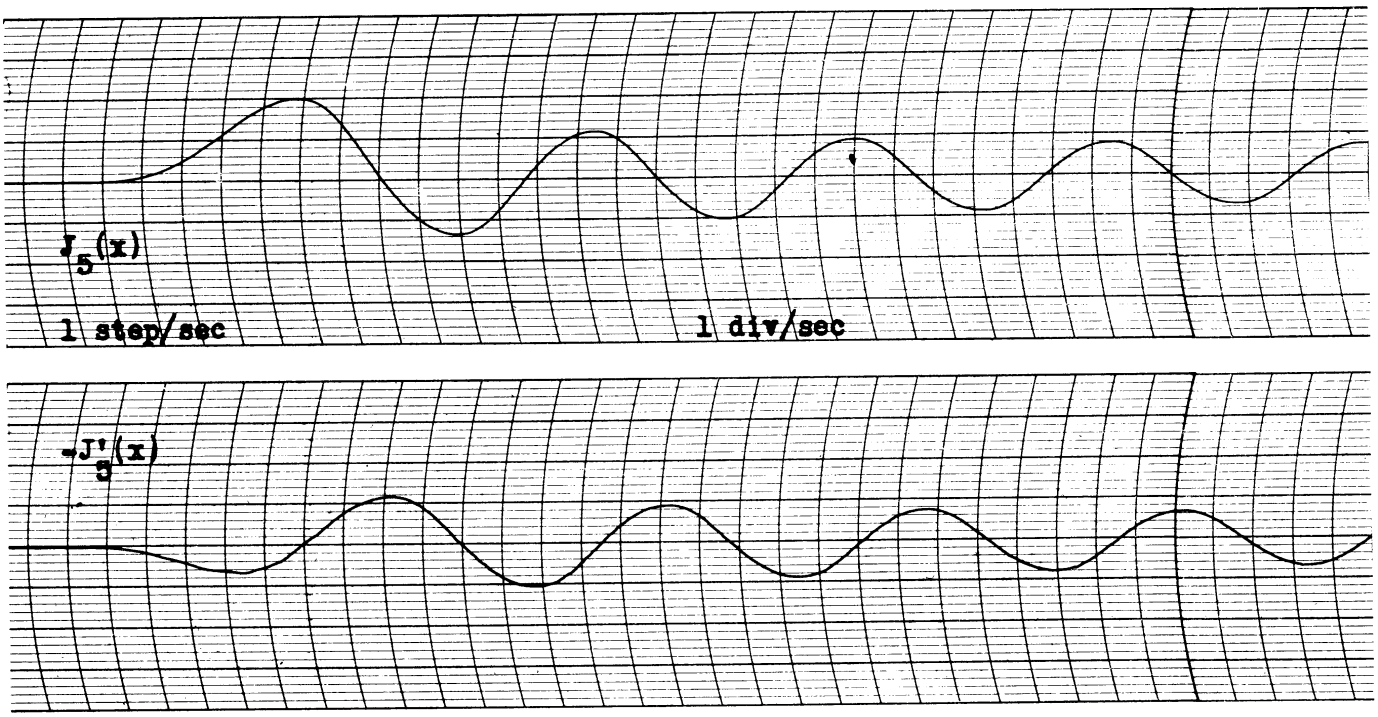

Figure 7-24. Computer solution for $J_5(x)$.

CHAPTER 8

SOLUTION OF LEGENDRE'S EQUATION BY MEANS OF THE ANALOG COMPUTER

8.1 Introduction

Another classical linear differential equation with variable coefficients which can be solved with the analog computer is Legendre's equation,

$$(1 - x^2)\frac{d^2y}{dx^2} - 2x\frac{dy}{dx} + n(n+1)y = 0. \qquad (8\text{-}1)$$

The computer circuit is shown in Figure 8-1.

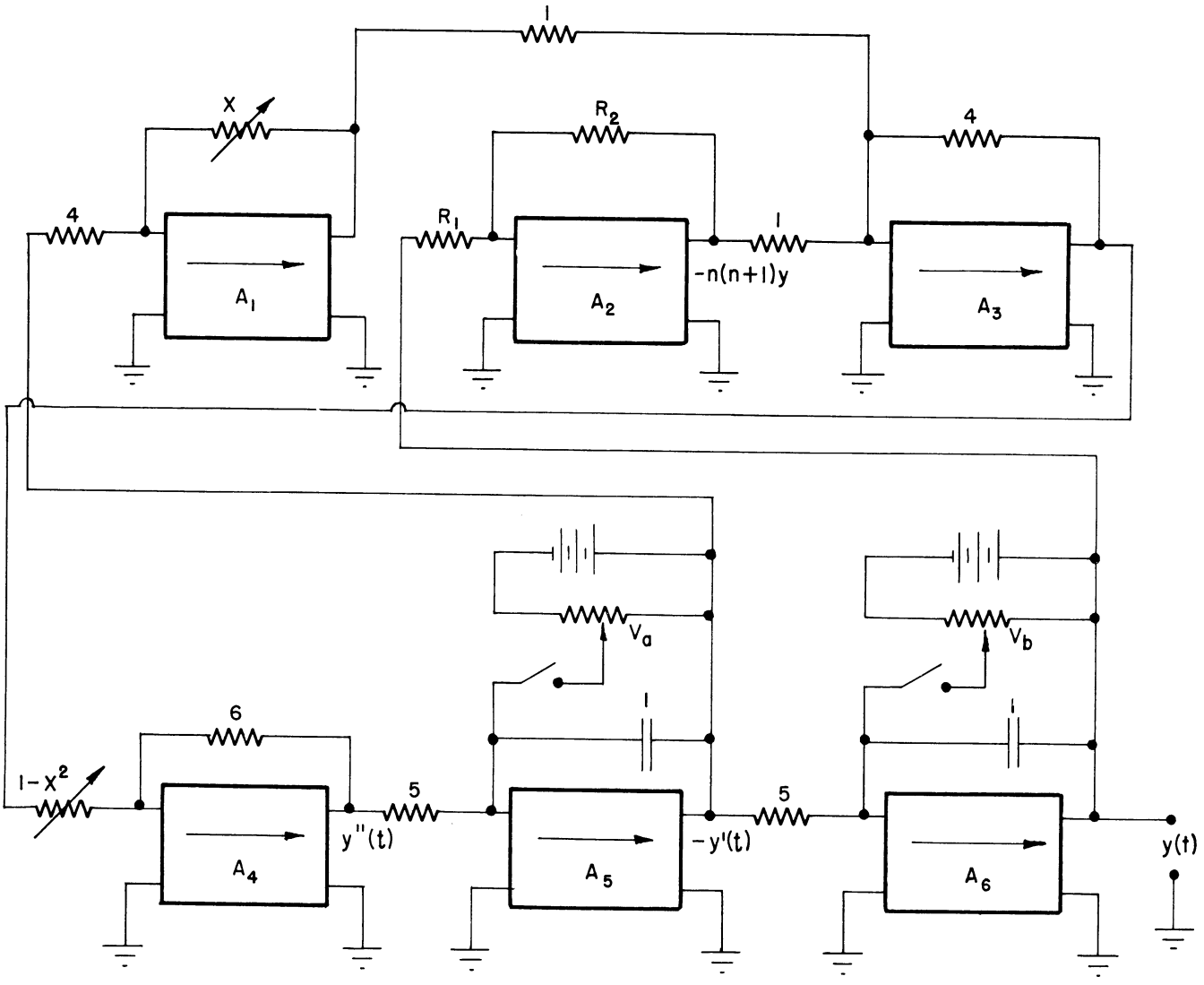

Figure 8-1. Computer circuit for solving the Legendre equation.

The function $(1 - x^2)$ is obtained in steps merely by changing the output lead (coming from the resistors on the terminal board) from the first resistor to the last resistor in the x^2 set-up used for Bessel's equation. This makes the first step 24 meg -5k; the second, 24 meg-30k-5k; the third, 24 meg-60k-30k-5k, etc. To proceed in this manner we must assume that $0 < x < 1$. The function x is obtained in steps exactly as in the case of Bessel's equation, the first step being 100k, the second, 300k, etc., up to 7.9 meg. At the beginning of the first step ($x = 0$) we wish to have the gain of A_4 be unity, hence the feedback resistor should be 24 meg. We actually use 6 meg, giving a net gain of 1/4 at $x = 0$, and to compensate for this the feedback resistor of A_3 is made 4 meg instead of 1 meg.

One unit of x is made 5 seconds of time for the computer; therefore the input resistors of the integrators are 5 meg. 8 steps/sec are used for the stepping relays in order to take 5 seconds for the 40 steps.

For integer values of the constant n in equation (8-1) there are polynomial solutions $P_n(x)$ called "Legendre polynomials". For values of n from 0 to 6 the solutions take the following forms:

$$P_0(x) = 1$$

$$P_1(x) = x$$

$$P_2(x) = 1/2(3x^2-1)$$

$$P_3(x) = 1/2(5x^3-3x)$$

$$P_4(x) = 1/8(35x^4-30x^2 + 3)$$

$$P_5(x) = 1/8(63x^5-70x^3 + 15x)$$

$$P_6(x) = 1/16(231x^6 - 315x^4 + 105x^2 - 5)$$

For even values of n the initial conditions are

$$P_n(0) = 0,\ P_n'(o) = \text{constant},\ n \text{ even}. \qquad (8\text{-}2)$$

The feedback capacitor across A_6 in Figure 8-1 is initially shorted, and V_a is varied until the first maximum of $P_n(x)$ is the desired number of deflection units on the recorder.

For odd values of n the initial conditions are

$$P_n(0) = \text{constant},\ P_n'(o) = n \text{ odd}. \qquad (8\text{-}3)$$

The feedback capacitor across A_5 is initially shorted, and V_b is varied until $P_n(0)$ is the desired number of deflection units on the recorder.

Oscillograms of $P_n(x)$ and $P_n'(x)$ for n = 1, 2, 3, 4, 5, 6, and 7 are shown in Figures 8-2, 8-4, 8-6, 8-8, 8-10, 8-12, and 8-14 respectively. The two-channel dc impedance matcher of our own design was used in taking these records; hence the curves are subject to small corrections.

Curves showing the computer solutions compared with the theoretical solutions from Jahnk-Emde for n = 1, 2, 3, 4, 5, 6, and 7 are shown in Figures 8-3, 8-5, 8-7, 8-9, 8-11, 8-13, and 8-15 respectively.

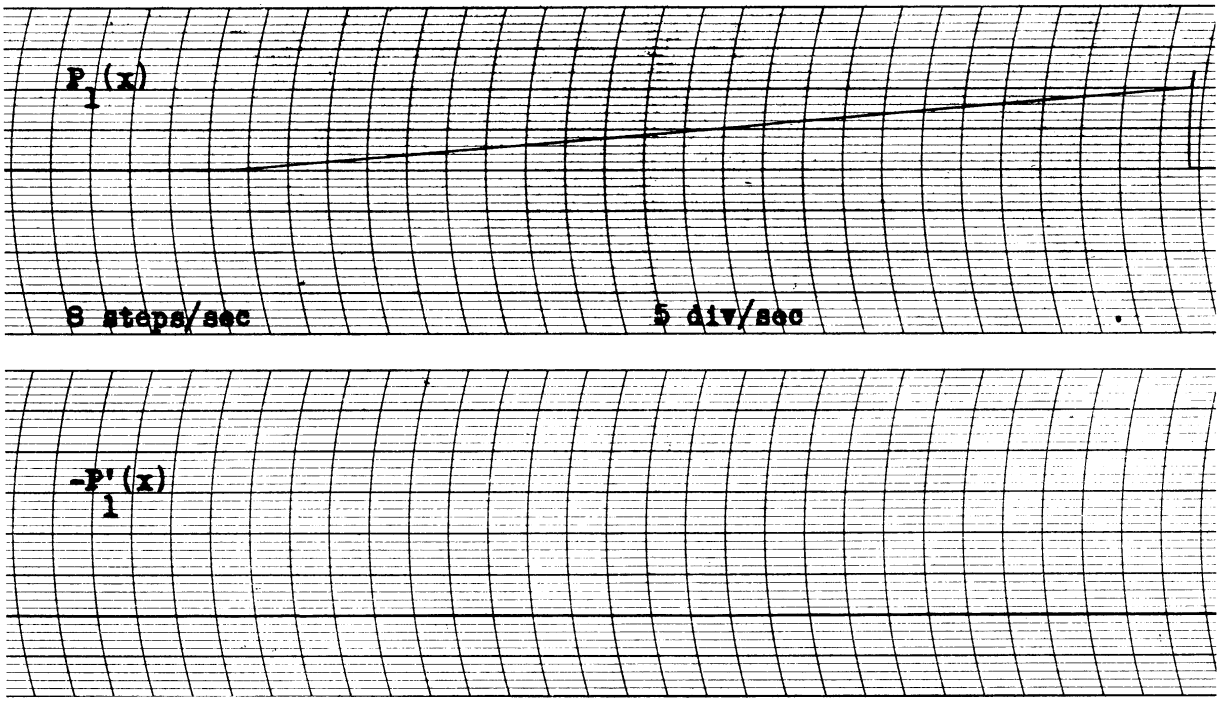

Figure 8-2. Computer solution for $P_1(x)$.

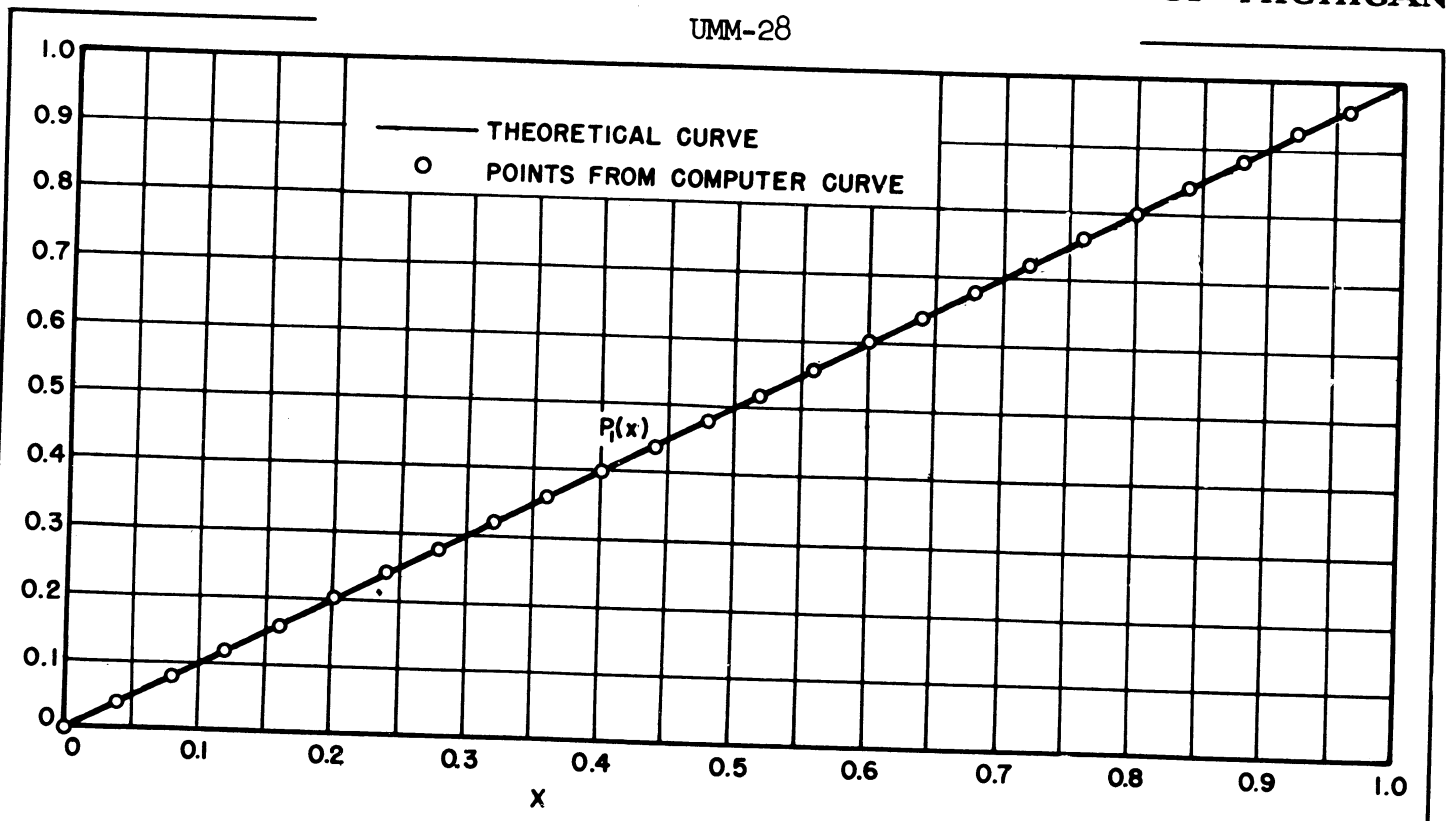

Figure 8-3. Theoretical $P_1(x)$ with computer solution.

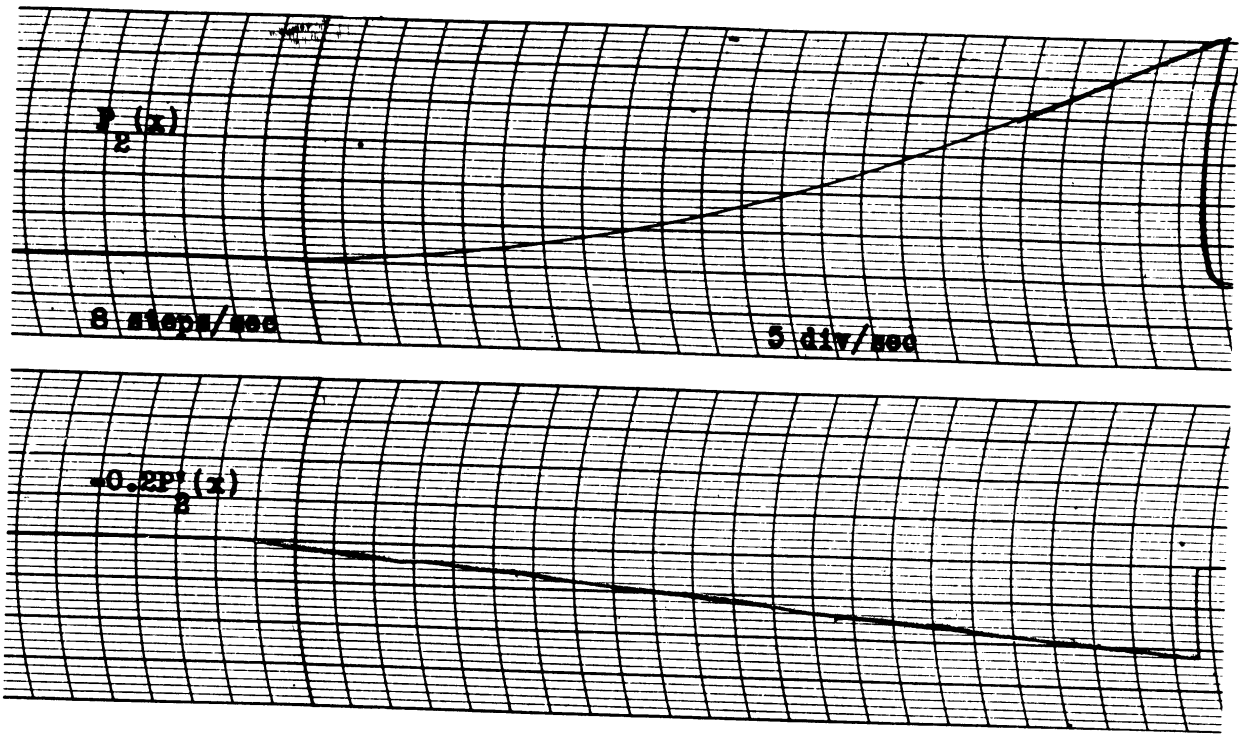

Figure 8-4. Computer solution for $P_2(x)$.

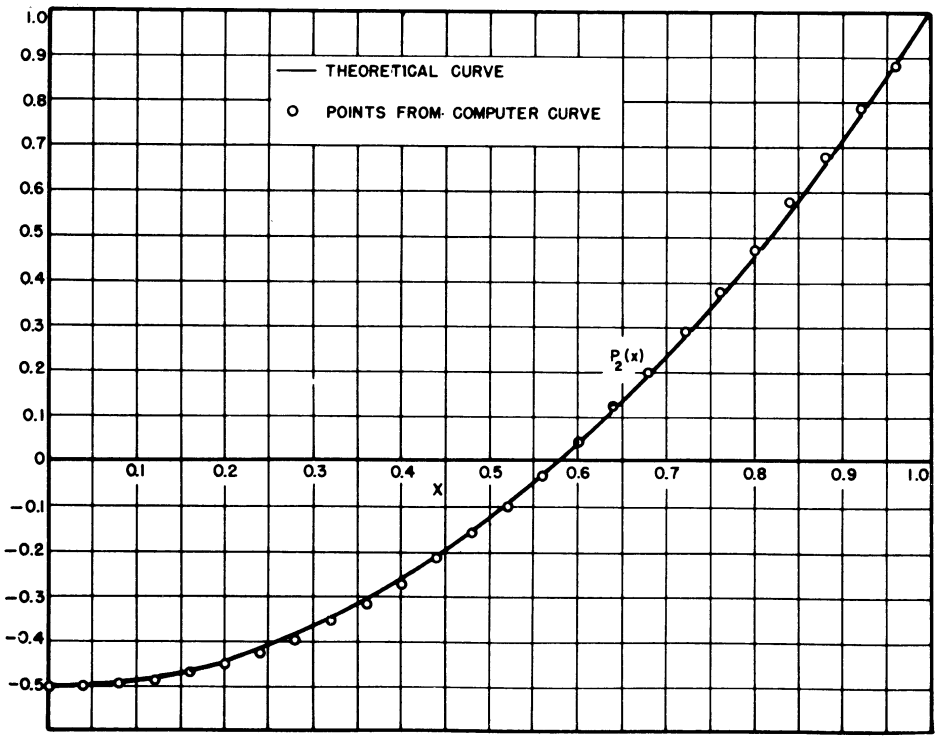

Figure 8-5. Theoretical $P_2(x)$ with computer solution.

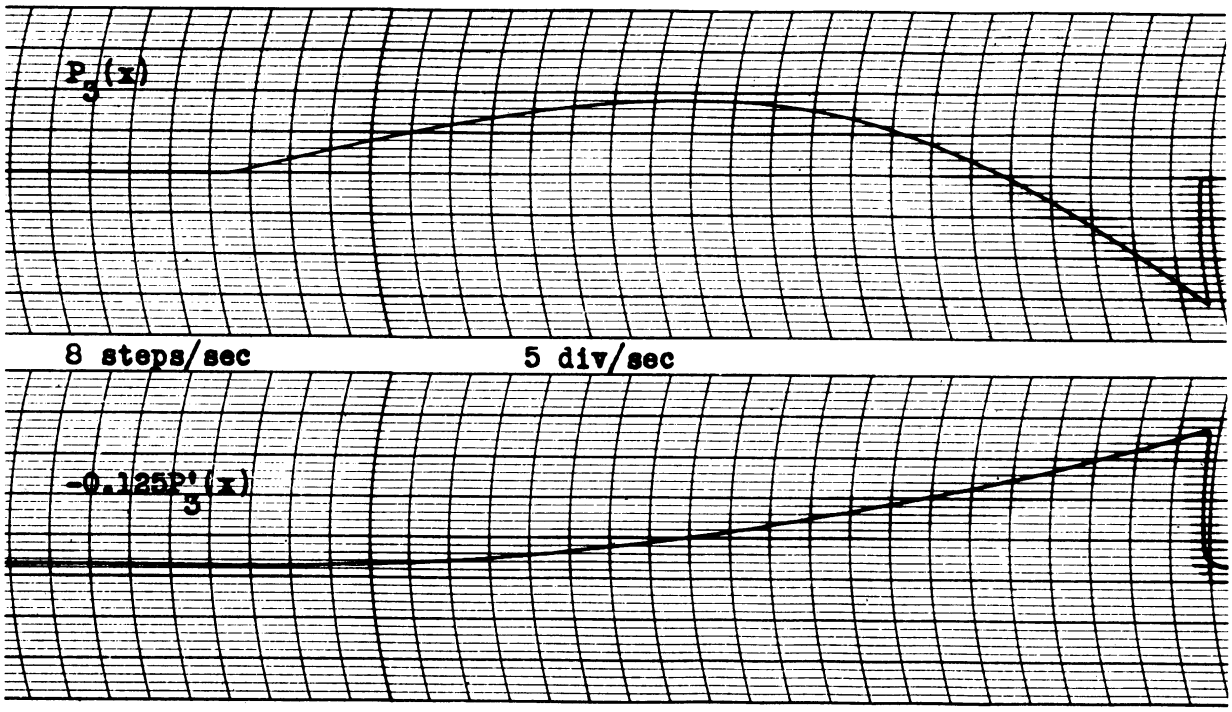

Figure 8-6. Computer solution for $P_3(x)$.

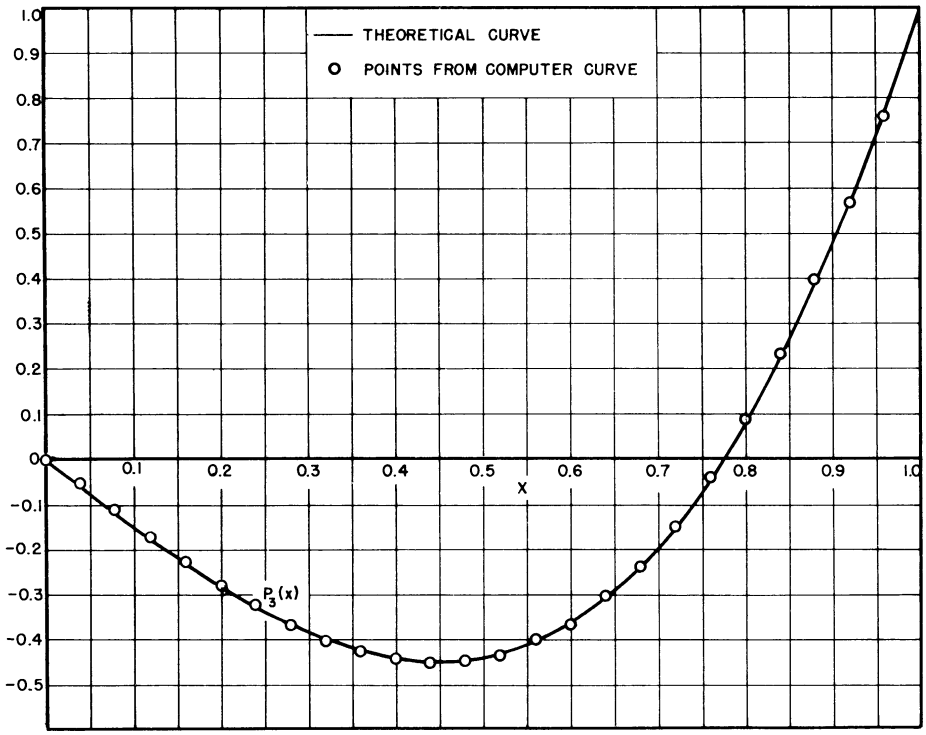

Figure 8-7. Theoretical $P_3(x)$ with computer solution.

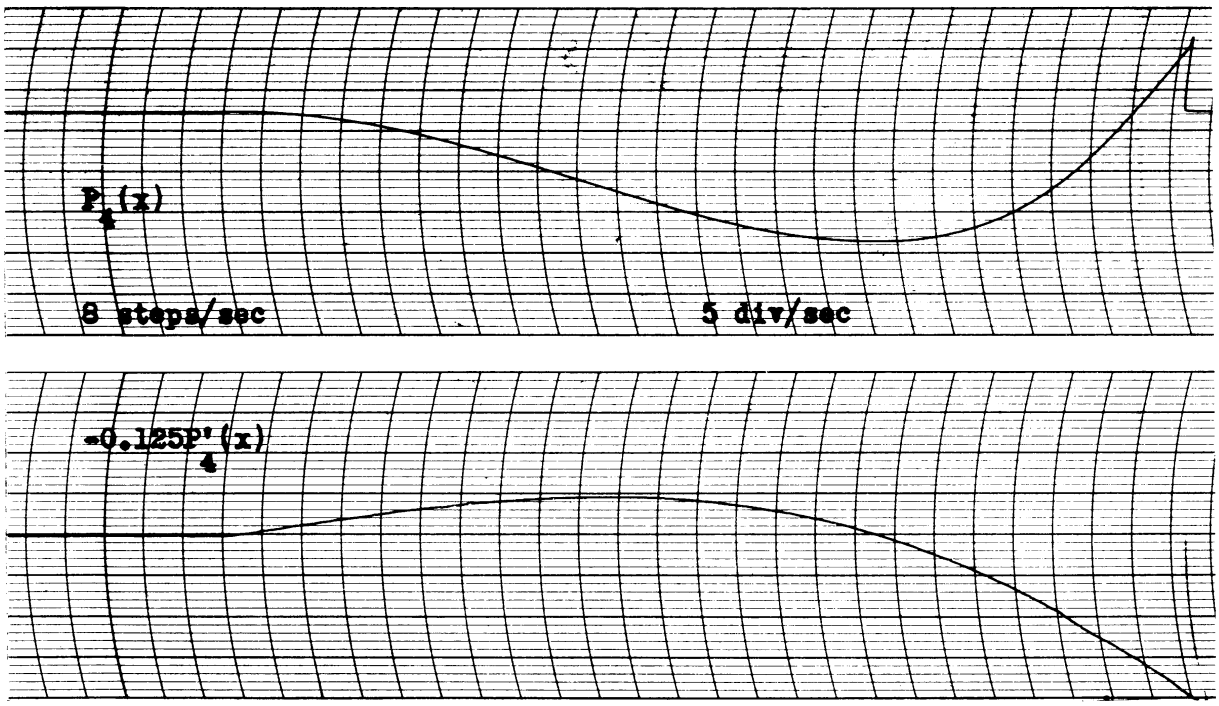

Figure 8-8. Computer solution for $P_4(x)$.

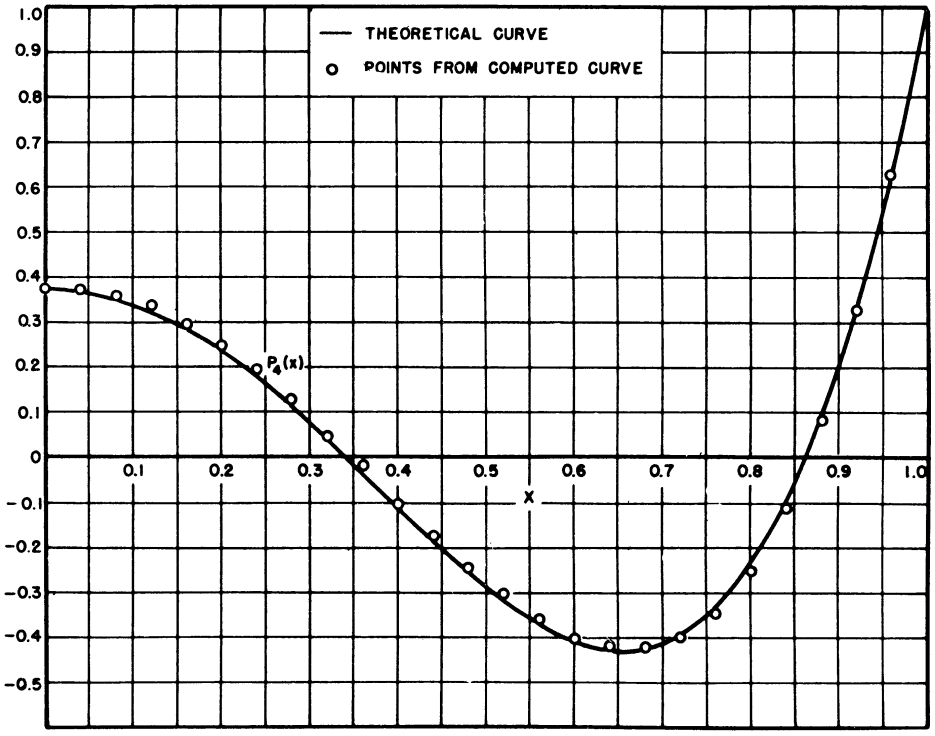

Figure 8-9. Theoretical $P_4(x)$ with computer solution.

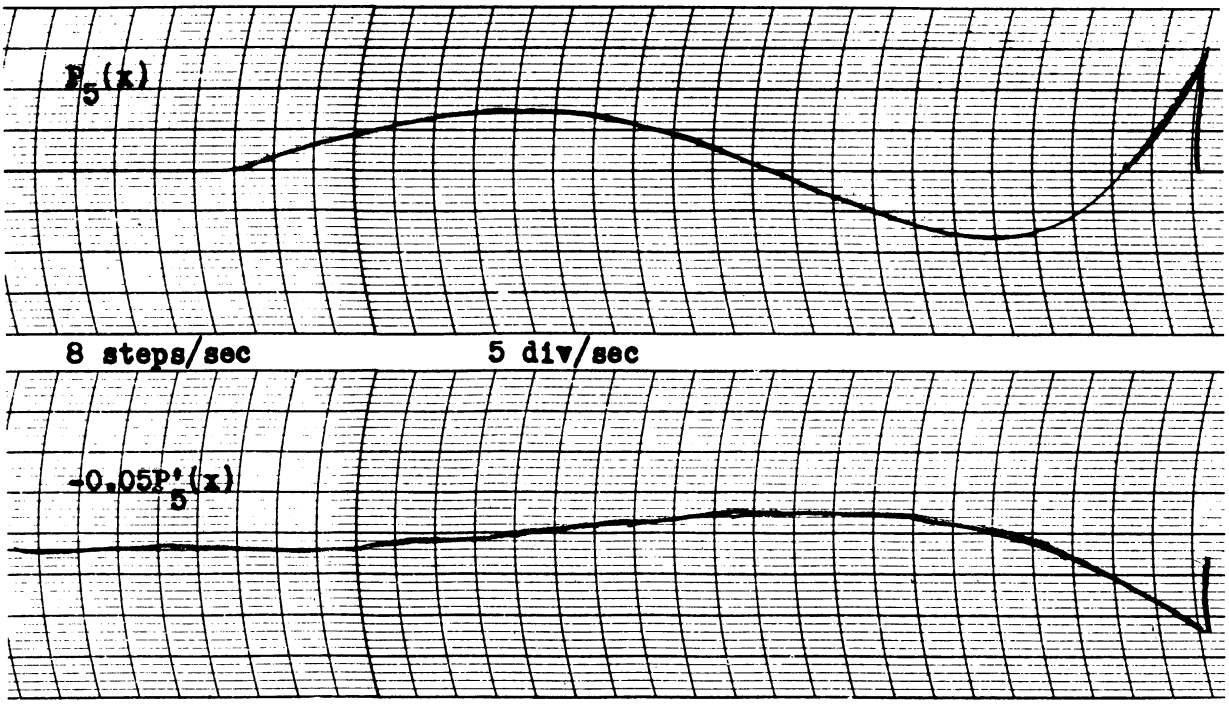

Figure 8-10. Computer solution for $P_5(x)$.

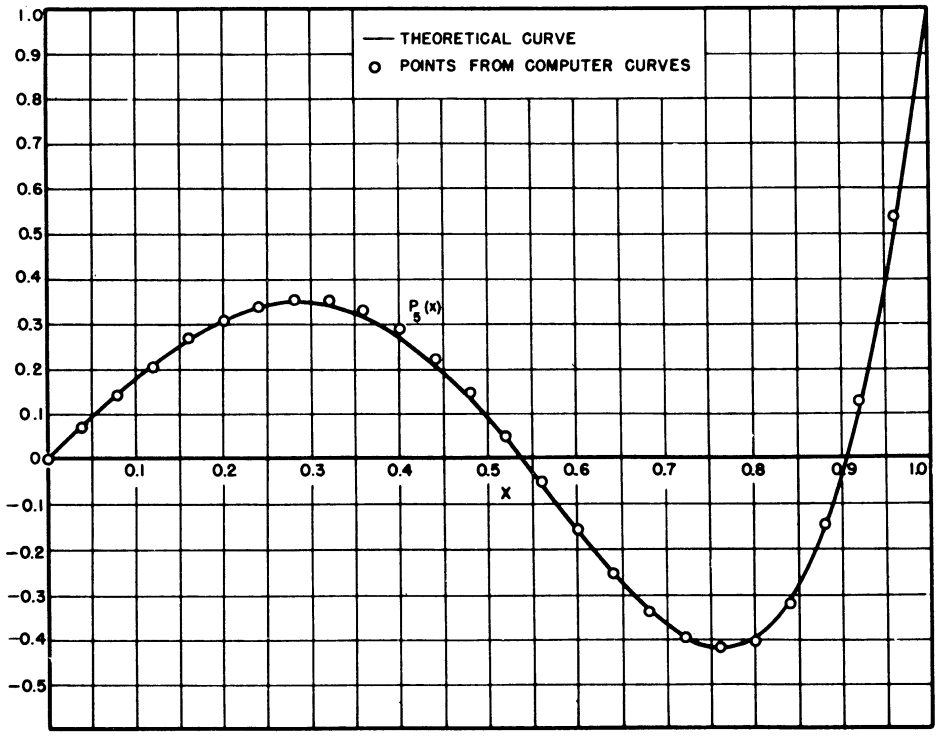

Figure 8-11. Theoretical $P_5(x)$ with computer solution.

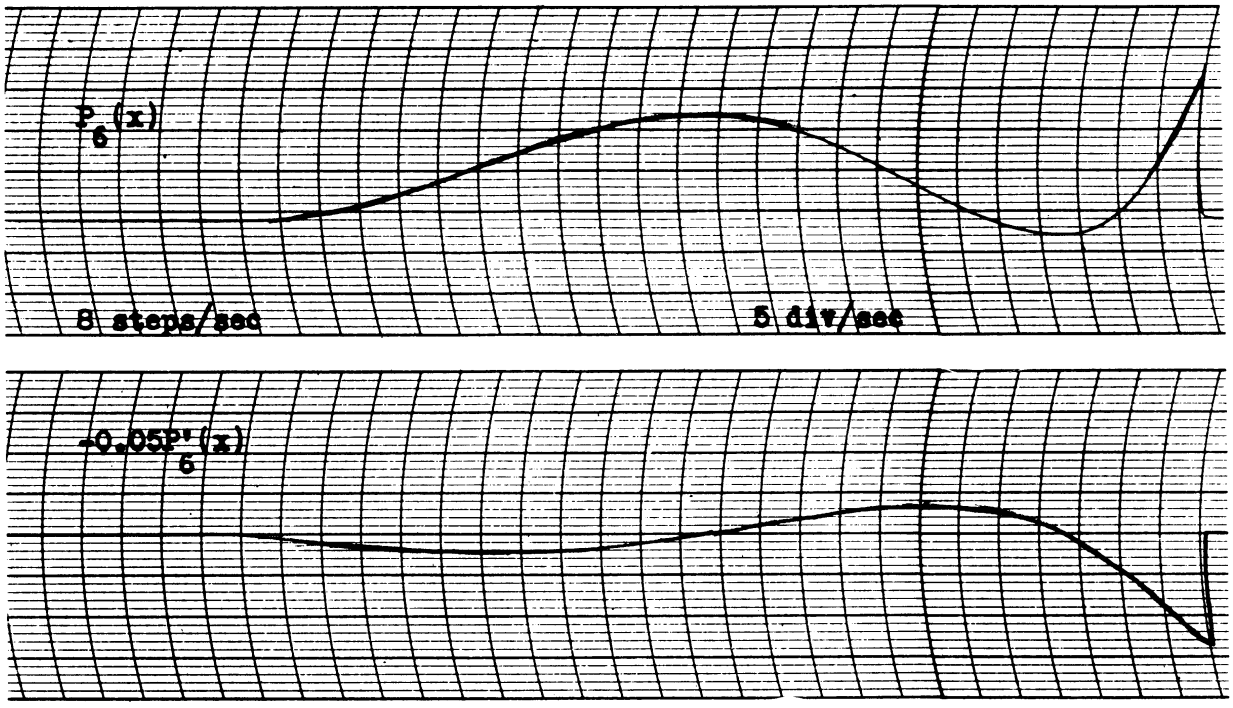

Figure 8-12. Computer solution for $P_6(x)$.

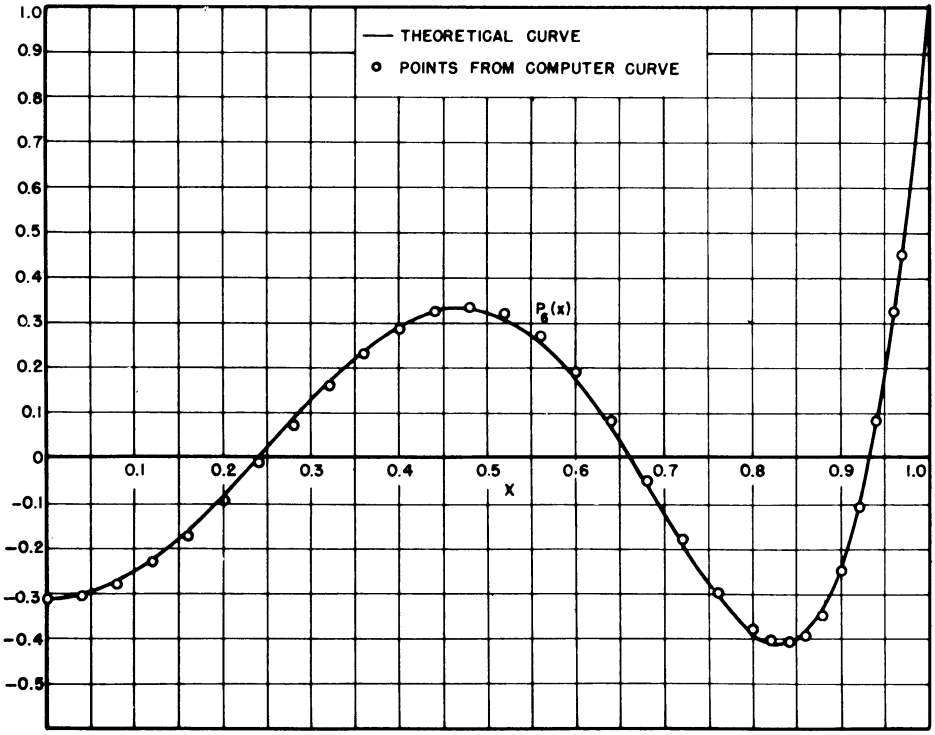

Figure 8-13. Theoretical $P_6(x)$ with computer solution.

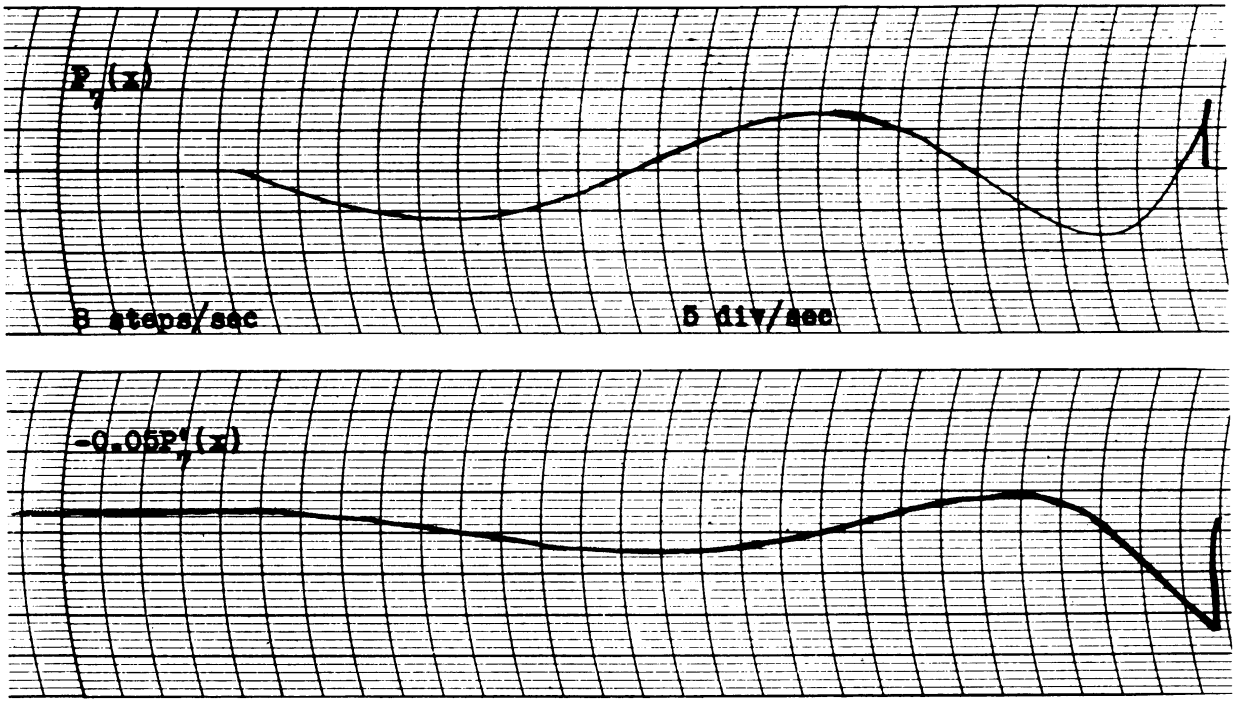

Figure 8-14. Computer solution for $P_7(x)$.

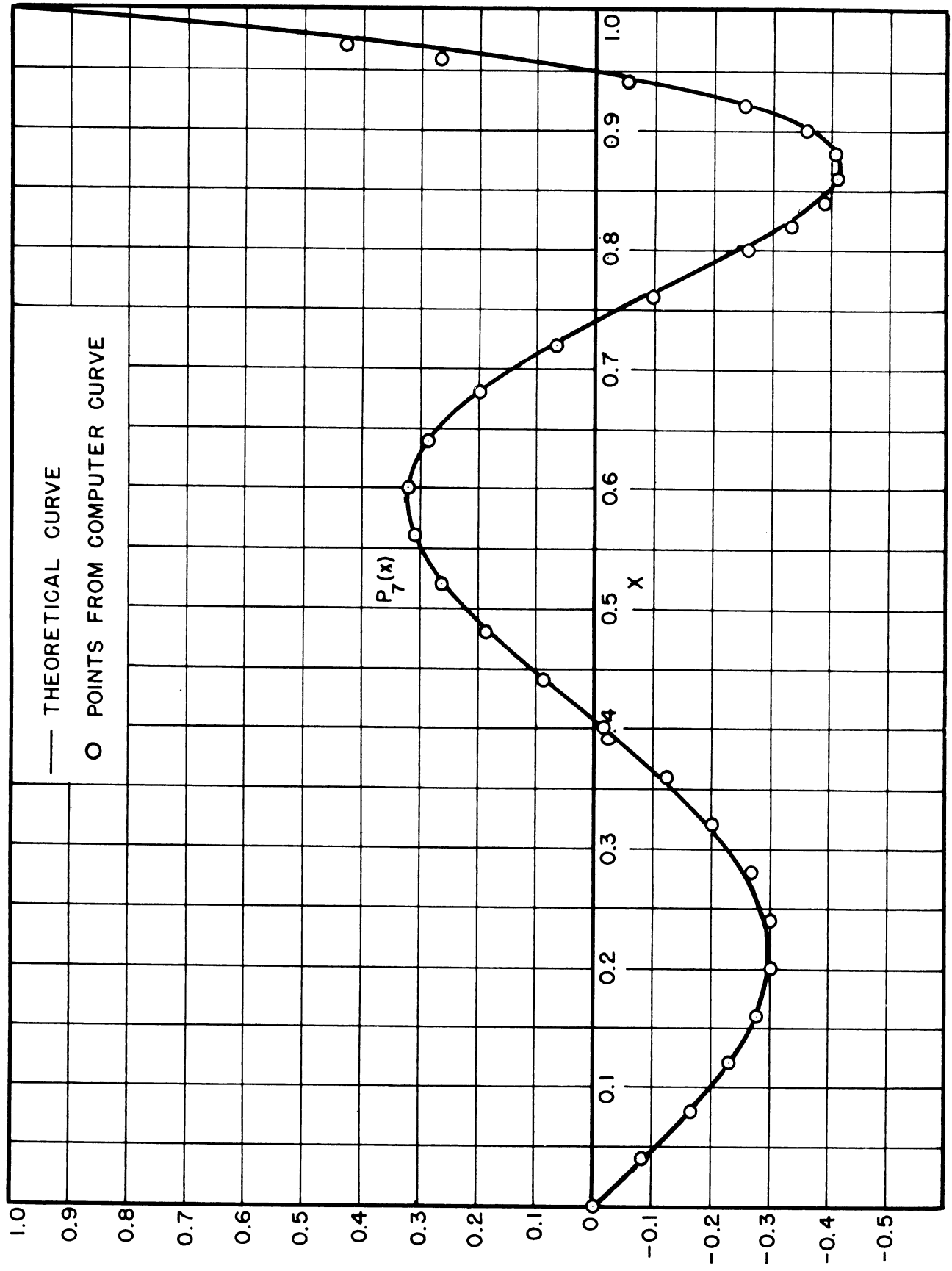

Figure 8-15. Theoretical $P_7(x)$ with computer solution.

CHAPTER 9

BOUNDARY VALUE PROBLEMS WITH VARIABLE COEFFICIENTS

9.1 Static Deflection of Uniform Beams with Variable Load

In Section 5.1 we saw that the equation for the static deflection of a uniform beam is

$$\frac{d^4y(x)}{dx^4} = aW(x) \quad , \qquad (5\text{-}2)$$

where $a = 1/EI$ = a constant and $W(x)$ is the load distribution along the beam. In Section 5.1, equation (5-2) was solved by means of the analog computer for $W(x)$ = a constant and $a = 1$. Reference to Figure 5-2 shows that $W(x)$ was simulated by a constant voltage applied to the input of the computer. In this section we simulate a variable $W(x)$ by means of a constant voltage input to amplifier A_1 in Figure 9-2, where A_1 has a feedback resistor R_m variable by means of the stepping relays.

A. Uniform Beam with Concentrated Load.

Let us first simulate a beam hinged on both ends and with a concentrated load in the middle (Figure 9-1).

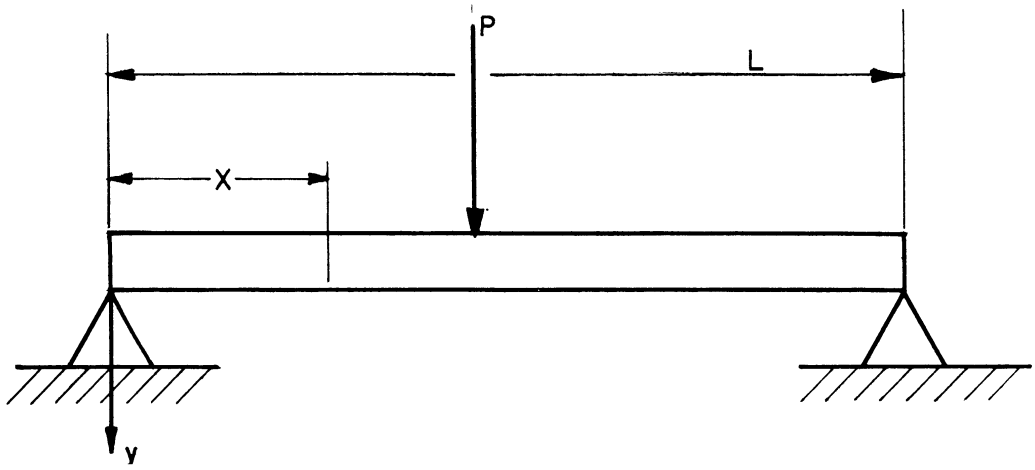

Figure 9-1. Uniform "hinged-hinged" beam with concentrated load at center.

We will simulate the concentrated force P by means of a load distributed over a quarter-second interval, where the total time interval is 4.75 seconds. In Figure 9-2 the feedback resistor R_m is made zero for the first 9 steps (0 to 2.25 sec), 10 megohms for the 10th step (2.25 to 2.50 sec), and zero for the next 9 steps (2.50 to 4.75 sec.). Actually the feedback resistor is shorted for a total of some 6 seconds (we were using a 25-step relay for these tests) in order to provide a continuous problem after 4.75 seconds.

As described in Section 1, the starting button, when pressed, automatically starts the stepping relays which simultaneously energize the initial condition relays, thus starting the solution of the problem. At the end of 6 seconds the stepping relays are automatically stopped and the initial condition relays automatically de-energized, resetting the initial conditions and hence stopping the solution of the problem. The voltage V_a in Figure 9-2 is varied until a correct solution, $X''(L) = X(L) = 0$, is obtained for a value of L different from the one desired. Then R_i is varied and the above process repeated until a correct solution is obtained for the desired length (L = 4.75 sec). Usually only four or five settings of R_i are required to obtain a solution of the proper length.

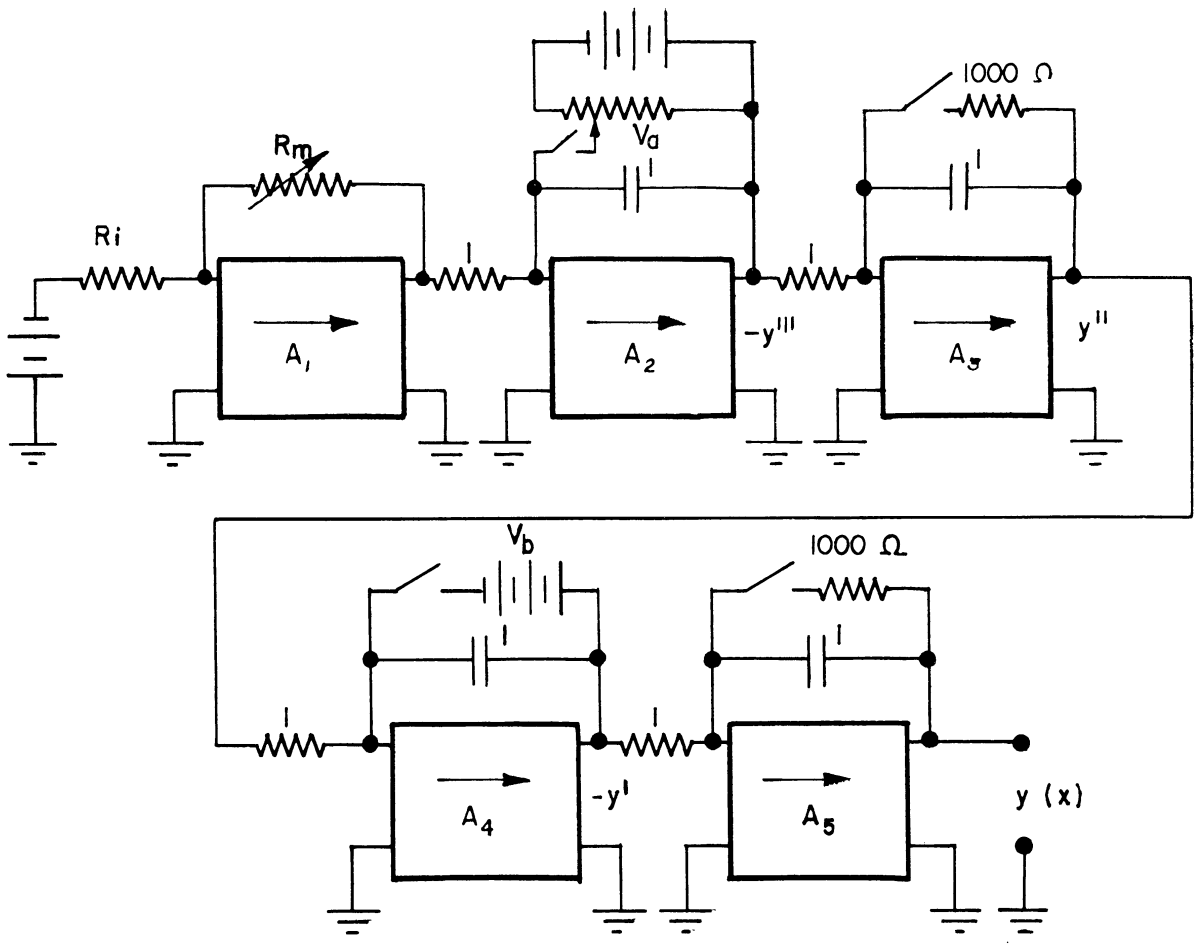

Figure 9-2. Computer circuit for solving static deflection of uniform beams under variable loads.

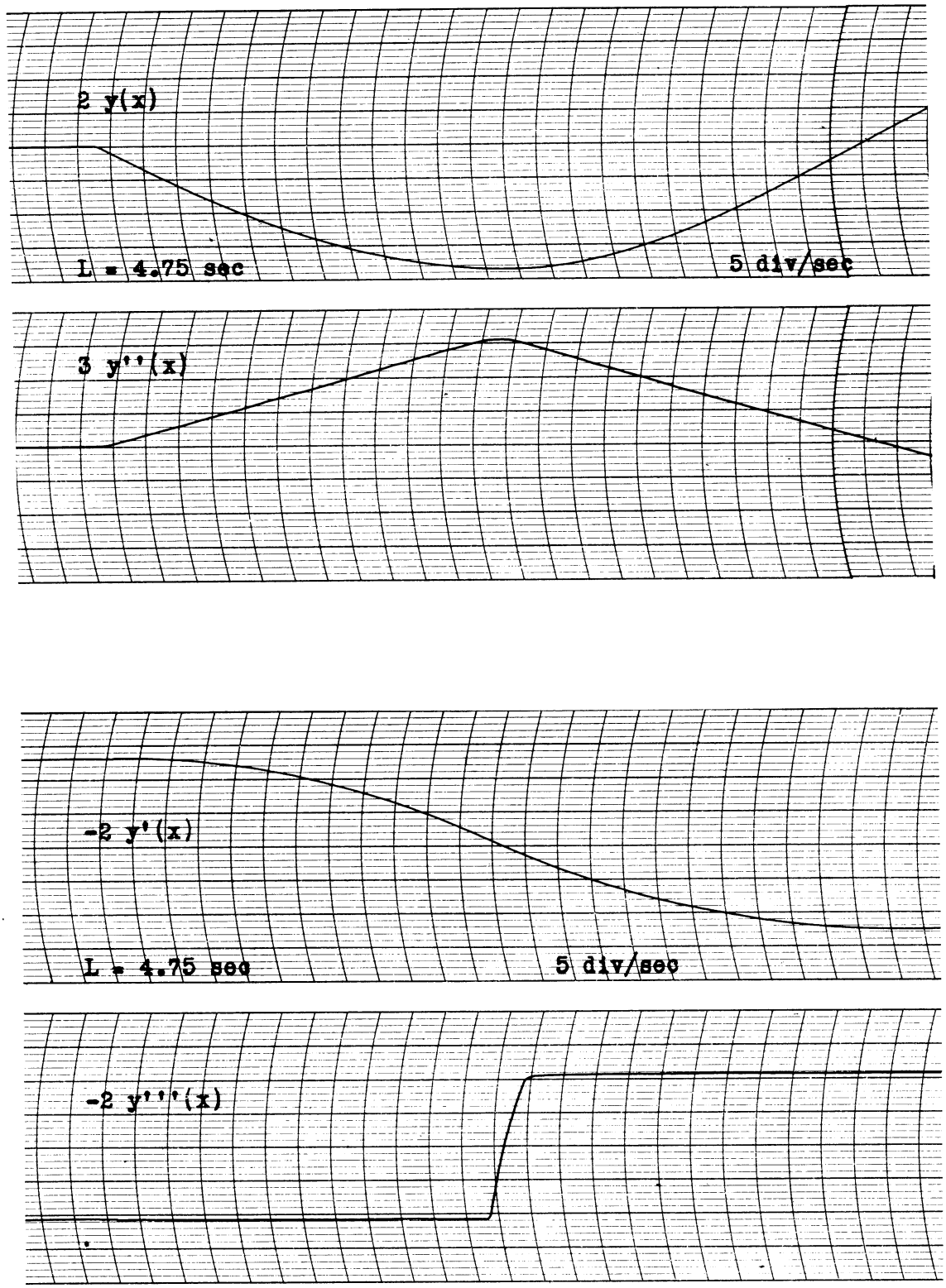

Figure 9-3. Static deflection of uniform "hinged-hinged" beam with concentrated load at center.

Oscillograms of y, y', y" and y''' as well as W(x) are shown in Figures 9-3 and 9-4. From Figure 9-4

$$P = \frac{W(x)}{4} = \frac{18.1}{4} = 4.53 \quad .$$

The theoretical values[11] for M_{MAX} and y_{MAX} are

$$M_{MAX} = \frac{PL}{4} = \frac{4.53(4.75)}{4} = 5.37$$

and

$$y_{MAX} = \frac{PL^3}{48EI} = \frac{4.53(4.75)^3}{48} = 10.1$$

From Figure 9-3

$$M_{MAX} = \frac{15.6}{3} = 5.2$$

and

$$y_{MAX} = \frac{18.8}{2} = 9.4$$

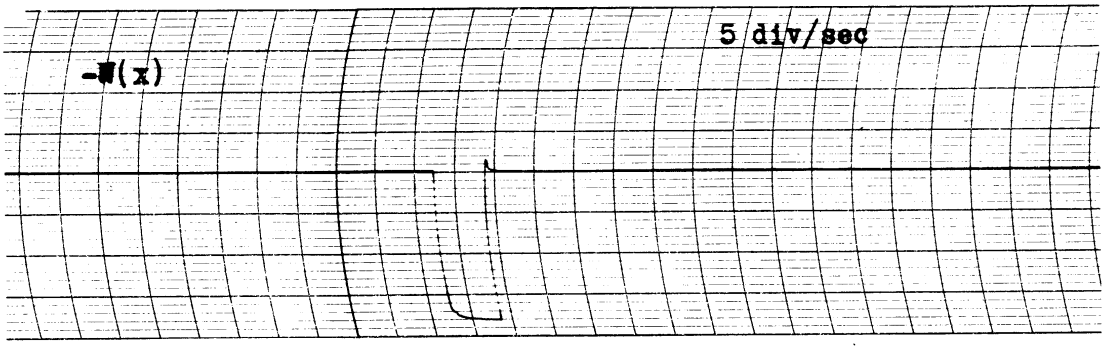

Figure 9-4. W(x) to simulate concentrated load.

B. Cantilever Beam with Tapered Load

The cantilever beam with tapered load is shown in Figure 9-5. In this case $W(x)$ is simulated in 16 quarter-second steps. This is accomplished by letting R_m of Figure 9-2 assume the values 775 K, 725 K, 675 K, 625 K, ..., 75 K, 25 K.

The 17th and 18th steps are made 25 K, and the 19th to 25th steps, 775 K in order to make a continuous problem. The computer circuit is exactly the same as in Figure 9-2 except that V_a and V_b are applied across the feedback capacitors of A_2 and A_3, respectively, and the initial short-circuits across the feedback capacitors of A_4 and A_5. V_a is varied until the end condition $y''(L) = y'''(L) = 0$ is met. R_i is varied and the above process repeated until L = 4 sec.

Oscillograms of y, y', y'' and y''' along with $W(x)$ are shown in Figures 9-6 and 9-7. From Figure 9-7

$$W = \text{total weight} = \frac{14.3 \times 4}{2 \times 10} = 2.86$$

The theoretical values[12] for M_{MAX} and y_{MAX} are

$$M_{MAX} = \frac{WL}{3} = \frac{(2.86)(4)}{3} = 3.81$$

and

$$y_{MAX} = \frac{WL^3}{15EI} = \frac{(2.86)(4)^3}{15} = 12.2$$

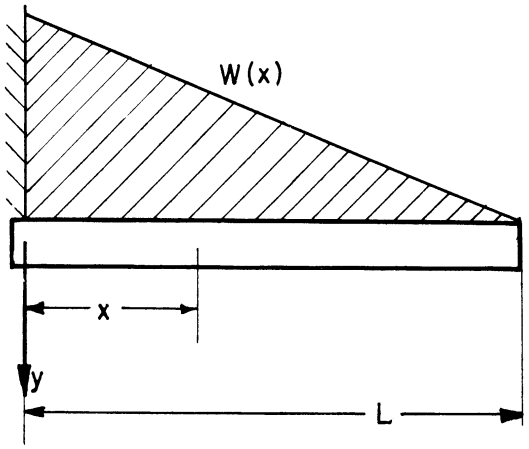

Figure 9-5. Uniform cantilever with tapered load.

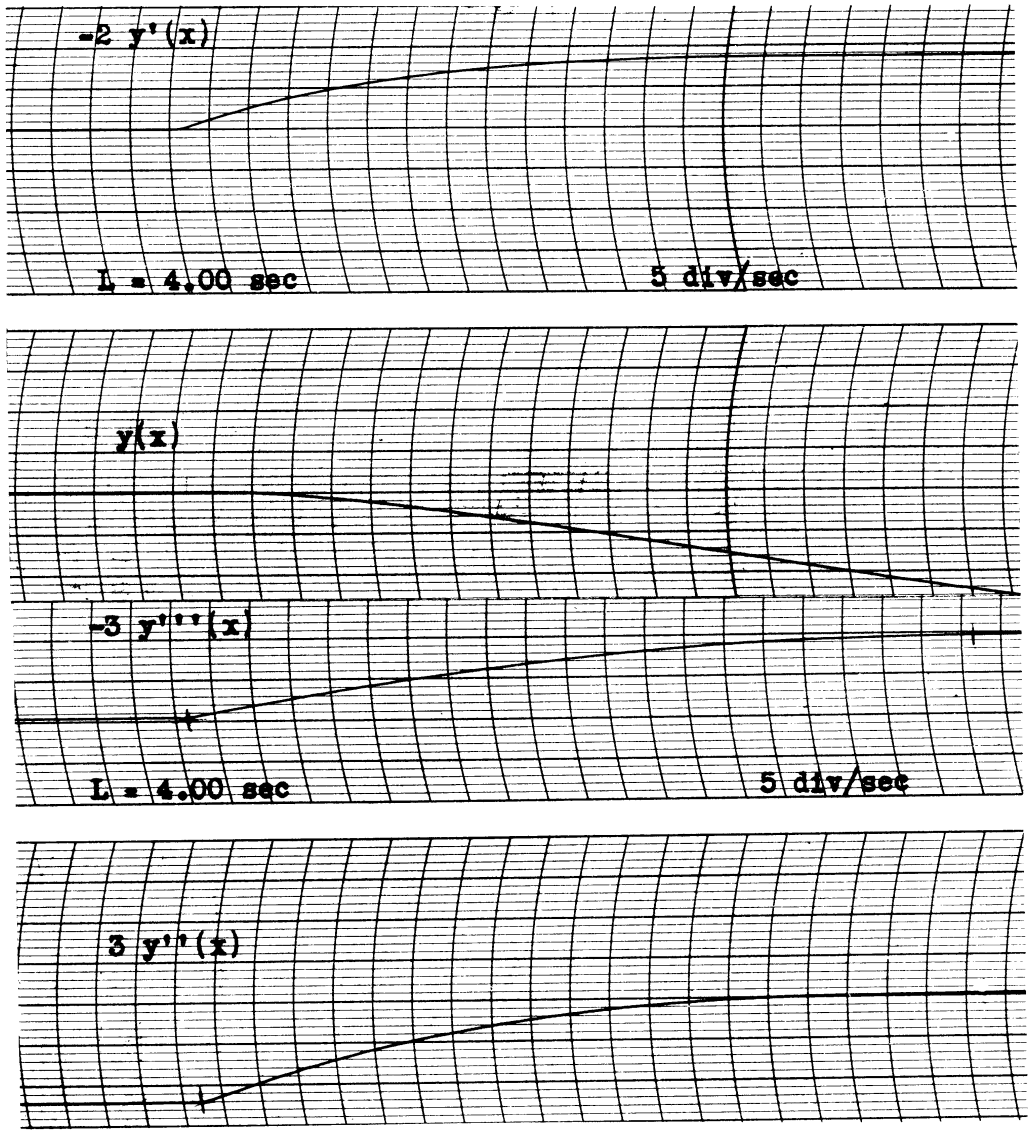

Figure 9-6. Solution of static deflection of cantilever beam with tapered load.

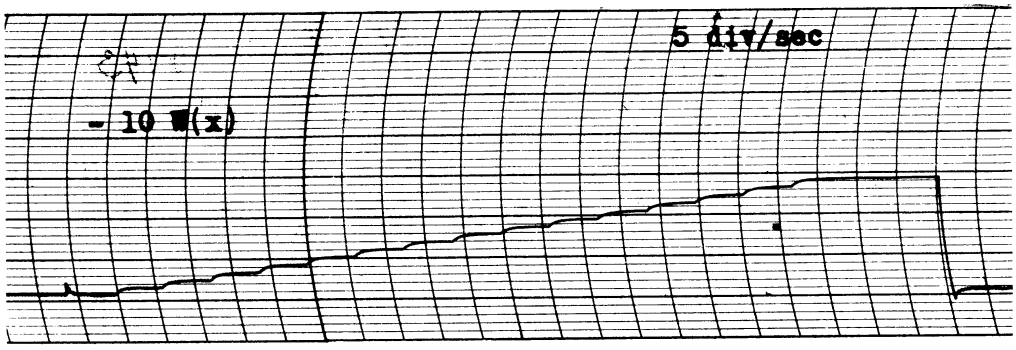

Figure 9-7. W(x) to simulate tapered load.

From Figure 9-6

$$M_{MAX} = \frac{12}{3} = 4.0$$

$$y_{MAX} = \frac{12.3}{1} = 12.3$$

9.2 First Normal Mode of Oscillation of a Uniform Beam with a Concentrated Load.

The beam which we consider in this section is supported by hinges at both ends and has a concentrated mass in the center (see Figure 9-8). To simulate the concentrated mass at the center we solve the problem for a mass of finite width 1/4 of a second, where L, the total length of the beam, is 3.25 seconds. From equation (5-29) we obtain as our equation

$$\frac{EIL^4}{\mu \lambda^2 \ell^4} \frac{d^4X}{d\bar{x}^4} - f(\bar{x})\ X = 0 \qquad (9\text{-}1)$$

where

$$\begin{aligned} f(\bar{x}) &= 1 && 0 < x < 1.5 \\ f(\bar{x}) &= K && 1.5 < x < 1.75 \\ f(\bar{x}) &= 1 && 1.75 < x < 3.25 \end{aligned} \qquad (9\text{-}2)$$

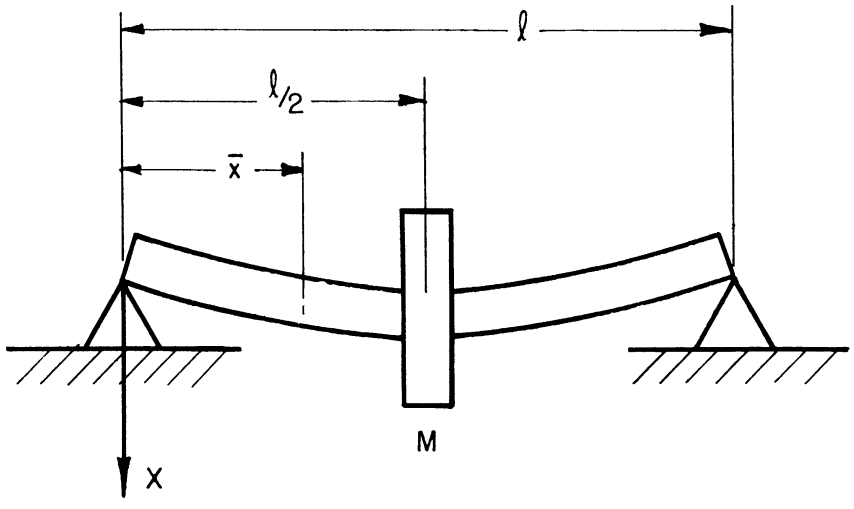

Figure 9-8. Uniform "hinged-hinged" beam with concentrated mass at center.

K is the relative increase in the mass distribution along the beam due to M. If m is the total mass of the beam without the load, the ratio

$$\frac{M}{m} = \frac{K-1}{4(3.25)} = \frac{K-1}{13} .$$

Our end conditions are

$$X(0) = X''(0) = X(L) = X''(L) \quad , \tag{5-37}$$

where L = 3.25 seconds.

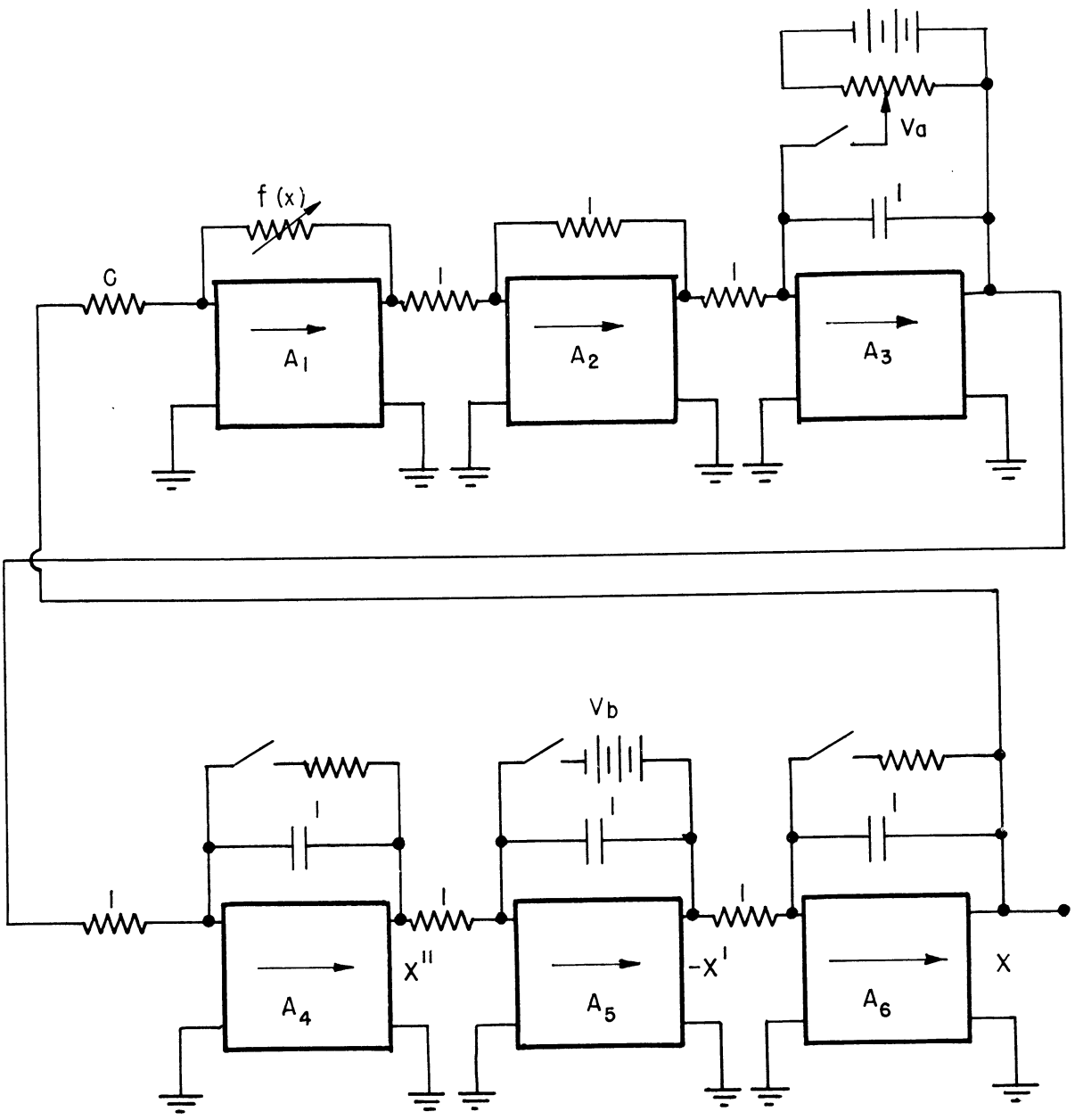

Figure 9-9. Computer circuit for solving normal modes of vibration of a uniform beam bearing a load.

The computer circuit for solving the problem is shown in Figure 9-9. The feedback resistor of A_1 is varied by means of the stepping relays as follows: first 6 steps, 1 meg; 7th step, 6 megs; 8th to 13th steps, 1 meg. In order to make a continuous problem after 3.25 seconds, the rest of the steps (14 through 25) were also 1 meg. In this case $K = 6$ and $\frac{M}{m} = \frac{5}{13}$ (see above).

The initial voltage V_a is varied until a solution with the correct end conditions is obtained. The value of C is varied until the length L of the correct solution is exactly 3.25 seconds.

Oscillograms of X, X', X" and X''' are shown in Figure 9-10, and f(x) is shown in Figure 9-11.

The theoretical value of the frequency for the first mode is given by[13]

$$\lambda = \sqrt{\frac{48EI}{m(\frac{M}{m} + 0.5)\ell^3}}$$

Since $m = \mu\ell$

$$\lambda = \sqrt{\frac{48}{\frac{M}{m} + 0.5}} \cdot \sqrt{\frac{EI}{\mu\ell^4}}$$

and

$$\alpha = \sqrt{\frac{48}{\frac{M}{m} + 0.5}} \qquad (9\text{-}3)$$

For $L = 3.25$ and $\frac{M}{m} = \frac{5}{13}$

$$\alpha = \sqrt{\frac{48}{5/13 + 0.5}} = 7.37$$

For a correct solution with L = 3.25 sec, C was found to be $\frac{1}{0.481}$ from the computer.

Then from equation (5-34)

$$\alpha = \frac{L^2}{\sqrt{C}} = (3.25)^2 \sqrt{0.481} = 7.36$$

Experimental $\alpha = 7.36$

Theoretical $\alpha = 7.37$

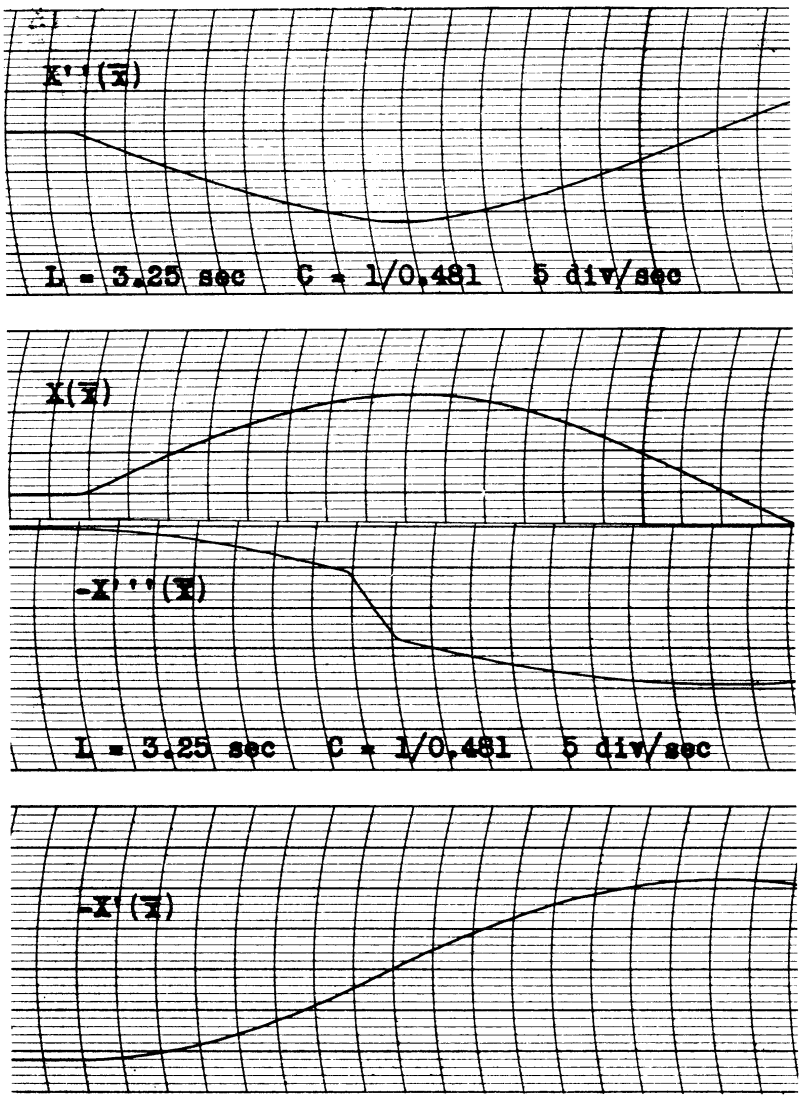

Figure 9-10. First-mode solution of "hinged-hinged" beam bearing a concentrated load at the center.

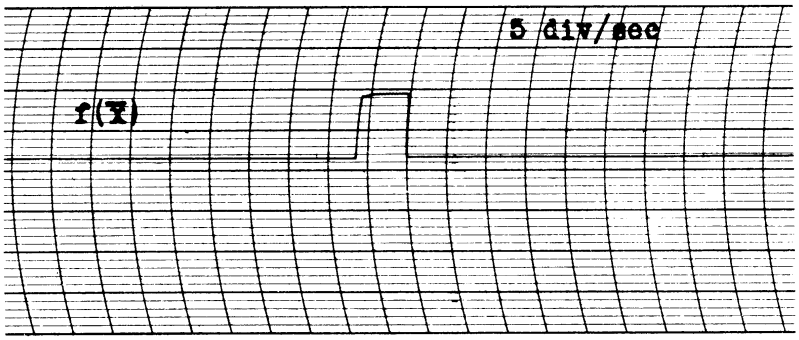

Figure 9-11. f(x) to simulate beam with concentrated load.

9.3 Normal Modes of Oscillation of a Non-Uniform Beam.

For a beam of variable cross-section our equation becomes, after separation of variables,

$$\frac{d^2}{dx^2}\left(EI\ \frac{d^2X}{dx^2}\right) - \mu\lambda^2 X = 0. \qquad (5\text{-}24)$$

We let

$$I = I_o i(x), \qquad (9\text{-}4)$$

$$\mu = \mu_o \beta(x), \qquad (9\text{-}5)$$

where I_o and μ_o are the maximum moment of inertia and mass per unit length respectively. If ℓ is the length of our original beam, and L is the length for the computer circuit, we let

$$\bar{x} = \frac{L}{\ell}\ x\ , \qquad (5\text{-}26)$$

and from equations (9-4), (9-5) and (5-26), equation (5-24) becomes

$$\frac{EI_oL^4}{\mu_o\ell^4\lambda^2}\ \frac{d^2}{d\bar{x}^2}\left[i(\bar{x})\ \frac{d^2X}{d\bar{x}^2}\right] - \beta(\bar{x})\ X = 0\ . \qquad (9\text{-}6)$$

Letting

$$\alpha = \lambda\sqrt{\frac{\mu_o\ell^4}{EI_o}} \qquad (9\text{-}7)$$

we get

$$\frac{L^4}{\alpha^2}\ \frac{d^2}{d\bar{x}^2}\left[i(\bar{x})\ \frac{d^2X}{d\bar{x}^2}\right] - \beta(\bar{x})\ X = 0\ , \qquad (9\text{-}8)$$

where we designate $C = \frac{L^4}{\alpha^2}$. The equation which we solve on the computer, then, is

$$C\ \frac{d^2}{d\bar{x}^2}\left[i(\bar{x})\ \frac{d^2X}{d\bar{x}^2}\right] - \beta(\bar{x})\ X = 0 \qquad (9\text{-}9)$$

The computer circuit for solving equation (9-9) in the case of a beam free at both ends is shown in Figure 9-12. From equation (5-3) it is apparent that the

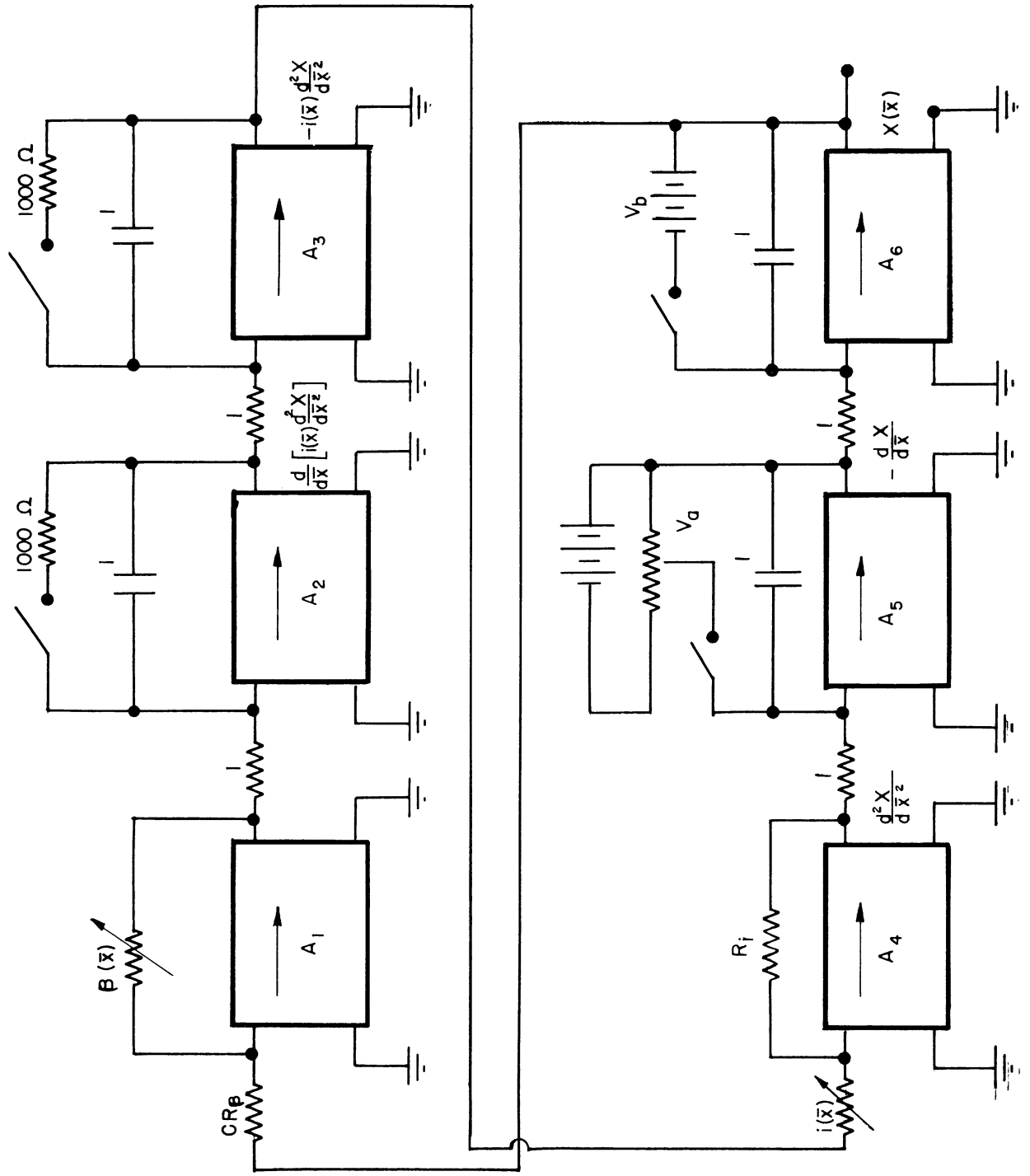

Figure 9-12. Computer circuit for solving normal modes of vibration of non-uniform beams.

bending moment $M(\bar{x})$ will be proportional to $i(\bar{x})\ \frac{d^2X}{d\bar{x}^2}$ and that the shearing force $Q(\bar{x})$ will be proportional to $\frac{d}{d\bar{x}}\left[i(\bar{x})\ \frac{d^2X}{d\bar{x}^2}\right]$.

The end conditions for the "free-free" beam become

$$i(0).\ \frac{d^2X(0)}{d\bar{x}^2} = \frac{d}{d\bar{x}}\left[i(0)\ \frac{d^2X(0)}{d\bar{x}^2}\right] = i(L)\ \frac{d^2X(L)}{d\bar{x}^2} = \frac{d}{d\bar{x}}\left[i(L)\ \frac{d^2X(L)}{d\bar{x}^2}\right] = 0 \qquad (9\text{-}10)$$

As an example of a beam with varying cross-section, we chose a problem for which an analytic solution has already been worked out for the first mode of vibration.(14) We consider the vibration of the hull of a ship, where the hull is assumed symmetrical with respect to the middle section. We assume that if we place the origin of longitudinal coordinates at the middle section, the moment of inertia I and mass distribution μ can be represented by the following formulas:

$$I = I_o\ (1 - bx^2) \qquad (9\text{-}11)$$

$$\mu = \mu_o\ (1 - cx^2) \qquad (9\text{-}12)$$

where x varies from $-\ell/2$ to $+\ell/2$, ℓ being the length of the ship.

The values of the constants given for the ship are: ℓ = 100 meters, I_o = 20 (meters)^4, μ_o = 7 x 9.81 tons/meter, b = c = 0.0003 1/(meter)^2, E = 2 x 10^7 tons/(meter)^2.

The calculated value of the frequency for the first mode is given as

$$\lambda = 21.6 \text{ radians/sec}$$

Solving for the frequency constant α from equation (9-7) we find that

$$\alpha = 21.6\sqrt{\frac{7(100)^4}{2 \times 10^7 \times 20}} = 28.6$$

We will now compute α on the analog computer and compare the result with the value given above.

We simulate $i(\bar{x})$ and $\beta(\bar{x})$ by means of 40 steps, 4 steps per second. This means that L = 10 sec for the computer solution. From equations (9-11) and (9-12) for b = c = 0.0003 we obtain

$$\beta(\bar{x}) = i(\bar{x}) = 1 - 0.75\left(\frac{2\bar{x}}{L}\right)^2,$$

where $-\frac{L}{2} < \bar{x} < \frac{L}{2}$. The resistances added for each step to simulate equation (9-13), as calculated from equation (6-4), are given in the following table.

Step	Resistance Added Each Step
1	0.765 meg
2	0.190
3	0.180
4	0.170
•	•
•	•
•	•
•	•
•	•
18	0.030
19	0.020
20	0.010

For steps 21-40 the same resistances were subtracted in reverse order by connecting steps 21 to 40 to the same terminals as steps 20 to 1. At $\bar{x} = 0$, $i(\bar{x}) = 1$. If the stepping resistors above are used as a feedback impedance, then for the amplifier to have a gain of unity at $\bar{x} = 0$ (between the 20th and 21st steps) the input resistor required is 2.667 meg.

The end conditions for our problem are

$$i(-L/2)\frac{d^2X(-L/2)}{d\bar{x}^2} = \frac{d}{d\bar{x}}\left[i(-L/2)\frac{d^2(-L/2)}{d\bar{x}^2}\right] = i(L/2)\frac{d^2X(L/2)}{d\bar{x}^2} =$$

$$\frac{d}{d\bar{x}}\left[i(L/2)\frac{d^2X(L/2)}{d\bar{x}^2}\right] = 0, \qquad (9\text{-}13)$$

where

$$-\frac{L}{2} < \bar{x} < \frac{L}{2}$$

The circuit for solution of the problem is shown in Figure 9-12, where $R_i = R\beta = 2.667$ meg. V_a is varied until a solution with the proper end conditions is obtained. C is then varied until the length L for a correct solution is 10 seconds. The quickest way to arrive at a correct

value of C is to plot a curve of C vs L as soon as the values of L are within 0.5 second of 10 seconds. Only a few points on this curve are necessary to locate C such that L = 10 sec ± 0.02 sec.

Oscillograms of X, $i(\bar{x})X''$ and $(i(x)X'')$ are shown in Figure 9-13. For L = 10.00 sec C = 12.20 and from equation (5-34)

$$\omega = \frac{L^2}{\sqrt{C}} = \frac{(10)^2}{\sqrt{12.20}} = 28.65$$

Experimental = 28.65

Theoretical = 28.6

In order to obtain L for the second mode it was found necessary to use the method of interpolation of higher modes described in Section 5.2A.

For L = 10.02 sec, C = 1.932. From equation (5-34)

$$\omega = \frac{L^2}{\sqrt{C}} = \frac{(10.02)^2}{\sqrt{1.932}} = 72.2$$

Even by means of interpolation of results solutions of the third mode are almost impossible to obtain because of failure of the computer to repeat curves from solution to solution. The following values were obtained using symmetry of the curves.

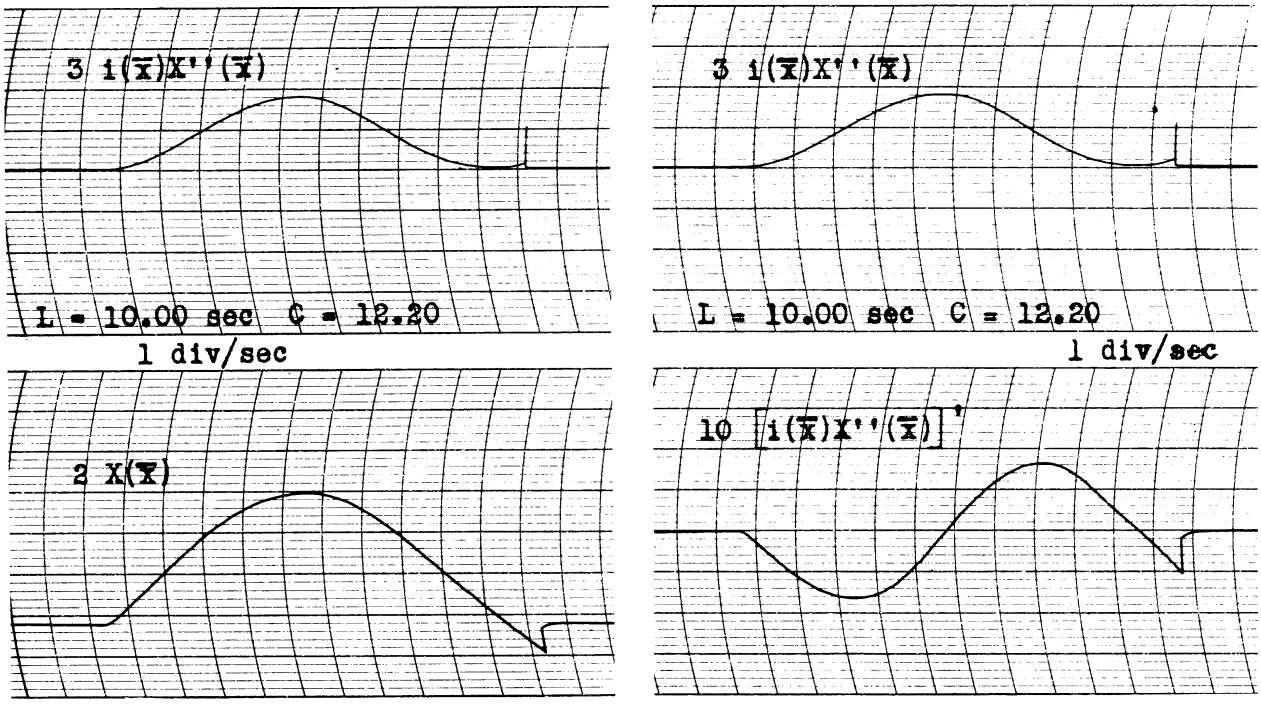

Figure 9-13. First-mode solution of ship hull.

For the third mode, C = 0.5335 for L = 9.96 sec. From equation (5-34)

$$\phi = \frac{L^2}{\sqrt{C}} = \frac{(9.96)^2}{\sqrt{.5335}} = 135.7$$

Summary of Data - Ship Problem

Mode	Experimental	Theoretical
1	28.65	28.6
2	72.2	
3	135.7 ± 1	

Several remarks on the solution of this type of problem by means of the analog computer should be made at this time. The first is that extensive tests have showed that the highest accuracy is attainable when the gains of all amplifiers in the system are kept as close to unity as possible. This means that the factor C, if different from unity by more than a factor of ten, should not be embodied all in one resistor or one amplifier, but should be distributed over several amplifiers, such as A_1 and A_2 in Figure 9-12. The length L of the solution should be selected so that C does not become larger than about 20, if high accuracy is desired. In all of these problems with coefficients varied in steps the length L can be conveniently changed by an integral factor merely by changing the number of contacts per second on the curve which steps the relays.

This brings up a second point. Despite the fact that the cams running the stepping relays (see Figure 2-11) were made on a milling machine, there was enough lack of symmetry between the flat-surfaces to cause wide variation in solution forms for the higher modes (2nd mode and up), depending on which surface the problem happened to start. For this reason the master cam with one contact per second was utilized to trip the multi-contact cams always on the same surface.

Variation in 60 cycle frequency must, of course, be considered, not only for corrections to the length L, but as having a disturbing effect on the consistency or repetition of solutions for higher modes. It would therefore be highly desirable to have a constant frequency source of 60 cycle power available.

For actual problems there will always be an effect due to shear and rotary inertia terms (see Section 5.3). By including a constant X" term to take care of the estimated average effect of these terms, and by neglecting the λ^4 term in equation (5-43), a very tolerable accuracy could probably be attained, as well as a considerable stabilizing effect on the computer due to the X" feedback (see Section 5.3).

In order to obtain solutions for higher modes it is possible to take advantage of symmetry of curves with respect to the center of the beam, if the beam is symmetrical. Then an accurate solution for the first half of the normal mode curve is all that need be obtained. The actual length L is twice the length of the first half. In order to eliminate pen lag errors in this procedure, it would be highly desirable to "blow-up" the curve being used to determine the length L. (See Sec. 5.4 for a description of this technique.)

CHAPTER 10

A SIMPLE SERVOMECHANISM

10.1 Definition of a Servomechanism

A servomechanism[15] may be defined as a system which attempts to impose upon an output signal y(t) the same functional form as the input signal x(t), i.e., attempts to make

$$y(t) = Kx(t) \tag{10-1}$$

where K is a constant. However, there are two restrictions which must be added to our definition. (1) The energy associated with the output shall be derived from a local source and not furnished by the input signal. (2) The effective cause which operates the system must be proportional to an "error signal", the latter being defined as

$$\text{error signal} = \epsilon(t) = x(t) - \frac{y(t)}{K} \tag{10-2}$$

This error signal $\epsilon(t)$ is obtained by taking the output y(t), dividing it by K, and feeding the result back to the input, where it is subtracted from the input signal x(t).

Thus we see that a servomechanism is a feedback amplifier.

10.2 Physical Example with Computer Analog

For a simple example of a servomechanism consider the system shown schematically in Figure 10-1. Here the problem is to cause the heavy weights W shown on opposite ends of the transverse shaft to turn in accordance with the movement of the handle H on the potentiometer control unit. Note that the control potentiometer is not connected mechanically to the shaft S which turns the weights. The movement is to be in one to one correspondence; i.e., if the control handle is moved ten degrees counter-clockwise, the heavy weights are to move ten degrees counter-clockwise.

The sliding arm A is fastened to the shaft S and makes contact with the potentiometer P. This potentiometer has its center-tap connected to ground (zero potential) and its ends connected to +V and -V volts respectively. Denoting the output of our servo (position of the shaft S) with respect to a fixed reference line as y(t), and the input signal (position of H) with respect to the reference line as x(t), then the potential difference between the center-tap on the pot and the contact-arm A will be proportional to x(t) - y(t). This voltage is then proportional to the error signal of equation (10-2) where K = 1, since our servo has a gain of unity. We will denote this error voltage as ϵ_1. Then

$$\epsilon_1 = k_1 \left[x(t) - y(t) \right] , \tag{10-3}$$

where k_1 is a constant depending upon the voltage applied to the potentiometer.

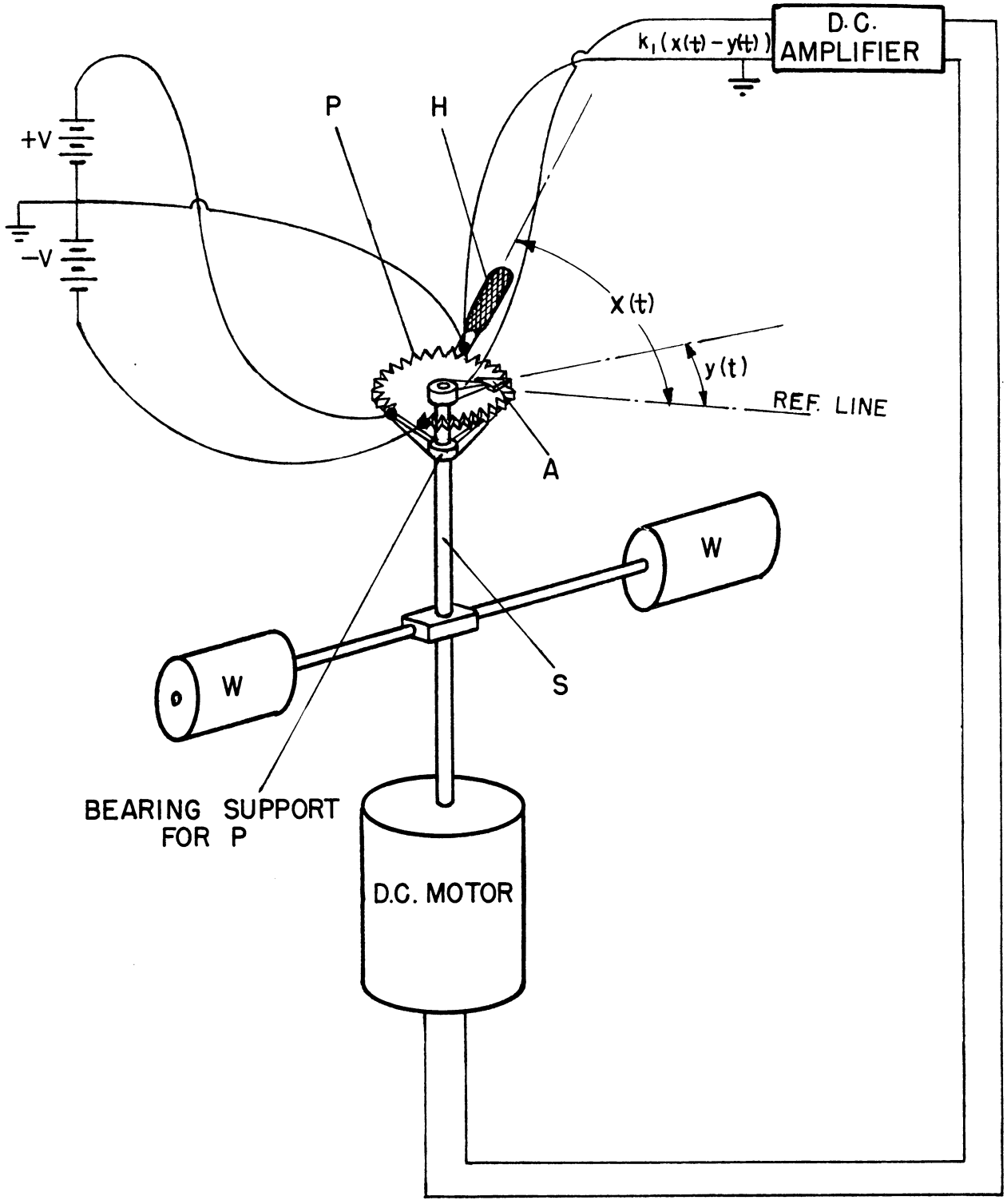

Fig. 10-1. Example of a simple servomechanism.

The error voltage is fed into a dc amplifier, the output voltage of which we shall assume is directly proportional to the input voltage. The power output of the dc amplifier is used to driva a dc motor. The output shaft of the motor is our servo output shaft S. The polarity of the input voltage to the motor is arranged so that the output torque of the motor tends to turn S toward H, i.e., to reduce $\epsilon(t)$ of equation (10-2) to zero.

Looking at our system we see that we have a system which imposes (or at least attempts to impose) upon an output signal y(t) the same functional form as the input signal x(t). We see also that the energy driving the output is not furnished directly by the input signal but rather is derived from a local source (in this case the dc amplifier). We note also that effective cause which operates the system is the error signal of equation (10-2), where K = 1. Hence our system satisfies the definition of a servomechanism.

We will now write the equation of motion of the system. Let I = moment of inertia of the mechanical system; c = damping coefficient (viscous), i.e., the retarding torque due to a unit velocity; k = torque output of the motor for a unit error signal input $\left[x(t) - y(t)\right]$.

Then our equation of motion is

$$I \frac{d^2y}{dx^2} + c \frac{dy}{dx} - k\left[x(t) - y(t)\right] = 0 \qquad (10\text{-}4)$$

In order to have a numerical problem which we can set up on the computer we assume the following values for the constants:

$$I = 0.25$$
$$c = 0.25$$
$$k = 1.00$$

Then equation (10-4) becomes

$$0.25 \frac{d^2y}{dx^2} + 0.25 \frac{dy}{dx} + y = x \qquad (10\text{-}5)$$

The computer circuit for solving equation (10-4) is shown in Figure 10-2.

10.3 Step Response

With the analog computer set up to simulate our servomechanism we can record the output or response y(t) of our servo to any input signal x(t). In Figure 10-3 is shown the response of the servo to a step-function input.

If there were no viscous damping in our servomechanism (c = 0), the response of the system to a step signal would be undamped oscillations about the new equilibrium position. The oscillogram of this condition is shown in Figure 10-4. To simulate this case the y feedback loop in Figure 10-2 is disconnected.

The frequency of these oscillations will be the natural frequency of the system and is given by the relation

$$f = \frac{1}{2\pi}\sqrt{\frac{k}{I}} \qquad (10\text{-}6)$$

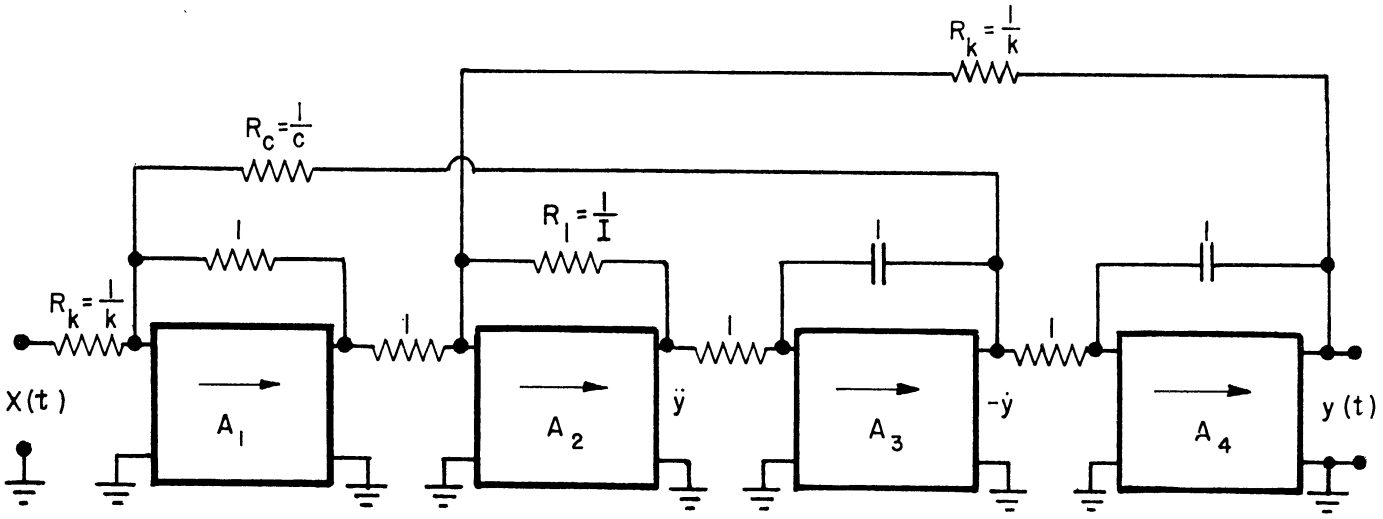

Fig. 10-2. Computer analog for simple servomechanism.

For our problem

$$f = \frac{1}{2\pi}\sqrt{\frac{1}{.25}} = \frac{1}{\pi} = 0.318 \text{ cycles/sec.}$$

From the computer

$$f = 0.317 \text{ cycles/sec.}$$

On the other hand suppose that our servo had more damping than we originally assumed. For critical damping

$$c = \sqrt{4Ik} = \sqrt{4 \times 0.25} = 1 \qquad (10\text{-}7)$$

In this case the resistor R_c in our computer is changed from 4 meg to 1 meg. The response of the servo to a step input for critical damping is shown in Figure 10-5.

It is apparent that we can change any of the constants in our problem merely by changing appropriate resistors in the computer circuit.

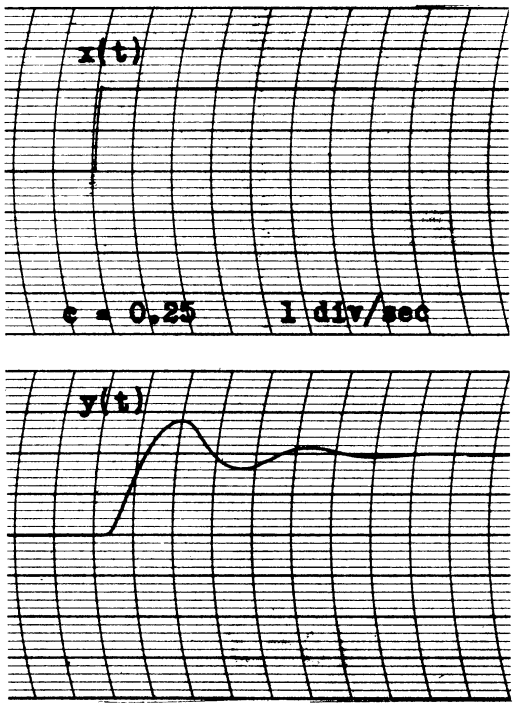

Fig. 10-3. Step response of the servo; c = 0.25.

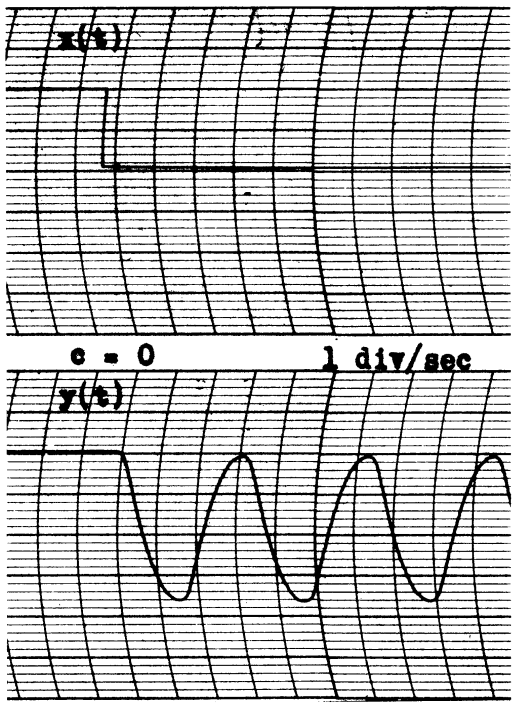

Fig. 10-4. Step response; c = 0.

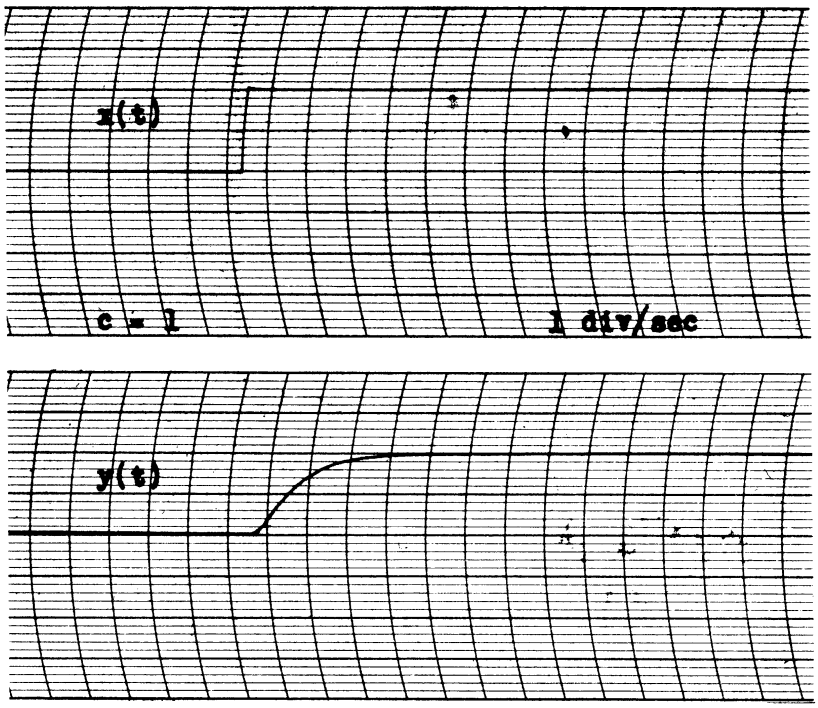

Fig. 10-5. Step response; c = 1 (critical damping).

10.4 Steady state Frequency Response

It is of considerable interest to know what the response of our servomechanism is to sinusoidal input signals of various frequencies. Using the well-known p-operator notation, we can rewrite equation (10-4) as

$$(Ip^2 + cp + k)\, y(t) = kx(t) \tag{10-8}$$

or

$$y(t) = \left(\frac{1}{\frac{I}{k}p^2 + \frac{c}{k}p + 1} \right) x(t) \tag{10-9}$$

For steady-state oscillations, $p = j\omega$ and we have

$$\frac{y(t)}{x(t)} = \frac{1}{1 - \frac{I}{k}\omega^2 + j\frac{c}{k}\omega} \tag{10-10}$$

Substituting the constants of our servomechanism in equation (10-10) we get

$$\frac{y(t)}{x(t)} = \frac{1}{1 - 0.25\omega^2 + j0.25\omega} \tag{10-11}$$

From equation (10-11) we can calculate the steady-state gain of our servo for any given frequency, the gain being defined as the output divided by the input. Note that in general this will be a complex quantity.

We can experimentally determine the steady-state response of our servo by taking the output from the low-frequency oscillator (see Chapter 2, Section 2.10), and feeding it into the analog computer as x(t). By recording x(t) and y(t) simultaneously on the Brush Oscillograph we can find the absolute gain ratio and relative phase shift of y(t)/x(t) for each driving frequency.

The servo steady-state gain curve showing both calculated and experimental values of y(t)/x(t) for various frequencies is plotted using complex coordinates in Figure 10-6. Curves showing absolute gain and relative phase shift as a function of frequency are given in Chapter 3, Figures 3-6 and 3-7, for the same system.

10.5 Summary of Theory of Servo Mechanisms

The Nyquist[16] method of analysis is a means of predicting the transient response (stability, accuracy, response time, etc.) of a servomechanism from its known steady state response to a sinusoidal signal. A brief summary of some of the results of the theory of servomechanisms follows.

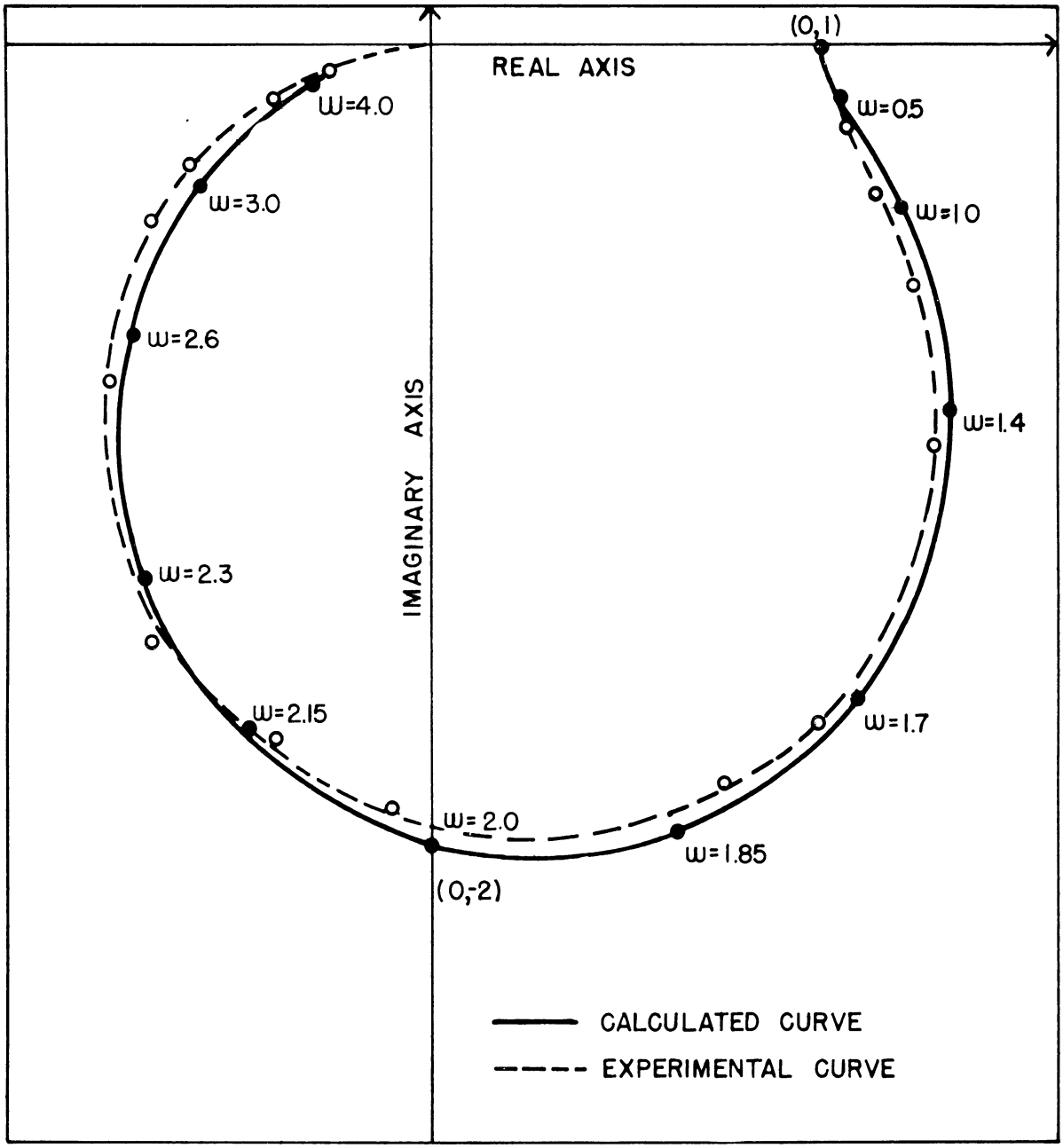

Fig. 10-6. Steady-state gain curve for the simple servomechanism.

Consider a unit having an input x(t) and an output y(t). If we apply a signal $x = \xi e^{pt}$ (p, imaginary) after transients have died out, the output will be $y = \eta e^{pt}$. The transfer function Y of the unit is defined by

$$Y = \frac{\eta}{\xi} \tag{10-12}$$

In general Y is complex and a function of p.

If the transfer function of a servomechanism with its feedback loop opened is $Y_o(p)$, then when the loop is connected, the transfer function of the servomechanism will be of the form $\frac{Y_o}{1 + Y_o}$.

For example, in Fig. 10-7 the transfer function of the amplifier Y(p) is given by

$$Y(p) = \frac{y(t)}{\epsilon(t)} \quad . \tag{10-13}$$

(To measure Y(p) we break the feedback loop at P_1, P_2 and apply a sinusoidal $\epsilon(t)$ to the input of the amplifier). When the feedback path is closed, we have

$$Y(p) = \frac{y(t)}{\epsilon(t)} = \frac{y(t)}{x(t) - C\, y(t)}$$

and

$$\frac{y(t)}{x(t)} = \frac{Y(p)}{1 + C\, Y(p)} = \frac{1}{C} \frac{Y_o(p)}{1 + Y_o(p)} \tag{10-14}$$

where $Y_o(p) = C\, Y(p)$.

Looking at equation (10-14) we see that our definition of a servomechanism holds as long as

$$\left|Y_o(p)\right| \gg 1$$

for then we have

$$C\, y(t) = x(t)$$

We expect the behavior of the servomechanism to be very dependent on $Y_o(p)$ in the region where

$$\left|Y_o(p)\right| \cong 1$$

and especially those values of p near that for which

$$Y_o(p) + 1 = 0 \tag{10-15}$$

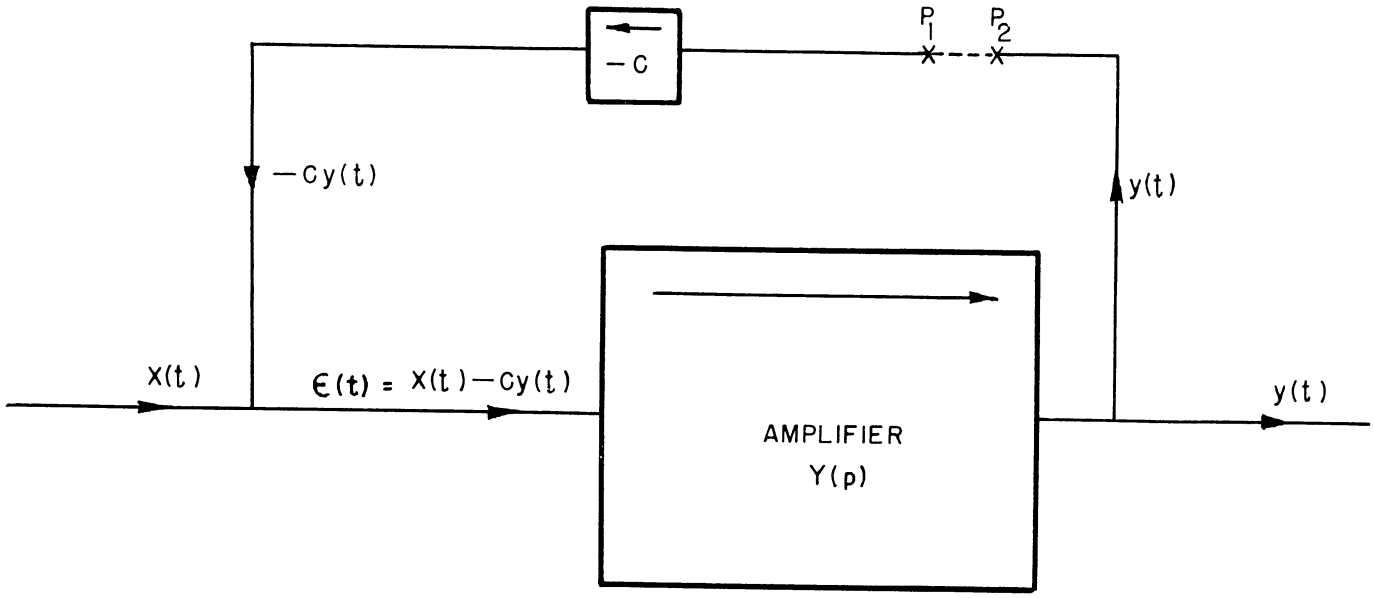

Fig. 10-7. Typical Feedback Amplifier.

Many of the transient input functions in which we are interested can be expressed in the form

$$x(t) = \frac{x_o}{2\pi i} \int_{\Gamma} \frac{1}{p^m} e^{tp} \, dp \qquad (10\text{-}16)$$

the path of integration Γ being the imaginary axis in the complex plane of p looping around the right side of the origin.

The integral of equation (10-16) has the value $x(t) = 0$ for $t < 0$

$$= x_o \frac{t^{m-1}}{(m-1)!} \text{ for } t > 0 \qquad (10\text{-}17)$$

Thus when $m = 1$ $x(t)$ is a step function Fig. 10-8; $m = 2$ gives a ramp function Fig. 10-9 and $m = 3$ gives the t^2 function Figure 10-10.

If we apply an input signal of the form of equation 10-16 to a servomechanism having the transfer function $\frac{1}{C} \frac{Y_o}{1 + Y_o}$ the output is zero for negative t and for positive t is given by

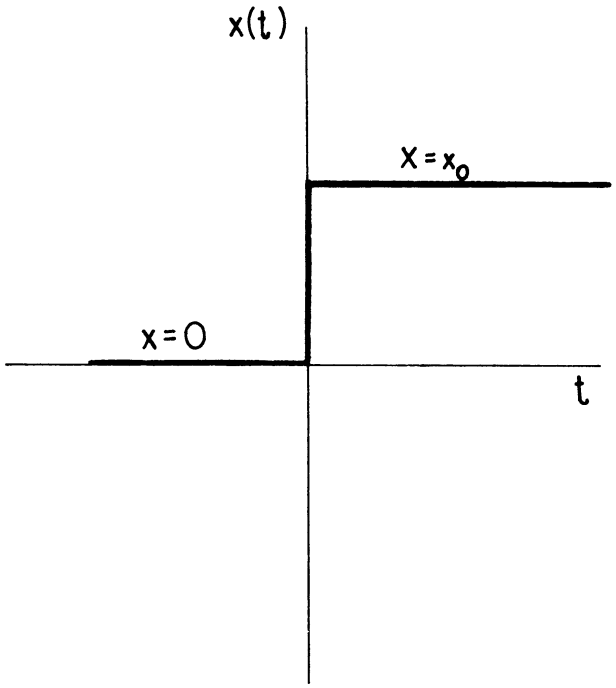

Fig. 10-8. Step function.

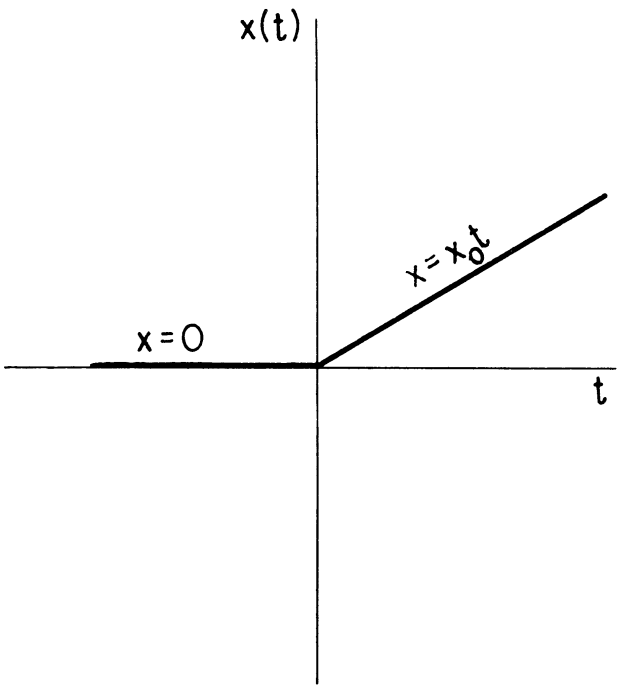

Fig. 10-9. Ramp function.

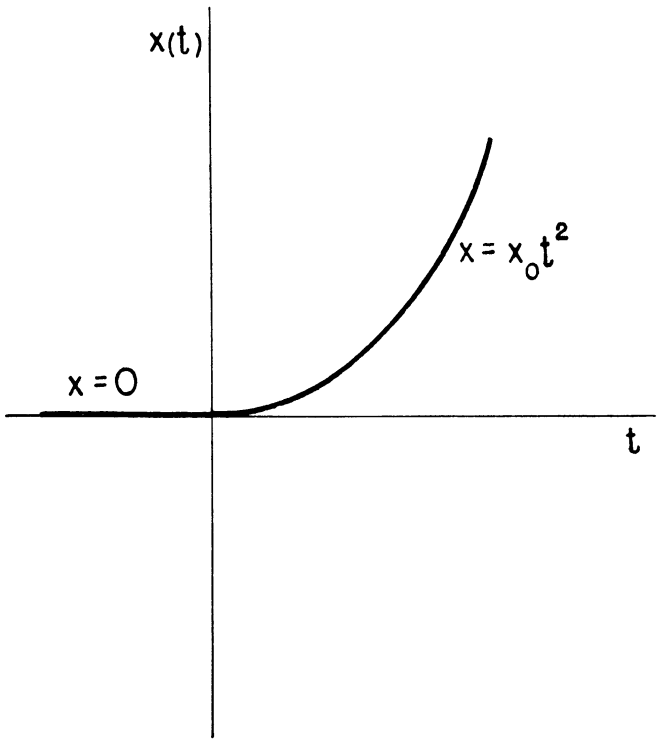

Fig. 10-10. The t^2 function.

$$y(t) = \frac{x_o}{2\pi i C} \int_{\Gamma} \frac{1}{p^m} \frac{Y_o(p)}{1 + Y_o(p)} e^{tp} dp \qquad (10\text{-}18)$$

Where the path of integration Γ is the imaginary axis distorted so as to pass to the right of any roots of $p^m (1 + Y_o(p)) = 0$.

Stability

Equation (10-18) can be integrated by making a Heaviside Expansion and using Cauchy's Theorem to give

$$y(t) = \sum_n K_n e^{p_n t} \qquad (10\text{-}19)$$

Where p_n are the poles of $\frac{1}{p^m} \frac{Y_o(p)}{1 + Y_o(p)}$ and K_n are constants (or at most polynomials in t if any of the poles are multiple).

It is frequently very difficult to determine the poles in an actual problem; however equation (10-19) will give information on the stability of the servomechanism without knowing the exact value of the poles. Suppose one of the poles p_n has a positive real part then y(t), equation (10-19), is exponentially increasing in time and the system is unstable. In any real single loop system $Y_o(p)$ is finite for all frequencies and hence the only poles which might have positive real parts are the roots of

$$1 + Y_o(p) = 0 \qquad (10\text{-}20)$$

The stability of a servomechanism is determined by whether or not equation (10-20) has any roots in the right half of the p-plane. (We shall see later the effect of roots at the origin.)

It can be shown that if we encircle the right half of the p-plane by going along the imaginary axis (passing to the right of the origin) and returning in a semicircle of infinite radius (Fig. 10-11), the curve which $Y_o(p)$ follows in its complex plane will encircle the point (-1, j0) once for every root of equation (10-20) having a positive real part. This curve of $Y_o(p)$ in its complex plane is called a Nyquist curve and whether or not it encircles the point (-1, j0) is Nyquist's stability criterion. Figures 10-12 and 10-13 show stable Nyquist curves while Figure 10-14 shows an unstable Nyquist curve. (Note that the stability can depend on the behavior of $Y_o(p)$ for large positive real values of p. The similar situation can also occur for small positive real values near the origin.

Transient Response

For the following we assume that the servomechanism is stable. The transient response is very dependent on the behavior of $\frac{Y_o}{1 + Y_o}$ near p = 0.

Applying a step function (Fig. 10-8), m = 1 in equation (10-16), what are the conditions that y(t) will approximate a step function? For an actual servomechanism, we can make a power series expansion in the neighborhood of p = 0

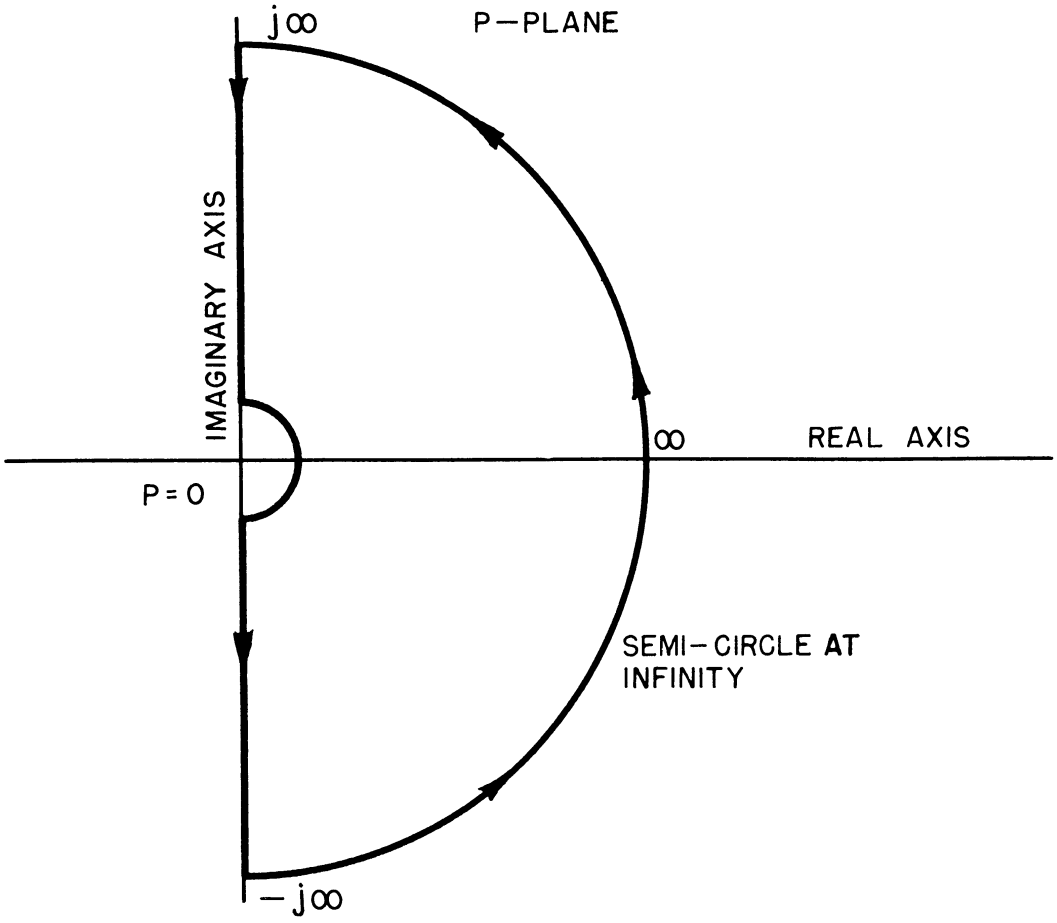

Fig. 10-11. Integration Path

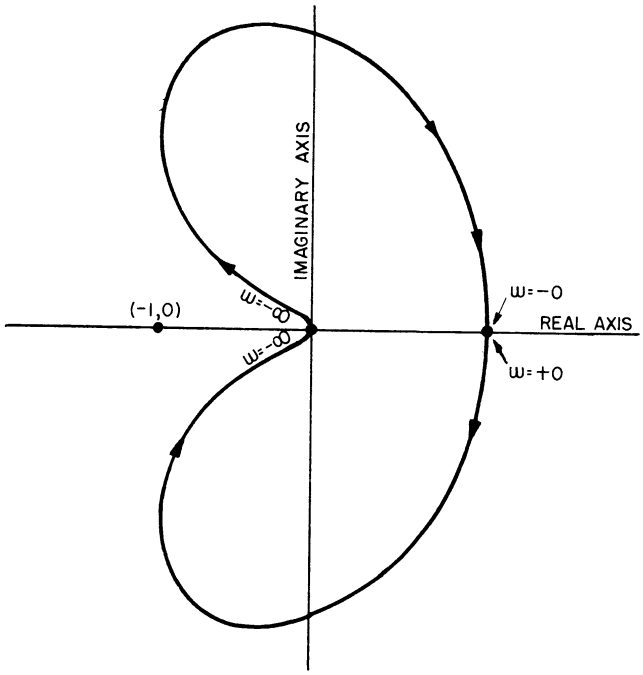

Fig. 10-12.

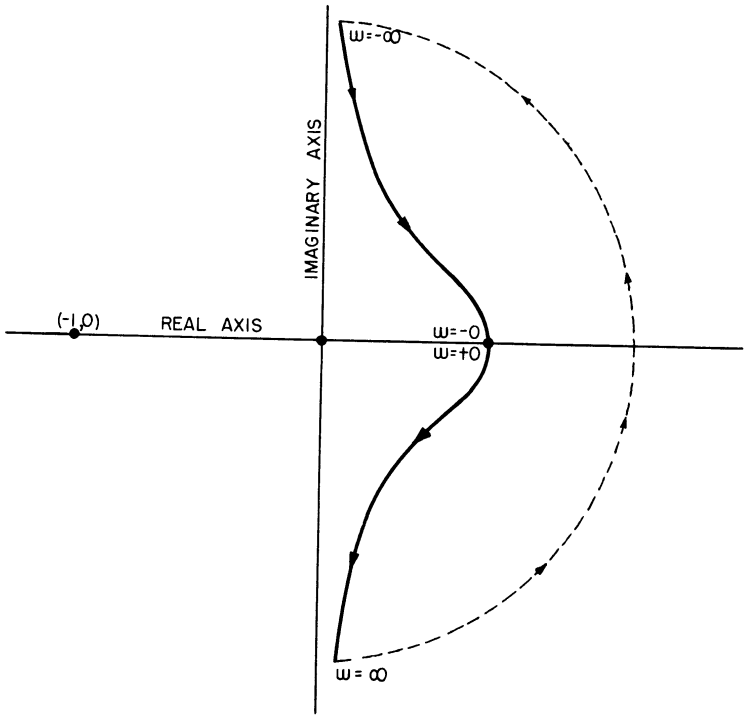

Fig. 10-13.

Stable Nyquist Curves.

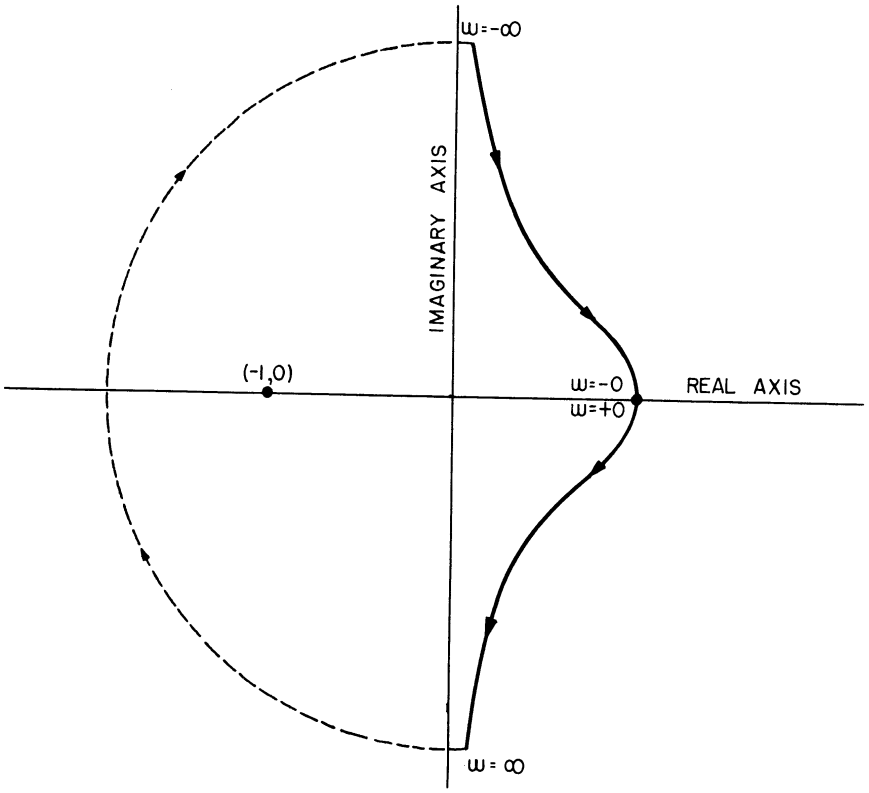

Fig. 10-14. Unstable Nyquist Curve.

$$\frac{Y_o(p)}{1 + Y_o(p)} = p^{-n} (a_o + a_1 p + a_2 p^2 + ...) \qquad (10\text{-}21)$$

where $a_o \neq 0$ and $n \geq 0$.

Substituting this in equation (10-18) and using equation (10-17), we get (for large t)

$$y(t) = \frac{1}{C} x_o \left[a_n + a_{n-1} t + \ldots + a_o \left(\frac{t^n}{n!} \right) \right] \qquad (10\text{-}22)$$

If y(t) is to be a constant then we must have n = 0 (no pole at the origin). Further if the system is to have no static error (Cy = x) then we must have $a_o = 1$.

If our system is to have zero static error, equation (10-21) must be

$$\frac{Y_o(p)}{1 + Y_o(p)} = 1 + a_1 p + a_2 p^2 + ... \qquad (10\text{-}23)$$

Assuming that equation (10-23) holds, let us now apply a ramp function (Figure 10-9, m = 2 in equation [10-16]). Substituting equation (10-23) in equation (10-18), and using equation (10-17) gives (for large t)

$$y(t) = \frac{x_o}{C} (t + a_1) = \frac{x_o}{C} (a_o t + a_1) \qquad (10\text{-}24)$$

It can be seen that the output y (in the limit) lags behind the input x by a_1 seconds. This is illustrated in Fig. 10-15, which shows the lag for the more general case where the static error is not zero. Here K = 1/C. If the lag is to be zero then equation (10-23) must become

$$\frac{Y_o(p)}{1 + Y_o(p)} = 1 + a_2 p^2 + a_3 p^3 + ... \qquad (10\text{-}25)$$

This method of analysis can be continued. If a t^2 function is applied, the lag in velocity can be determined.

Again assuming that equation (10-23) holds, let us apply a $t^2/2$ function (Fig. 10-10, m = 3 in equations [10-16] and [10-18]). Substituting equation (10-23) in equation (10-18) and using equation (10-17) gives (for large t)

$$y(t) = \frac{x_o}{C} \left(\frac{t^2}{2} + a_1 t + a_2 \right) \qquad (10\text{-}25a)$$

$$y(t) = \frac{x_o}{C} \left[\frac{(t + a_1)^2}{2} + a_2 - \frac{a_1^2}{2} \right]$$

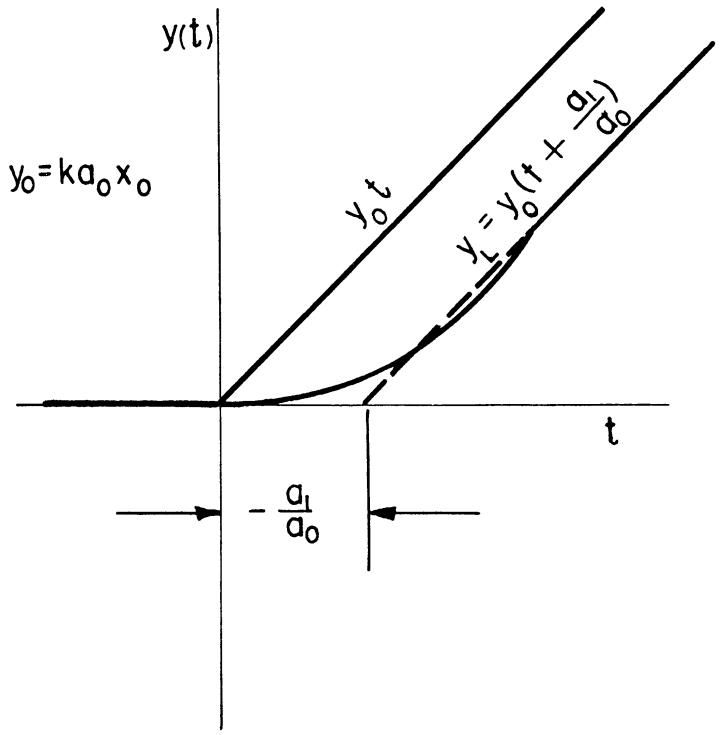

Fig. 10-15. Lag in case of ramp function.

It can be seen that for large t the impressed $t^2/2$ function is delayed by a_1 seconds and that a static error $a_2 - a_1^2/2$ is introduced. The derivative is simply delayed a_1 seconds.

10.6 Experimental Verification of Nyquist Stability Criterion.

We shall illustrate the Nyquist stability curve by placing an additional feedback loop in our servomechanism, a feedback proportional to $-C\frac{dy}{dt}$. The resulting servomechanism is shown schematically in Fig. 10-16 where the transmission ration Y(p) is the $\frac{y(t)}{x(t)}$ given in equation (10-11) for our original servo (not the Y(p) of equation [10-13]).

Let us define

$$Y_1(p) = \frac{dy/dt}{\epsilon} = \frac{\dot{y}}{\epsilon} \qquad (10\text{-}26)$$

where $\epsilon = x - C\dot{y}$. Then we have from equation (10-14) that $(x - C\dot{y})Y_1 = \dot{y}$, or

$$\frac{\dot{y}}{x} = \frac{Y_1}{1 + C\,Y_1} \qquad (10\text{-}27)$$

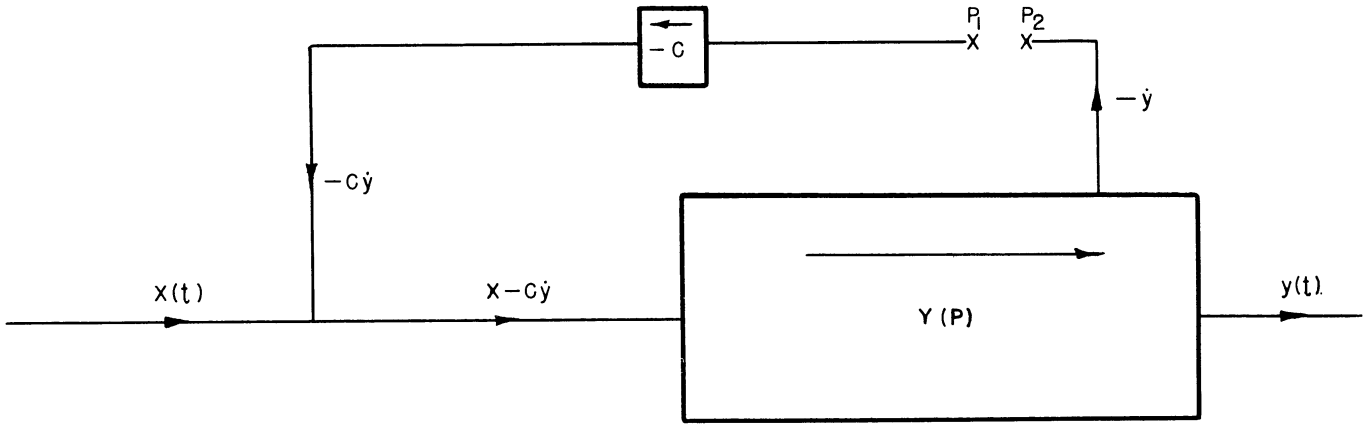

Fig. 10-16. Servomechanism with additional feedback loop.

Letting

$$Y_o = CY_1 \tag{10-28}$$

(not the Y_o of equation [10-14])

we get

$$\frac{\dot{y}}{x} = \frac{1}{C}\left(\frac{Y_o}{1 + Y_o}\right). \tag{10-29}$$

This is now in our standard form for stability investigations. We break our feedback loop at P_1 and feed our steady state frequency into P_1. The output $\frac{dy}{dt}$ at P_2 is recorded. Denoting the input at P_1 as ϵ (t) (= A sin t), (not the ϵ of equation [10-26]), we see that $\frac{\dot{y}}{\epsilon} = -CY_1 = -Y_o$.

The curve of $Y_o(j\omega)$ is then plotted in the complex plane for the frequency range (see Fig. 10-17). The computer circuit for determining $-\frac{\dot{y}}{\epsilon}$ is shown in Figure 10-18.

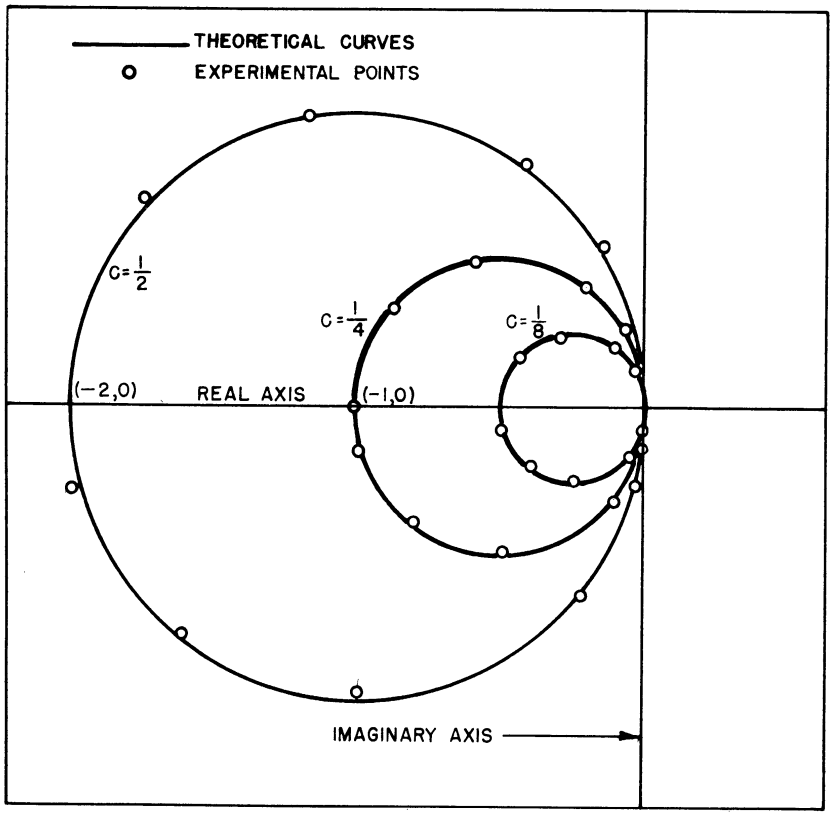

Fig. 10-17. Theoretical and experimental plot of $Y_{oj}(\omega)$.

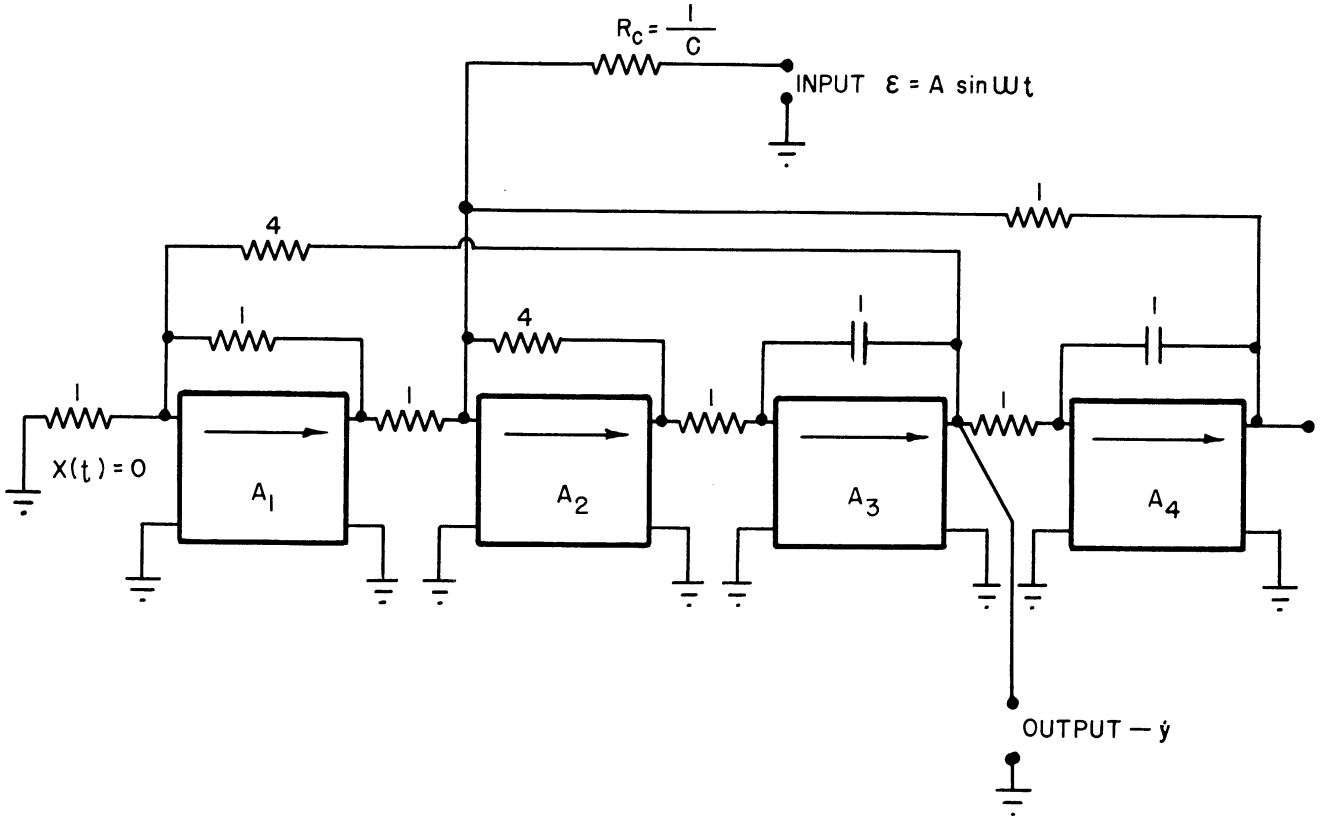

Fig. 10-18. Computer circuit for determining - Ẏ.

Let us calculate $Y_o(p)$ from our knowledge of the basic equation of motion. We have, with the loop open,

$$Y_o(p) = CY_1 = \frac{C\dot{y}}{x} \qquad (10\text{-}30)$$

Using the operator p notation we have also shown that

$$\frac{y}{x} = \frac{1}{0.25p^2 + 0.25p + 1} \quad . \qquad (10\text{-}31)$$

From equation (10-30) we can write

$$Y_o(p) = \frac{Cp}{0.25p^2 + 0.25p + 1} \quad . \qquad (10\text{-}32)$$

For steady state frequency response, $p = j\omega$, and we have

$$Y_o(j\omega) = \frac{j\omega C}{1 - 0.25\ ^{2} + j\ 0.25} \qquad (10\text{-}33)$$

It can be shown that equation (10-33) represents a family of circles in the Y_o plane. The centers of the circles lie on the negative real axis, the right-hand edges of all the circles go through the origin, and the radius of the circles is 2C. In Fig. 10-17 are shown three of these circles for values of C of 1/8, 1/4, and 1/2. The experimental points as obtained from the computer are also plotted in Fig. 10-17. As can be seen the agreement between experimental and theoretical points is within the limits of recording accuracy.

As ω goes from 0 to 00 the $Y_o(j\omega)$ curve starts down from the origin, curves around to the left and up through the negative real axis at $\omega = 2$ (the natural frequency of the system), and comes in to the origin from above as $\omega \longrightarrow \infty$. As ω goes from -00 to 0 the $Y_o(j\omega)$ curve makes another clockwise revolution of the circle, making a net of two revolutions as p goes from + j0 to - j0. Since $Y_o(j\omega) = Y_o(-j\omega) = 0$, the total curve is closed and the stability investigation is complete.

For C = 1/8 reference to Figure 10-17 will show that $Y_o(j\omega)$ does not encircle (-1,0) and the system is stable. In this case the net effect on the servomechanism when the feedback loop is connected is to reduce the damping coefficient c in equation (10-5) from 1/4 to 1/8. The servomechanism output y(t) is shown for a step input in Fig. 10-19.

For C - 1/4 the $Y_o(j\omega)$ curve goes through the point (-1,0). Hence the system is just unstable. When the feedback loop is connected the net effect is to reduce the damping in the servomechanism to zero. The response to a step input will be undamped oscillations of the natural frequency of the servo. Reference to Fig. 10-20 shows this.

For C = 1/2 the $Y_o(j\omega)$ curve circles well around the point (-1,0). Hence the system will be unstable, as reference to Fig. 10-21 corroborates. In this instance no signal is put into the servo. Any minute unbalance is enough to cause the increasing oscillations to build up as soon as the feedback loop is connected.

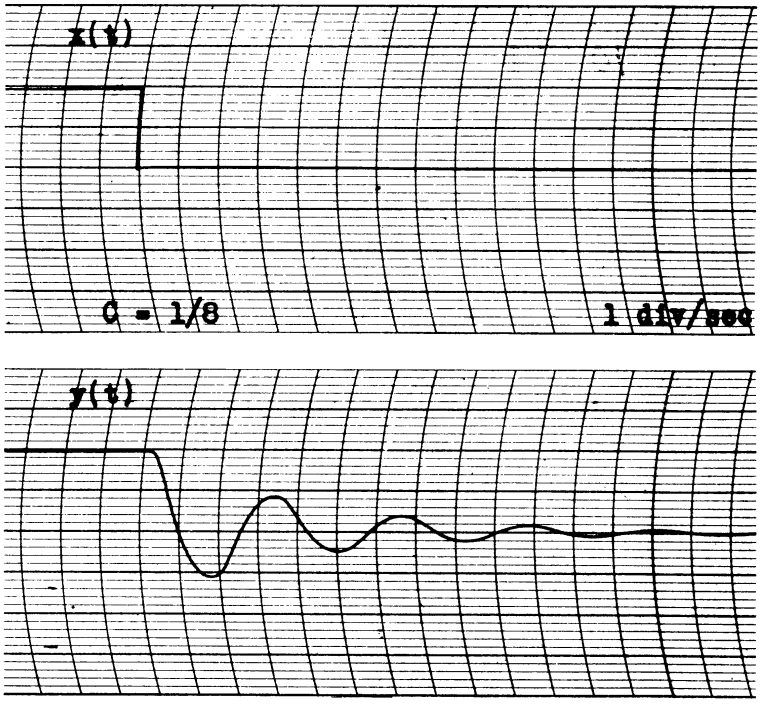

Fig. 10-19. Step response; C = 1/8.

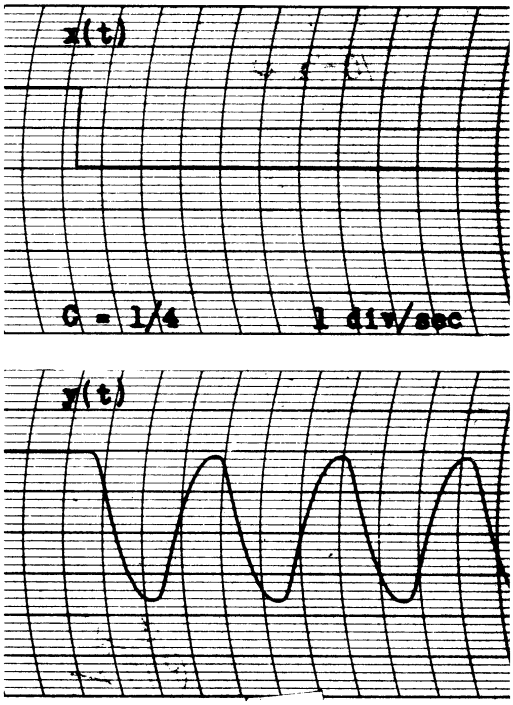

Fig. 10-20. Step response; C = 1/4

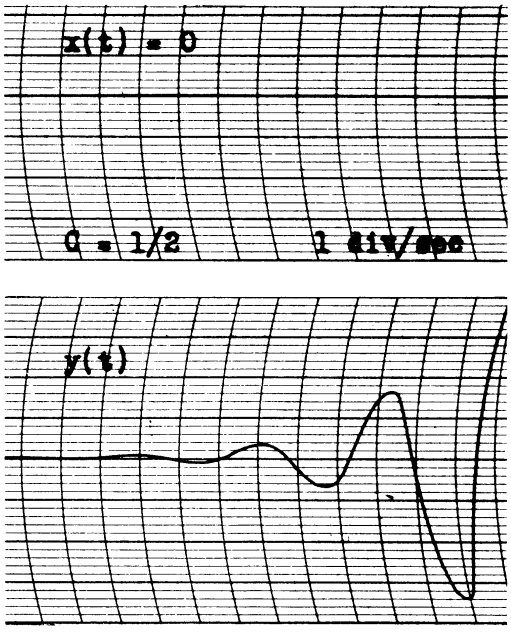

Fig. 10-21. Step response; c = 1/2.

10.7 Evaluation of Power Series Coefficients using the Analog Computer.

As an example of determining the transient response of a servomechanism, let us consider the servo described in Section 10.2, where the constants of equation (10-5) have the following values:

$$I = 0.5$$
$$c = 0.5$$
$$k = 1.00$$

Then our equation of motion, using operator p notation, becomes

$$(1 + 0.5p + 0.5p^2)\, y(t) = x(t) \qquad (10\text{-}34)$$

or

$$Y(p) = \frac{y(t)}{x(t)} = \frac{1}{1 + 0.5p + o.5p^2} \; . \qquad (10\text{-}35)$$

In order to solve for Y(p) in terms of a power series in p, we divide the denominator of equation (10-35) into the numerator.

$$\begin{array}{l} 1 + 0.5p + 0.5p^2 \;\;)\overline{1} \\ \qquad \underline{1 + 0.5p + 0.5p^2} \\ \qquad\quad - 0.5p - 0.5p^2 \\ \qquad\quad \underline{- 0.5p - 0.25p^2 - 0.25p^3} \\ \qquad\qquad\quad - 0.25p^2 + 0.25p^3 \\ \qquad\qquad\quad \underline{- 0.25p^2 - 0.125p^3 - 0.125p^4} \\ \qquad\qquad\qquad\qquad 0.375p^3 + 0.125p^4 \end{array} \qquad \begin{array}{l} 1 - 0.5p - 0.25p^2 + 0.375p^3 + \ldots\ldots\ldots \end{array}$$

Thus we see that Y(p) has the form

$$Y(p) = 1 - 0.5p - 0.25p^2 + 0.375p^3 + \ldots\ldots \qquad (10\text{-}36)$$

and hence that

$$a_0 = 1$$
$$a_1 = 0.5$$
$$a_2 = 0.25$$
$$a_3 = 0.375 \quad \text{etc.}$$

In Fig. 10-22 is shown the computer circuit used to solve equation (10-34) which represents our servomechanism.

A. Step Response

For the servomechanism under consideration $\frac{1}{C} = 1$ and $a_o = 1$. Hence the servo has no static error, and the limiting response to a step input should be an output of the same magnitude. Reference to Fig. 10-23, which shows the output y(t) of the servo analog for a step input, corroborates this. In Fig. 10-24 is shown the error signal y(t) - x(t). The static error is seen to be zero.

Fig. 10-22. Computer circuit representing the servo of equation (10-34).

B. Ramp Response.

The ramp-function shown in Fig. 10-9 is generated by means of an integrator with a constant voltage input supplied by a battery. A relay is connected across the feedback capacitor so that when the relay is not energized the capacitor is short-circuited through 1000 ohms. With the relay not energized (i.e., the capacitor shorted) the amplifier is balanced for zero voltage output. Then when the relay is energized, the short circuit is removed from the capacitor, and because of the input battery voltage, a ramp function of the form $x_o t$ is generated.

It would be possible to measure the time lag of $y_L(t)$ behind x(t) by extending $y_L(t)$ back to the origin as shown in Fig. 10-15. However, a much more accurate measurement of the time lag can be achieved by recording the error signal $\epsilon(t) = x(t) - y(t)$. For a ramp-function input where $\frac{1}{C} = a_o = 1$ we have

$x(t) = x_o t$ and $y_L t = x_o t + x_o a_1$ from which

$$x_o t - y_L(t) = - x_o a_1$$

$$\text{or} \quad a_1 = \frac{y_L(t) - x_o t}{x_o} \; . \qquad (10\text{-}37)$$

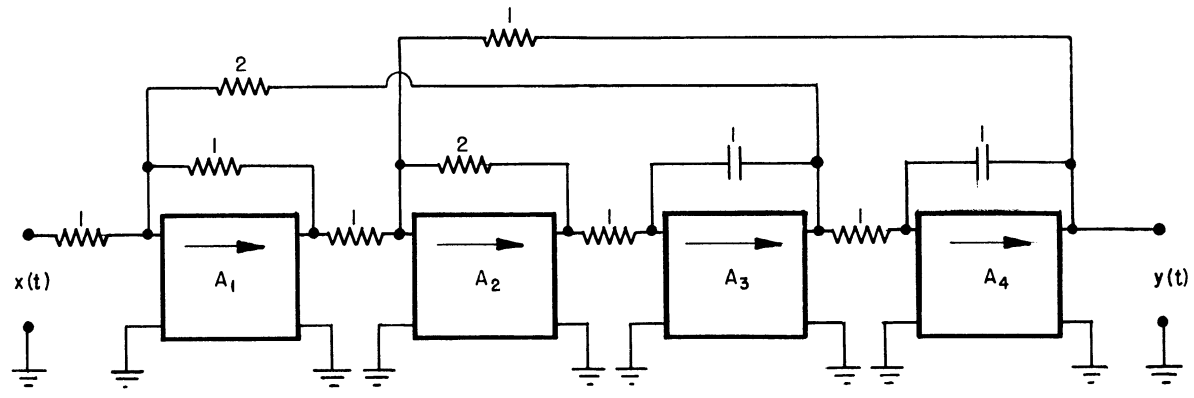

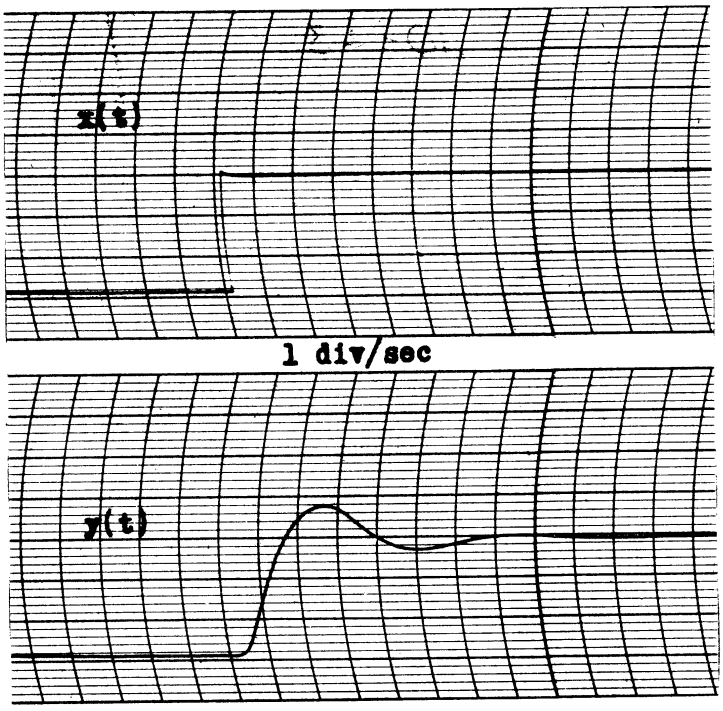

Fig. 10-23. Servo response to a step input.

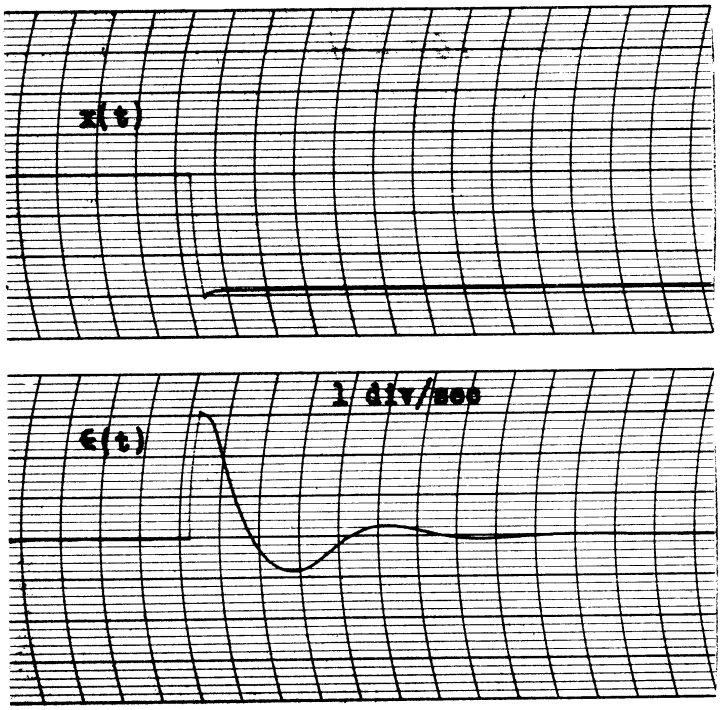

Fig. 10-24. Error signal $\epsilon(t)$ for a step input.

Since we record $x_o t$ as well as $y_L(t) - x_o t$ we can measure the slope x_o of the ramp-function and hence determine a_1 from equation (10-37). The computer circuit for accomplishing this is shown in Fig. 10-25.

As soon as the relay is energized the ramp-function $x_o t$ starts, and the solution of the problem has begun. In Fig. 10-26 the oscillogram of $x_o t$ and $y(t) - x_o t$ is shown. Note that the error signal is amplified by a factor of twenty. Because of slight inaccuracies in the values of the components in the computers, the gain of the servo simulator may not be exactly unity. Any small deviation from a gain of exactly unity will be amplified by a factor of twenty in the $\epsilon(t)$ output. The net result is that the limiting error signal $\epsilon_L(t)$ may not be a constant but may drift slowly in either direction. Hence the 1 meg y(t) input resistor to amplifier A_3 is changed by a resistance $\pm$ R until the above mentioned drift becomes negligible. The magnitude of R is usually around 2000 ohms.

Note that $y_L(t) - x_o t$ is negative and hence a_1 is negative.

Using three different values of the slope x_o the following values of a_1 were obtained experimentally using equation (10-36)

- 0.482 sec.
- 0.480
- 0.479

Average a_1 = - 0.480 sec.

Theoretical a_1 = - 0.500 sec.

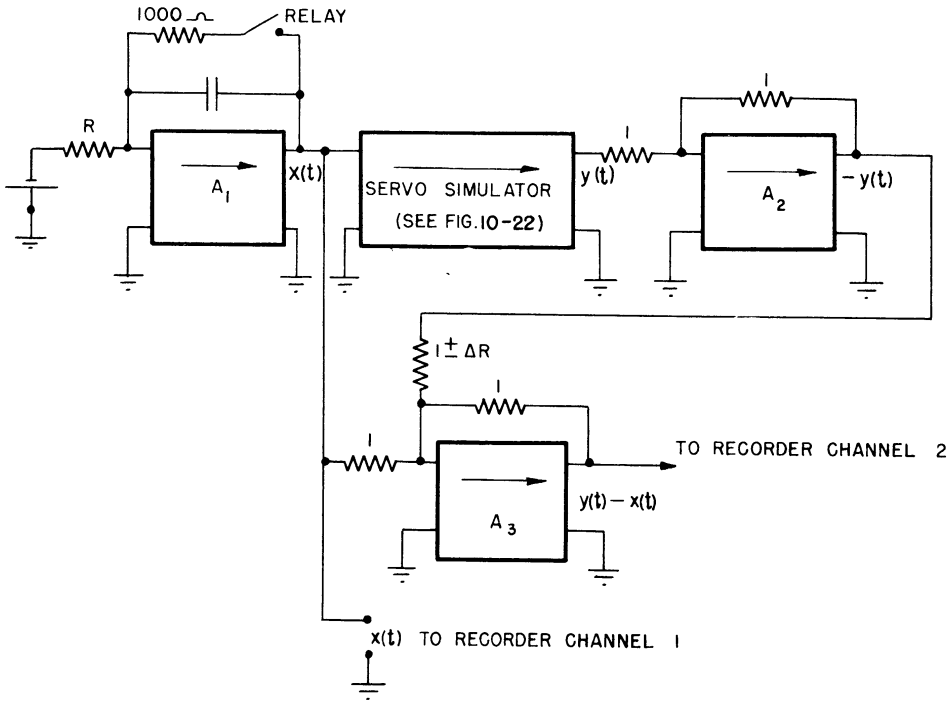

Fig. 10-25. Circuit for measuring a_1 by means of a ramp function input.

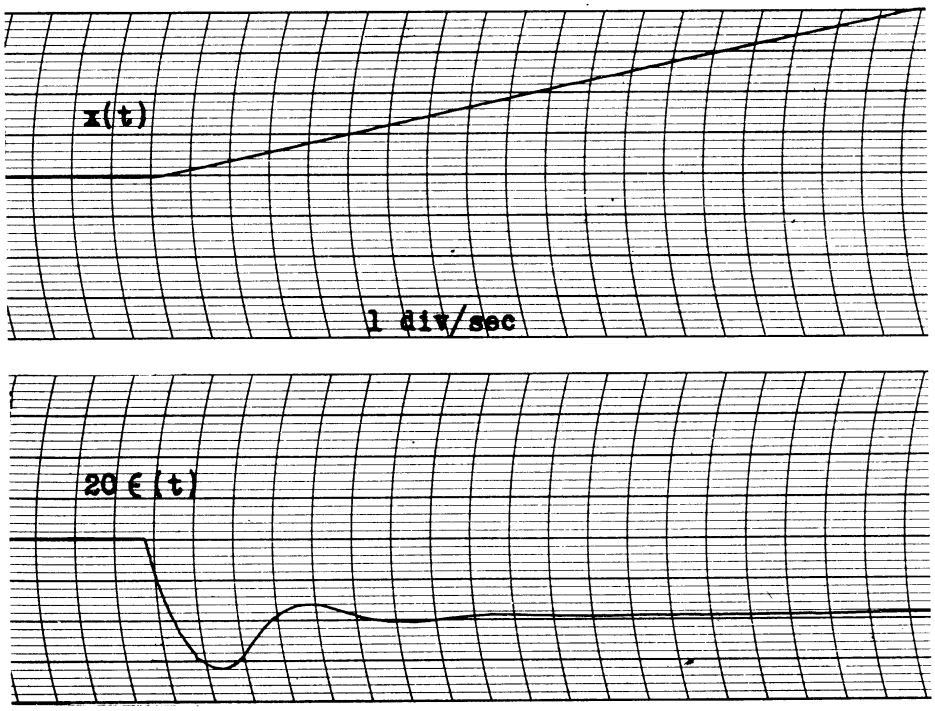

Fig. 10-26. $\epsilon(t)$ for a ramp function input.

Before we take up the response of our servomechanism to the $x_o t^2$ input, let us consider the evaluation of a_1 in the case where the damping coefficient is 0.25 instead of 0.5. The equation of motion becomes

$$0.5\ddot{y} + 0.25\dot{y} + y = x.$$

Rewritten in operator p notation, the equation becomes

$$(1 + 0.25p + 0.5p^2)\, y(t) = x(t).$$

The expansion of $y(t)/x(t)$ if found to be

$$Y(p) = \frac{y(t)}{x(t)} = 1 - 0.25p - 0.4375p^2 + \ldots\ldots$$

In this case the theoretical value of a_1 is - 0.25 sec. Proceeding as before we obtained the following experimental values for a_1 for various slopes x_o of the input ramp:

- 0.242 sec
- 0.245
- 0.232
- 0.242

Average a_2 = - 0.240 sec.

Theoretical a_2 = - 0.250 sec.

(Note that the ramp-function lag a_1 is independent of the moment of inertia I of the servomechanism. This fact is easily demonstrated with the analog computer.)

C. t^2 Response.

The input function $x(t) = x_o t^2$, Figure 10-10, is generated by taking a constant voltage and integrating it twice. The circuit is shown as a part of Figure 10-27. Both feedback capacitors in the two integrators are short-circuited through 1000 ohms until the relays are energized. Both amplifiers are carefully balanced with the feedbacks shorted, and a battery is connected to the input of the first integrator. When an initial-condition button is pressed, energizing the relays and thereby releasing the short-circuits across the capacitors, generation of the function $x_o t^2$ begins at the output of the double integrator.

If both the integrators of Fig. 10-27 have a gain of G, and the input battery voltage is V, the output of A_1 will be -GVt, and the output of A_2 will be $\frac{G^2 V t^2}{2}$. Therefore

$$2x_o = G^2 V . \tag{10-38}$$

For $K = a_o = 1$ and $a_1 = - 0.5$

$$y_L(t) = x_o t^2 - x_o t + 2x_o a_2$$

$$\text{or} \quad a_2 = \frac{y_L(t) - x_o t^2 + x_o t}{2x_o} = \frac{\epsilon'_L}{2x_o} , \tag{10-39}$$

where ϵ'_L is the limiting form of $\epsilon = y(t) - x_o t^2 + x_o t$.

We record ϵ' and -GVt. From the slope of GVt we can calculate V (since G is known) in units of recorder divisions in deflection. From V and G we can find $2x_o$ from equation (10-38) and from equation (10-38) calculate a_2 using the observed value of ϵ'_L. In Fig. 10-27 is shown the computer circuit for obtaining ϵ' and $2x_o t$. The R is maintained at the same value found optimum for the evaluation of a_1, and R' is adjusted until ϵ'_L is a constant without any drift.

The oscillogram of -GVt and ϵ' is shown in Fig. 10-29. Note that ϵ' is amplified by a factor of 40. A sample calculation of a_2 from Fig. 10-29 follows.

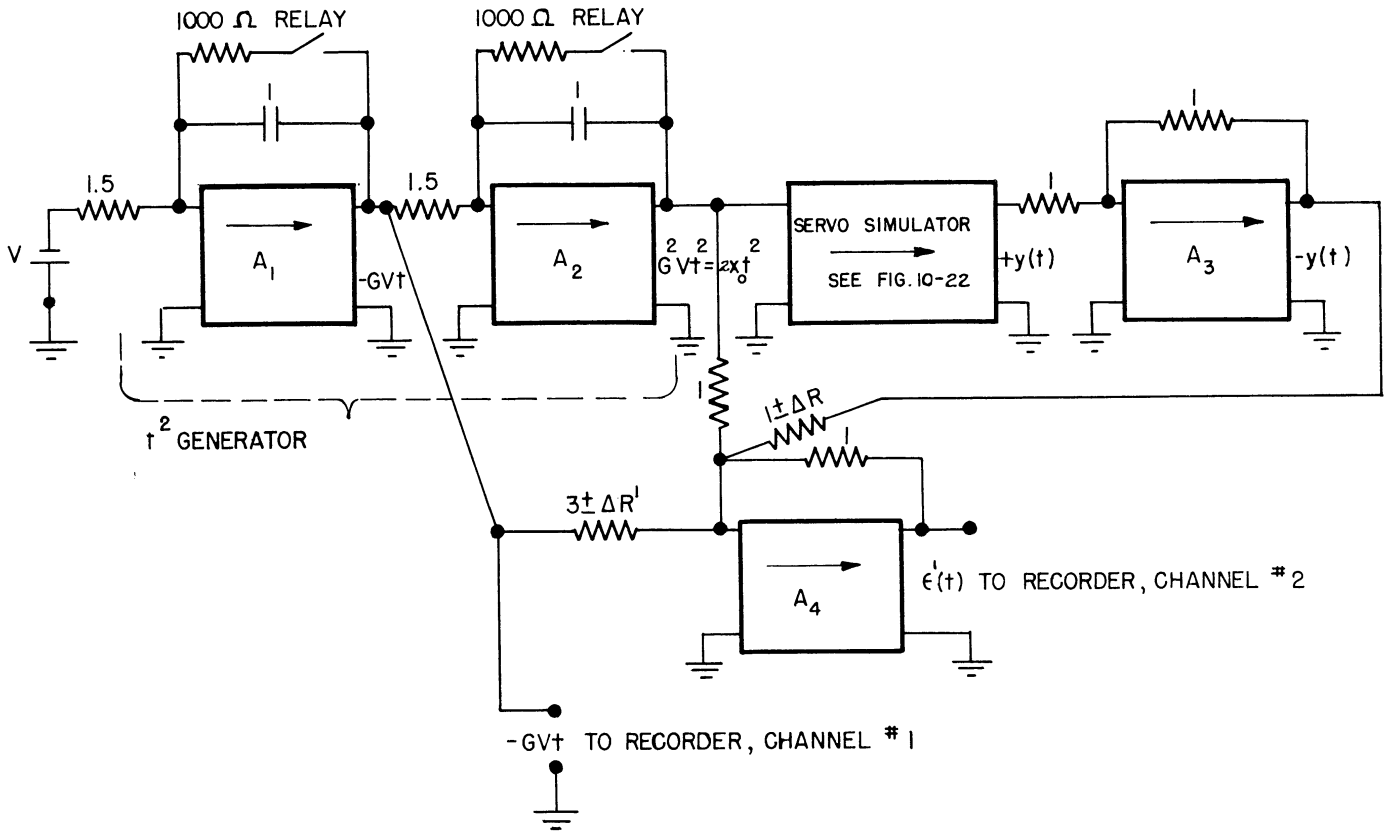

Fig. 10-27. Circuit for measuring a_2 by means of t^2 input.

From Fig. 10-29 $-GV = \dfrac{11.0 - 1.0}{10} = 1.0$ div/sec

$$G = \frac{1}{1.5} \text{ 1/sec} \qquad V = -1.5 \text{ div.}$$

From equation (10-38)

$$2x_0 = G^2V = -\left(\frac{1}{1.5}\right)^2 (1.5) = \frac{1}{1.5} \text{ div/sec}^2$$

From Fig. 10-29

$$\epsilon'_L = \frac{7.5}{40} = 0.187 \text{ div.}$$

From equation (10-39)

$$a_2 = \epsilon'_L / 2x_0 = -1.5\,(0.187) = -0.281 \text{ sec}^2$$

For the input voltage to A_1 equal to + 1.5 volts, a_2 = - 0.281 sec^2

- 1.5 volts, a_2 = - 0.305 sec^2

Average a_2 = - 0.29 sec^2

Theoretical a_2 = - 0.25 sec^2

It will be noted that both in Fig. 10-25 and Fig. 10-27 an extra amplifier was needed to reverse the servo output y(t) to - y(t). In Fig. 10-28 is shown a computer circuit which gives the required output of -y(t) directly. The only difference from the circuit of Fig. 10-22 is that the input x(t) is fed into amplifier A_2 instead of A_1.

D. Response

The summary of the numerical results appears below.

Servo equation: 0.5 y + 0.5 y + y = x(t)

	Theoretical Value	Experimental Value
a_0	1	1.00
a_1	- 0.5 sec	- 0.48 sec
a_2	- 0.25 sec^2	- 0.29 sec^2

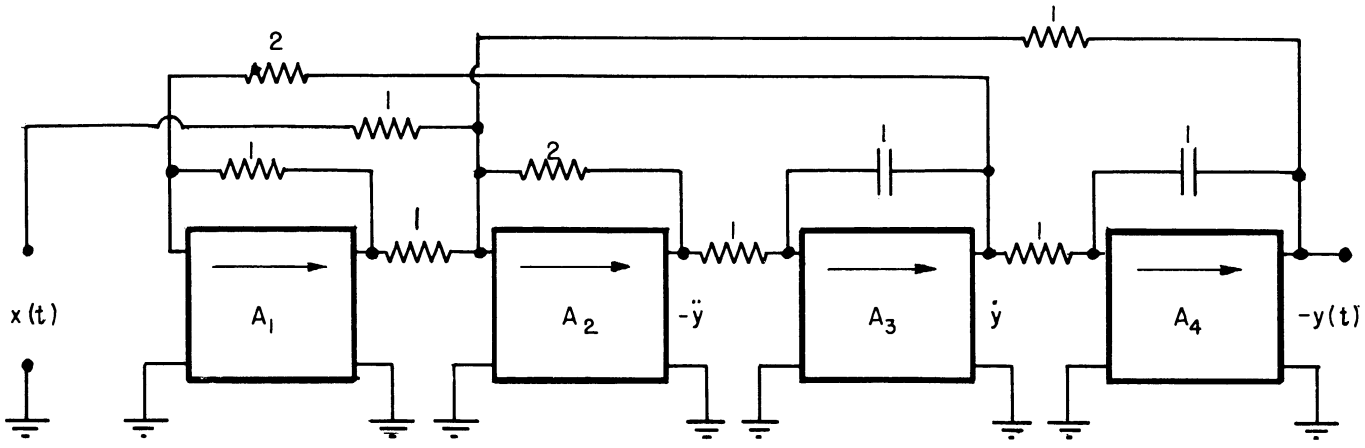

Fig. 10-28. Circuit to furnish - y(t) instead of y(t).

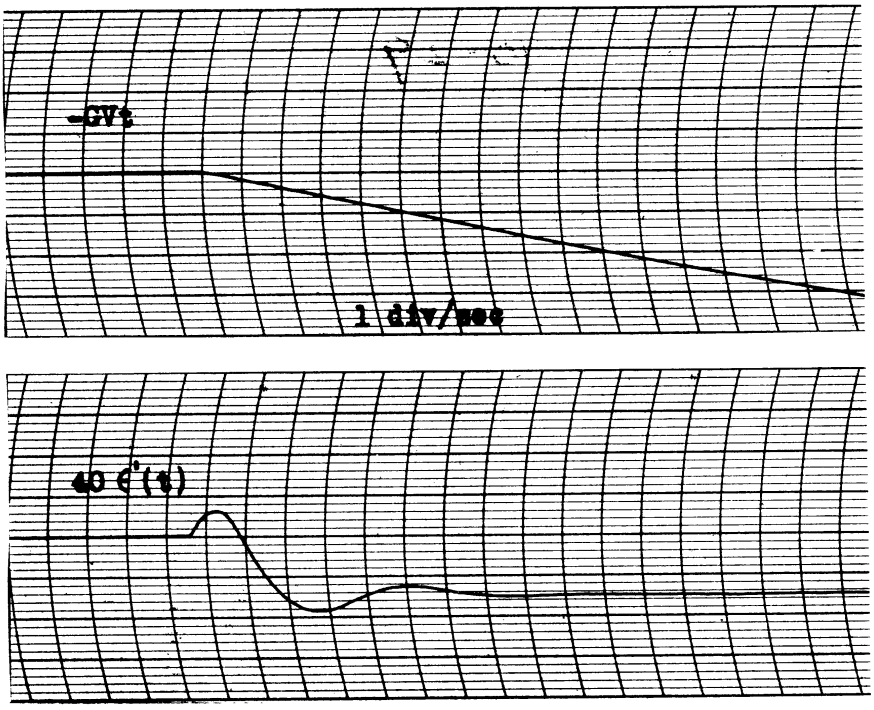

Fig. 10-29. $\in'(t)$ for a t^2 input.

Servo Equation: $0.5\,y + 0.25\,y + y = x(t)$

	Theoretical Value	Experimental Value
a_o	1	1.00
a_1	- 0.25 sec	- 0.24 sec

In conclusion it might be noted that although the results of the determination of the power series coefficients a_1 and a_2 by means of the analog computer seem to show rather poor agreement with the theoretical values, it must be remembered that these results were obtained by amplifying the difference between two voltages of very nearly the same level. For example, in the determination of a_1 the discrepancy between the experimental and theoretical values was 4%. However, the final output signal $\epsilon_L(t)$ was only about one-twentieth of the order of magnitude of the ramp-function input voltage. Hence the actual error in the analog computer output voltage was 4% / 20 or only 0.2%.

In view of these results we conclude that the method for determining the power-series coefficients of the servomechanism transmission ratio is not very accurate experimentally, and gives decreasing accuracy for coefficients of

higher powers. However, it would seem that the power-series coefficients are of interest more in a qualitative sense for a particular servomechanism, the idea being to make the lower order coefficients as small as possible.

The output of a servomechanism having the coefficient $a_1 = 0$ would not lag behind a ramp-function input after the transients had died out. In the same manner the output of a servomechanism having $a_1 = 0$ would not lag behind a t^2 input function after the transients had died out, but there would be a static error of $\frac{x_o a_2}{C}$. If $a_2 = \frac{a_1^2}{2}$ then there is a delay of a_1 seconds, but no static error. Therefore the approximate values of the power-series coefficients give a considerable insight into the effectiveness of a servomechanism.

CHAPTER 11

A COMPLETE SERVO-LOOP; AIRPLANE, AUTO-PILOT, ELEVATOR

11.1 Summary of the Problem

It was desired to investigate the suitability of the analog computer for simulating a more complicated servomechanism. We chose as our example the control of an airplane in elevation or pitch by means of an auto-pilot. Since we were not interested in results for design purposes, but rather in results for the purpose of determining the applicability of the computer, we were not too particular in selecting certain constants in the problem or in making certain simplifying assumptions. The main objective was to solve a problem which would embody typical features of an airplane control problem.

The general approach consists of: (1) determining the equations of motion of (a) the airplane, (b) the auto-pilot and (c) the elevator; (2) simulating each of these equations of motion by means of analog computers; and (3) properly tying the three components together so as to represent the complete system. The block diagram of the complete system is shown in Fig. 11-1.

After the equation of motion of each of the three component parts is determined, the corresponding analog computer is set up. Steady state response curves for various input frequencies are obtained experimentally and checked against the theoretical curves for each component part. From these data the steady state frequency response curve for the whole system is calculated. The calculated response is then compared with the experimental steady state frequency response of the whole system of analog computers as set up in Fig. 11-1. In addition, step response and ramp response curves are run to determine the power series coefficients, as described in Chapter 10.

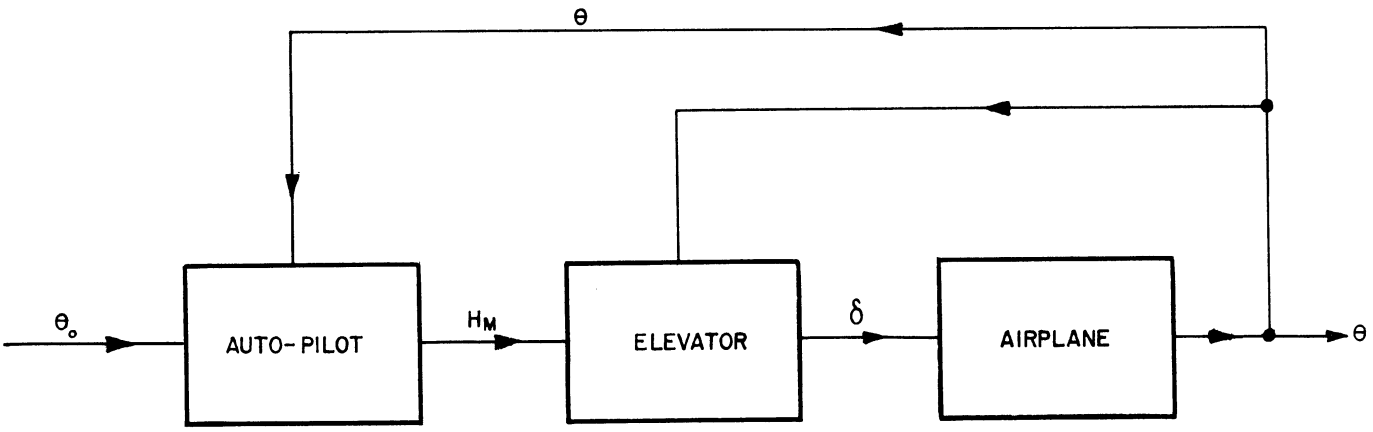

Fig. 11-1. Block diagram of the complete system.

Stability is also investigated. Nyquist curves for a part and for the whole system are plotted in order to make predictions about the stability.

11.2 Airplane Simulator.

We arrived at the equation of motion of an airplane in elevation in a rather roundabout manner. In a report[17] covering the steady state response of a B-25 J airplane to sinusoidal oscillations of the elevator for a range of frequencies of oscillation, the following formula is given:

$$\left|\frac{\theta}{\delta}\right| = |M_\delta| \cdot \sqrt{\frac{1 + (Z_\omega/\omega)^2}{\omega^4 + (C_1^2 - 2C_2)\,\omega^2 + C_2^2}}\,, \qquad (11\text{-}1)$$

where θ is the angle of pitch of the airplane with respect to the horizontal.

δ is the angle of the elevator with respect to the stabilizer.

ω is the forcing frequency applied to the elevator.

M_δ, C_1, C_2 and Z_ω are constants.

Equation (11-1) is the formula for the absolute value of the frequency response of the airplane. From Equation (11-1) we can deduce that for steady state oscillations,

$$\frac{\theta}{\delta} = -M_\delta \cdot \frac{1 + j\,Z_\omega/\omega}{-\omega^2 + C_2 - j\omega C_1} \cdot \qquad (11\text{-}2)$$

The signs of all terms above cannot be directly deduced from Equation (11-1), but a subsequent check of points on the curves for the phase angle of θ/δ versus frequency in the report[17] establishes the signs in Equation (11-2).

Since for steady state oscillations $p = j\omega$, we assume, using operator p notation, that we can write from Equation (11-2),

$$\theta(t) = -M_\delta \cdot \frac{1 - Z_\omega/p}{p^2 - C_1 p + C_2}\,\delta(t)\,, \qquad (11\text{-}3)$$

where we are no longer limited to the steady state. Rewriting Equation (11-3) in the usual notation we obtain as the equation of motion of the airplane:

$$\frac{d^2\theta}{dt^2} - C_1\frac{d\theta}{dt} + C_2\theta = -M_\delta\left(\delta - Z_\omega\int\delta\,dt\right). \qquad (11\text{-}4)$$

Note that Equation (11-4) is a linear, third order differential equation with constant coefficients. In its derivation it is assumed that the angles δ and θ are small enough so that the forward velocity U of the airplane remains constant.

Below are the values of the constants in Equation (11-4) as given in Table 1 of the report[17] for U = 175 m.p.h.

$$Z_\omega = -0.864 \text{ / sec}$$

$$C_1 = -3.75 \text{ / sec}$$

$$C_2 = 4.31 \text{ / sec}^2$$

$$M_\delta = -8.98 \text{ / sec}^2$$

Before we set up Equation (11-4) on the computer it is convenient to divide through by $-M_\delta$, obtaining:

$$-\frac{1}{M_\delta}\ddot{\theta} + \frac{C_1}{M_\delta}\dot{\theta} - \frac{C_2}{M}\theta = \delta - Z_\omega\int\delta\,dt\,. \qquad (11\text{-}5)$$

The computer circuit used for solving Equation (11-5) is shown in Fig. 11-2. Response of the airplane angle of pitch θ to a square pulse input of the elevator angle δ is shown in Fig. 11-3.

Using Equation (11-2) and the values of the constants given above, we calculate the steady state frequency response curve of the airplane. Following the method outlined in Chapter 3, we determine experimental steady state frequency response data. The solid-line curves in Fig. 11-4 show the calculated steady state response (amplitude and phase shift). The experimental points as obtained from the computer are also shown. It is evident that agreement is well within the limits of recording error.

11.3 Auto-Pilot Simulator

The auto-pilot frequency response curves were based on actual curves for a B-24 auto-pilot amplifier.[18] A circuit was designed which would give roughly the same gain and phase characteristics except for a frequency ratio of approximately two, i.e., it was assumed that the frequencies for a B-25 would be about double for the same response as a B-24.

The auto-pilot circuit is shown in Fig. 11-5. Assuming that the point P is at ground potential we see that

$$i_3 + i_4 = i_5 \,. \qquad (11\text{-}6)$$

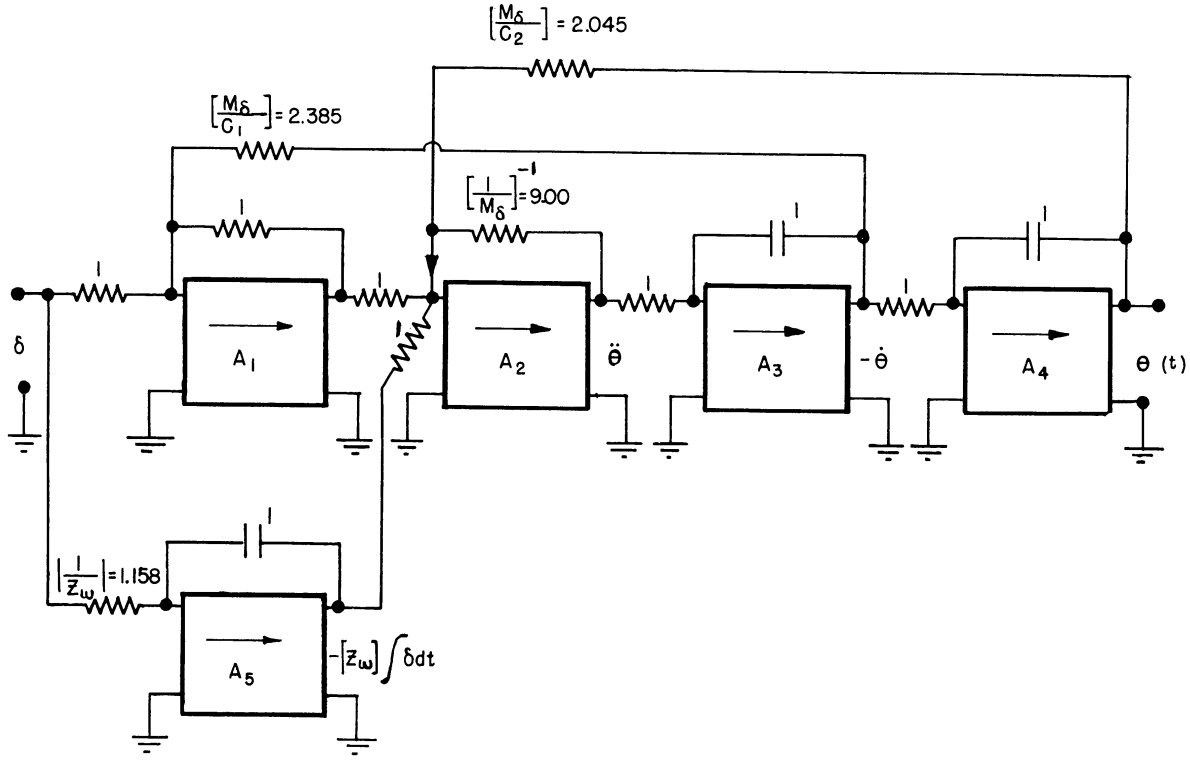

Fig. 11-2. Computer circuit for Equation (11-5).

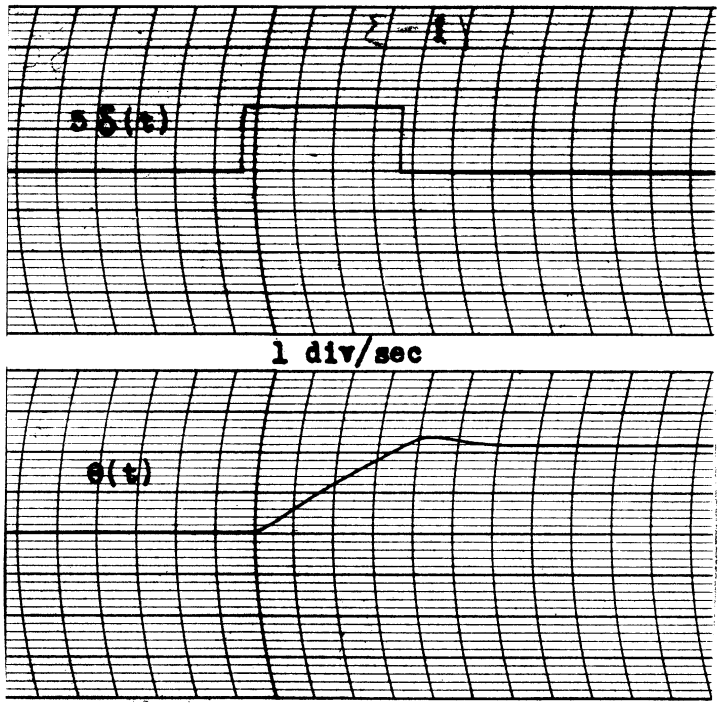

Fig. 11-3. Response θ of airplane to square pulse input

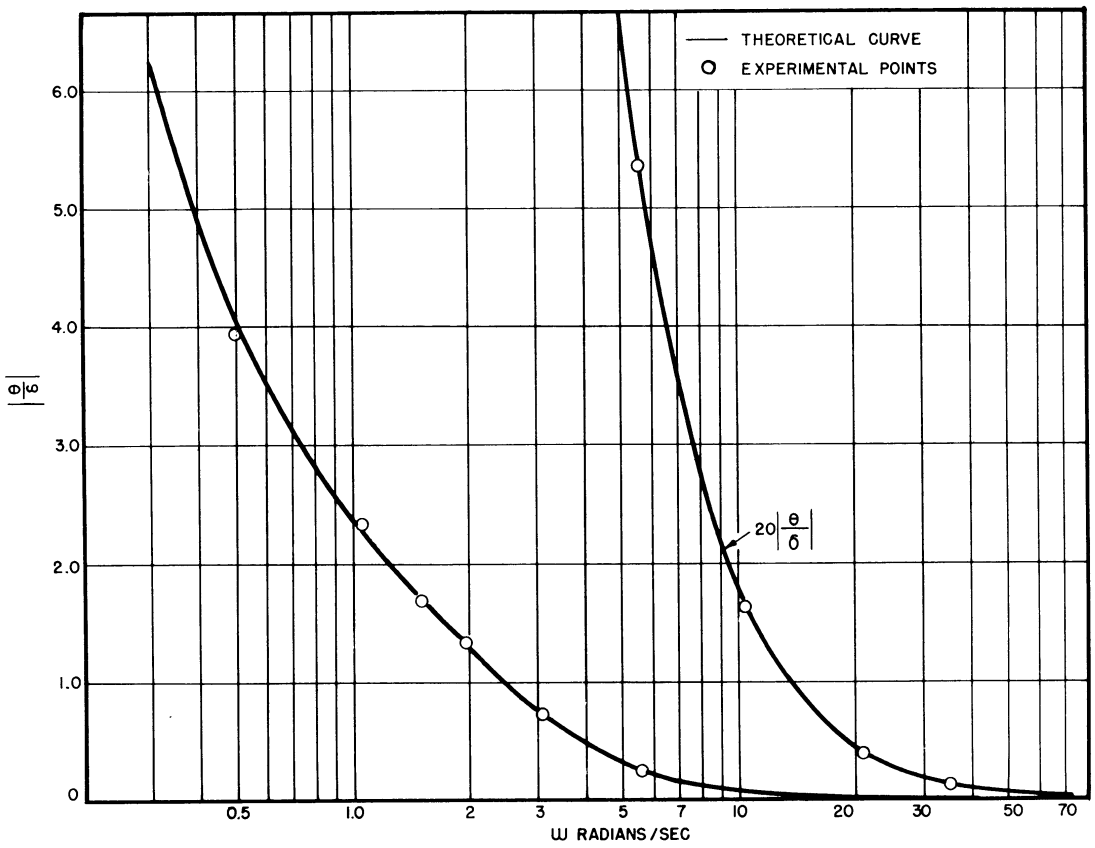

Fig. 11-4(a)

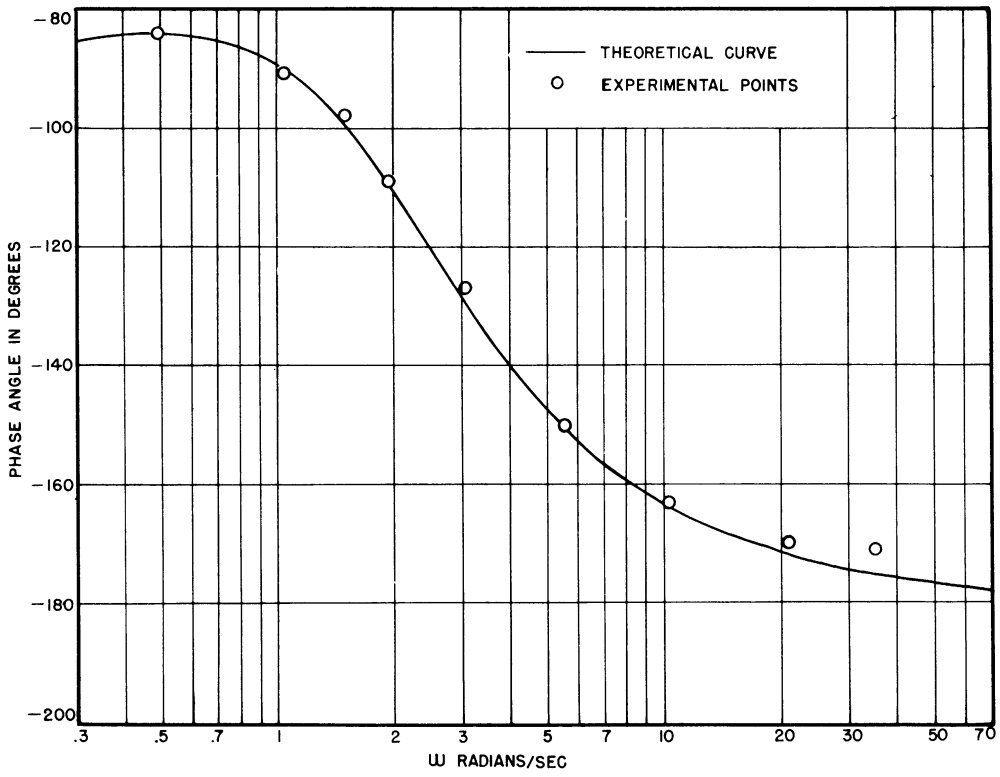

Fig. 11-4(b)
Experimental and calculated steady state response curves.

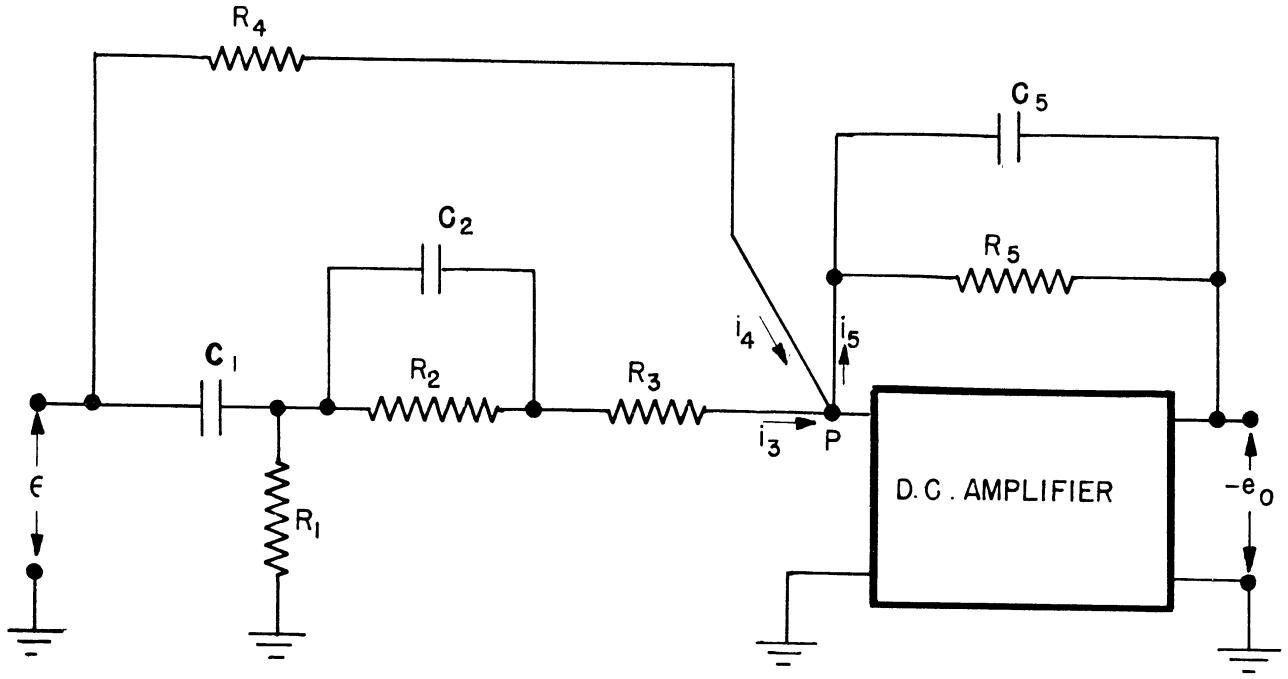

Fig. 11-5. Auto-pilot circuit.

Denoting the output of the auto-pilot amplifier as $-e_o$ (the negative sign is necessary because the d.c. amplifier reverses the phase by 180 degrees) and the input as ϵ we can derive, using Equation (11-6), the following formula for $\frac{e_o}{\epsilon}$.

$$\frac{e_o}{\epsilon} = \left(\frac{R_4}{R_5}\right)^{-1} \frac{\alpha_2 p^2 + \alpha_1 p + \alpha}{\beta_3 p^3 + \beta_2 p^2 + \beta_1 p + \alpha} \qquad (11\text{-}7)$$

where

$$\alpha = \frac{R_2 + R_3}{R_1} + 1$$

$$\alpha_1 = \left(\frac{R_3}{R_1} + 1\right) R_2 C_2 + (R_2 + R_3 + R_4) C_1$$

$$\alpha_2 = (R_3 + R_4) R_2 C_1 C_2$$

$$\beta_1 = \left(\frac{R_2 + R_3}{R_1} + 1\right) R_5 C_5 + (R_2 + R_3) C_1 + \left(\frac{R_3}{R_1} + 1\right) R_2 C_2$$

$$\beta_2 = R_5 C_5 \left[(R_2 + R_3) C_1 + \left(\frac{R_3}{R_1} + 1\right) R_2 C_2 \right] + R_2 R_3 C_1 C_2$$

$$\beta_3 = R_2 R_3 R_5 C_1 C_2 C_5$$

$$p = \frac{d}{dt} \quad , \quad p^2 = \frac{d^2}{dt^2} \quad , \text{ etc.}$$

The following values for the circuit constants were used:

R_1	= 0.500 meg	C_1	= 0.195 mfd
R_2	= 9.95 meg	C_2	= 0.099 mfd
R_3	= 0.200 meg	C_5	= 0.006 mfd
R_4	= 3.00 meg		
R_5	= 3.00 meg		

Substituting the above circuit constants in Equation (11-7) we get

$$\frac{e_o}{\epsilon} = \frac{0.615\,p^2 + 3.943p + 21.30}{0.000680p^3 + 0.0967p^2 + 3.730p + 21.30} \,. \qquad (11\text{-}8)$$

For steady state ($p = j\omega$) Equation (11-8) becomes

$$\frac{e_o}{\epsilon} = \frac{21.30 - 0.615\omega^2 + j\,3.943\,\omega}{21.30 - 0.0967\,\omega^2 + j\,(3.73\omega - 0.000680\,\omega^3)} \,, \qquad (11\text{-}9)$$

From equation (11-9) the steady state response curves of the autopilot can be calculated. Both the calculated curves and those obtained experimentally from the simulator are shown in Fig. 11-6.

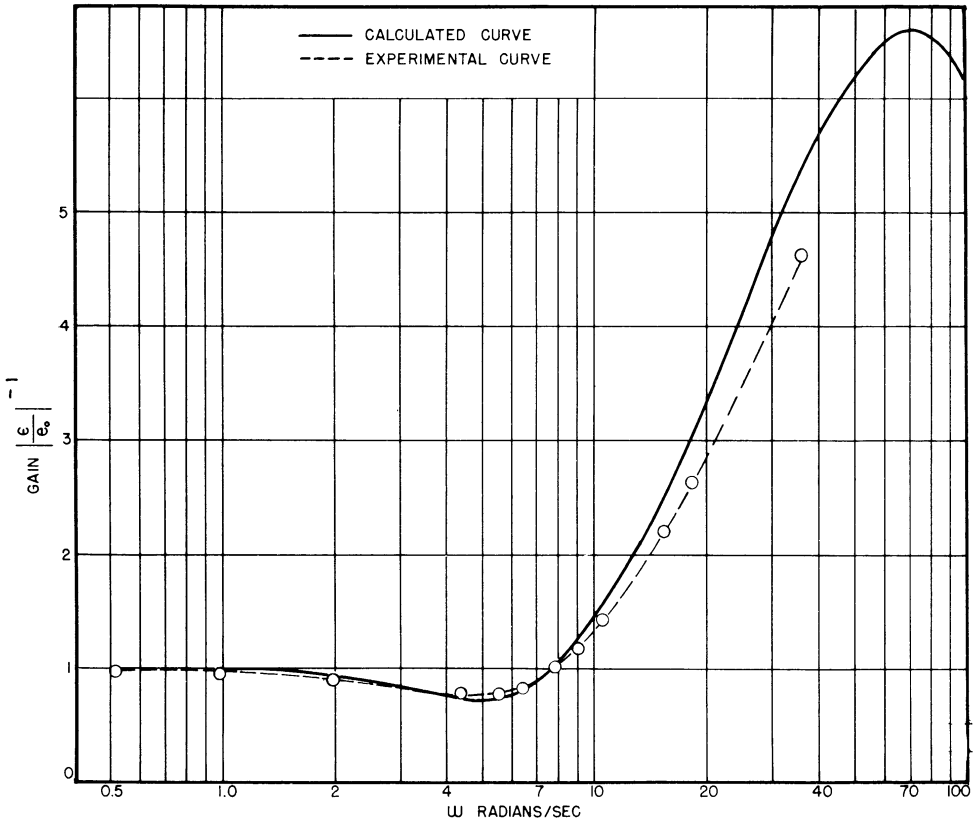

Fig. 11-6(a)

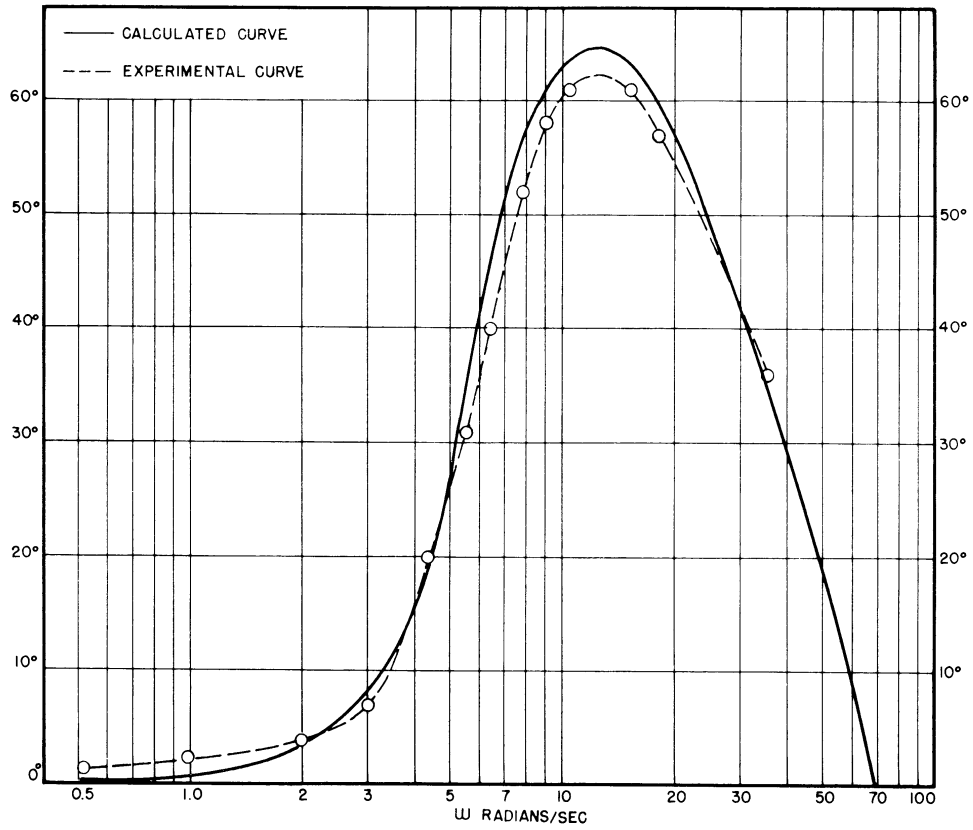

Fig. 11-6(b)
Experimental and calculated steady state response curves.

Lack of perfect agreement may be due to the fact that G. E. Pyranol capacitors were used in the auto-pilot circuit instead of the polystyrene capacitors normally used in our computer circuits.

Note that for high frequencies the gain of the auto-pilot decreases sharply due to the presence of C_5 in the circuit. The circuit acts as an integrator for these high frequencies.

11.4 Elevator Simulator.

Before we consider the complete elevator problem, let us first assume a relationship between the net torque T_δ applied to the elevator, the hinge moment H_m applied to the elevator, and the angle of pitch θ of the airplane. We will ignore the effect of the normal acceleration of the airplane, not because this is justifiable in the actual problem, but because it considerably simplifies our simulator problem. That is, we wish to simplify the problem as much as possible and yet still retain a legitimate problem. Thus, we assume that

$$T_\delta = K_1 H_m + K_2 \theta \quad . \tag{11-10}$$

Now consider the equation of motion of the elevator. We assume it to be of the form:

$$I \frac{d^2\delta}{dt^2} + C \frac{d\delta}{dt} + K\delta = T_\delta \quad , \tag{11-11}$$

where

$\delta(t)$ = the elevator angle with respect to the stabilizer.

I = moment of inertia of the elevator.

C = aerodynamic damping coefficient

K = aerodynamic restoring torque for a unit deflection of δ

$T_\delta(t)$ = the net torque applied to the elevator.

The following numerical values for the constants of Equation (11-11) were used.

$$I = \frac{0.000315}{1.2} \text{ sec}^2 \text{ radian}^{-1}$$

$$C = \frac{0.0119}{1.2} \text{ sec}^2 \text{ radian}^{-1}$$

$$K = \frac{1}{1.2} \text{ radian}^{-1}$$

The equation of motion of the elevator now becomes:

$$0.000315\ddot{\delta} + 0.0119\dot{\delta} + \dot{\delta} = 1.2T_{\delta} \qquad (11\text{-}11a)$$

The computer circuit used as the elevator simulator is shown in Fig. 11-7.

Note that the natural frequency of the elevator is given by:

$$\omega = \sqrt{\frac{K}{I}} = \frac{1}{0.000315} = 56.5 \text{ radians/sec} .$$

The elevator response to step-function input T_{δ} is shown in Fig. 11-8.

Writing Equation (11-11) in operator p notation we get

$$\frac{\delta}{T_{\delta}} = \frac{1.2}{0.000315p^2 + 0.0119p + 1} \qquad (11\text{-}12)$$

For steady state oscillations, $p = j\omega$ and

$$\frac{\delta}{T_{\delta}} = \frac{1.2}{1 - 0.000315\omega^2 + 0.0119\omega} \qquad (11\text{-}13)$$

From Equation (11-13) the steady state frequency response of the elevator is calculated. Calculated and experimental curves of elevator frequency response (as obtained from the analog computer) are shown in Fig. 11-9. Here again the discrepancy between theoretical and experimental curves is perhaps due to the use of paper condensers in the integrating amplifiers.

Referring again to Equation (11-10) we assign the value unity to K_1 and K_2. We also denote H_m as Be_o, where H_m is the hinge-moment applied to the elevator, e_o is the output of the auto-pilot circuit shown in Figure 11-5, and B is a constant which we will call the auto-pilot gain-factor. Then Equation (11-10) becomes:

$$T_{\delta}(t) = Be_o(t) + \theta(t) , \qquad (11\text{-}14)$$

and Equation (11-11) becomes

$$0.000315\ddot{\delta} + 0.0119\dot{\delta} + \dot{\delta} = 1.2(\theta + Be_o) \qquad (11\text{-}15)$$

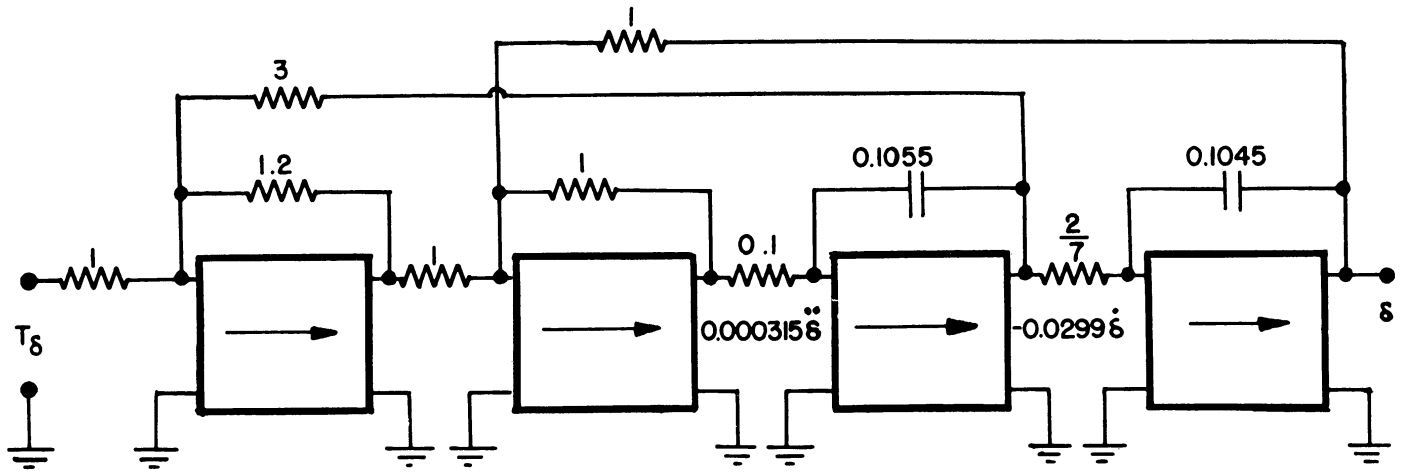

Fig. 11-7. Computer circuit for elevator.

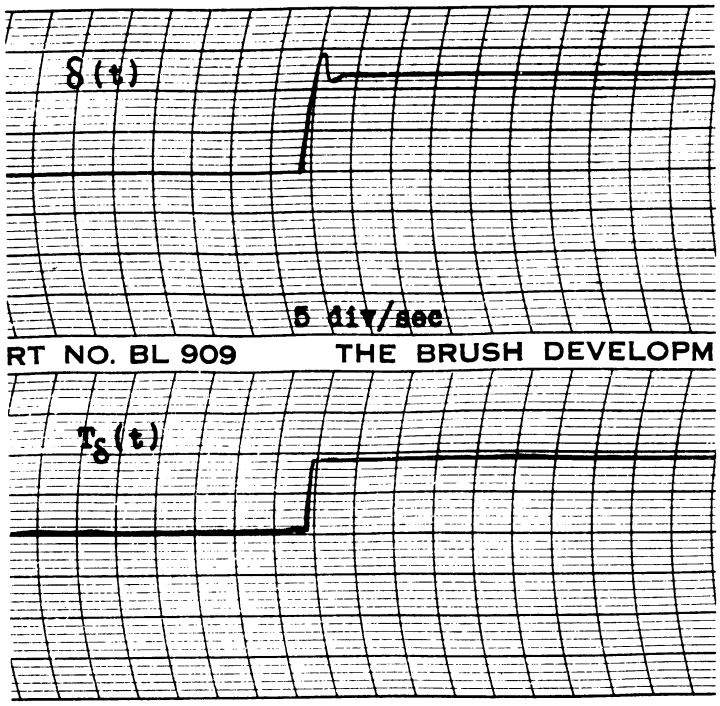

Fig. 11-8. Elevator response to step input T_δ.

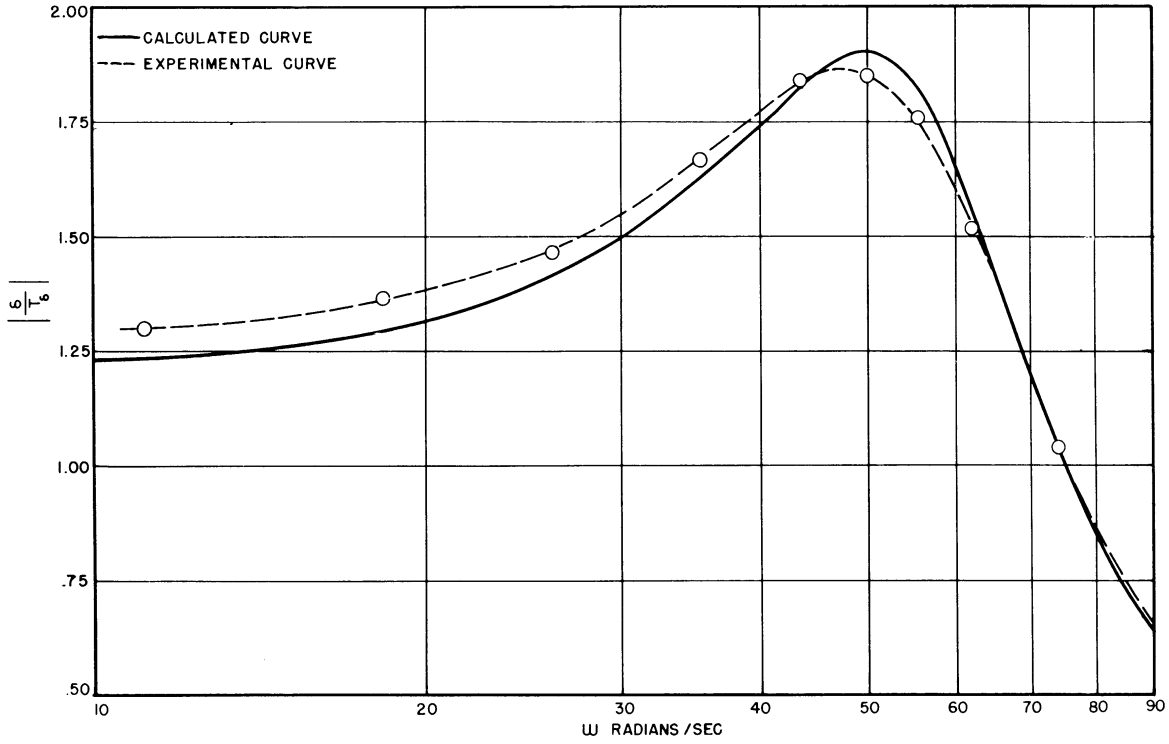

Fig. 11-9(a)

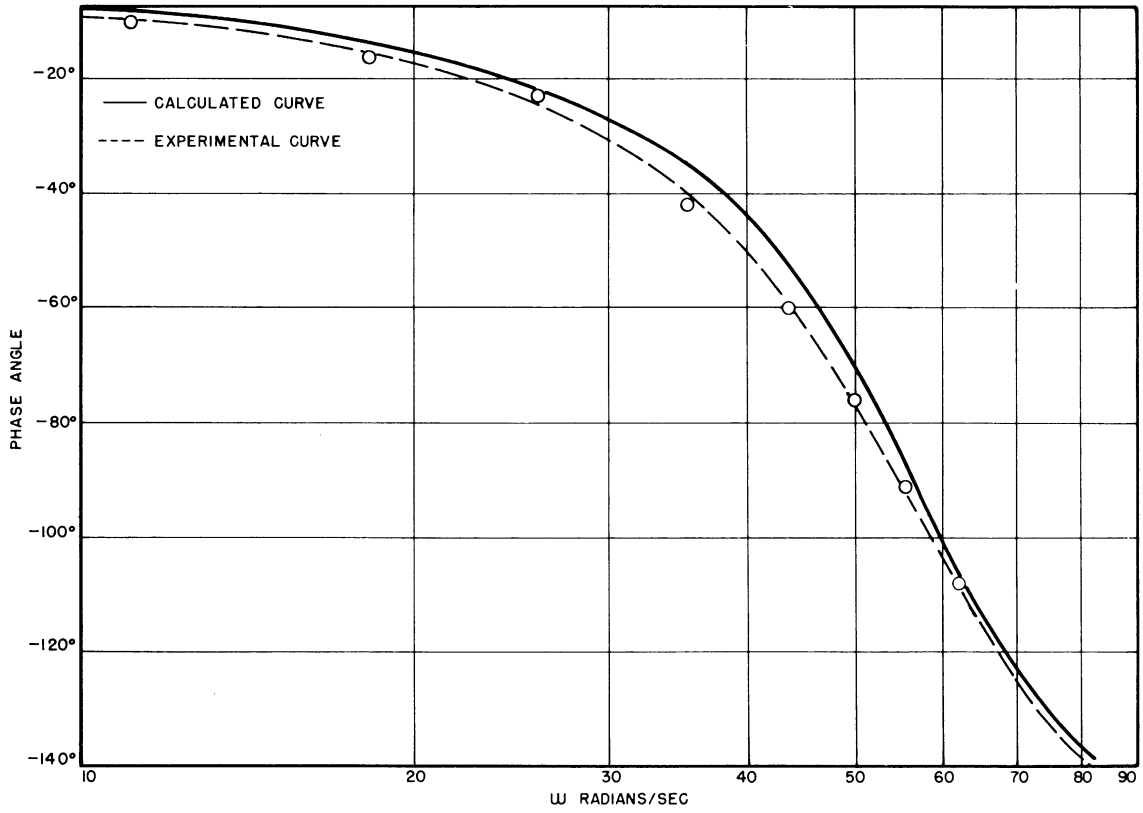

Fig. 11-9(b)
Experimental and calculated steady state response curves.

11.5 Steady-state Response of the Complete System.

We must now tie the auto-pilot, elevator, and airplane together in order to simulate the action of the complete control system. The following notation is used

$$Y_1 = \frac{H_m(t)}{\epsilon(t)} = B\,\frac{e_o(t)}{\epsilon(t)} = \text{transmission ratio of auto-pilot}$$

$$Y_2 = \frac{\delta(t)}{T_\delta(t)} = \frac{\delta(t)}{\theta(t) + Be_o(t)} = \text{transmission ratio of elevator}$$

$$Y_3 = \frac{\theta(t)}{\delta(t)} = \text{transmission ratio of airplane.}$$

Our complete servomechanism in terms of the transmission ratio is shown in Figure 11-10.

From Figure 11-10:

$$H_m = (\theta_o - \theta)\,Y_1 \qquad (11\text{-}15a)$$

$$\delta = (\theta + H_m)\,Y_2 = \theta Y_2 + \theta_o Y_1 Y_2 - \theta Y_1 Y_2 \qquad (11\text{-}16)$$

But $$\delta = \frac{\theta}{Y_3} \qquad (11\text{-}17)$$

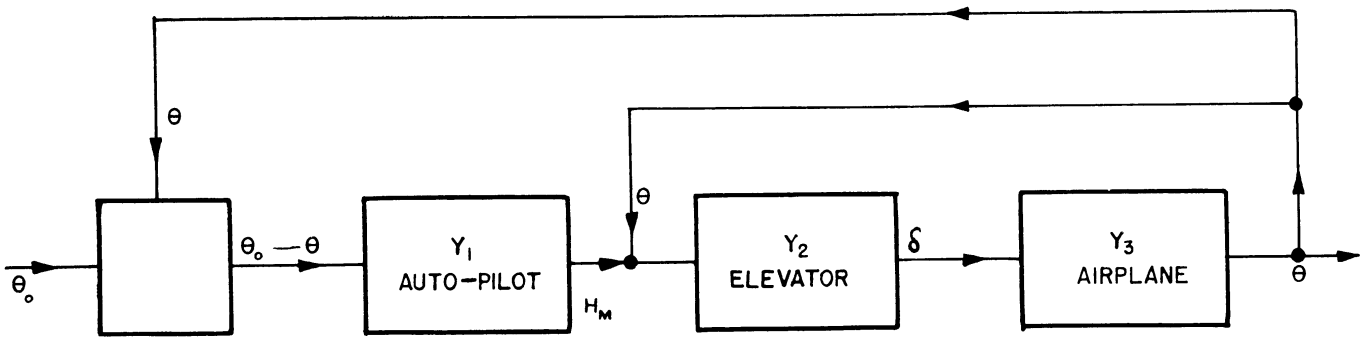

Fig. 11-10. Complete servomechanism.

Therefore, we can write from Equations (11-16) and (11-17):

$$\theta = Y_2Y_3\theta + Y_1Y_2Y_3\theta_o - Y_1Y_2Y_3\theta \ ,$$

or

$$\frac{\theta(t)}{\theta_o(t)} = \frac{Y_1Y_2Y_3}{Y_1Y_2Y_3 - Y_2Y_3 + 1} \qquad (11\text{-}18)$$

Since we already know Y_1, Y_2 and Y_3, we can calculate $\frac{\theta(t)}{\theta_o(t)}$ from Equation (11-18).

The complete analog computer circuit for simulating Figure 11-10 is shown in Figure 11-11.

In Figure 11-12 are shown the steady state frequency response curves as calculated from Equation (11-18) using the theoretical or calculated values of the transmission ratios.

The auto-pilot gain constant B was chosen as 3 for these steady state curves. The experimental points for steady state frequency gain as determined from the computer are also shown in Fig. 11-12. Note that the agreement is fairly close except at the higher frequencies. This is due to the discrepancy in theoretical and experimentally determined auto-pilot gain curves (See Fig. 11-6).

The steady state frequency response curves for the complete system as calculated from the separate experimental transmission ratio curves are shown in Figure 11-13.

11.6 Stability Considerations.

Whenever a servomechanism has more than one feedback loop, the simple Nyquist theory as presented in Section 10.5 is not adequate. Each feedback loop system within the main outside feedback loop must be investigated separately for stability by means of a Nyquist diagram.[19] The net number of loops about the critical point for each feedback system is determined. The net total number of encirclements of critical points for all the inner feedback systems is determined. For the complete system to be stable when the final feedback loop is connected, the Nyquist curve for the complete system must encircle the critical point exactly as many times as the net revolutions of the critical points of the inner systems, but in the opposite direction.

Thus the net number of encirclements of the critical point for all the feedback systems is zero.

In our particular problem we have two feedback loops and we must first investigate the stability of the inner loop. Let $\overline{\overline{Y}}_o$ denote Y_2Y_3. The steady state frequency curve of $\overline{\overline{Y}}_o$ as calculated from Y_2 and Y_3 for ω running from +0 to ∞ is shown in Figure 11-14. The reflection of the curve about the real axis gives the $\overline{\overline{Y}}_o$ curve for ω going from $-\infty$ to - 0. Note that $\overline{\overline{Y}}_o\ (-j\,0) = j\infty$, and $\overline{\overline{Y}}_o\ (+j\,0) = -j\infty$. In order to join the two ends at infinity we must find

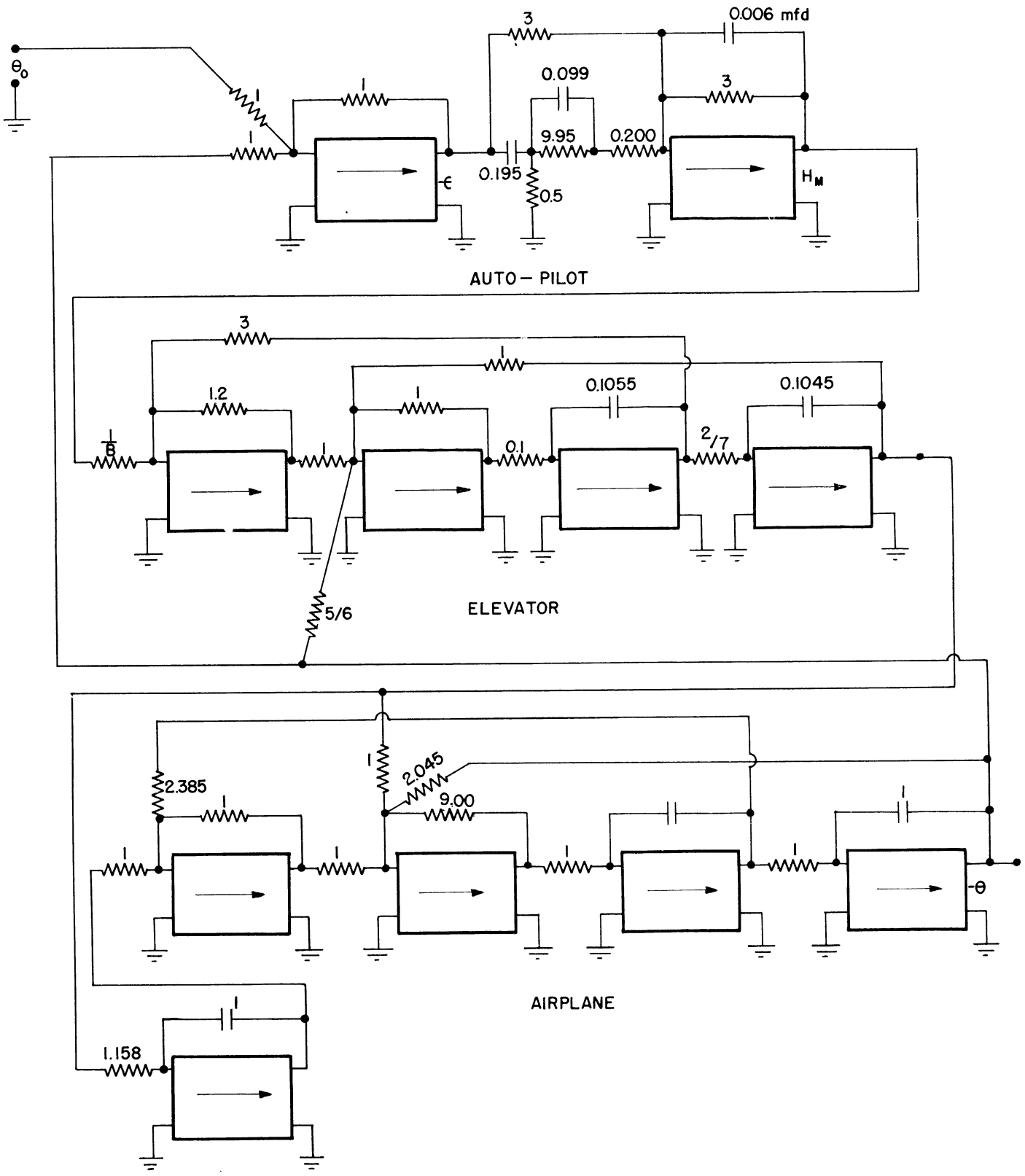

Fig. 11-11. Computer circuit for entire system.

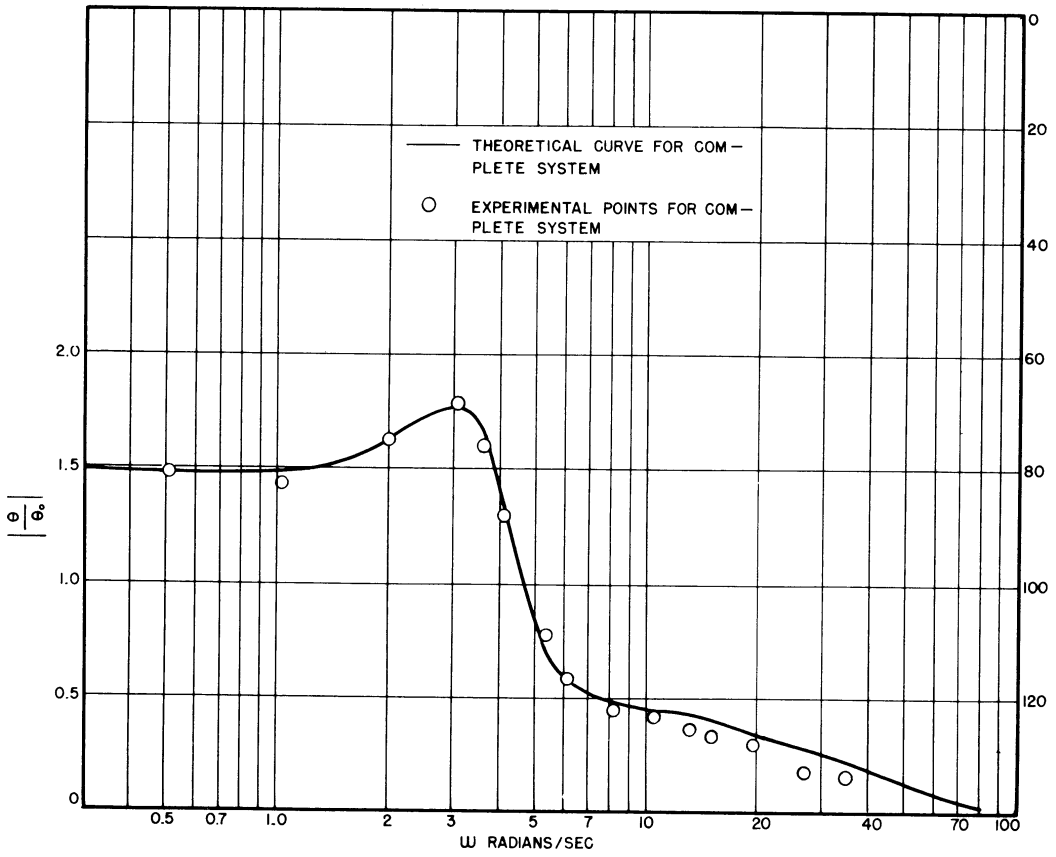

Fig. 11-12(a).

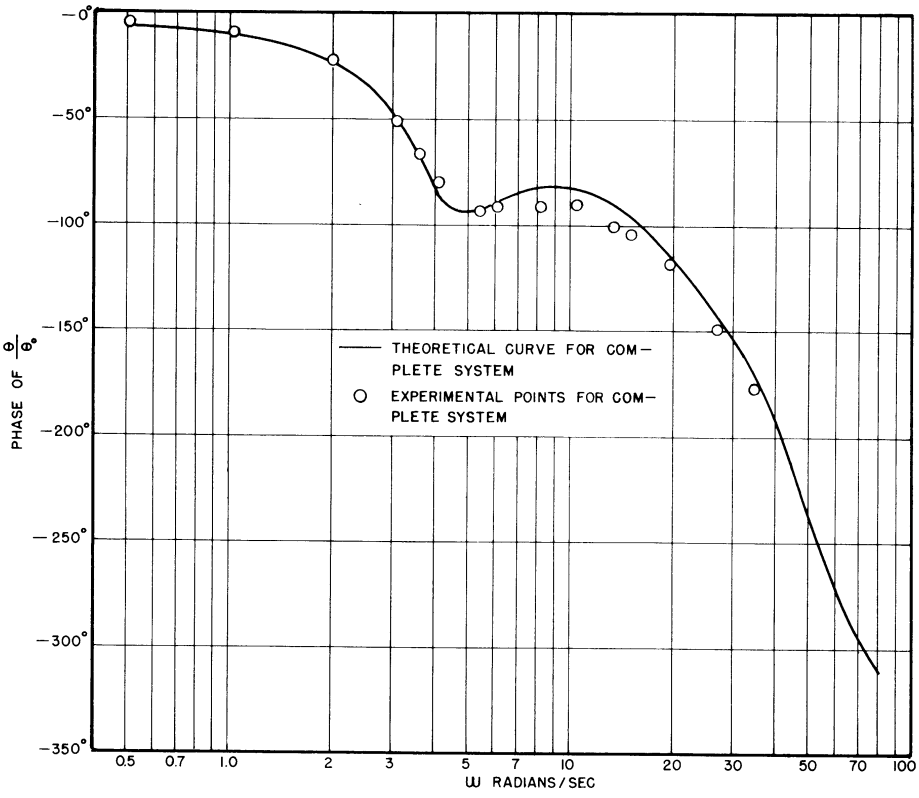

Fig. 11-12(b).
Experimental and Theoretical steady state response curves.

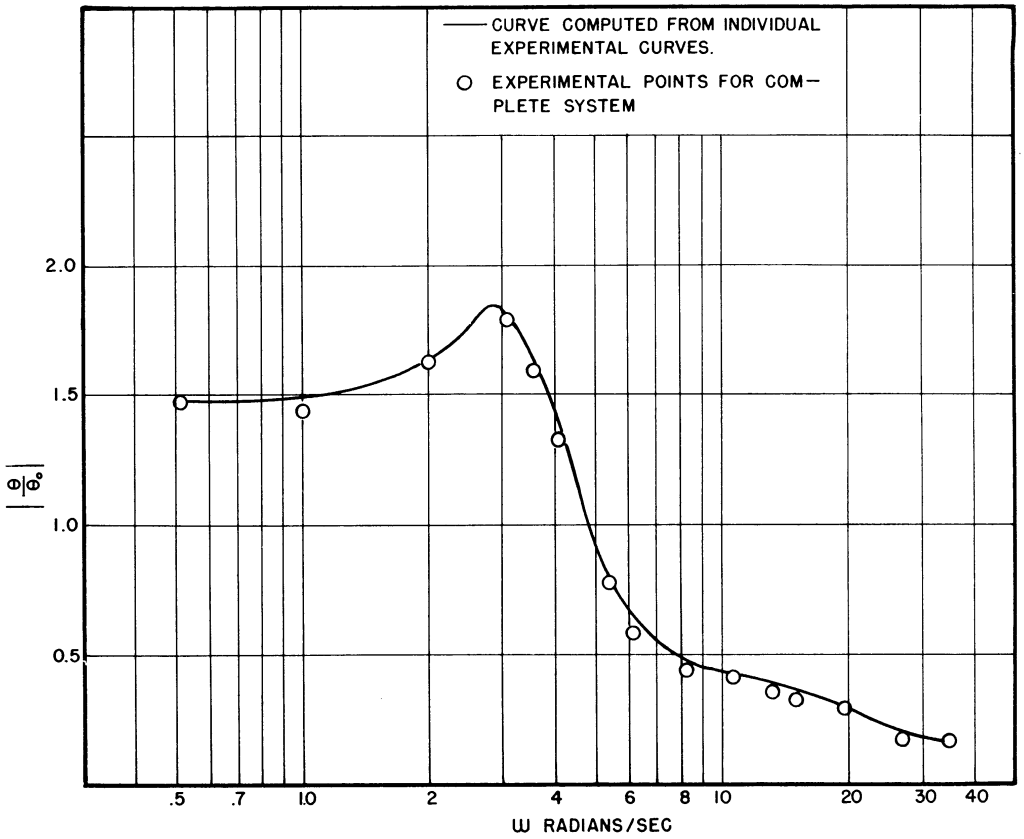

Fig. 11-13(a).

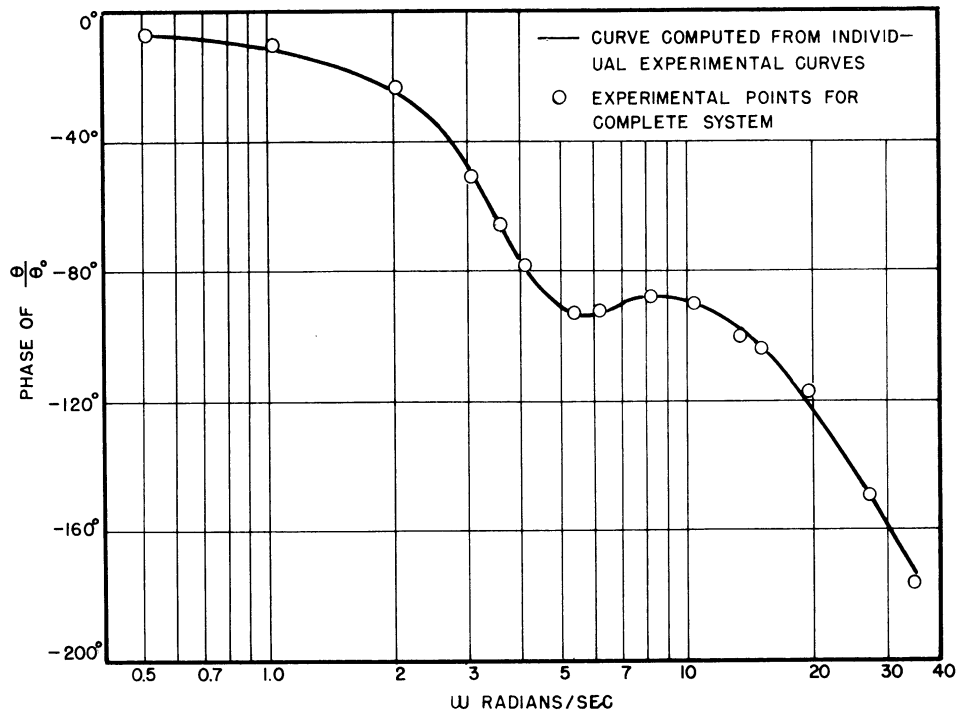

Fig. 11-13(b).

Experimental and calculated steady state response curves.

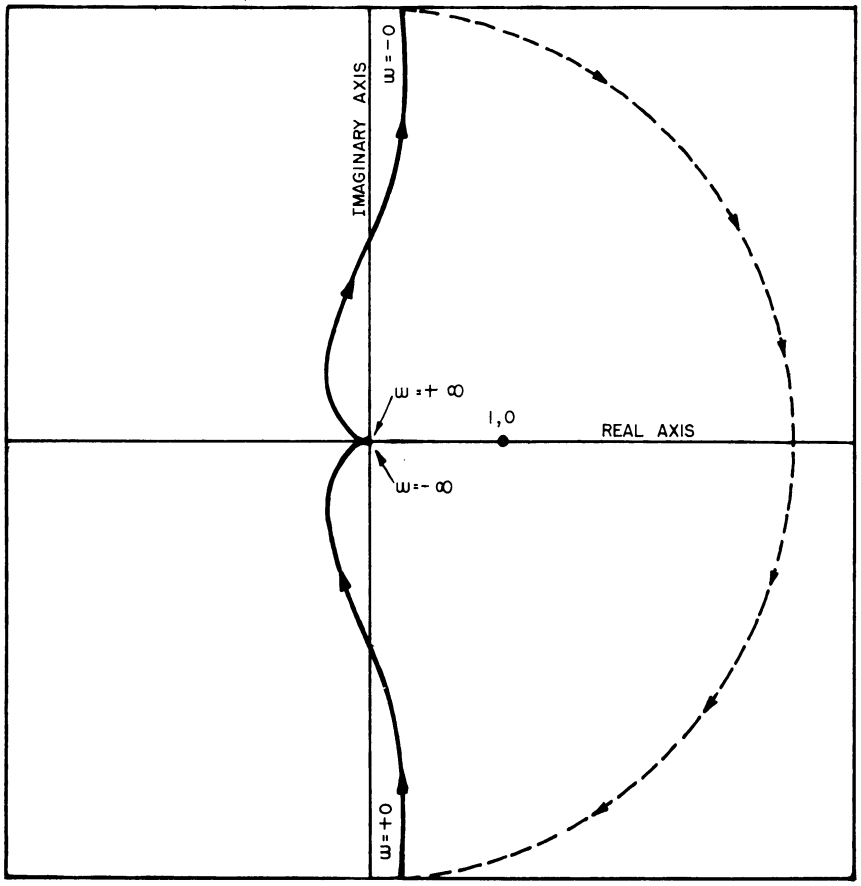

Fig. 11-14. Nyquist diagram for inner loop.

out on which side of the real axis the semi-circle at infinity crosses. Hence, we wish to find the limit of $Y_2(p) \cdot Y_3(p)$ as p approaches zero along the real axis.

From Equation (11-12) we see that

$$\lim_{p \to 0} Y_2(p) = 1.2$$

Remembering that Z_ω is negative, we get from Equation (11-3)

$$\lim_{p \to 0} Y_3(p) = +\infty$$

Then it follows that

$$\lim_{p \to 0} \bar{\bar{Y}}_0(p) = \lim_{p \to 0} Y_2(p) Y_3(p) = +\infty \qquad (11\text{-}19)$$

Thus the circle at infinity is in the right half plane and the Nyquist loop for $\bar{\bar{Y}}_0$ is completed as shown in Fig. 11-14.

Referring to Figure 11-10 we see that

$$(\theta + H_M)\, Y_2 = \quad = \frac{\theta}{Y_3}$$

and

$$\frac{\theta}{H_m} = \frac{Y_2\, Y_3}{1 - Y_2 Y_3} = \frac{Y_o}{1 - Y_o} \qquad (11\text{-}20)$$

From equation (11-20) it is apparent that the critical point is (1,0), and from Fig. 11-14 we see that the loop does encircle the critical point, and in a clockwise direction.

From equation (11-18) we can write

$$\frac{\theta}{\theta_o} = \frac{\dfrac{Y_1 Y_2 Y_3}{1 - Y_2 Y_3}}{1 + \dfrac{Y_1 Y_2 Y_3}{1 - Y_2 Y_3}}$$

Letting

$$Y_o = \frac{Y_1 Y_2 Y_3}{1 - Y_2 Y_3} \qquad (11\text{-}21)$$

we get

$$\frac{\theta}{\theta_o} = \frac{Y_o}{1 + Y_o} \qquad (11\text{-}22)$$

The critical point is (-1,0).

In Fig. 11-15 the Nyquist loop for Y_o as calculated from the theoretical values of Y_1, Y_2, and Y_3 according to Equation (11-19) is plotted. Note that the critical point is encircled in a counterclockwise direction. Since the Y_o loop encircled the critical point in a clockwise direction, the Nyquist Criterion for stability has been met and the system will be stable.

In Figure 11-16 the Y_o points as calculated from experimental computer curves of Y_1, Y_2, and Y_3 are shown against the theoretical curve of Y_o.

The response θ of the system to a step input θ_o as recorded from the computer is shown in Fig. 11-17. The elevator angle δ is also shown for a step input θ_o in Fig. 11-18. The response of the system when the elevator angle δ is held at a constant deflection from zero for a short length of time is shown in Fig. 11-19.

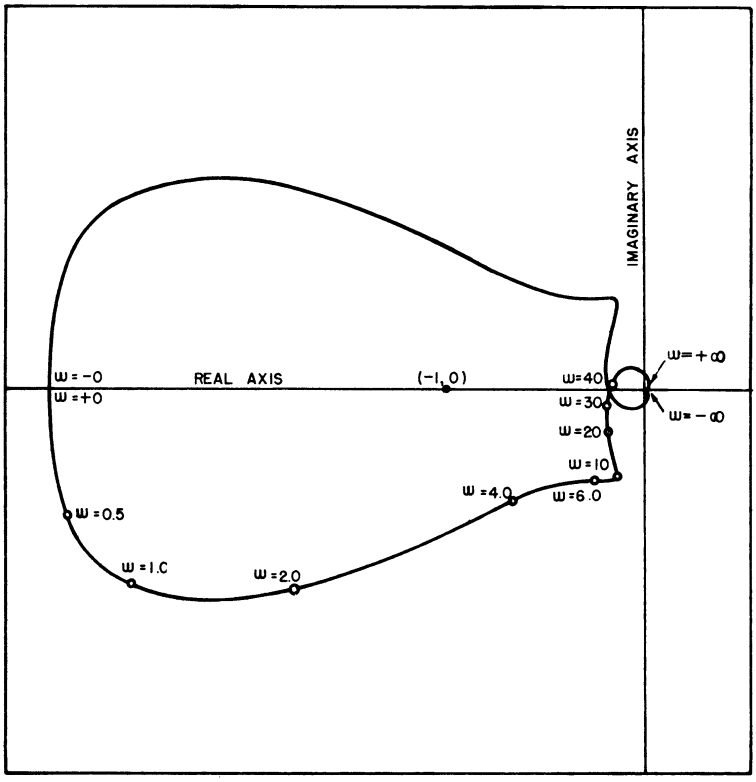

Fig. 11-15. Nyquist diagram for entire system.

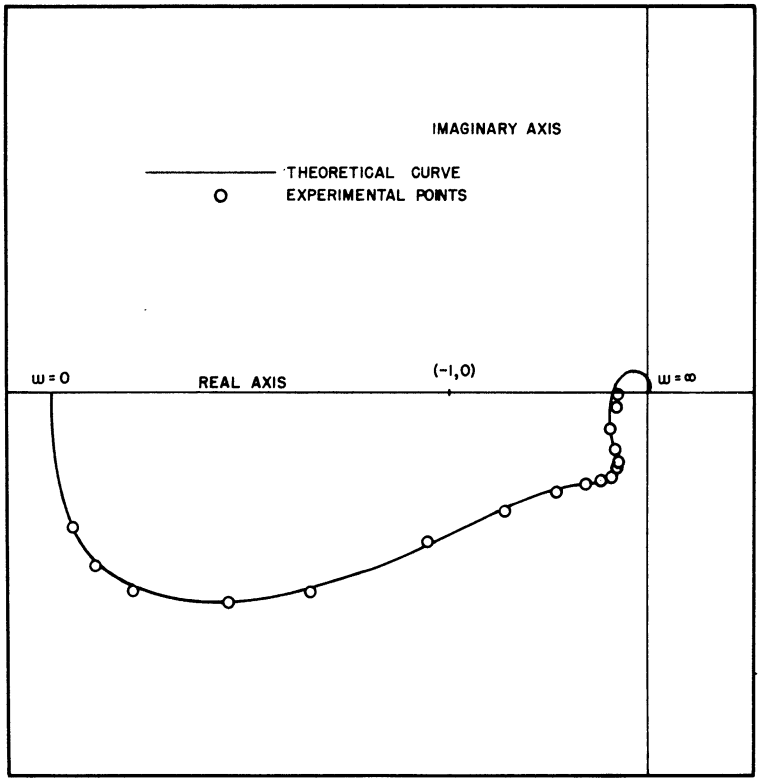

Fig. 11-16. Comparison of experimental and theoretical performance of entire system on the Nyquist plane.

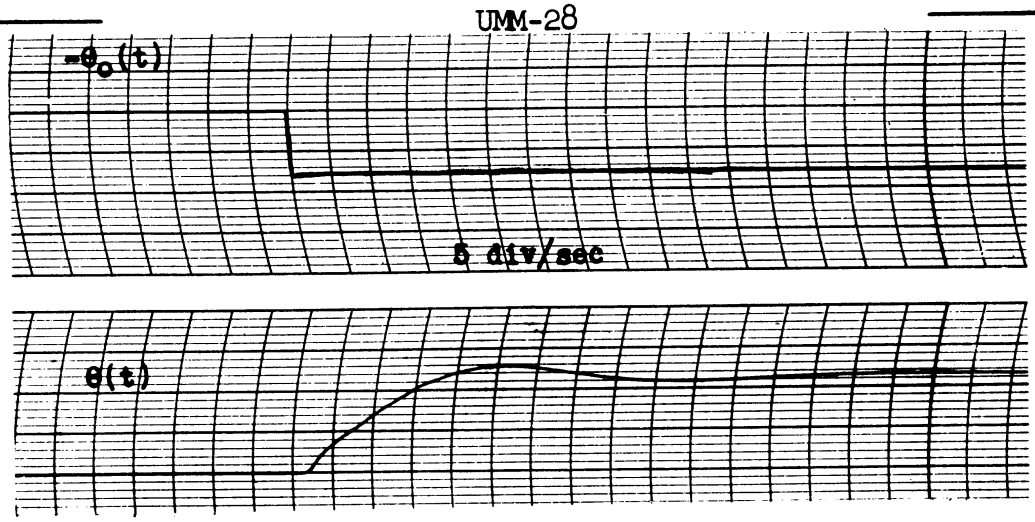

Fig. 11-17. Response θ to a step input θ_o.

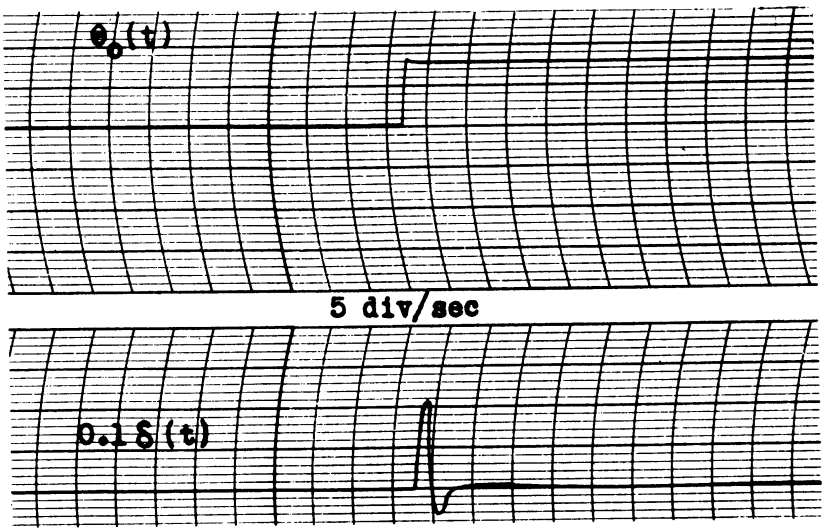

Fig. 11-18. Response δ to a step input θ_o.

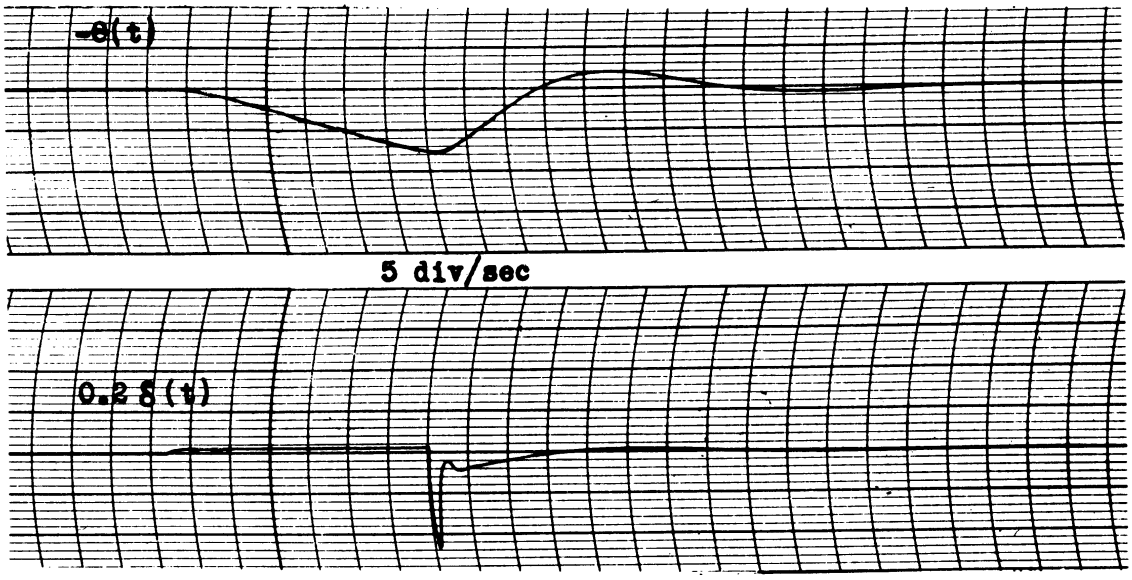

Fig. 11-19. System response to elevator transient.

It is interesting to consider the effect of removing the first and second derivative components of the auto-pilot system, i.e., letting $Y_1 = B =$ constant. For B = 3 the resulting Y_o Nyquist diagram is shown in Figure 11-20.

Since the loop still encircles the critical point once in a counter-clockwise direction, we would expect a stable system. But note that the curve is closer to the critical point by roughly a factor of two. Hence we would not expect the system to be quite as stable for Y_1 = constant.

In Fig. 11-21 the response θ to a step input θ_o bears out this expectation; the oscillations of the angle of pitch θ die out much more slowly than in Fig. 11-17.

From Equation (11-21) it is evident that changing the auto-pilot transmission ratio Y_1 by a constant factor will change Y_o by only a constant factor. Thus far we have considered the problem only for the auto-pilot gain factor B = 3. As the gain factor of the auto-pilot is made larger, the $Y_o\ (j\omega)$ curve of Figure 11-15 is expanded out from the origin by the same factor. If we neglect scale effect in Figure 11-15, we see that this is equivalent to moving the critical point (-1,0) in toward the origin along the real axis. In fact, if the auto-pilot gain B is made large enough, the critical point will be inside the small inner loop of Fig. 11-15, and the Nyquist loop encircles the critical point in a clockwise instead of a counterclockwise direction. Hence the system will be unstable.

By blowing up the region of Y_o about the origin it is determined that the curve crosses the real axis at about the point (-0.175,0). For B = 15 instead of 3 (auto-pilot gain increased by a factor of 5) the crossover point is moved out to the point (-0.875,0).

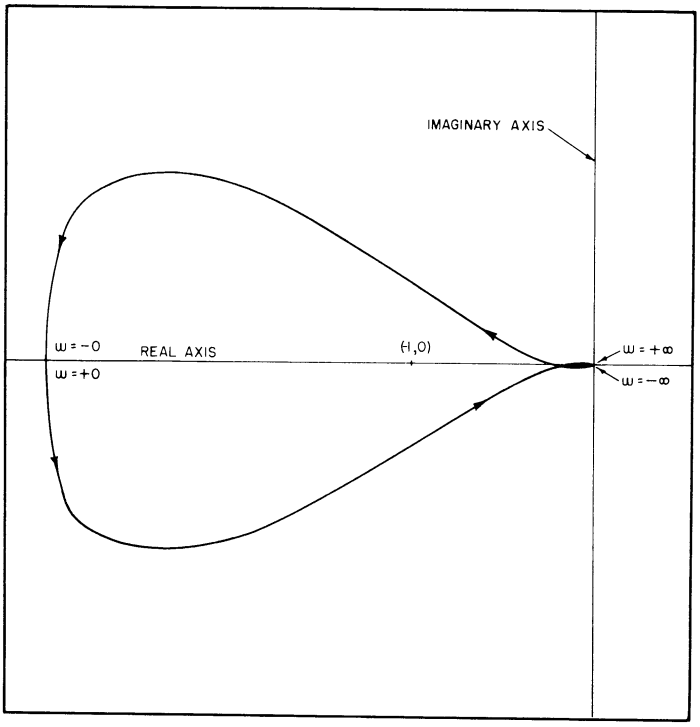

Fig. 11-20. Y_o Nyquist diagram.

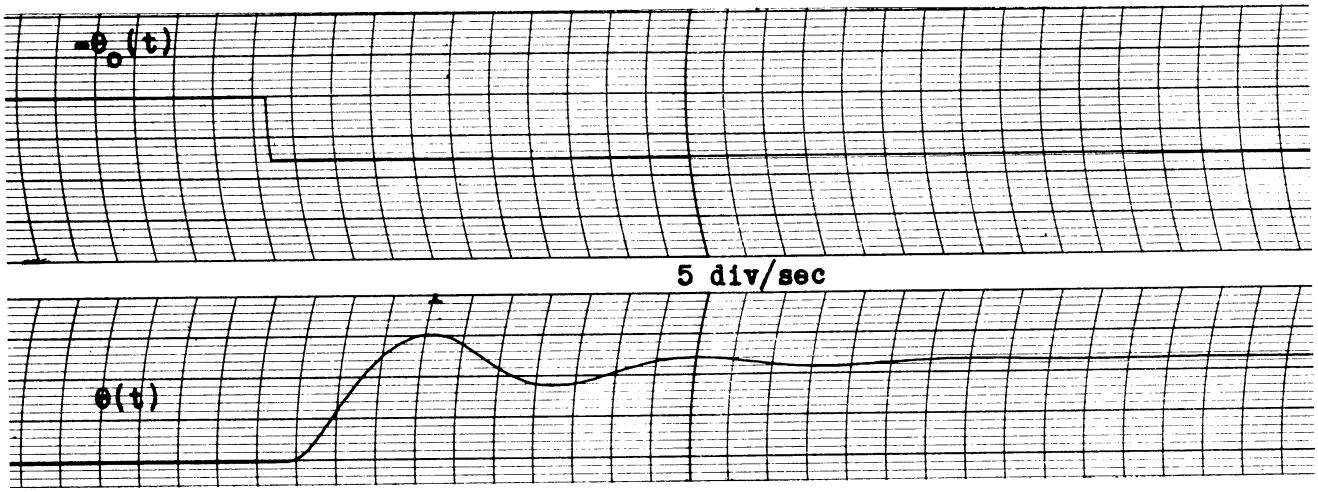

Fig. 11-21. Response θ to a step input θ_o for $Y_1 = 3$.

Figure 11-22 shows that in this case the system shows much less stability in response to a step function input.

The value of B such that the system oscillated continuously for a step input was determined from the computer and found to be 18.0. According to the theoretical curve of Y_o this value of B should be $\frac{3 \times 1}{0.175} = 17.2$. The response of the system to a step function input is shown in Figure 11-23. The frequency of oscillation as determined from Fig. 11-23 is 36.4 radians/sec.

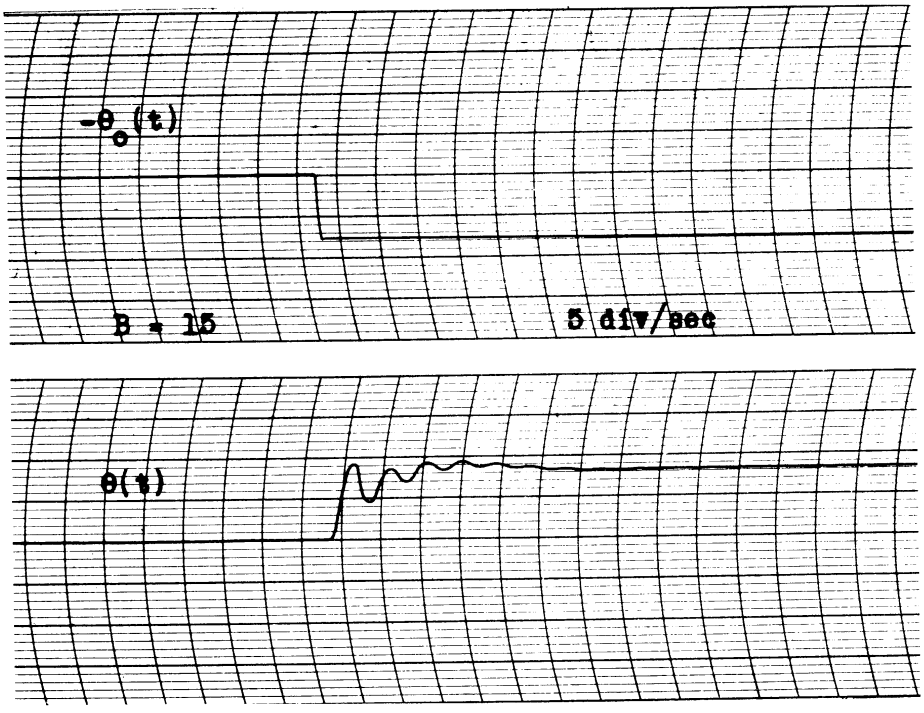

Fig. 11-22. Response θ to a step input θ_o for autopilot gain-factor B = 15.

The theoretical rrequency is 36.8 radians/sec. The experimental data here shows fair agreement with the theoretical values when one considers that the auto-pilot and elevator simulators themselves are not too accurate at these higher frequencies.

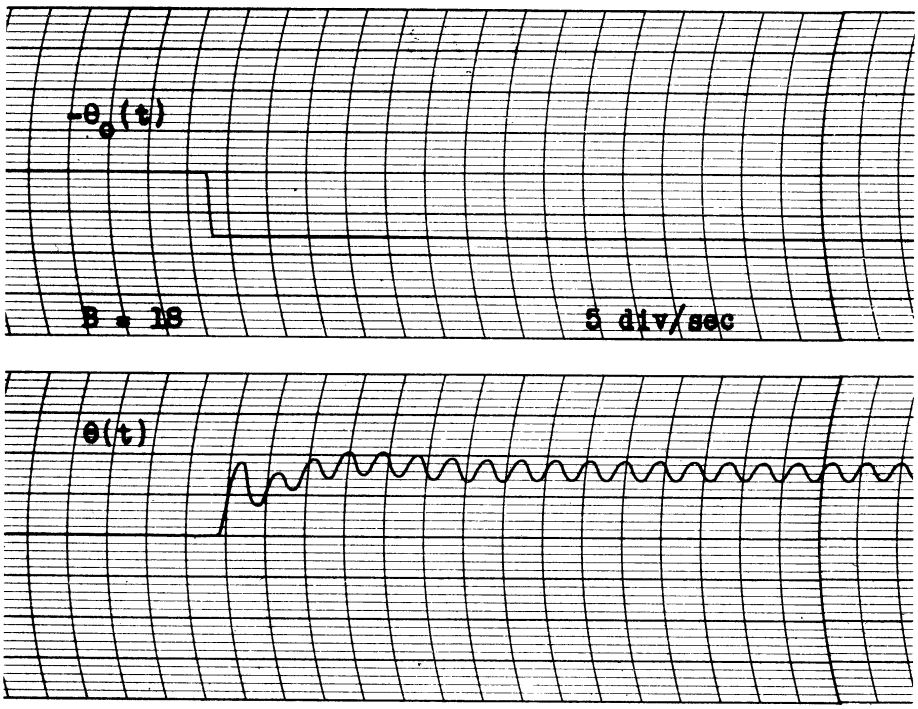

Fig. 11-23. Response θ to step input θ_o for auto-pilot gain-factor B = 18.

11.7 Evaluation of Power Series Coefficients.

Following the met l of Chapter 10, we will calculate the theoretical power series representatio .or $\frac{\theta}{\theta_o}$ and check the first two coefficients experimentally on the analog computer.

From Equatior (11-8) we have for the auto-pilot

$$\frac{e_o}{\epsilon} = \frac{0.615p^2 + 3.943p + 21.30}{0.000680p^3 + 0.0967p^2 + 3.730p + 21.30} \qquad (11\text{-}8)$$

From Section 11.5 we remember that $Y_1 = B\frac{e_o}{\epsilon}$. Letting B = 3 and dividing the denominator of Equation (11-8) into the numerator, we obtain the power series expansion for $Y_1(p)$.

$$Y_1(p) = 3 + 0.03p + 0.678p^2 + 0.0121p^3 + \ldots \qquad (11\text{-}23)$$

Referring to equation (11-12) we find that for the elevator

$$Y_2 = \frac{}{T} = \frac{1.2}{0.000315p^2 + 0.011} \cdot \frac{}{1} \quad . \qquad (11\text{-}12)$$

Substituting the values of the airplane constants given in Section 11.2 into Equation (11-3) we get

$$Y_3 = \frac{\theta}{\delta} = (8.98). \frac{1 + .864p}{p^2 + 3.75p + 4.31} \qquad (11\text{-}24)$$

Multiplying Equation (11-12) and (11-24) together, the following expression for $Y_2 Y_3$ is obtained when terms of order higher than p^3 are neglected.

$$Y_2Y_3 = p^{-1} \cdot \frac{9.31 + 10.8p}{4.31 + 3.80p + 1.046p^2 + 0.0131p^3}$$

Dividing numerator by denominator, we find that

$$Y_2(p) \cdot Y_3(p) = \frac{2.16}{p} + 0.603 - 1.06p + 0.778p^2 + \ldots\ldots \qquad (11\text{-}25)$$

Substituting the power series expansions for $Y_1(p)$ and $Y_2(p) \cdot Y_3(p)$ in Equation (11-18) and neglecting all terms of order higher than p^3 we obtain the following power series expansion for $\frac{\theta}{\theta_o}$ when the numerator of the expression is divided by the denominator.

$$\frac{\theta}{\theta_o} = 1.5 - 0.354p + 0.167p^2 - 0.243p^3 + \ldots\ldots \qquad (11\text{-}26)$$

For a step function input we have

$$\theta_o = 0 \ , \ t < 0$$

$$\theta_o = A = \text{constant}, \quad t > 0, \qquad (11\text{-}27)$$

and from Equation (11-26) it is apparent that

$$\frac{\theta_L}{\theta_o} = 1.5, \qquad (11\text{-}28)$$

where θ_L is the limiting angle of pitch after all transients have died out.

In Figure 11-17 the step response curve is shown. Note that $\frac{\theta_L}{\theta_o} = 1.5$ within the limits of recorder error.

In general it is desirable to have a servomechanism for which the zero order coefficient a_o is unity or near unity (so that the static error is zero; see 10.5). Reference to Fig. 11-22 shows that when we increase the auto-pilot gain factor B from 3 to 15, the ratio a_o becomes very nearly one. In fact it can be shown that

$$a_o = \frac{B}{B-1} \qquad (11\text{-}29)$$

However, B cannot be increased beyond the value 18 without making the system unstable, as shown in Section 11.6. Even for B = 15 the system shows oscillatory tendencies (see Fig. 11-22). A more practical value for B would be between 5 and 10.

For a ramp function input we write

$$\theta_o = 0 \quad , \quad t < 0 \ .$$
$$\theta_o = At \quad , \quad t > 0 \ . \qquad (11\text{-}30)$$

and from Equation (11-26) we get

$$\frac{\theta_L}{\theta_o} = (1.5t - 0.354) \ ,$$

or

$$\frac{\theta_L}{\theta_o} = 1.5\,(t - 0.236) \ . \qquad (11\text{-}31)$$

As explained in Section 10.5, this means that the θ_L "ramp" should lag behind the input ramp function θ_o by 0.236 seconds.

Assuming that a_o is known to be 1.5, but that a_1, the coefficient of t, is unknown, we can write for a ramp input

$$\theta_L = 1.5\,At + Aa_1 = 1.5\theta_o + Aa_1 \ ,$$

or

$$\theta_L - \theta_o = \frac{Aa_1}{1.5} \qquad (11\text{-}32)$$

If we record θ_o (= At) along with $\theta_L/1.5 - \theta_o$, we can calculate a_1 following the method of Section 10.5.

The circuit for obtaining these values is shown in Fig. 11-24.

The ramp response for the system is shown in Figure 11-25 and the quantities θ_o and $\frac{\theta}{1.5} - \theta_o$ are shown in Fig. 11-26.

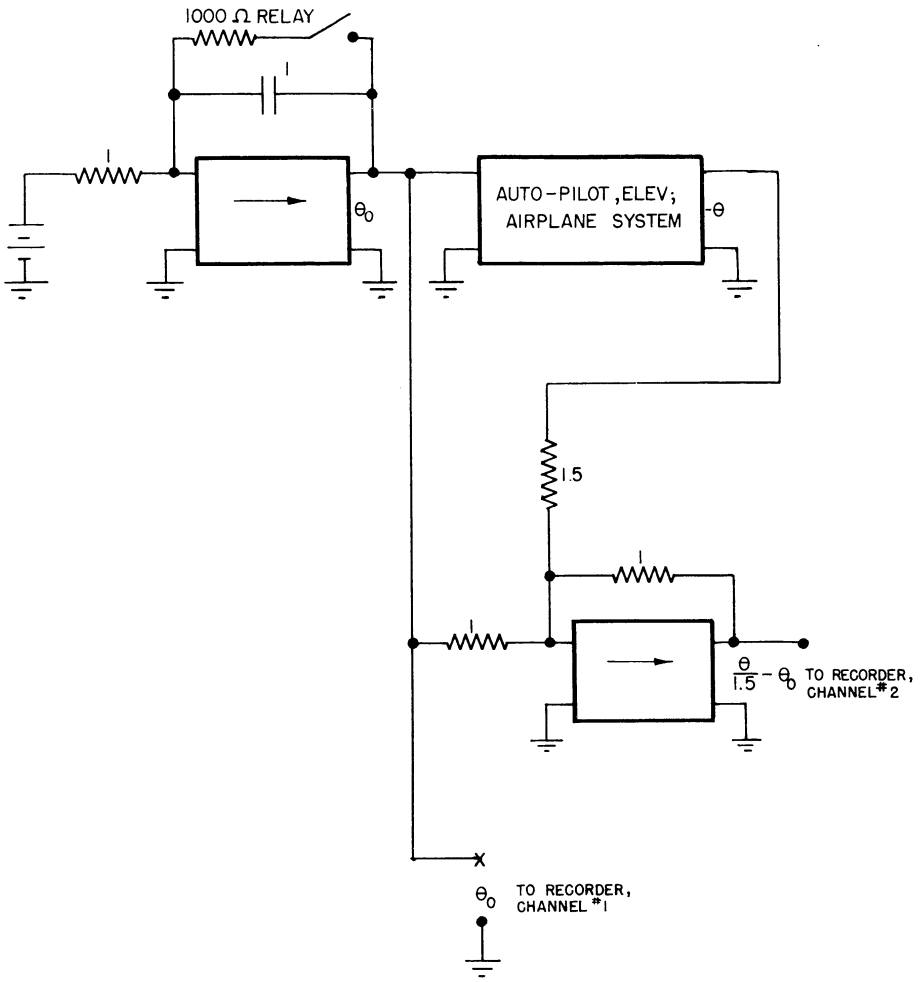

Fig. 11-24. Computer circuit for obtaining a_1.

For different values of the slope A the following values of $\frac{a_1}{1.5}$ were determined experimentally using Equation (11-32).

$$\begin{array}{r} -0.184 \\ -0.198 \\ \underline{-0.182} \end{array}$$

Average -0.19 sec

$$a_1 = -0.19\ (1.5) = -0.29 \text{ sec}$$

theoretical $a_1 = -0.35$ sec

At first consideration this discrepancy seems rather large, but when it is remembered that we are measuring the difference between two very similar quantities and that the total error is only 0.06 sec, the result is not so alarming.

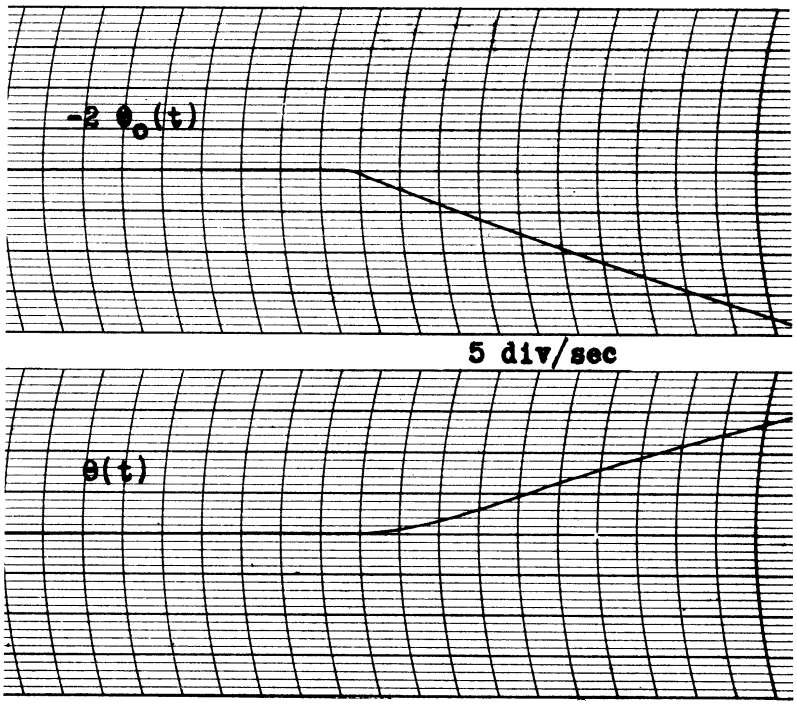

Fig. 11-25. Response θ to a ramp input function.

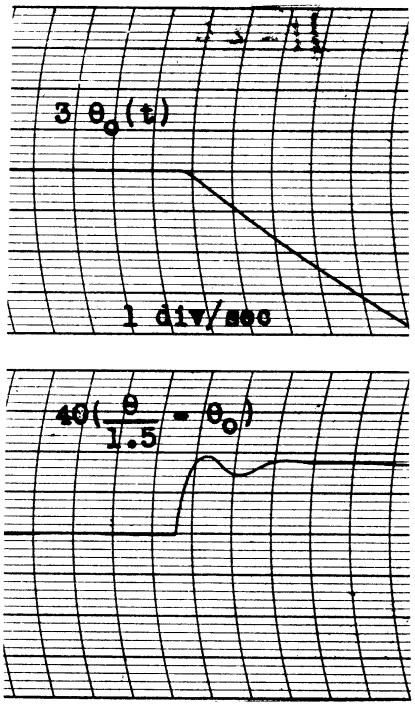

Fig. 11-26. Curves of $\frac{\theta}{1.5} - \theta_o$ and θ_o.

11.8 Conclusions.

In conclusion it might be said that the analog computer shows great possibility in the simulation of complicated servo systems. Response of the system to any kind of input signal can immediately and accurately be observed and recorded. System constants can be changed merely by changing resistors. Stability of the system is easily observed and checks well with the Nyquist Criterion.

It is to be noted that the overall accuracy of the simulator would have been considerably improved by using polystyrene capacitors throughout.

BIBLIOGRAPHY

1. Ragazzini, Randall, and Russell; Proc. IRE, 35, 444 (1947)

2. Frost; Electronics, 21, 116, (1948)

3. Den Hartog; Mechanical Vibrations, 2nd Edition, pp. 99-104 (McGraw Hill)

4. Churchill; Modern Operational Methods in Engineering, pp. 68-70, (McGraw Hill)

5. Den Hartog; Ibid., paragraph 33

6. Hudson; The Engineers Manual, p. 121

7. Timoshenko; Vibration Problems in Engineering, Section 54 (D. Van Nostrand)

8. Timoshenko; Ibid., Section 55

9. Timoshenko; Ibid., Section 57

10. Ormondroyd, Hess, and Hess; University of Michigan Engineering Research Institute, Third Progress Report, (March 1, 1949) Office of Naval Research Contract N5Ori-116 (Univ. of Mich. No. M670-4). Title: Theoretical Research on the Dynamics of a Ship's Structure.

11. Hudson; Ibid., page 121

12. Hudson; Ibid., page 122

13. Den Hartog; Ibid. Appendices II, III

14. Timoshenko; Ibid., Section 65

15. MacColl; Fundamental Theory of Servomechanisms, pp. 2-3, (D. Van Nostrand)

16. MacColl; Ibid., pp. 23-28

17. Millikan; JAS. 14, 493 (1947)

18. Halpert and Esval; Proc. AIEE, 63, 861, (1944)

19. Bode; Network Analysis and Feedback Amplifier Design, Chapter VIII, Section 8.8 (D. Van Nostrand)

DISTRIBUTION

Distribution of this report is made in accordance with ANAF-GM Mailing List No. 8, dated April 1949, to include Part A, Part B, and Part C.